NASA/TM–2014-218512 (Corrected Copy)
NESC-RP-13-00869

International Space Station (ISS) Plasma Contactor Unit (PCU) Utilization Plan Assessment Update

Amri Hernandez-Pellerano
Goddard Space Flight Center, Greenbelt, Maryland

Christopher J. Iannello/NESC
Langley Research Center, Hampton, Virginia

Henry B. Garrett, Andrew T. Ging, Ira Katz, and R. Lloyd Keith
Jet Propulsion Laboratory, Pasadena, California

Joseph I. Minow, Emily M. Willis, and Todd A. Schneider
Marshall Space Flight Center, Huntsville, Alabama

Albert C. Whittlesey
Jet Propulsion Laboratory, Pasadena, California

Edward J. Wollack
Goddard Space Flight Center, Greenbelt, Maryland

Kenneth H. Wright
University of Alabama in Huntsville, Huntsville, Alabama

August 2014

NASA STI Program . . . in Profile

Since its founding, NASA has been dedicated to the advancement of aeronautics and space science. The NASA scientific and technical information (STI) program plays a key part in helping NASA maintain this important role.

The NASA STI program operates under the auspices of the Agency Chief Information Officer. It collects, organizes, provides for archiving, and disseminates NASA's STI. The NASA STI program provides access to the NASA Aeronautics and Space Database and its public interface, the NASA Technical Report Server, thus providing one of the largest collections of aeronautical and space science STI in the world. Results are published in both non-NASA channels and by NASA in the NASA STI Report Series, which includes the following report types:

- TECHNICAL PUBLICATION. Reports of completed research or a major significant phase of research that present the results of NASA Programs and include extensive data or theoretical analysis. Includes compilations of significant scientific and technical data and information deemed to be of continuing reference value. NASA counterpart of peer-reviewed formal professional papers, but having less stringent limitations on manuscript length and extent of graphic presentations.

- TECHNICAL MEMORANDUM. Scientific and technical findings that are preliminary or of specialized interest, e.g., quick release reports, working papers, and bibliographies that contain minimal annotation. Does not contain extensive analysis.

- CONTRACTOR REPORT. Scientific and technical findings by NASA-sponsored contractors and grantees.

- CONFERENCE PUBLICATION. Collected papers from scientific and technical conferences, symposia, seminars, or other meetings sponsored or co-sponsored by NASA.

- SPECIAL PUBLICATION. Scientific, technical, or historical information from NASA programs, projects, and missions, often concerned with subjects having substantial public interest.

- TECHNICAL TRANSLATION. English-language translations of foreign scientific and technical material pertinent to NASA's mission.

Specialized services also include organizing and publishing research results, distributing specialized research announcements and feeds, providing information desk and personal search support, and enabling data exchange services.

For more information about the NASA STI program, see the following:

- Access the NASA STI program home page at *http://www.sti.nasa.gov*

- E-mail your question to help@sti.nasa.gov

- Fax your question to the NASA STI Information Desk at 443-757-5803

- Phone the NASA STI Information Desk at 443-757-5802

- Write to:
  STI Information Desk
  NASA Center for AeroSpace Information
  7115 Standard Drive
  Hanover, MD 21076-1320

NASA/TM–2014-218512 (Corrected Copy)
NESC-RP-13-00869

International Space Station (ISS) Plasma Contactor Unit (PCU) Utilization Plan Assessment Update

Amri Hernandez-Pellerano
Goddard Space Flight Center, Greenbelt, Maryland

Christopher J. Iannello
Langley Research Center, Hampton, Virginia

Henry B. Garrett, Andrew T. Ging, Ira Katz, and R. Lloyd Keith
Jet Propulsion Laboratory, Pasadena, California

Joseph I. Minow, Emily M. Willis, and Todd A. Schneider
Marshall Space Flight Center, Huntsville, Alabama

Albert C. Whittlesey
Jet Propulsion Laboratory, Pasadena, California

Edward J. Wollack
Goddard Space Flight Center, Greenbelt, Maryland

Kenneth H. Wright
University of Alabama in Huntsville, Huntsville, Alabama

National Aeronautics and
Space Administration

Langley Research Center
Hampton, Virginia 23681-2199

August 2014

Acknowledgments

The NESC team would like to acknowledge the following individuals who provided their time to answer questions and/or contribute information to this effort: Steven Koontz, Johnson Space Center (JSC), Ronald Galvez (JSC), Mathew Scudder (JSC/Boeing), Doug Hamilton (Wyle), Tamra George (JSC/Hamilton), Orbital Sciences Corporation (OSC) EVA Tool Personnel (JSC), Raymond Kaminski (JSC/Boeing), and Penni Dalton, Glenn Research Center (GRC).

The NESC team would also like to thank the following peer reviewers for their thorough review and commentary: Tim Brady (JSC/Systems Engineering Office (SEO)), Bob Kichak (GSFC), Dawn Emerson (GRC/NESC Chief Engineer (NCE)), Mike Patterson (GRC), Scott West (JSC/NCE), Steve Gentz (MSFC/NCE), and Rob Boyle (JSC/ Crew and Thermal Systems Division of JSC Engineering, see Appendix J).

Available from:

NASA Center for AeroSpace Information
7115 Standard Drive
Hanover, MD 21076-1320
443-757-5802

ERRATA

NASA/TM–2014-218512

Issue Date: 07/21/2015

On each page of body of report in NESC header, Version number changed from 1.0 to 2.0.

Revised Section 4.0, Executive Summary, page 11, by adding two additional paragraphs at the end to reference the new Appendix K, pp. 226-294.

Block 18 of Report Documentation Page adjusted to include additional pages (from 230 to 299).

International Space Station (ISS) Plasma Contactor Unit (PCU) Utilization Plan Assessment Update

July 10, 2014

Report Approval and Revision History

NOTE: NOTE: This document was submitted to the NESC Director for out-of-board approval on July 21, 2015, for configuration control.

Approved: *Original Signature on File* 7/22/15

NESC Director Date

Version	Description of Revision	Office of Primary Responsibility	Effective Date
1.0	Initial Release	Dr. Christopher Iannello, NASA Technical Fellow for Electrical Power, KSC	7/10/14
1.1	Roeschel references changed from year 2010 to 2013. *(No Signature Required)*	Dr. Christopher Iannello, NASA Technical Fellow for Electrical Power, KSC	8/28/14
2.0	Revised Section 4.0, Executive Summary, by adding 2 additional paragraphs at the end to reference the addition of Appendix K.	Dr. Christopher Iannello, NASA Technical Fellow for Electrical Power, KSC	7/16/15

Table of Contents

Technical Assessment Report

List of Figures

List of Tables

Technical Assessment Report

1.0 Notification and Authorization

The NASA Engineering and Safety Center (NESC) received a request to support the Assessment of the International Space Station (ISS) Plasma Contactor Unit (PCU) Utilization Update. This assessment was co-led by Dr. Christopher Iannello, NASA Technical Fellow for Electrical Power, and Ms. Amri Hernández-Pellerano, NASA Electrical Power Technical Discipline Team (TDT) member. The NESC conducted an earlier assessment of the use of the PCU in 2009 (NESC Request #07-054-E[1]) [NASA, 2009]. The objective for that assessment was to evaluate whether leaving PCUs off during non-extravehicular activity (EVA) time frames presented any risk to the ISS through assembly completion. Dr. Steven Koontz asked the previous assessment be extended to include the following possible additions to the PCU utilization plan:

- Nominally leaving the PCUs off during EVA if pre-EVA hazard severity measurements and short-term ionospheric environment forecasts support that decision.
- Disabling the EVA shunt fault detection, isolation and recovery (FDIR) logic and the supporting operational hazard controls if two PCUs are in discharge during the EVA.
- Possible long-term marginalization of the ISS EVA-312 shock hazard report so that no active hazard controls are required.

The key stakeholders for this assessment were Dr. Steven Koontz and the ISS Program (ISSP).

[1] NESC-RP-07-054/NASA/TM-2010-216683

2.0 Signature Page

Submitted by:
Team Signature Page on File – 7/29/14

Ms. Amri Hernandez-Pellerano Date

Significant Contributors:

Dr. Christopher J. Iannello Date

Dr. Henry B. Garrett Date

Mr. Andrew T. Ging Date

Dr. Ira Katz Date

Mr. R. Lloyd Keith Date

Dr. Joseph I. Minow Date

Ms. Emily M. Willis Date

Mr. Todd A. Schneider Date

Mr. Albert C. Whittlesey Date

Dr. Edward J. Wollack Date

Dr. Kenneth H. Wright Date

Signatories declare the findings, observations, and NESC recommendations compiled in the report are factually based from data extracted from program/project documents, contractor reports, and open literature, and/or generated from independently conducted tests, analyses, and inspections.

3.0 Team List

Name	Discipline	Organization
Core Team		
Christopher Iannello	NASA Technical Fellow for Electrical Power	KSC
Amri Hernandez-Pellerano	EPS TDT/PMAD and Power	GSFC
Linda Anderson	MTSO Program Analyst	LaRC
Dan Burbank	Mission Specialist	JSC
Michael Engle	Flight Operations	JSC
Henry Garrett	Space Environments & Effects Scientist	JPL
Ira Katz	Charging Specialist	JPL
Lloyd Keith	NESC Chief Engineer	JPL
Shannon Melton	Medical Team	JSC/Wyle
Kathy Messersmith	Aerospace Flight Systems	JSC
Joseph Minow	Flight Vehicle Space Environment	MSFC
Jack Rasbury	Medical Team	JSC/Wyle
Eduardo Roeschel	Safety & Mission Assurance	JSC
Todd Schneider	Basic Properties of Materials	MSFC
Jason Vaughn	Basic Properties of Materials	MSFC
Albert Whittlesey	Electromagnetic Engineer	JPL
Emily Willis	Flight Vehicle Space Environment	MSFC
Edward Wollack	Research Astrophysicist	GSFC
Kenneth Wright	Research Scientist: Plasma-Body Interactions	UAH
Consultant		
Andrew Ging	Mission Operations	JPL
Administrative Support		
Linda Burgess	Planning and Control Analyst	LaRC/AMA
Melinda Meredith	Project Coordinator	LaRC/AMA
Erin Moran	Technical Writer	LaRC/AMA

3.1 Acknowledgements

The NESC team would like to acknowledge the following individuals who provided their time to answer questions and/or contribute information to this effort: Steven Koontz, Johnson Space Center (JSC), Ronald Galvez (JSC), Mathew Scudder (JSC/Boeing), Doug Hamilton (Wyle), Tamra George (JSC/Hamilton), Orbital Sciences Corporation (OSC) EVA Tool Personnel (JSC), Raymond Kaminski (JSC/Boeing), and Penni Dalton, Glenn Research Center (GRC).

The NESC team would also like to thank the following peer reviewers for their thorough review and commentary: Tim Brady (JSC/Systems Engineering Office (SEO)), Bob Kichak (GSFC), Dawn Emerson (GRC/NESC Chief Engineer (NCE)), Mike Patterson (GRC), Scott West (JSC/NCE), Steve Gentz (MSFC/NCE), and Rob Boyle (JSC/ Crew and Thermal Systems Division of JSC Engineering, see Appendix J).

4.0 Executive Summary

The International Space Station (ISS) vehicle undergoes spacecraft charging as it interacts with Earth's ionosphere and magnetic field. The interaction can result in a large potential difference developing between the ISS metal chassis and the local ionosphere plasma environment. If an astronaut conducting extravehicular activities (EVA) is exposed to the potential difference, then a possible electrical shock hazard arises.

The control of this hazard was addressed by a number of documents within the ISS Program (ISSP) including *Catastrophic Safety Hazard for Astronauts on EVA* (ISS-EVA-312-4A_revE). The safety hazard identified the risk for an astronaut to experience an electrical shock in the event an arc was generated on an extravehicular mobility unit (EMU) surface. A catastrophic safety hazard, by the ISS requirements, necessitates mitigation by a two-fault tolerant system of hazard controls. Traditionally, the plasma contactor units (PCUs) on the ISS have been used to limit the charging and serve as a "ground strap" between the ISS structure and the surrounding ionospheric plasma.

In 2009, a previous NASA Engineering and Safety Center (NESC) team evaluated the PCU utilization plan (NESC Request #07-054-E) with the objective to assess whether leaving PCUs off during non-EVA time periods presented risk to the ISS through assembly completion. For this study, *in situ* measurements of ISS charging, covering the installation of three of the four photovoltaic arrays, and laboratory testing results provided key data to underpin the assessment. The conclusion stated, "*there appears to be no significant risk of damage to critical equipment nor excessive ISS thermal coating damage as a result of eliminating PCU operations during non-EVA times.*"

In 2013, the ISSP was presented with recommendations from Boeing Space Environments for the "Conditional" Marginalization of Plasma Hazard [Mikatarian, R., et al., 2013]. These recommendations include a plan that would keep the PCUs off during EVAs when the space environment forecast input to the ISS charging model indicates floating potentials (FP) within specified limits. These recommendations were based on the persistence of conditions in the space environment due to the current low solar cycle and belief in the accuracy and completeness of the ISS charging model. Subsequently, a Noncompliance Report (NCR), ISS-NCR-232G, *Lack of Two-fault Tolerance to EVA Crew Shock in the Low Earth Orbit Plasma Environment*, was signed in September 2013 specifying new guidelines for the use of shock hazard controls based on a forecast of the space environment from ISS plasma measurements taken prior to the EVA [ISS-EVA-312-AC, 2012].

This NESC assessment re-evaluates EVA charging hazards through a process that is based on over 14 years of ISS operations, charging measurements, laboratory tests, EMU studies and modifications, and safety reports. The assessment seeks an objective review of the plasma charging hazards associated with EVA operations to determine if any of the present hazard controls can safely change the PCU utilization plan to allow more flexibility in ISS operations during EVA preparation and execution.

The following approach was used:

1) Review shock hazard-related data as provided in the measurements from the floating potential measuring unit (FPMU) aboard the spacecraft and other ISSP sources.
2) Compare the ISS charging model output versus FPMU measurement.
3) Review existing ISS documentation related to shock hazards and controls.
4) Provide preliminary analysis and data observations related to the shock hazard severity, available controls, and forecast tool capabilities.

The NESC recommends continuing the catastrophic hazard assumption and the use of three controls for the typical two-fault tolerant hazard control during all EVAs regardless of FP predictions or EVA location. These recommendations include the use of the two PCUs in discharge for EVAs and propose the ISS/EVA team evaluate the use of the low probability of contact (which includes the isolation features in the ISS-suit-crew path) as the third control while discontinuing the use of the solar array wing shunt fault detection, isolation and recovery (FDIR). In addition, it is recommended that the Plasma Interaction Model version 3 (PIM3.0) "predictions" (i.e., forecast) be constrained to planning purposes and not be used to determine the use of active hazard controls. Refer to Appendix I for a Summary of Key Points from this assessment.

The NESC team's work in this report considers the positive charging hazard to EVA crew and assumes a single galvanic contact case the team deemed most concerning. Other contact cases might result in higher current collection. However, those require multiple simultaneous galvanic contacts and therefore these were considered worst-on-worst, hence overly conservative.

At the completion of this report, the requester specifically asked that the team go back and evaluate this worst current collection case regardless of the additional conditions for the situation to arise. Appendix K provides the current collection of individual pieces of the system that might contribute and can be used to consider randomly generated cases, including the multiple galvanic contact cases previously considered overly conservative. The ISS Program can use this data to assess severity of the individual contact cases, and coupled with accurate probabilistic risk assessment (PRA), determine quantitatively, which is the driving risk case based on the product of severity and likelihood.

5.0 Assessment Plan

This assessment started with the assembly of a team that included plasma physicists, space environment scientists, EVA safety specialists, medical team specialists, system engineers, power system engineers, and administrative support.

The plan was divided (according to the request) into three main re-phrased questions:

(1) Is it acceptable for PCUs to be off during EVAs?
(2) Can the FDIR be disabled if two PCUs are in discharge?
(3) Is it acceptable to conduct an EVA without active shock hazard controls?

Several key documents and presentations related to the use of controls and environment "forecasting" were reviewed to understand the hazard and available controls and guidelines. For example, these included the ISS-EVA-312-AC (1/26/2012): *Electric Shock to EVA Crew Resulting from EMU Arcing in Plasma* [ISS-EVA-312-AC, 2012]; the ISS-NCR-232F (1/26/2012): *Lack of Two-fault Tolerance to EVA Crew Shock in the Low Earth Orbit Plasma Environment* [ISS-NCR-232F, 2012] and the ISS-NCR-232G (9/2013) [ISS-NCR-232G, 2013]. Data from the FPMU, International Reference Ionosphere (IRI), and calculations from the PIM3.0 were reviewed to understand the forecast limitations and the types of charging events at the ISS. The known magnitudes of these charging events and the ISS FP levels were considered in the assessment.

Documents were reviewed and direct communication was established with ISS power engineering to understand the FDIR basic functionality. Data related to charging events due to shunting or unshunting solar arrays were considered. Alternatives to the use of the FDIR were considered based on the shock hazard severity, the likelihood of completing an electrical circuit current path, possible conditions affecting the ISS power positive state during the FDIR use, and available information related to the validation of the process.

The following is an outline of the assessment plan:

1. Basis of PCU as a control
    i. Proposed forecast adequacy to determine PCU control utilization review hazards [ISS-EVA-312-AC, 2012]
    ii. Review the forecasting process
        1. Sources
        2. Limits
        3. Proposed changes
    iii. Review of PIM3.0 charging model adequacy for forecasting
        1. Prediction capabilities
        2. Error bars
        3. Accuracy of prediction for the FP
            a. Magnitude of values
            b. Forecast time length: Can it accurately predict 2 to 3 or up to 14 days?

            c. What boundaries shall be in place based on what can and cannot be predicted?
        iv. FPMU role and criticality
        v. Review assumptions for the probabilistic risk assessment (PRA)
2. Evaluate the FDIR
    i. Two-fault tolerance requirement
        1. Two operational PCUs are considered single fault tolerant
        2. For two-fault tolerance the ISS-NCR-232F list the two PCUs and have the FDIR (solar array shunt control algorithm) as third control
    ii. Risks
        1. Is there a risk to the ISS power configuration?
        2. Are there risks of large negative events with the array shunting?
        3. How reliable is the system? Is it programmed for every EVA?
        4. Severity of hazard if one PCU fails
3. Hazard controls marginalization
    i. Recommended analyses
        1. Worst-case positive and negative potentials
        2. How much electrical circuit path current collection is realistic for a positive EMU charging?
            a. Compare to medical limits
        3. Evaluate charging events
            a. Eclipse exit normal charging
            b. Eclipse exit rapid charging event
            c. Auroral charging
            d. Array unshunt in sunlight

The NESC team did not evaluate the EMU systems (i.e., electrical systems and instruments) to understand their susceptibility to the assessment hazards. In addition, the analysis in this assessment focused on the present ISS configuration and did not attempt to address the effects of possible configuration changes (e.g., future Russian solar arrays).

6.0 Problem Description and Proposed Solutions

6.1 Problem Description Summary

The ISS vehicle undergoes spacecraft charging as it interacts with Earth's ionosphere and magnetic field. The interaction can result in a large potential difference developing between the ISS metal chassis and the local ionosphere plasma environment. If an astronaut conducting an EVA is exposed to the potential difference, then a possible electrical shock hazard arises.

This assessment evaluated the approach and methodology adopted by the ISSP, which relies on modeling to determine if hazardous charging conditions exists. The modeling was contrasted with the use of active charge mitigation devices (i.e., PCUs), which are in place on the ISS and directly limit the potential difference between the ISS and the ionosphere plasma when they are operational.

6.2 Background Information

6.2.1 ISS and the Ionosphere/Plasma Environment

The ISS orbits the Earth at an altitude of approximately 400 km. In this orbit, the ISS is continually moving through Earth's ionosphere and magnetic field. The ionosphere, which is a plasma environment, is made up of a superheated gas in which the neutral atoms are converted into charged particles via ionization. The principle constituents of the ionosphere plasma are electrons (i.e., negatively charged particles) and oxygen ions (positively charged particles). Since the ionosphere plasma is comprised of charged particles, the interaction with the ISS can occur because of direct collisions or as a result of electrostatic attraction/repulsion. As opposite charges attract (e.g., positive attracts negative), like charges repel (e.g., positive repels positive). An example of electrostatic attraction of charged particles is the solar arrays on the ISS. The solar arrays are made up of silicon solar cells with an exposed edge. When illuminated by sunlight, the cells produce electrical power and achieve a positive voltage. Electrons in the plasma near a solar cell will be pulled towards the solar cell due to electrostatic attraction. Some fraction of the electrons attracted to the cell will be collected by the cell (since it is an electrical semi-conductor) and result in spacecraft charging.

6.2.2 ISS Power System and Spacecraft Charging

The ISS power system was electrically configured as a negative ground system. To understand this configuration, a solar array can be treated as a simple battery. The negative terminal of this "battery" is connected to the ISS aluminum (Al) structure (or chassis) and the positive terminal is immersed in the ionosphere plasma. Accordingly, if electrons in the plasma are collected by a positively biased solar cell, they will ultimately accumulate on the ISS chassis as part of the negative ground power system arrangement. To characterize the amount of charge that might accumulate on the ISS chassis, an electrical reference point must be defined. On Earth's surface, this reference point is Earth Ground. For the ISS, it is not practical to use Earth Ground as a reference. Instead, it is easier to choose the local plasma environment around the vehicle as the electrical reference point or "plasma ground." Using this convention, the potential difference (voltage) that develops between the ISS chassis and the local plasma can be described. In the scenario where the solar cells collect electrons, which end up on the ISS chassis, a negative voltage developing on the chassis with respect to the local plasma can be described.

6.2.3 Charged Particle Collection: Ions, Electrons, and FP

A corollary to the electron collection scenario is ion collection. Exposed metal surfaces on the ISS chassis that are negatively biased with respect to the local plasma can collect ions (i.e., positive charges). In the spacecraft-charging arena, it is understood that equilibrium potential must be arrived at where the ion current collection balances the electron current collection. Known as the FP, it is dependent on the amount of ion collection area, the electron collection area, and the mass and energy of the electrons and ions in the plasma. For the ionosphere plasma, the ions are massive compared to the electrons and the ions have very little thermal energy. Ions are mostly collected as a result of the ISS colliding with them – which is called RAM collection. The electrons, however, are very light and have a modest thermal energy, so they interact with all the surfaces on the ISS and can be easily collected by positively biased conductive (or semi-conductive) surfaces. Combining all of these factors, one finds that the typical equilibrium FP of the ISS chassis is a negative potential.

6.2.4 Mitigating ISS Spacecraft Charging – PCUs

When the design decision was made to use high-voltage (+160 volts (V)) solar arrays on the ISS, scientists and engineers familiar with the ionosphere plasma environment predicted that the ISS would experience significant spacecraft charging. To limit the ISS chassis charging due to solar array electron current collection, the spacecraft charging design team in the early 1990s recommended the use of PCUs. The PCUs would act as an effective "ground strap" to the local plasma. The PCUs operate by creating a plasma bridge between the ISS chassis and the ionosphere plasma. They move the excess charge accumulated on the ISS chassis back into the ionosphere, thereby minimizing any spacecraft charging. Thus, the ISSP developed and deployed two robustly designed PCUs. Each PCU was rated to continuously emit as much as 10 amps of accumulated charge back into the ionosphere and respond to changes in the ISS current collection in a fraction of a second. The PCUs were designed and verified such that ISS chassis potential would never go more negative than −40V when the PCUs were operating.

6.2.5 Potentials Generated by Magnetic Induction

Charging on the ISS chassis is actually a combination of current collection by charged surfaces (described above) and induced potentials created by magnetic induction. The magnetic induction occurs as a result of the long metallic ISS truss structure moving through field lines in the Earth's magnetic field. Like a wire in a conventional electric generator, the ISS develops a potential difference (voltage) across its length as it moves through a magnetic field. The formula that governs the induction voltage is $\varepsilon_{induced} = \mathbf{v} \times \mathbf{B} \bullet \mathbf{L}$, where **v** is the spacecraft velocity vector, |**B**| is the magnetic field strength, and |**L**| is the length of the conductor. This equation is actually a vector equation, which means that the orientation of the conductor with respect to the magnetic field is important. Often referred to by the shorthand "v cross B", the magnetic induction potential can have a net magnitude as high as about 38V (see Appendix G) measured from truss tip to truss tip. Thus, the potential that is created by magnetic induction ($\mathbf{v} \times \mathbf{B} \bullet \mathbf{L}$) across the ISS is a function of position along the truss.

6.2.6 Insulating Surfaces, Anodized Components, and Capacitors

Like most other spacecraft, the ISS is made up of a wide variety of materials, including electrically conductive and electrically insulating materials. When electrically insulating materials or dielectric materials are exposed to the ionosphere plasma environment, their surface can become electrically charged. An important example of an insulating material charging on the ISS is the case of the micrometeoroid and orbital debris (MMOD) shields. The MMOD shields are anodized Al. The anodizing process creates a significant thin oxide layer on the Al surface (for corrosion protection). The Al metal is a good electrical conductor, the anodization layer, however, is a good electrical insulator (dielectric). The MMOD shields form the outer surface of the ISS pressurized modules. The Al metal in the MMOD shields is attached to the chassis and the oxide layer (anodized coating) is exposed to the ionosphere plasma. This arrangement can be described in electrical circuitry terms as a parallel plate capacitor.

Recall that a parallel plate capacitor is a device made up of two electrically conductive plates separated by a dielectric material. To characterize the MMOD shields as a capacitor: one of the capacitor plates is the Al metal, the dielectric material between plates is the anodization layer, and the other "plate" is the plasma. Given the large amount of surface area associated with the MMOD shields and the significant thin anodization layer, it turns out that the capacitance of the ISS modules can be quite large – on the order of milli-Farads [Carruth, 2001].

Three important features of capacitors are:

1. Charge Storage – a large capacitance translates to a capacity to store a large amount of charge.
2. Direct Current (DC) Blockage – only changing or pulsed currents can pass through a capacitor.
3. Pulse Discharge – shorting across the plates of a charged capacitor or dielectric breakdown can produce a large pulse of current out of the capacitor.

Given the large capacitance of the ISS MMOD debris shields, it can be expected that a great deal of charge can be stored and, in turn, sourced as a large current pulse when the capacitor terminals are shorted. An electrical arc across a capacitance is equivalent to shorting the capacitor with a switch.

Of the many external surfaces on ISS that can be characterized as capacitors, three areas figure prominently in this assessment: 1) the main ISS structure capacitance associated with the MMOD shields, 2) the solar array capacitance, and 3) the EMU capacitance. It should be noted that the capacitance associated with the MMOD shields is very large compared to the solar array and EMU capacitances.

Reference:

1. Carruth, Jr., M.R., et al. (2001): "ISS and Space Environment Interactions without Operating Plasma Contactor," AIAA-2001-401, *Aerospace Sciences Meeting and Exhibit, 39th,* Reno, Nevada, January 9-11, 2001.

6.3 Detailed Problem Description

6.3.1 ISS Charging

The conditions that generate a plasma hazard on ISS arise when a difference in potential develops between the ISS chassis and the surrounding ionosphere plasma, which is the defined electrical reference point. The two sources that create this potential difference (voltage) are: (1) electron current collection on the high voltage (+160V) solar arrays which drives the ISS chassis to negative potentials, and (2) the magnetic induction voltage generated across the long truss structure as it moves through the Earth's magnetic field.

The electron collection on the solar array occurs when the solar array is illuminated by sunlight and connected to the power system. The array output can be short-circuited through an operation known as shunting. If an array is shunted, the electron current collection from the plasma does not charge the ISS chassis since it is also short-circuited. The magnetic induction voltage generated across the length of the truss changes depending on the orientation of the truss to the magnetic field.

6.3.2 Plasma Shock Hazard for EVA Astronauts

The plasma hazard occurs when an astronaut conducting EVAs is exposed to the potential difference between ISS and the local plasma as a result of an electrical connection being made to the EMU (spacesuit). The magnitude and the nature of the hazard condition are dependent on the astronaut's location along the vehicle as well as some vehicle operations (e.g., PCU on/off, solar array state, etc.). Figure 6.3-1 provides a pictorial representation of the ISS spacecraft charging that results from solar array current collection and magnetic induction (i.e., **v × B • L**). Figure 6.3-1 shows that the **v × B • L** voltage is distributed along the truss such that one end of the truss can be at a more positive voltage than the other end.

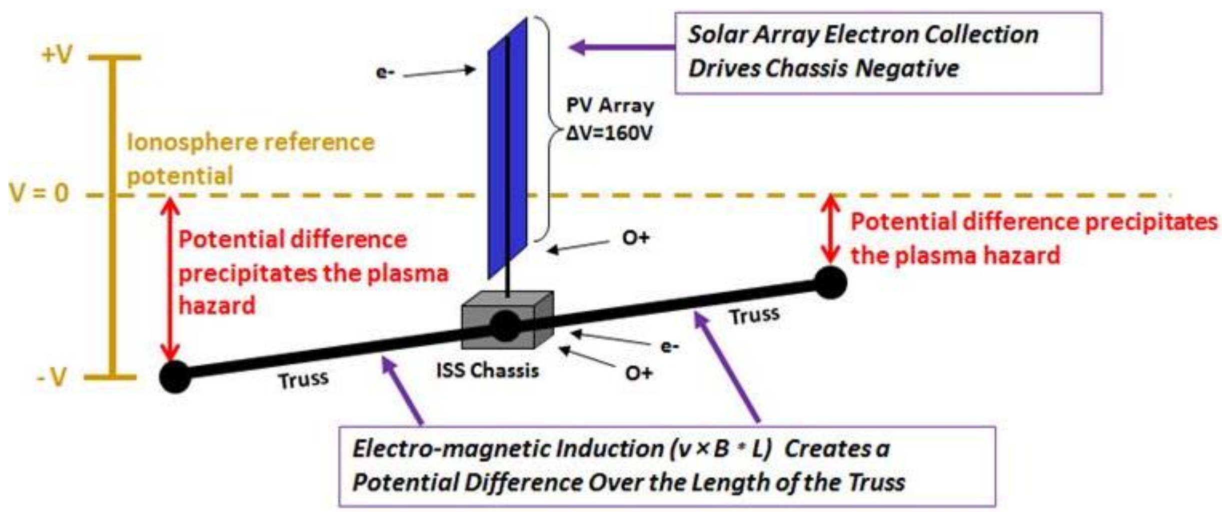

Figure 6.3-1. ISS Potential with Respect to the Local Ionosphere Plasma. The ISS potential is a combination of solar array current collection and magnetic induction (or v × B • L).

6.3.3 PCUs

To dramatically reduce the negative charging that occurs on the ISS chassis due to solar array electron collection, the PCU was developed for the ISS. The PCU acts as an effective "ground strap" to the local plasma. The purpose of this device is to mitigate the negative charging hazard by returning excess charge accumulated on the ISS chassis back to the ionosphere plasma. This provides mitigation to the negative FP hazard by keeping the station chassis potential more positive than −40V. There are two independently powered and controlled PCU systems installed on the ISS and together they provide a single-fault tolerant control against the negative FP hazard (Figure 6.3-2). A third unit is in storage at the ISS. For operational description of the PCU, see Appendix H for reference to Section 2.3.4 of the *International Space Station Electrical Power Systems Training Manual ISS EPS TM 21109* [Anon., 2004].

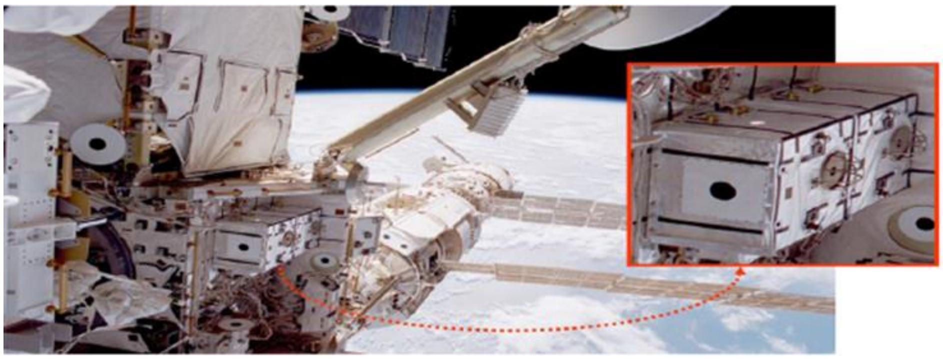

Figure 6.3-2. PCU Installed on ISS (Source: NASA)

Reference:

1. Anon. (2004): ISS Electrical Power Systems Training Manual, ISS EPS TM 21109, Mission Operations Directorate, Space Flight Training Division, NASA Johnson Space Center, 2004.

6.3.4 Hazard Classification and Protection Systems

Given that the plasma hazard is an electrical shock hazard for an EVA astronaut, it has been classified as a catastrophic hazard. In this classification, a two-fault tolerant hazard control must be employed. To meet the two-fault tolerant requirement, the ISSP has employed two PCUs and an automatic array shunting algorithm referred to here as solar array shunt FDIR, or just FDIR. The solar array FDIR algorithm is enabled after the two PCUs are in discharge. If the FDIR detects that one of the two PCUs have failed, the algorithm will shunt solar arrays (refer to the B9-908 document, "Plasma Hazard Mitigation during EVA"). Appendix F provides information received from the electrical power system (EPS) hardware operator in relation to the FDIR. To support the ISS power demands, ground commands to unshunt the arrays may occur any time, in or out of sunlight. However, to reduce the RAM electrical current collection, the commands are issued after the corresponding array is off-pointed from the velocity vector by >105 degrees. No more than two arrays can be unshunted and auto-tracked while being less than 105 degrees from the velocity vector.

The EVA pre-planning efforts involve a short-term forecast where environment measurements are taken 14 days prior to the EVA (per ISS-NCR-232G). The ionosphere plasma environment measurements are made with the FPMU. The PCUs are off when the FPMU measurements are made so corresponding ISS potentials are indicative of the conditions uncontrolled by the PCUs. Calculations of the ISS chassis potential are made by using FPMU data in the empirical model PIM3.0. Configurations of the solar arrays resulting in calculated FPs more positive than −40V are acceptable and within the limits. In the event of a PCU failure, if the solar array management necessary to maintain the ISS in a "power positive" mode produces a chassis potential more negative than −40V, then additional safety risk will be accepted up to the level of −45.5V. The hazard limit for the negative potential was set as −40V [ISS-EVA-312-AC, 2012]. However, side notes included on the ISS-provided overview presentations suggest an increased risk acceptance level for arc occurrence has been established to tolerate potentials as negative as −45.5V (1/14/2009 ISS Safety Review Panel (SRP)). However, the rationale for this move has not been documented in any reference this team has uncovered.

Reference:

1. ISS-EVA-312-AC (2012): *Electric Shock to EVA Crew Resulting from EMU Arcing in Plasma*, 1/26/2012.

6.3.5 FPMU

The FPMU is a multi-probe instrument designed to measure: (1) FP, (2) plasma density, and (3) electron temperature from the ISS local ionospheric environment (see Figure 6.3-3). Refer to Figure 6.3-4 for the location of the PCUs and FPMU through the ISS assembly. The FPMU was installed with the goal to use its data for refinement and validation of the ISS spacecraft charging models and to determine the severity and frequency of ISS charging events.

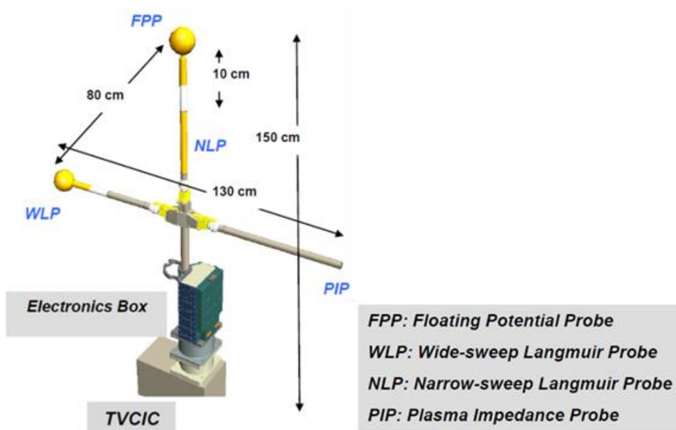

Figure 6.3-3. FPMU Probes and Layout

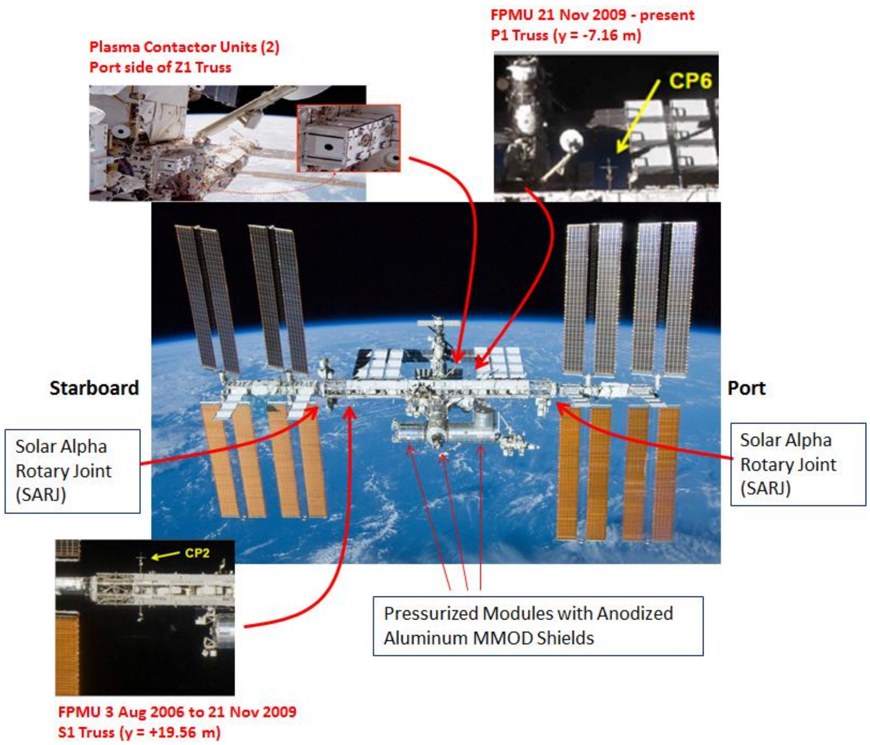

Figure 6.3-4. Location of the PCUs and the FPMU at the ISS. The FPMU has been in two different locations on ISS over the course of its lifetime.

Reference:

1. Wright, et al. (2008): "Charging of the ISS as Observed by the FPMU: Initial Results," *IEEE Transactions on Plasma Science*, Vol. 36, No. 5, October 2008.

6.3.6 PIM3.0 Charging Model

The initial PIM charging model was developed by Science Applications International Corporation and Boeing Space Environments and is currently maintained by Boeing Space Environments. The latest revision of the PIM3.0 is used to calculate the ISS chassis potential and includes various processes such as: 1) the magnetic induction potentials due to motion of the vehicle through the Earth's geomagnetic field; 2) the charging due to solar array and other current collection processes from the ionosphere plasma; and 3) PCU effects. Figure 6.3-5 shows examples of the calculated potentials on the ISS using the PIM3.0 model. Figure 6.3-5 also shows that the use of PCUs affects the potential distribution across the vehicle. Figure 6.3-6 shows the effectiveness of the PCU at controlling the chassis potential (i.e., potentials with PCU on versus potentials with PCU off). The PCUs keep the ISS within the −40V limit when the PCUs are in discharge.

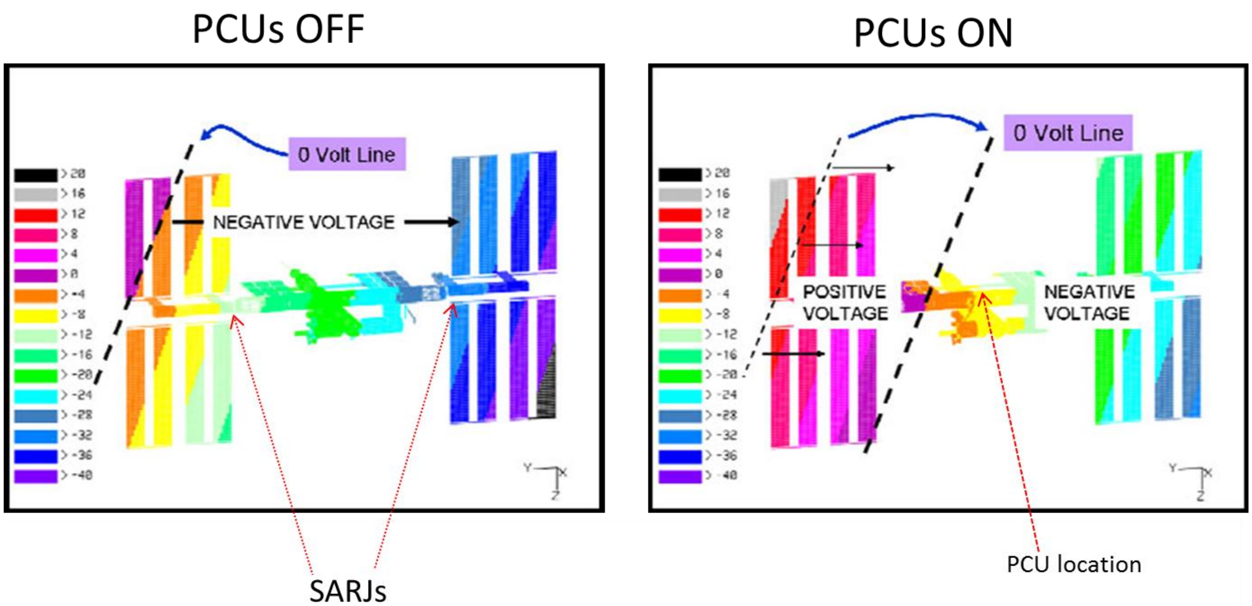

Figure 6.3-5. 2010 Comparison of Potential Calculations with PCUs On and Off [Kramer, et al., 2010]

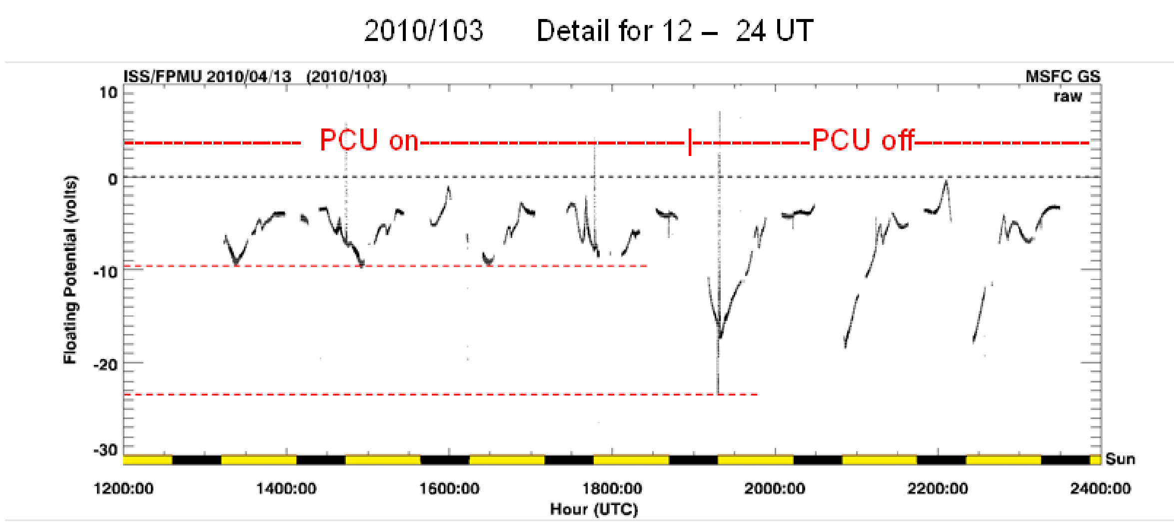

Figure 6.3-6. Example of FPMU Data showing the Effect on the Peak Chassis Potential (i.e., FP) when the PCUs are On and Off

Reference:

1. Kramer, L.; Hamilton, D.; Mikatarian R.; Thomas J.; and Koontz, S. (2010): "Positive Voltage Hazard to EMU Crewman from Currents through Plasma," *Proc. 4th IAASS Conference 'Making Safety Matter'*, Huntsville, Alabama, USA, 19–21 May 2010 (ESA SP-680, September 2010).

6.3.7 Electrical Shock Hazard Scenarios

The electrical shock hazard associated with EVAs is based on a situation in which an electrical circuit is established that could inject an electrical current into a crew member inside an EMU. Critical to the establishment of a shock hazard is the fact that EMU crew members wear a cooling garment against their skin, which quickly becomes soaked in perspiration as an EVA commences. The close confines of the EMU, combined with the layer of perspiration that covers the crew member's body, results in a situation where there is electrical contact between the crew member and the metal components used at several locations in the EMU construction. Thus, if electrical current flows through an EMU, there will be a parallel path through the crew member's body, which represents a hazardous situation for the crew member (i.e., a shock hazard). The severity of this hazard ranges from a small shock on the skin that causes the astronaut to be startled, to a catastrophic situation in which current flows through the astronaut's thoracic cavity and causes defibrillation or arrest of the heart (see Appendices A and B).

Two charging scenarios on the ISS must be assessed to determine if they give rise to an electrical shock hazard:

1) Negative charging
2) Positive charging

Given that astronaut safety is at stake, the most conservative approach is taken to assess the electrical circuit associated with each charging scenario. Specifically, the circuit that is evaluated is the one that can lead to electrical current flow through the astronaut's thoracic cavity. This circuit is created when current enters a lower portion of the EMU (i.e., the waist area), and then flows through crew member's body and exits at a point in the upper portion of the EMU (e.g., the neck area).

6.3.8 Hazard Circuit Associated with Negative Charging

In the case of a negative charge being applied to the EMU, the hazard that arises is from current flow due to an electrical discharge (arc) on an anodized Al component somewhere on the EMU. With a crew member in a perspiration-soaked garment that is in electrical contact with portions of the EMU, as current flows through the EMU to an arc site, a portion of the current can flow through the crew member's body. The arcing scenario associated with negative potentials on the ISS and applied to the EMU can be visualized in Figures 6.3-7a through 6.3-7e. The choice to separate the negative charging hazard circuit into several circuit diagrams was made to not only illustrate how the situation develops, but to also indicate that multiple events must occur simultaneously in order for the actual hazard to be created.

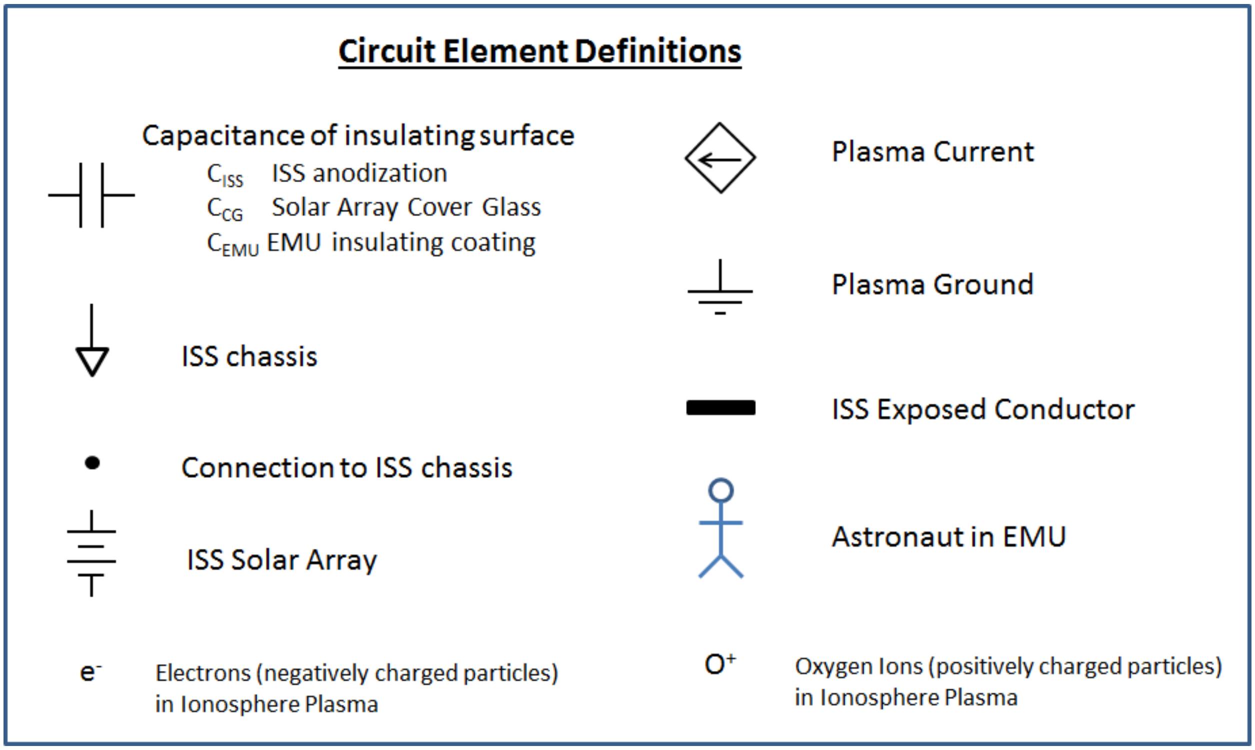

Figure 6.3-7a. Circuit Element Definitions used in Circuits #1, #1a, #2, and #3 (below)

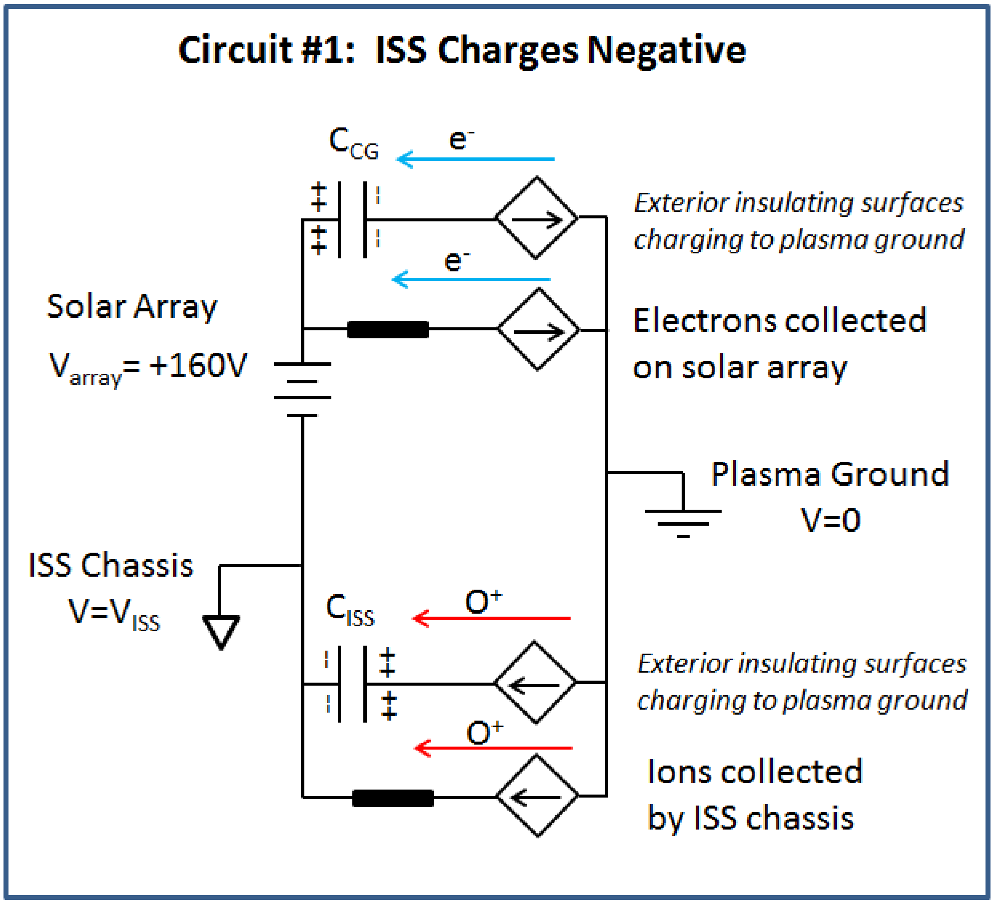

Figure 6.3-7b. Circuit Diagram showing Solar Array Current Collection and related Charging of the ISS. In steady state, the ISS chassis potential (or FP) adjusts to achieve current balance, such that the Ion Current = Electron Current.

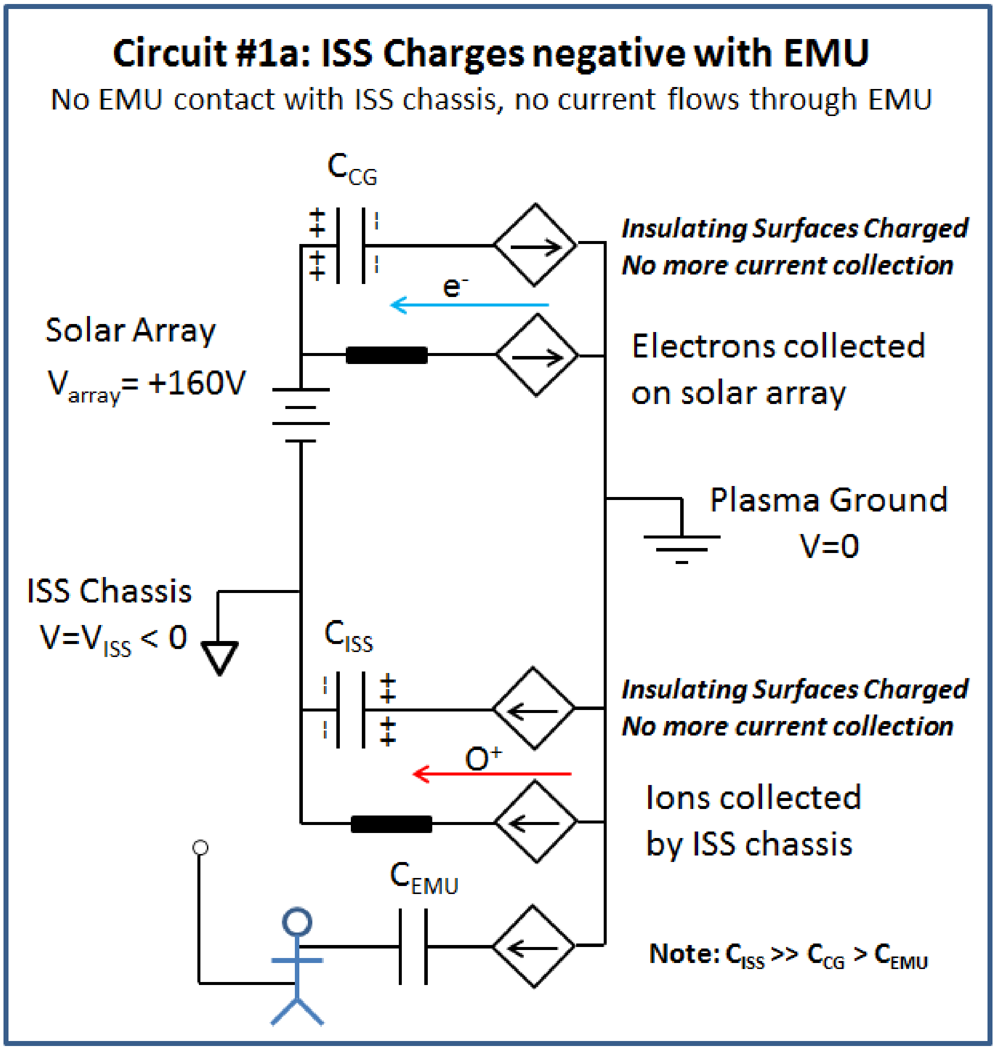

Figure 6.3-7c. Circuit Diagram showing the Scenario where an EVA is being Conducted. There is no direct electrical connection between the charged ISS chassis and the EMU (space suit).

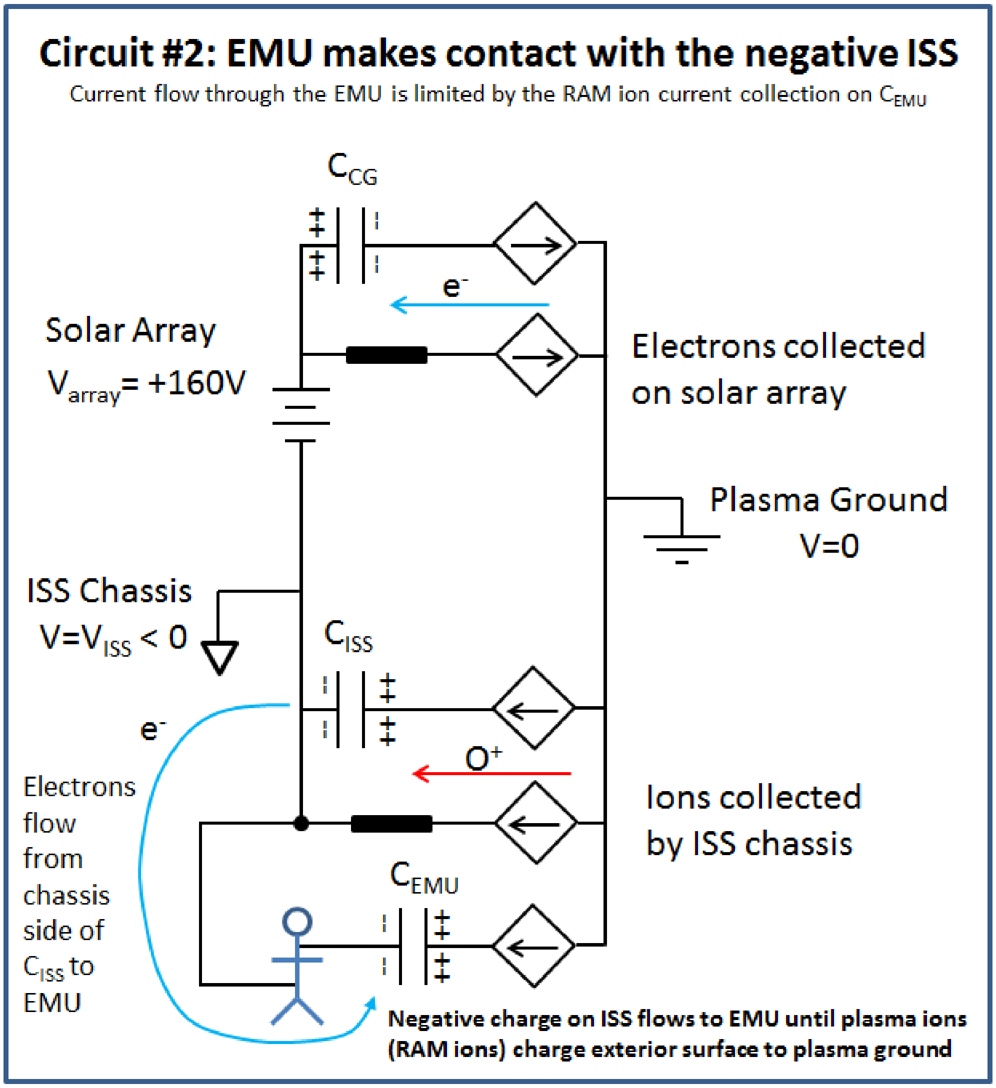

Figure 6.3-7d. Circuit diagram showing the scenario where a direct electrical connection is established between the charged ISS chassis and the EMU (space suit). In this situation, there is a small electron current that flows from the ISS chassis to the EMU. Only a small amount of electron current flows to the EMU due to limitations in RAM ion current collection on C_{EMU}.

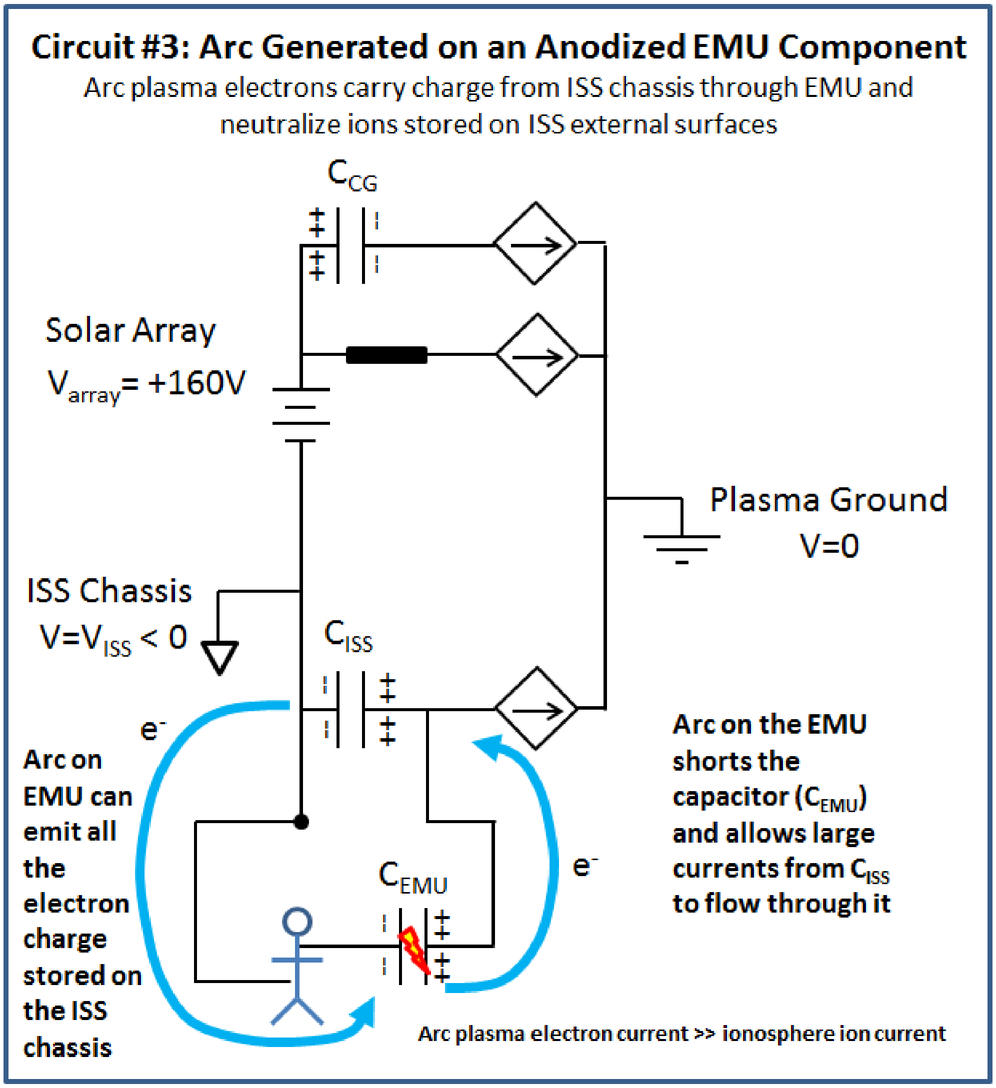

Figure 6.3-7e. Circuit diagram showing the scenario where an arc occurs on an anodized component of the EMU (space suit). A large current of electrons flows through the EMU to the arc site. With a crew member inside a perspiration-soaked garment in the EMU, there is electrical contact between the crew member and various EMU metal components. Current flowing to the arc site can follow a parallel path through the crewmember. Arc current magnitude can exceed 10 amps as electrons in the arc plasma neutralize nearby anodized surfaces on the ISS vehicle (one side of C_{ISS}). If a fraction of the arc current flows through the crew member, a significant hazard occurs. The source of the large arc current is the C_{ISS}, which is a very large capacitor.

Summary – Negative Charging Hazard

The shock hazard associated with negative charging on the ISS vehicle is by a situation in which an electrical discharge (arc) forms on an EMU component. The simple application of a negative charge on the EMU does not create a hazard. The application of a negative charge on the EMU must result in an arc occurring before the hazardous situation arises. The crew member in an EMU is inside a perspiration-soaked garment, which provides electrical contact between the crew member's body and metal components that make up the EMU. Therefore, if current flows in an EMU due to an arc occurring on an external component, the crew member's body may be subjected to current flow as it represents a parallel path for a portion of the arc current.

The formation of an arc on an EMU requires the simultaneous occurrence of multiple events, which means the likelihood of an arc occurring is very low. As depicted in Figures 6.3-7a through 6.3-7e, for an arc to occur on an EMU, the following must happen:

1) The ISS vehicle must experience spacecraft charging to negative potentials, as shown in Figure 6.3-7b.
2) A bare metal component on an EMU must make electrical contact with a bare metal component on the ISS chassis. This situation is shown in Figure 6.3-7d.
3) Anodized Al components on the EMU must develop a potential difference across their anodization (oxide) layers (i.e., negative charge on the surface against the Al metal and positive charge on the surface exposed to the plasma). In Figure 6.3-7d, the potential across the anodization layer is represented by the electrical charges on the element "C_{EMU}."
4) An anodization (oxide) layer must breakdown and generate an arc. In Figure 6.3-7e, the arc on an anodized component is shown as the lightning bolt across the element "C_{EMU}."
5) Charge from the ISS vehicle must flow through the EMU to the arc site – which means the EMU must remain electrically connected to the ISS chassis throughout the charging and arcing process. In Figure 6.3-7e, the large current through the arc site is provided by the capacitance of the ISS vehicle represented by "C_{ISS}."

If such a set of events were to occur, and an arc was generated on an EMU, the astronaut inside the EMU would most likely experience an electrical shock as electric charges move from the ISS chassis through the EMU into the arc site and return to the local plasma environment. With the crew member in electrical contact with EMU metal components, due to the perspiration-soaked garment covering the crew member's body, some of the arc current can split into the parallel path created by the crew member's body. Because the United States (U.S.) modules on the ISS are constructed in a manner that results in a large effective capacitance, the magnitude of current flow (charge movement) through an EMU arc site is possibly very large (>10 amps). If only a small fraction of the arc current goes through the crew member's body, a potentially catastrophic situation can be created.

A key to all electrical shock hazards associated with the EMU is that bare metal on the EMU must make electrical contact with bare metal on the ISS vehicle in order to charge the EMU. Due to the nature of the construction of the EMU and ISS vehicle, it is very unlikely that an electrical contact can be established, let alone maintained, for the time period required to establish a hazardous charging situation (negative or positive).

6.3.9 Hazard Circuit Associated with Positive Charging

A crew member inside an EMU is in electrical contact with the metal surfaces in the EMU because the crew member's body is covered in a perspiration-soaked garment (the liquid cooling and ventilation garment (LCVG)). The crew member can, therefore, become part of an electrical circuit in which current can flow and a shock can be delivered. In the case of the negative charging hazard (described in Section 6.3.8), an arc generates the hazardous situation. In the case of positive charging of the EMU, current flow in the EMU (and the crew member's body), can occur as the capacitance of the EMU is charged by electron current from the local plasma. A bare metal component on the EMU must contact a bare metal component on a positively charged section of the ISS vehicle. In this scenario, the EMU metallic structure becomes positively charged and electrons are attracted to the external surfaces of the EMU. Anodized components of the EMU act as capacitors and can be collectively treated as a single capacitance "C_{EMU}." It is possible that as the capacitance of the EMU charges due to electron current from the plasma, the crew member's body, that is part of the EMU circuit, will be impacted by the current flow. The positive charging hazard, therefore, is initiated when the EMU metallic structure charges to positive potentials with respect to the local plasma.

While the PCUs are in discharge, the ISS is grounded close to the center of the station where the units are located. At precisely the PCU location, the potential is around −10V since there is a 10V drop across the device. The difference in potential across the truss due to $\mathbf{v} \times \mathbf{B} \cdot \mathbf{L}$ is on the order of ~38V. With the PCUs on, a maximum positive potential is on the order of 10V (accounting for the PCU potential drop) can be seen as the calculated FP in Figure 6.3-5. Considering the positive potential electrical current path (Figure 6.3-8), the hazard is from the electron current collection during charging of the EMU capacitance (i.e., the capacitance due to external anodized components). The plasma impedance for collecting electrons when the potential is positive is high, thus limiting the electrical current in the path. This current lasts on the order of 1 microsecond (ms) and it is in the order of 1 milliampere (mA). See Section 7.10 of this report for details. The hazard control documents ISS-EVA-312-AC and the ISS-NCR-232F/G do not specify a positive potential or electrical current collection limit. References to electrical current threshold for human reaction can be found in Appendices A and B of this report.

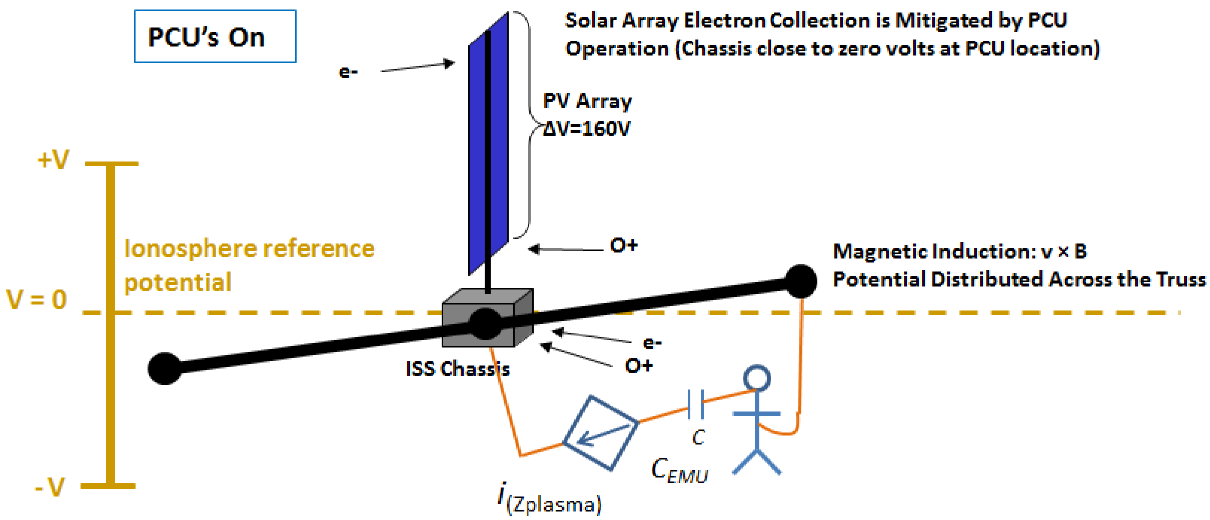

Figure 6.3-8. Positive Potential Electrical Current Path through the Crew Member. Note the crew member's body can become part of the electrical circuit due to contact of the perspiration-soaked cooling garment covering the crew member with internal metal structures in the EMU.

6.3.10 Shock Hazard Probabilities

The probability of a shock hazard developing during an EVA involves the probability of large chassis potentials developing combined with the probability of completing the electrical current path through the EMU. The ISS Probabilistic Risk Assessment for Shock Hazard, ISS-PRA-12-56 (May 17, 2013), lists the simultaneous events for a shock hazard to occur and reports the probability as 6.72E-06, which can be improved to 9.44E-08 with additional isolation to the operational bioinstrumentation system (OBS).

Fundamental to the establishment of both the negative and positive shock hazard circuit are the following two conditions:

1) The crew member's body must be in electrical contact with exposed metal inside the EMU at two separate locations.
2) An electrical connection must be made between ISS structure and the EMU (i.e., exposed metal on the exterior of the vehicle must connect to/touch exposed metal on an exterior surface of the EMU).

With respect to the first condition, the crew member's body is covered with a LCVG, which quickly becomes soaked with perspiration as an EVA begins. The wet LCVG increases the likelihood of electrical contact between the crew member's body and metal components on the interior of the EMU. Figure 6.3-9 shows the locations of possible metal contact in the EMU suit.

Electrical connection between exterior bare metal surfaces on the ISS vehicle and the EMU is a low probability condition due to the prolific use of anodized Al on both the vehicle and the EMU. (Recall that anodized coatings are electrically insulating). To further decrease the probability of bare metal contact between the exterior surfaces on the vehicle and the EMU, isolation features were implemented (circa 2009) into the EMU's Modular Mini Workstation (MMWS) exposed metal (refer to ISS-NCR-232F, Attachment 7 and Appendix D). Kapton® film was placed between the Al baseplate and the stainless steel receptacles (Figure 6.3-10) and hard anodized washers were used to isolate conductive paths through the fasteners. These modifications were validated through ground testing [Castillo, 2010], which included isolation and mechanical stress tests.

Figure 6.3-9. EMU Suit External Metal Locations [ISS-NCR-232F Attachment 5, 2012]

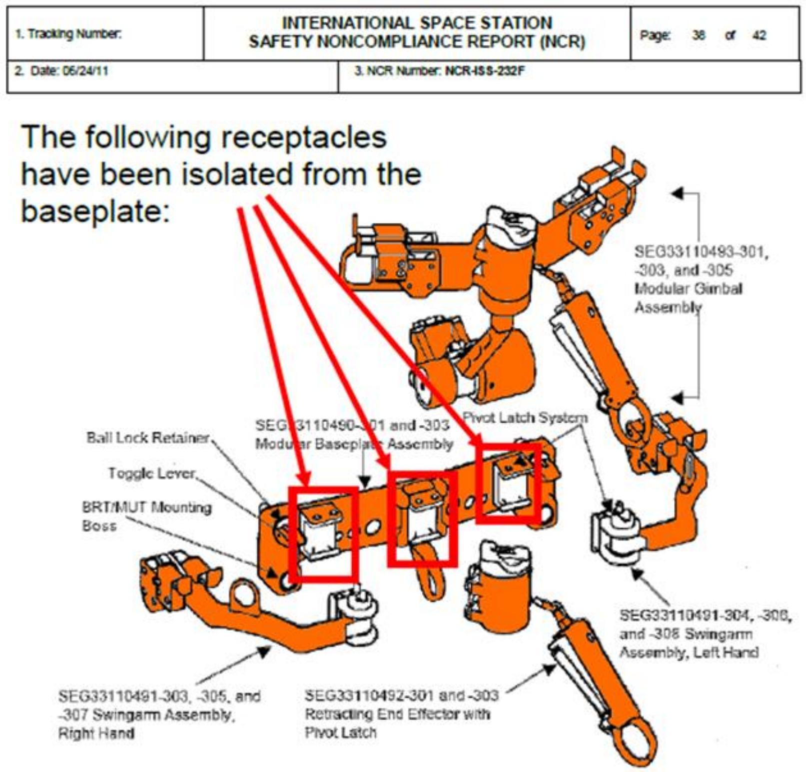

Figure 6.3-10. Modifications to the MMWS ("tool belt") [ISS-NCR-232F, Attachments 5 and 7, 2012]

References:

1. Castillo, M. (2010): *Modular Baseplate Assembly/Body Restraint Tether/Handrail Electrical Continuity Test*, dtd. 05/04/10.
2. ISS-NCR-232F (2012): Lack of Two-fault Tolerance to EVA Crew Shock in the Low Earth Orbit Plasma Environment, 1/31/2012. Attachment 5.
3. ISS-NCR-232F (2012): Lack of Two-fault Tolerance to EVA Crew Shock in the Low Earth Orbit Plasma Environment, 1/31/2012. Attachments 5 and 7.

6.3.11 Approach to EVAs Without a Two-Fault Tolerant Hazard Control

The negative potential limits and hazard controls discussed so far are referenced in the ISS-NCR-232F. This version of the "*Lack of Two-fault Tolerance to EVA Crew Shock in the Low Earth Orbit Plasma Environment*" document was the active hazard control guidelines at the start of this assessment. However, on September 2013, a new version, G, of the document was signed. Figure 6.3-11 summarizes the differences between the two guidelines as well as the recommendations from this assessment relative to the controls. In summary, the new guidelines (1) extends the "short-term" forecast to 14 days prior to an EVA, (2) updates the FP risk acceptance limit to −45.5V, and (3) provides guidelines for the use of controls based on the 14-day FP calculations from the forecast. The extension of the forecast based on the environment measurements taken 14 days prior to the EVA is based on the environments persistence of condition (the environment today is the same as it would be in 14 days) and the solar cycle predictions remaining "benign" at least through Solar Cycle 25 which extends through 2030 (ISS mission). Because operation of the PCUs increases the magnitude of the positive potential at certain points on the vehicle, the new control guidelines are biased towards not operating the PCUs (i.e., PCUs not in discharge).

The new NCR document establishes the following for controls based on the calculation of the ISS potentials 14 days in advance of an EVA:

1) When the 14-day forecast calculates FP more positive than −45.5V, then:
   - for EVAs inboard the solar alpha rotary joint (SARJ), use of the PCUs is optional and the array shunt FDIR is not required.
2) When the 14-day calculates FP more negative than −45.5V, then:
   - for EVAs inboard of the SARJ, use the two PCUs in discharge with the array shunt FDIR enabled.
3) Because of the positive FP outboard of the SARJ when the PCU is on, the PCU will not be used for EVAs outboard of the SARJ.
4) If the PCUs are required due to extreme negative potentials, the ISS will be placed in the y-axis in the velocity vector (YVV) orientation to mitigate the positive hazard.
5) If the YVV orientation is not possible, then the ISS-PRA-12-56 low probability of shock hazard (which includes the isolation modifications to the MMWS) will be used as justification against the hazard. Additional isolation to the OBS would be added.

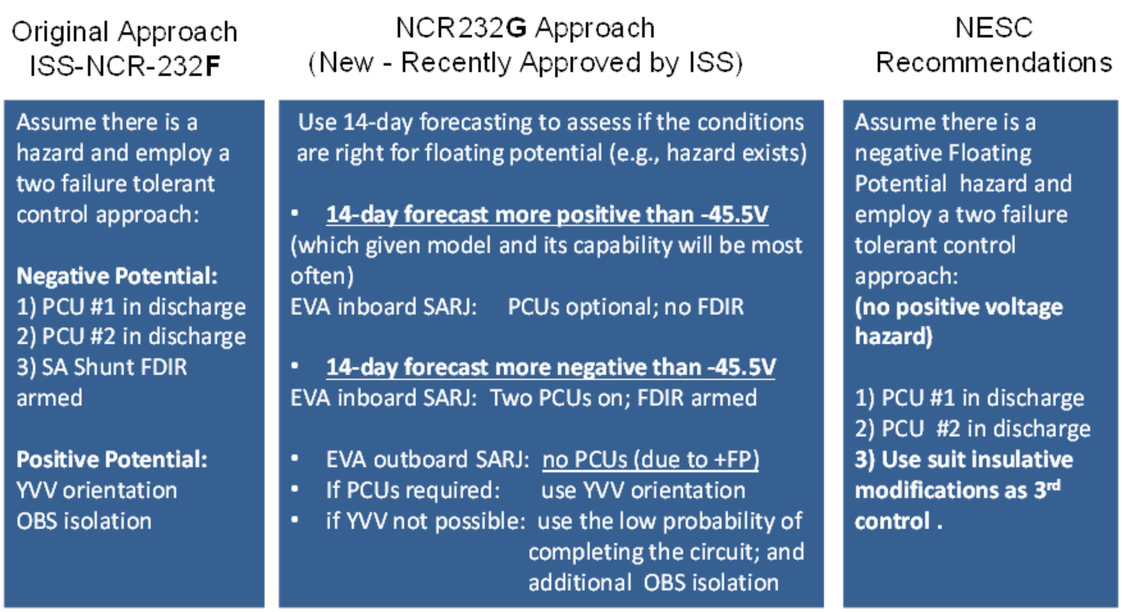

Figure 6.3-11. Comparison of Hazard Control Approaches

6.3.12 Data Supporting NESC Recommendations

Section 7.0 presents the supporting information for the NESC recommendations to revise the new guidelines [ISS-NCR-232G, 2013]. However, the NESC team recommends a combination of controls different from the earlier version [ISS-NCR-232F, 2012] of the guidelines. The recommended hazard control plan is to use the two PCUs in discharge for all EVAs regardless of location, and the EMU isolation features, which predict a low probability of contact, as the three controls. As for the positive potential hazard, the NESC position is that it is not a threat even under the worst-case positive potential (+15V) and the maximum exposed metal area in the EMU.

References:

1. ISS-NCR-232G (2013): *Lack of Two-fault Tolerance to EVA Crew Shock in the Low Earth Orbit Plasma Environment*, NCR-20264-R7, 18 September 2013.
2. ISS-NCR-232F (2012): Lack of Two-fault Tolerance to EVA Crew Shock in the Low Earth Orbit Plasma Environment, 1/31/2012.

7.0 Data Analysis

The use of active controls to prevent the shock hazard (e.g., PCUs and shunt array FDIR) was evaluated based on the data and analyses presented in this section. The recent ISS Safety team's proposed control-use approach triggered questions related to the adequacy of the forecast and the tools associated with the output calculations and limits for FP subsequently used for safety-critical decisions. The various FP scenarios and events were considered and examples are provided below. These examples of charging events were considered along with the solar array shunt FDIR operations to identify non-characterized issues during the array management.

Several aspects of the PCU utilization were studied to determine reasons that would merit the discontinuation or limitation of the PCU use. The PCU adequacy to support the ISS mission (up to 2030) was considered from the capability and reliability perspective. The positive ISS truss FP bias introduced when the PCUs are in discharge seems to have been a factor against its use. Therefore, the electrical current collection scenario under the positive FP conditions was analyzed with the purpose to understand the severity of the positive potential hazard.

Other aspects studied in this assessment involve the probability of completing an electrical current path from the ISS through the EMU suit through the crew member. This condition was studied considering the isolation layers in this path that include most recent modifications to the suit-tool configuration.

7.1 Shortcomings in the Space Weather Forecast Planning that Limits its Utility for Forecasting

The proposed strategy for forecasting ISS charging levels 14 days in advance of an EVA as described in ISS-NCR-232G has technical issues. The strategy involves forecasting space weather conditions and using the forecast conditions as input to the PIM3.0 charging model. The issues with the forecasting process must be addressed before the strategy is used by the ISSP for making safety critical decisions regarding EVAs.

7.1.1 Persistence of Conditions Assumption is Not Accurate

No sophisticated space weather modeling technique is being used in the 14-day space weather forecast. The plasma electron density (Ne) and plasma electron temperature (Te) "forecast" is a simple persistence of conditions method based on the assumption that space weather conditions in 14 days will be the same as on the day the FPMU measurements are obtained. FPMU measurements are obtained on a reference day about 14 days in advance of a scheduled EVA and used to document the current Ne and Te values along the ISS orbit. The FPMU data are then compared to output from a statistical version of the IRI model to determine which statistical estimate for Ne and Te deviations at $\pm 1\sigma$, $\pm 2\sigma$, and $\pm 3\sigma$ levels (where σ is the standard deviation) about the IRI model best represents the measured FPMU data. The selected statistical IRI model output is used to generate Ne and Te values along the ISS orbit that are input to the PIM3.0 charging model to predict ISS charging 14 days in advance of the EVA.

The National Oceanic and Atmospheric Administration's (NOAA) Space Weather Prediction Center (SWPC) (the Federal entity chartered with providing official U.S. government space weather forecasts) only issues 3-day forecasts of solar flare activity and geomagnetic storm conditions which could impact ionosphere electron density and temperature conditions (http://www.swpc.noaa.gov/wwire.html#swxdaypre).

NOAA SWPC does provide a 45-day forecast of geomagnetic Ap and solar F107 indices (http://www.swpc.noaa.gov/ftpdir/latest/45DF.txt) that could be used to provide the predicted F107 values required to run the IRI model. However, no guidance is provided in ISS-NCR-232G or the plasma hazard assessments available to the study team for review [Hartman, 2013a,b; Schmidl, 2013b] as to how future F107 values are obtained for use in the generating the plasma hazard assessments.

References:

1. Hartman, D. (2013a): *Plasma Hazard Relief Assessment for US EVA 22*, ISS-HOU-ENV-WAH-130032, 25 June 2013.
2. Hartman, D. (2013b): *Plasma Hazard Relief Assessment for US EVA 23*, ISS-HOU-ENV-WAH-130035, 2 July 2013.
3. Schmidl, D. (2013b): *Plasma Hazard Relief Assessment for US EVA 21*, ISS-HOU-ENV-WDS-110018, 10 May 2013.

7.1.2 Dependency on Benign Solar Cycle is Unreliable

ISS-NCR-232G provides a statement that *"the Space Environments community has concluded based on the downward trend of recent Solar Cycles that the environment will remain benign at least through Solar Cycle 25 which extends through 2030."* It is not clear from the document what group the term "Space Environments Community" is intended to represent. The general consensus of this NESC team is that, based on the poor results from the solar physics community in predicting the low activity state of the current Solar Cycle 24, it is unlikely there is any physical basis for making quantitative predictions of activity levels through the end of Solar Cycle 25.

The ability of the solar physics community to forecast solar activity for a complete solar cycle in advance is limited at best. Figure 7.1-1 from Pesnell [2008] shows a collection of predictions for the annual averaged sunspot number (Rnn) at the peak of Solar Cycle 24, which were all made before Solar Cycle 24 started.

A few of the prediction techniques gave values close to the local maximum of R = 67 that was observed in February 2012 [Biesecker et al., 2013]. However, a number of the predictions are lower than the observed maximum in 2012 and most of the predictions are significantly higher than the observed maximum. Some of the predictions even give values in the range of R = 180 with error bars extending over R = 200. Such high values typify the solar cycle maxima from past cycles, thereby demonstrating that pre-Solar Cycle 24 predictions varied from historic lows to typical highs. Predictions of Solar Cycle 25 activity using some, or all, of these same techniques will likely result in the same large range of predicted activity levels. Additional work is required before forecasts of solar activity in future cycles can be claimed with any real accuracy [Pesnell, 2008, 2012].

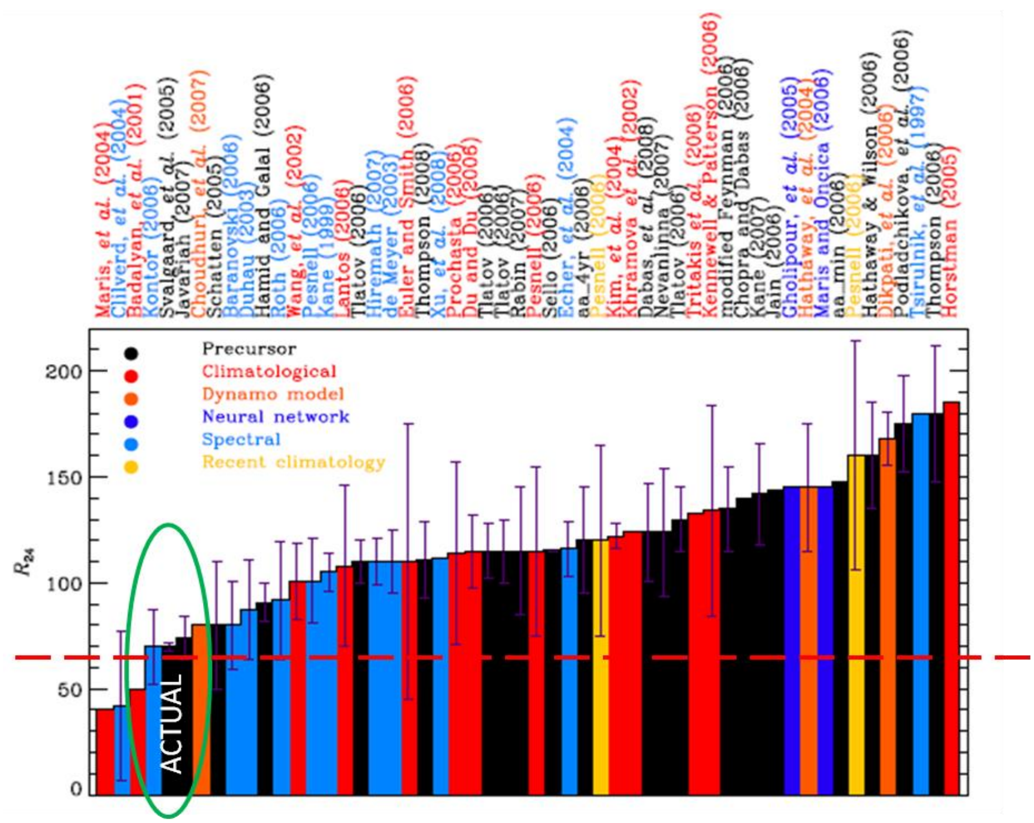

Figure7.1-1. Predictions of Solar Cycle 24 Sunspot Maximum
Colored bars show the wide range of Solar Cycle 24 sunspot maxima values obtained from different prediction techniques [Pesnell, 2008].

References:

1. Pesnell, W.D. (2008): “Predictions of Solar Cycle 24,” *Solar Phys*., 252, 209-220, 2008.
2. Biesecker, D.; Balch, C.; and McIntosh, S. (2013): “Where is Solar Cycle 24? Did it happen already? Is There More to Come?” Presented at the *NOAA 2013 Space Weather Workshop*, Boulder, Colorado, 16-19 April 2013.
3. Pesnell, W.D. (2012): “Solar Cycle Predictions (Invited Review),” *Solar Phys*., 281, pp. 507-532, 2012.

7.1.3 Use of the Climatological Model – IRI is Inadequate

Use of the IRI model to generate the input values required for the PIM3.0 charging model calculations is problematic in two significant areas. First, the IRI model itself is only a monthly average climatology model not intended for use in predicting changes in ionospheric Ne or Te values over shorter time periods. Second, the model is incapable of predicting the full range of environments responsible for ISS charging, including auroral electron flux and plasma depletions at low latitude eclipse exit where the strongest ISS charging to date has been observed. IRI models only the ambient background plasma conditions within the ionosphere and contains no model for the physics of energetic auroral electrons that are responsible for auroral charging. The eclipse exit rapid charging events that represent some of the largest ISS charging observed to date (in the −40 to −67V range) have been shown to occur in plasma density depletions at high latitudes and in dawn density depletions in the equatorial region. IRI does provide some representation of the low plasma density in high latitude ion troughs, but regularly underestimates their magnitude. The physics for dawn density depletions is not included in the IRI model.

7.1.4 Missing Short Term Changes in the Plasma Environment: Geomagnetic Storm Activity

Examples of the plasma hazard assessment’s provided to the ISS program before each EVA reviewed for this study [Hartman, 2013a,b; Schmidl, 2013b] do not include information on the current state of geomagnetic activity, which is a significant issue. Geomagnetic storm activity tends to deplete the ionosphere of plasma density and increase the electron temperature. These changes actually serve to suppress ISS solar array charging because the reduction in electron density reduces the amount of electron current to the solar cells and the higher electron temperature increases charging of the cover glass material on the solar cells. This, in turn, increases the barrier potentials and reduces the amount of electron current that reaches the solar cell. Measurement of the ionospheric Ne and Te values during a geomagnetic storm period will give values representative of suppressed ISS charging conditions. Once a geomagnetic storm ends—typically on time scales of 12 to 24 hours—the electron density and temperatures recover to the pre-storm values, which will result in higher charging levels. Obtaining the reference data for the 14-day forecast during a geomagnetic storm period almost certainly guarantees the charging environment will be underestimated for the time period of an EVA. There is no release documentation suggesting that this effect has been considered in development of the 14-day forecast products and no documented plans to deal with FPMU data obtained during disturbed periods when reference data may under represent environment in 14 days.

References:

1. Hartman, D. (2013a): *Plasma Hazard Relief Assessment for US EVA 22*, ISS-HOU-ENV-WAH-130032, 25 June 2013.
2. Hartman, D. (2013b): *Plasma Hazard Relief Assessment for US EVA 23*, ISS-HOU-ENV-WAH-130035, 2 July 2013.
3. Schmidl, D. (2013b): *Plasma Hazard Relief Assessment for US EVA 21*, ISS-HOU-ENV-WDS-110018, 10 May 2013.

7.1.5 Inconsistencies in Input Parameters

An additional issue identified with use of the forecast tools is an inconsistency in the use of different versions of the IRI models. The plasma hazard reports reviewed for this study [Hartman, 2013a, b; Schmidl, 2013b] indicate the IRI-2011 model is used for the plasma hazard assessment. However, the plasma variability model that is used to obtain the $\pm 1\sigma$, $\pm 2\sigma$, and $\pm 3\sigma$ level deviations in the Ne and Te values about the IRI model output was derived from comparing satellite data with the IRI-2001 model [Minow, 2004]. No evidence was presented to demonstrate that the statistical variability levels for Ne and Te values derived from the older IRI-2001 model are still applicable to the newer IRI-2011 version of the ionospheric climatology model.

References:

1. Hartman, D. (2013a): *Plasma Hazard Relief Assessment for US EVA 22*, ISS-HOU-ENV-WAH-130032, 25 June 2013.
2. Hartman, D. (2013b): *Plasma Hazard Relief Assessment for US EVA 23*, ISS-HOU-ENV-WAH-130035, 2 July 2013.
3. Schmidl, D. (2013b): *Plasma Hazard Relief Assessment for US EVA 21*, ISS-HOU-ENV-WDS-110018, 10 May 2013.
4. Minow, J.I. (2004): "Development and Implementation of an Empirical Ionosphere Variability Model," *Adv. In Space Res.*, 33, 887-892, 2004.

7.1.6 Limited Validation Studies

Reliability of the technique to give predicted ISS charging levels that are not exceeded during an EVA period would depend critically on the ionosphere exhibiting very low levels of Ne and Te variability over the forecast period. The ISS-NCR-232G argues that these conditions are met for the current Solar Cycle 24 because the lower than typical solar ultraviolet/extreme ultraviolet output has resulted in a depressed solar cycle with hotter electron temperatures that limit charging. What is required to test this prediction technique, however, is not an argument based on high electron temperatures, but rather comparisons of measured Ne and Te values on a reference day to those observed on the forecast day 14 days later. The only available material showing such a validation study [Hartman, 2013c] is limited to comparing FPMU Ne and Te measurements at approximately 7-, 14-, 21-, and 30-day intervals from a single reference day measurement in the two time intervals Greenwich Mean Time (GMT) 2011/120-150 and 2013 GMT 20-100. It is not clear why such a limited set of validation comparisons have been attempted since there are numerous long periods of FPMU data from recent years that can be used to conduct more extensive comparisons for validation. In addition, there are alternative data sets such as ground-based ionosonde measurements that can be used to test 14-day forecasts for periods of a year or more.

No complete verification of the ability to predict ISS potentials 14 days in advance has been demonstrated. The validation studies for the 14-day forecast and PIM3.0 charging modeling strategy available for review have only shown that Ne and Te values have not significantly changed over 14 days for a few limited time periods. No attempt to forecast the ISS charging levels and then compare the measured potentials after 14 days to validate that charging values never exceed the forecast was provided to the NESC team. As a result, pieces of the forecast technique appear to work at least for a couple of isolated time periods, yet there has been no full validation study to demonstrate the technique.

Reference:

1. Hartman, D. (2013c): *Extension of Plasma Forecasting, Boeing Space Environments*, 2013.

7.2 FPMU Role in the Forecast: Criticality and Alternate Data

FPMU data are critical to the 14-day plasma hazard forecast approach because FPMU Ne and Te measurements are used to constrain which statistical set of IRI-2001 statistical model output will be used as input to the PIM3.0 charging model calculations of the ISS potentials. In order to provide the plasma hazard forecast, a source of Ne and Te data to constrain the ionosphere model is required. A review of the NCR proposing to replace PCU operations with the plasma hazard forecast approach [ISS-NCR-232G, 2013] shows no explicit contingency procedure that outlines what to do if recent FPMU data are not available.

Reference:

1. ISS-NCR-232G (2013): *Lack of Two-fault Tolerance to EVA Crew Shock in the Low Earth Orbit Plasma Environment*, NCR-20264-R7, 18 September 2013.

7.2.1 Ambiguity in Dataset Requirements

The NESC team does note that in at least three of the plasma hazard relief assessment reports that were available to the team for review [Hartman, 2013a,b; Schmidl, 2013b], a statement is included indicating "if sufficient FPMU data are not available, then +2 σ results may be used. In that case, the Space Environments team will provide those results." If this vague statement is the contingency procedure intended to be followed when FPMU data are not available, then explicit information needs to be added describing what constitutes sufficient FPMU data and what conditions will require discontinuing use of the plasma hazard forecast process. For example, what total amount of data is the minimum required for the assessment? What quality of data is acceptable (and what metric is used for the quality assessment)? Which instrument(s) provide the data for the analysis? Can data from any of the FPMU instruments be used or must the data come from a specific instrument? Details of this procedure must be documented in the NCR for review and concurrence by the ISSP to assure that inadequate FPMU data are not being used in the process.

References:

1. Hartman, D. (2013a): *Plasma Hazard Relief Assessment for US EVA 22*, ISS-HOU-ENV-WAH-130032, 25 June 2013.
2. Hartman, D. (2013b): *Plasma Hazard Relief Assessment for US EVA 23*, ISS-HOU-ENV-WAH-130035, 2 July 2013.
3. Schmidl, D. (2013b): *Plasma Hazard Relief Assessment for US EVA 21*, ISS-HOU-ENV-WDS-110018, 10 May 2013.

7.2.2 Alternatives for Ionospheric Data

The FPMU is not the only source of ionospheric Ne and Te data. Alternative sources of ionospheric Ne and Te data should be evaluated by the ISSP for use as a contingency option for characterizing the plasma environment should FPMU data not be available. One possible example is the approximately 500 to 1000 electron density profiles provided by the FORMOSAT-3/COSMIC satellite constellation distributed over a wide range of latitudes and longitudes [Rocken, et al., 2000; Schreiner, et al., 2007; Anthes, 2011]. Another source of ionospheric plasma density data is the maximum F2-region electron density routinely measured by a global network of ionosonde stations and distributed by the NOAA SWPC every 30 to 60 minutes [NOAA, 2014]. ISS orbital altitudes are typically above the F2-peak where the electron density is less than the F2-region peak values so this data would characterize the worst-case electron density for ISS charging. Finally, availability of data from the Global Assimilative Ionospheric Model (GAIM), or other full physics ionosphere models, should be evaluated for use in providing Ne and Te along the ISS orbit. GAIM is of particular interest because the model output is constrained by real-time data from a number of sources including ionosondes and satellites.

References:

1. Rocken, C., Kuo, Y.H.; Schreiner, W.; Hunt, D.; Sokolovskiy, S.; and McCormick, C. (2000): “COSMIC system description,” *Terr. Atmos. Oceanic Sci*., 11, 21–52.
2. Schreiner, W.; Rocken, C.; Sokolovskiy, S.; Syndergaard, S.; and Hunt, D. (2007): Estimates of the Precision of GPS Radio Occultations from the COSMIC/ FORMOSAT-3 Mission, *Geophys. Res. Lett*., 34, L04808,doi:10.1029/2006GL027557.
3. Anthes, R. A. (2011): “Exploring Earth’s Atmosphere with Radio Occultation: Contributions to Weather, Climate and Space Weather,” *Atmos. Meas. Tech*., 4, 1077–1103, doi:10.5194/amt-4-1077-2011.
4. NOAA (2014), Space Weather Prediction Center, URL: http://www.swpc.noaa.gov/ftpdir/lists/iono_day/README, accessed 21 May 2014.

7.2.3 FPMU Reliability

A number of issues related to FPMU data availability and reliability must be considered when deciding whether to discontinue PCU operations in favor of the plasma hazard forecast approach. The FPMU was designed and built as Class 3 electronics (for a 3-year operational life). Reliability is provided by (a) redundant Ne and Te and FP measurements from multiple measurement techniques and (b) spare FPMU units to replace a failed unit [Swenson and Thompson, 2002]. Three flight and two engineering/qualification units were delivered to NASA with the assumption that flight units would be replaced with a spare when operational units failed. FPMU Serial Number 3 was deployed on the ISS during an EVA on August 3, 2006 with the first data received the same day. This same unit continues to serve as the operational FPMU instrument on the ISS and has collected data for approximately 709 days during the period starting August 3, 2006, and ending October 1, 2013, (the last time the data collection statistics were updated), representing 1.9 years of powered instrument operations over an on-orbit time of 7.2 years. The data collection time is only approximate (within a few days) since it was obtained from a count of daily file folders generated by the FPMU ground station and not a detailed measure of the actual instrument operations time. FPMU operations are typically limited to about 100 days a year although operations in 2012 exceeded 130 days with no operational FPMU issues.

Reference:

1. Swenson, C.; and D. Thompson (2002): “FPMU Systems Overview,” presented at *FPMU CDR*, February 19-20, 2002.

7.2.4 FPMU Design Life Limitations Compared To PCU

Any recommendation to discontinue the use of the PCUs in favor of a process requiring FPMU data should balance the remaining life expectancy of the operational FPMU unit and the two flight spares against the expected life of the PCUs. PCUs were designed for long-term use in the space environment and finding 7 (F-7) in this report demonstrates the two operational PCUs have adequate xenon gas and a hardware design life to support their use past 2028. In addition, a third spare PCU unit is located on board the ISS with a full tank of xenon gas and a hollow cathode that has seen little use.

In contrast, the cumulative design life for an FPMU unit is only three years and long-term reliability of the instrument is based on redundant measurements from the multiple probes and replacing failed units with flight spares. As of March 1, 2014, the operational FPMU unit will have been exposed to the space environment for 7.6 years, exceeding the cumulative 3-year life requirement for a single unit by 4.6 years. Limited life items used in the design of an FPMU include the cleaning lamp in the wide-sweep langmuir probe (WLP), and a thermal switch used in the survival heater. The cleaning lamp in the WLP sphere is not an issue because the cleaning lamp is no longer used in FPMU operations. The survival heater is required to run continuously when FPMU is outside the vehicle to protect the electronics from extremely cold temperatures. The thermostats are expected to cycle every 270 minutes and are rated for 10,000 cycles for a life of 5.1 years [Utah State University, 2002]. The current operational unit has successfully exceeded the survival heater rating by 2.5 years. Additionally, radiation damage to the electronics is an issue because the FPMU was not built using radiation hardened parts. The ISS radiation design environments (Space Shuttle Program (SSP) 30512) indicate the 1-year total ionizing dose, due to trapped protons and electrons in silicon behind 5 mm of Al-equivalent shielding, is approximately 123 radiation absorbed dose (rad) [Space Station Program Office, 1994]. Radiation sensitive components with this amount of shielding could exceed a total ionizing dose of 1000 rad in the next year based on the SSP 30512 specification, a benchmark where commercial parts not selected for tolerance to radiation environments begin to show degradation. SSP 30512 is a conservative design environment so the as-flown radiation dose is certainly lower, but a more thorough analysis of potential radiation effects on the FPMU is warranted to determine what additional time remains for the operational unit before replacement with the flight spare is required.

While the FPMU currently in operation on the ISS has exceeded the design life, it has not been shown that the remaining spare flight units can be expected to operate for a similar period beyond the design life. Should the operational FPMU fail in 2014, the conservative assumption is the two flight spares will last the 3-year design life and can be expected to support the proposed plasma hazard forecast process only until 2020. If the two units last for periods approaching the flight experience of the FPMU operating on ISS, then the plasma hazard process could possibly be supported by FPMU data until 2028.

References:

1. Utah State University (2002): SDL 2002, FPMU Limited-Life Items List, SDL/02-037, Space Dynamics Laboratory, Utah State University, 7 February 2002.
2. Space Station Program Office (1994): *Space Station Ionizing Radiation Design Environment*, Revision C, 3, SSP 30512, June 1994.

7.2.5 Spare FPMUs – EVA Deployment

Two additional FPMU flight units provide a backup to the operational unit on ISS. An FPMU (Serial Number 5) is stored on-board the ISS for use as a pre-positioned flight spare, but an EVA will be required to replace a failed unit. This EVA would have to be conducted without the benefit of FPMU data and the plasma hazard forecast process although operation of the PCUs during this EVA would mitigate the negative charging hazard. The third FPMU flight unit (Serial Number 2) is located in bonded storage at the Kennedy Space Center (KSC), but would require a flight to the ISS.

7.2.6 FPMU Power Supply Limitations

The use of the FPMU depends on availability of the television camera interface controller (TVCIC) and its power supply, because the TVCIC provides power to FPMU and the link between the FPMU and the ISS data telemetry system. The power supply in the TVCIC box currently in use with FPMU was launched with a known reliability issue [Kichak et al. 2009; Mikatarian, 2010] resulting in periodic shut down. Power cycling of the FPMU/TVCIC combination is occasionally required to re-establish FPMU data flow. Spare TVCIC power supplies with a new design to correct the supply failure mechanism exists on-orbit, but the details for refurbishing the TVCIC with a spare power supply would need to be worked out should a failure occur. Finally, note that options presented as part of the ISS-NCR-232 update do not show contingency plans against a TVCIC power supply failure.

References:

1. Mikatarian, R.(2010): *Operation of the FPMU to support plasma hazard assessments, FINAL-ShortVer-2010-04-13-SSPCB-FPMU-Requirements-revK.pdf,* April 13, 2010.
2. Kichak, R., E. Young, C. Pandipati, and R. Cooke, International Space Station (ISS) External Television (TV) Camera Shutdown Investigation, NASA TM-2009-215572, NESC-RP-06-49/06-001-E, February 2009.

7.3 Limitations of the ISS Charging Model PIM3.0

Calculated values of the maximum ISS eclipse exit potential obtained from PIM3.0 charging model using measured FPMU Ne and Te at the time of the potential maxima are not the same as the maximum ISS potential measured by the FPMU at eclipse exit. Discrepancies between the measured data and PIM3.0 modeled data show that there are deficiencies in the model and use of FPMU data that limit the accuracy of the output. These limitations and sources of error need to be identified, documented, and communicated to the critical decision makers as part of meeting the NASA-STD-7009 Standard for Models and Simulations requirements [NASA, 2013a].

The NESC team identified a number of limitations and sources of error in PIM3.0, which resulted in discrepancies between measured and modeled data. Fundamental issues with the physics-based algorithms used in the code include:

- Analytical approximations used in the numerical solutions for the potential barriers in the gaps between solar cells (solar array electrical current collection model).
- Assumption that every solar cell and solar array string collects the same electrical current.
- Use of a static (equilibrium) charging algorithm independent of ISS capacitance that cannot predict rapid charging events.
- Use of single capacitance in time-dependent charging algorithms that oversimplifies the physics of ISS charging and fails to model fast transient charging (i.e., rapid charging events).

The issue with the charging algorithms included in the PIM3.0 charging model is fundamental to whether the code will be able to predict the full range of charging behavior observed on the ISS. PIM3.0 in its current state is only capable of modeling the relatively slow change in ISS potential at eclipse exit, but fails to correctly model the rapid charging events observed at eclipse exit and when solar arrays are unshunted in sunlight. Refer to Section 7.6.

In addition, errors in input data used to run the model or configuration data used to constrain the ISS electrical current collection processes will also impact the model results. A number of these errors include:

- Uncertainties in FPMU Ne and Te input data (due to FPMU data reduction errors).
- Timing of FPMU data chosen for the PIM3.0 charging model input relative to the charging peak maxima.
- Errors in knowledge of (or values used for) solar array angles, ISS flight attitude, ISS velocity.
- Variations in ion collection area (free parameter adjusted to obtain best results).

While it may not be necessary to fully characterize each of these sources of error in the PIM3.0 charging model output, an error bound at some appropriate statistical level should be computed and applied to the PIM3.0 charging model output when used in safety assessments.

Reference:

1. NASA (2013a): NASA-STD-7009 Standard for Models and Simulations, July 10, 2013.

7.4 PIM3.0 Charging Model in the Critical Path to EVA

The Columbia Accident Investigation Board report [CAIB, 2003] and NASA's response to it, contained in the "A Renewed Commitment to Excellent" report [NASA, 2004], both emphasize that modeling and simulation (M&S) used as a basis for critical decisions must meet certain standards to ensure the credibility of the results and that analytical results derived from M&S are assessed and properly conveyed to those making critical decisions. NASA responded to the findings in CAIB, 2003 and PB2005-10096, 2004, by establishing a minimum set of requirements and recommendations for use of M&S to support critical decisions and published them in NASA-STD-7009, 2013. The requirements and recommendations contained in the standard are intended to address one or more of the following eight objectives:

1. *Identify best practices to ensure that knowledge of operations is captured in the user interfaces (e.g., users are not able to enter parameters that are out of bounds).*
2. *Develop a process for tool verification and validation, certification, verification, revalidation, and recertification based on operational data and trending.*
3. *Develop a standard for documentation, configuration management, and quality assurance.*
4. *Identify any training or certification requirements to ensure proper operational capabilities.*
5. *Provide a plan for tool management, maintenance, and obsolescence consistent with M&S environments and the aging or changing of the modeled platform or system.*
6. *Develop a process for user feedback when results appear unrealistic or defy explanation.*
7. *Include a standard method to assess the credibility of the M&S presented to the decision maker when making critical decisions (i.e., decisions that affect human safety or mission success) using results from M&S.*
8. *Assure that the credibility of M&S meets the project requirements.*

NASA-STD-7009 defines a critical decision as *"those technical decisions related to design, development, manufacturing, ground, or flight operations that may impact human safety or mission success, as measured by program/project-defined criteria."* A decision to discontinue the use of PCUs as a redundant hazard control to guard the safety of crew members during EVA (based on the results of the plasma hazard forecasts and PIM3.0 modeling of ISS shock hazards) meets the NASA-STD-7009 definition of a critical hazard. However, the PIM3.0 charging model, when used to provide results in support of a critical decision, falls short of the requirements and recommendations contained in the NASA-STD-7009 in almost every regard. Examples of the more serious PIM3.0 shortcomings include (but are not limited to):

- The limitations of the PIM3.0 are not explicitly known by the decision makers.
- User's manual and parameter definitions for the PIM3.0 code are not available.
- The configuration files that provide the PIM3.0 model input and control how the model is run are not documented in the pre-planning proposed procedure. No documented process exists to constrain the content of the configuration files assuring the model is used the same every time it is run.
- The model has not been independently peer reviewed.
- There is no process identified to update the PIM3.0 charging model to include physical changes to the station configuration.
- There is no clearly documented validation, verification, or certification process.
- Uncertainty in the model results are not documented and applied to model output.

The NESC team finds that the PIM3.0 charging model should not be in the critical path for EVA safety decisions as it lacks the pedigree associated with NASA standards for M&S.

References:

1. CAIB (2003): *Columbia Accident Investigation Board, Volume 1*, August 2003.
2. NASA (2004): *A Renewed Commitment to Excellence: An Assessment of the NASA Agency-wide Applicability of the Columbia Accident Investigation Board Report*, PB2005-100968, January 2004.

7.5 Example of PIM3.0 Error Estimate

Results from the PIM have been stated and used with a high level of accuracy. Sometimes PIM3.0 results are reported to the tenth of volt and in some cases reported to the hundredth of volt. Kramer et al. (2010) [Kramer, et al., 2010] in a contributed paper to a conference state that "The EVA worksite voltage exposure, as seen in Figure 6 and Figure 9, using Boeing-developed capability incorporated into the PIM3.0 is accurate." The authors attribute any error in the PIM3.0 results on inputs to the model. No evidence of PIM3.0 validation is referenced for their statement. No evidence of a validation exercise has been provided to the NESC team. In a hazard situation (e.g., the EVA scenario), statements implying "no error" should be regarded with skepticism. Scatter plots of PIM3.0 and FPMU visually do not support using PIM3.0 results to an accuracy of 0.1V. This note is to derive an error based on available PIM3.0 results as compared with FPMU data. The result of this method is not offered as the final value, but as motivation for the ISS Environments team to derive a value that is vetted and approved within the ISSP.

Figure 7.5-1 shows a scatter plot of PIM3.0 versus FPMU data. The time period that spans the data is day 188 of 2007 to day 105 of 2013. For each FP measurement of the FPMU, the simultaneous FPMU density and temperature measurements were input to the PIM3.0 with output calculation appropriate for the FPMU location. Note this data period includes both locations of the FPMU on the truss (i.e., S1 Truss from August 3, 2006, to November 21, 2009, and the P1 truss from November 21, 2009, to the present). The number of data points is 2164. Comparing charging events included the file used to generate Figure 7.5-1 [Boeing, 2013] with a Marshall Space Flight Center (MSFC) study of eclipse exit charging events [Wright, et al., 2009], the NESC team determined that not all of the rapid charging events are included in the Boeing, 2013 data set. Nevertheless, fundamental information about an error bar to associate with a PIM3.0 calculation can be obtained from this data set.

Figure 7.5-2 shows a plot of the difference between the PIM3.0 calculations and the FPMU FP measurement versus the FPMU measurement. As noted in the figure, ~74 percent of the data show a positive difference. Note that the values shown in Figure 7.5-1 are negative. A positive difference indicates that the PIM3.0 calculation is less negative, meaning that the model is underpredicting the FP of the ISS frame. In a hazardous situation (e.g., EVAs are treated), underpredicting should be viewed with concern.

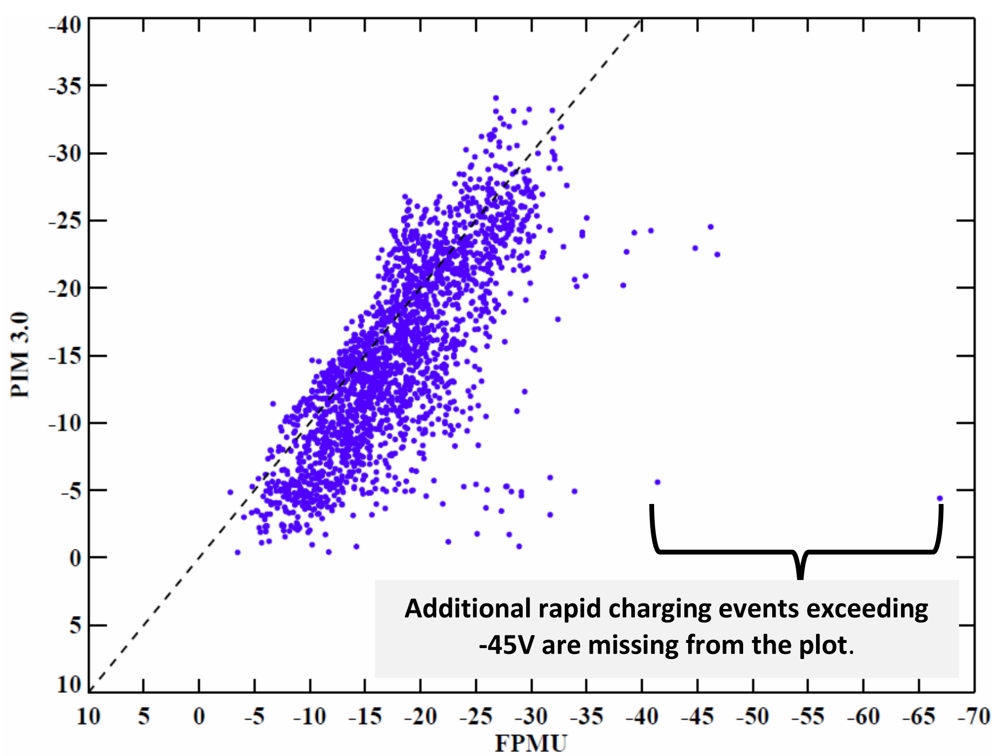

Figure 7.5-1. Scatter Plot of PIM3.0 Voltage Calculations versus FPMU FP Measurement. The dashed line represents a one-to-one correspondence; i.e., a slope of 1.

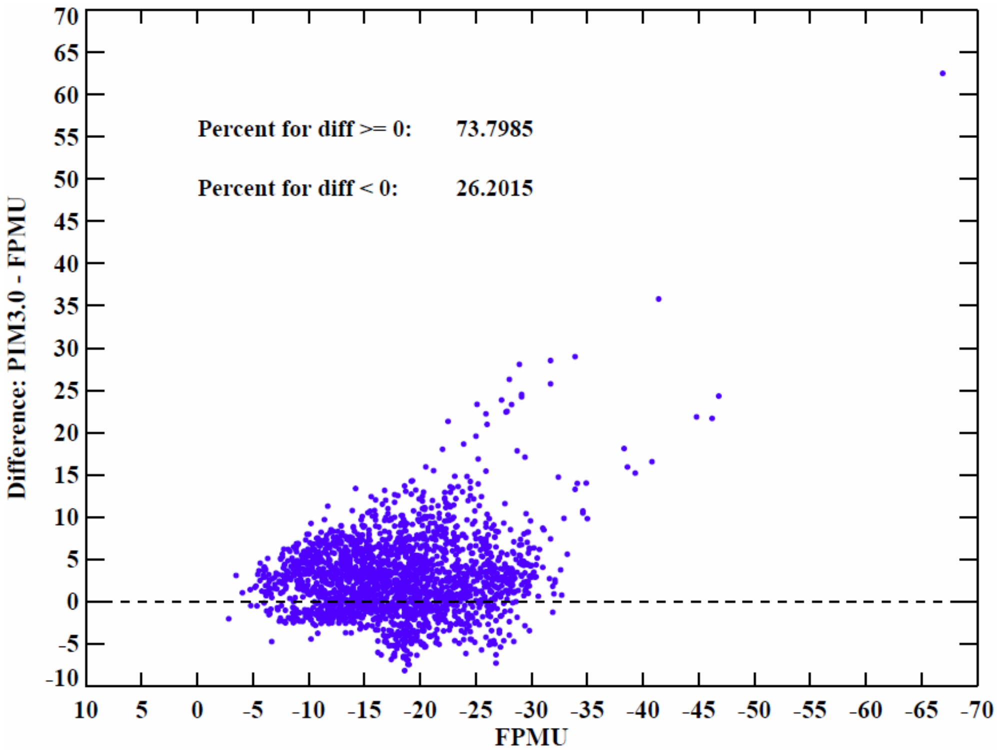

Figure 7.5-2. Plot of the (PIM3.0 calculation – FPMU Measurement) Difference versus FPMU FP Measurement. Dashed line indicates no difference between the model and measurement.

To get an idea of error from the PIM3.0 calculations, the distribution of occurrence of the model-measurement difference data was plotted. The histogram (blue line) in Figure 7.5-3 shows the number of occurrences in 1V bins versus the PIM3.0 calculation-FPMU measurement difference. Overlaid on the histogram is a Gaussian curve (dashed red line) defined in Eqs. (1) and (2).

$$\text{Gaussian} = A_0 \exp^{-(Z*Z)/2}, \text{ where} \qquad \text{Eq. (1)}$$

$$Z = (x-A_1)/A_2 \qquad \text{Eq. (2)}$$

A_0 was chosen to match the largest amplitude of the distribution. A_1 was chosen to match the location of the peak in the distribution. A_2 is the standard deviation and was determined by requiring that 68 percent of the distribution lie within one standard deviation of A_1. Visual examination of the distribution (blue curve) indicates that it is not quite Gaussian in shape. The exercise here is to demonstrate a non-zero error and the use of a Gaussian distribution is sufficient to do this.

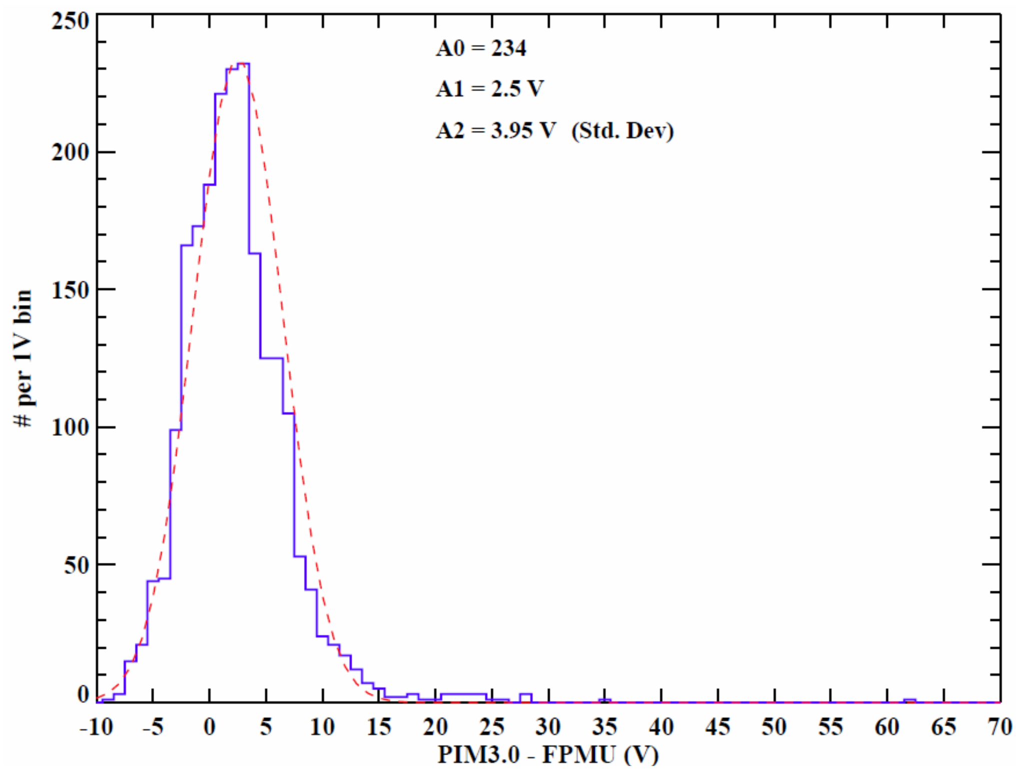

Figure 7.5-3. Histogram of PIM3.0, FPMU Measurement Difference for 1V bins. The red-dashed line overlay is a Gaussian curve-fit.

Figure 7.5-4 shows how the data points fall into the 1-, 2-, 3-, and beyond 3σ bands. The various data bands are colored-coded. The 2.5V difference bias in the data is denoted as the dashed line. The various rapid charging event data points are not known with certainty in this plot, but it is speculated that these events are the points denoted in red that lie outside the 3σ band and solicit inclusion in an updated PIM.

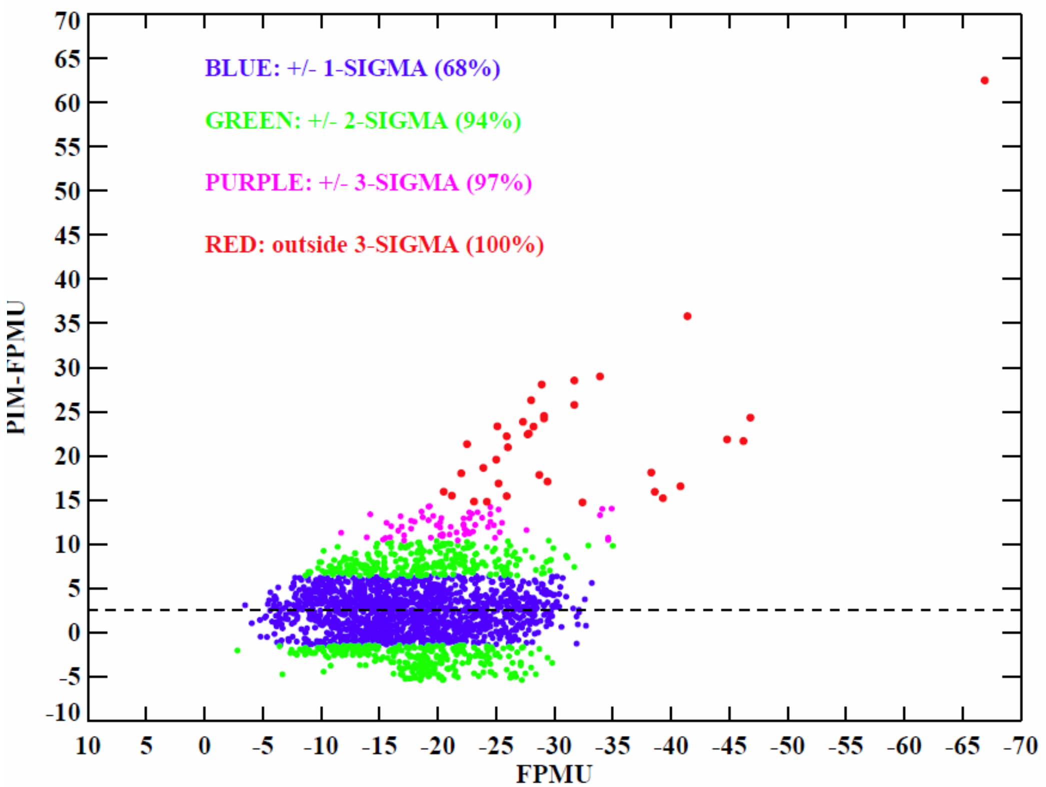

Figure 7.5-4. Data in Figure 7.5-2 re-plotted with color code to indicate points that lie inside 1-σ, 2-σ, and 3-σ boundaries and also points that lie beyond the 3-σ boundary. The dashed line is the 2.5V bias inherent in the PIM.

A suggested method to use for the purpose of deriving a FP value calculated by PIM3.0 is the following. First, consider the data plotted in Figure 7.5-5 as FPMU versus PIM3.0 calculation. The y-axis in this case could be considered a "prediction." The data were curve-fit to Eq. (3).

$$Y = A + B \bullet X, \text{ with} \qquad \text{Eq. (3)}$$

$$A = -7.89 \text{ and } B = 0.67$$

The best linear fit is marked by the black line. Also shown in Figure 7.5-5 are the 1-σ (±4V) boundary lines and the 2-σ (±8V) boundary lines drawn parallel to the best linear fit line.

If a plasma environment (i.e., density and temperature) is input to PIM, then a calculated value for a particular location is determined. This calculated value should be processed through Eq. (3) to obtain a corrected value. Note the difference between the black centerline and the green 1σ boundary lines for a given PIM3.0 value approximately ±3V. Once the corrected PIM3.0 value is obtained, an error of ±3V for the 1σ case should be assigned. In considering the 2σ case, an error of ±6V should be assigned. The risk posture of the ISSP should determine what amount to include of standard deviations.

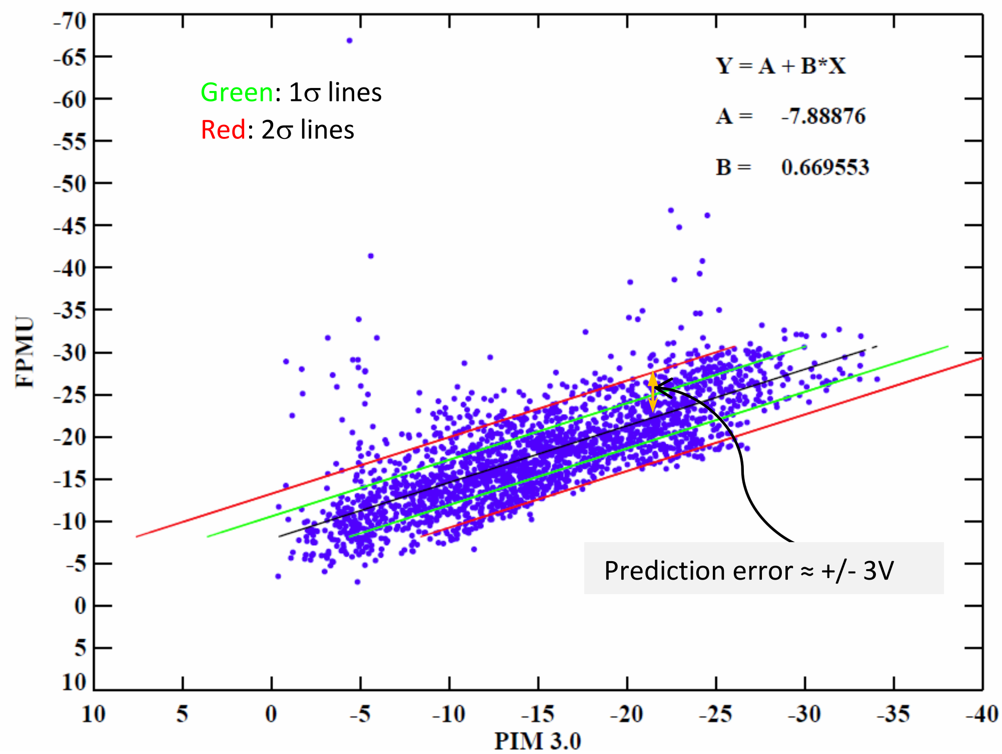

Figure 7.5-5. FPMU versus PIM3.0 calculation. The y-axis can be interpreted as a prediction based on a given environmental input.

Recommendation: The ISS Environments team should obtain a voltage error to assign to any PIM-calculated value and refrain from stating such calculated values to an accuracy of less than 1V.

References:

1. Kramer, L.; Hamilton, D.; Mikatarian R.; Thomas J.; and Koontz, S. (2010): "Positive Voltage Hazard to EMU Crewman from Currents through Plasma," *Proc. 4th IAASS Conference 'Making Safety Matter'*, Huntsville, Alabama, USA, 19–21 May 2010 (ESA SP-680, September 2010).
2. Boeing (2013): *PIMVar1_results.xls* file, 2013a.
3. Wright, et al. (2009): Wright, K.H., FPMURapidChargingEvents_KHW_2009Mar02.xls file, 2009.

7.6 Types of Charging Events

Figure 7.6-1 shows examples of the three basic types of negative charging events, due to solar array interactions with the plasma environment, which have been identified in FPMU data. The PCU was not operating during any of the charging events shown in the figure and the potentials refer to the ISS potential measured by the FPMU floating potential probe at the location of the FPMU instrument. Voltages at other locations on the truss will be shifted by the appropriate

v × B • L inductive potential at the time the data was obtained. Potentials due to normal charging (Figure 7.6-1a) are generally in the range of −20V to −30V, but the duration of the charging events may last for many minutes to 10s of minutes [Wright, et al., 2007]. Normal charging is the most commonly observed type of ISS eclipse exit charging event.

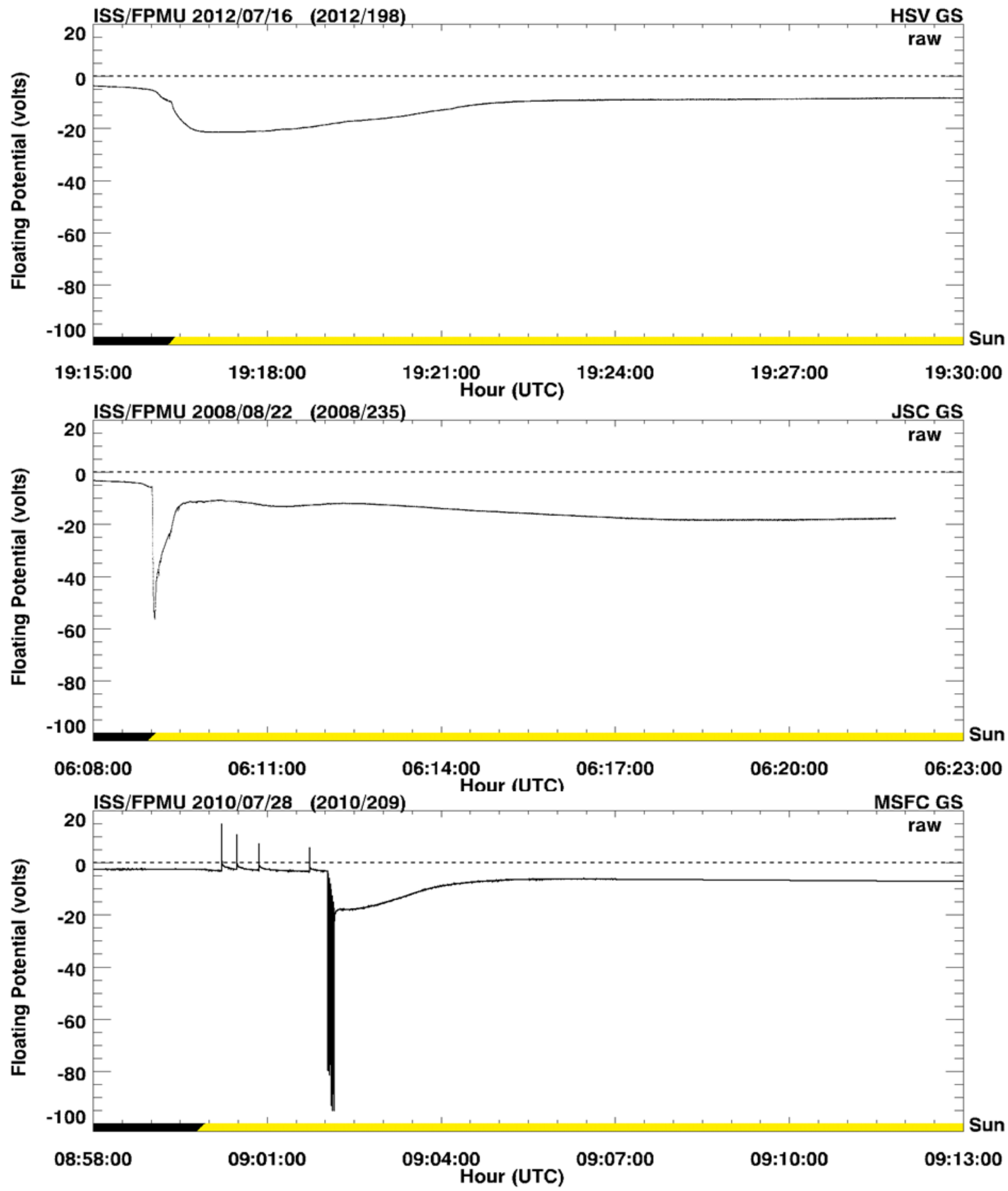

Figure 7.6-1. ISS Solar Array Charging

Charging events identified to date due to solar array interactions with the plasma environment include (a) normal eclipse exit charging, (b) eclipse exit rapid charging events, and (c) rapid charging events in sunlight following array unshunt operations.

Rapid charging events at eclipse exit (Figure 7.6-1b) are characterized by increases in potential over time scales of seconds followed by a rapid decrease in potential over a few seconds. While many rapid charging events remain within the −20 to −40V range, some of the largest eclipse exit charging events observed on the ISS have been rapid charging events with potentials in the −40 to −67V range [Craven, et al., 2009; Minow, et al., 2010]. Rapid charging events are less common than normal charging, and appear to be correlated to eclipse exit conditions with low plasma densities (less than 3×10^{10} m^{-3}) [Craven, et al., 2009].

Finally, a class of rapid charging events (Figure 7.6-1c) occur when fully shunted solar arrays are unshunted in full sunlight [Minow, et al., 2010]. Sunlight unshunt rapid charging events are transient events reaching the maximum potential within one FPMU sample period (≤7.8 milliseconds (msec)) followed by a rapid decrease in potential on times scales of 20 to 150 msec. Sunlight unshunt rapid charging events were first observed on GMT 2010/155 and over the period GMT 2010/205-212 during a set of 36 experiments in which all 8 ISS solar arrays were fully shunted for about 3 minutes following eclipse exit. Then each array wing was unshunted at 1-second intervals resulting in a set of eight charging peaks (Figure 7.6-2). Two additional events were observed on GMT 2013/130 when array power manipulation activities associated with the ammonia pump repair required shunting the 2B array and unshunting in sunlight. The largest recorded ISS negative charging events fall in this category. Maximum potentials for 288 of the 289 sunlight unshunt rapid charging event charging peaks observed to date are more negative than −45V, 265 events are more negative than −60V, and 16 events are more negative than −90V. Two charging events on GMT 2010/209 reached −95V and are the largest negative charging events observed to date on the ISS. Sunlight unshunt rapid charging events have been observed in all cases where FPMU data is available following unshunt of a solar array in sunlight.

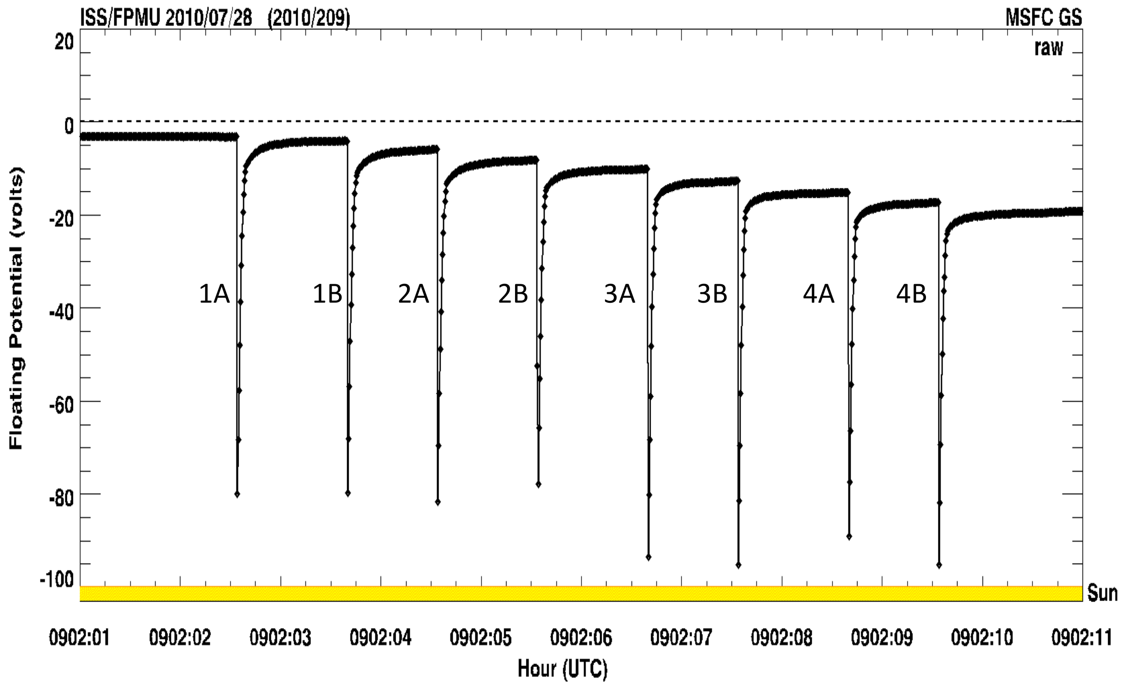

Figure 7.6-2. Detail of Sunlight Unshunt Rapid Charging Event

The time scale for the sunlight unshunt rapid charging event from Figure 7.6-1 is expanded to better show the rapid rise time and decay of each of the eight events. Rise time from background to maximum potential is ≤7.8 msec and the charging peaks decay within ~100 msec. The array responsible for each charging peak is indicated and the highest negative charging observed to date on the ISS are the events from the 3B and 4B arrays.

Figure 7.6-3 provides a summary of the ISS eclipse exit charging levels and examples of the most extreme negative and positive charging events observed to date. PCUs were off for all of the events in the summary so it provides examples of the range of charging that can be observed when PCUs are not used to control the vehicle potential. The figure and analysis of the data used to generate it highlights three important findings. First, ISS charging is variable with approximately 95 percent of the observed charging events remaining within 0 to −45V. Second, FPMU data provide a record of a number of ISS charging events more negative than −45V contradicting the ISS-NCR-232G that states "*FPMU measurements since 2007 have indicated no ISS charging in excess of -45V*." Third, positive potentials are not due solely to PCU operations so discontinuing use of the PCUs will not eliminate exposure to positive potentials.

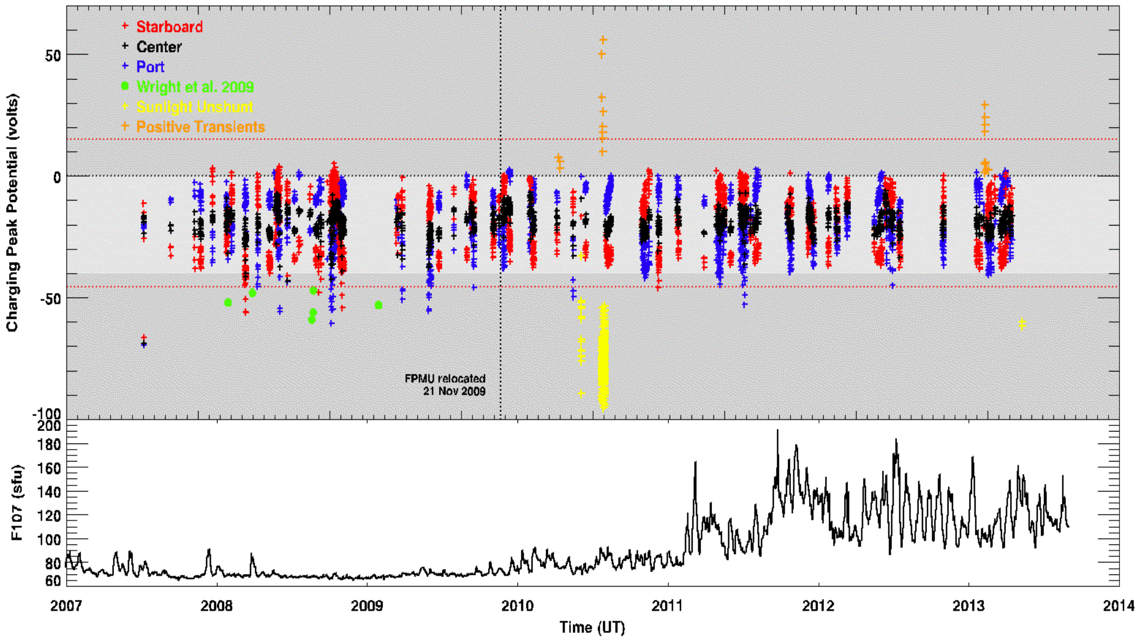

Figure 7.6-3. ISS FPMU Charging Event Summary

(Top Panel) Colored symbols indicate the maximum potential in individual charging events as a function of time. (Bottom Panel) The F107 index is a measure of the solar 10.7 cm radio flux (in solar flux units) showing the phase in solar cycle.

The majority of the data points in Figure 7.6-3 are from a Boeing study [Boeing, 2013] of the maximum negative ISS frame potential due to solar array charging following eclipse exit. The data cover 2,164 orbits during the period starting 2007/188 through 2013/105. The ISS potential measurements at the FPMU location are adjusted for the **v** × **B** • **L** potential difference between the measurement location and the ISS centerline (black symbols), starboard Truss tip (red symbols), and port truss tip (blue symbols).

The Boeing data were checked against a MSFC study of rapid charging events during the period from 2007/027 through 2009/037 [Wright, et al., 2009] to determine if all rapid charging events more negative than 45V in the MSFC study are in the Boeing data set. Seven events were identified that exceed −45V (green symbol) that are missing from the Boeing study. These values are from the original location of the FPMU on the starboard Truss and have not been adjusted by the **v** × **B** • **L** potential to the locations used in the Boeing study. However, they can be directly compared because all seven events occur near the geographic equator where **v** × **B** • **L** effects along the Truss are small. A total of 2,171 eclipse exit charging events are available including the 2164 from the Boeing 2013 study [Boeing, 2013] and the seven additional events from Wright, et al. 2009. Table 7.6-1 provides a summary of the eclipse exit charging events from these studies providing the number of events more negative than −45V and the number of events more positive than 0V.

Figure 7.6-3 also includes all 287 of the sunlight unshunt rapid charging events (yellow symbols) from the 2010 solar array charging experiments and the two on GMT 2013/130 during the ammonia pump repair activities. Charging events more negative than −45V are summarized in Table 7.6-1. Two important points regarding sunlight unshunt rapid charging events are worth emphasizing: (1) the FDIR process currently used to protect the crew in case of a PCU failure during an EVA automatically shunts all eight solar arrays if one of the PCUs is not operational, and (2) the ISS can operate on batteries for only a limited amount of time. Ground control will have to unshunt a subset of the arrays to restart the solar array electrical current collection sometime after the FDIR has been activated. Present flight rules provide no guidelines on when to unshunt the arrays, so there is a risk the operation could be implemented in sunlight, and expose the EVA crew to the large sunlight unshunt rapid charging events. Developing a new flight rule to require the array unshunts to be implemented during night or discontinuing use of the FDIR will eliminate this risk.

Finally, transient positive charging events were also observed on the ISS with maximum potentials often reaching some 10s of volts. Figure 7.6-4 shows examples of three positive charging events from GMT 2010/208. The largest event exceeded 0V for over 200 msec, reaching a maximum potential of approximately +55V. This is the largest positive charging event that has been identified in the FPMU data to date. Additional examples of four transient positive charging events can be seen in Figure 7.6-1c. Maximum potentials from 21 positive charging events (orange symbols) are included in Figure 7.6-3 and Table 7.6-1, including the record event from GMT 2010/208. No attempt was made to identify all positive charging events in the FPMU data records. The values shown in Figure 7.6-3 only provide examples for the range of positive potentials that have been seen on a few dates. The ISS environments community currently has no explanation for origin of these events. It is worth noting, however, that discontinuing use of the PCUs will not protect an EVA crew from the transient positive charging events since the examples included in Figures 7.6-3 and 7.6-4 were all observed when the PCUs were not operating.

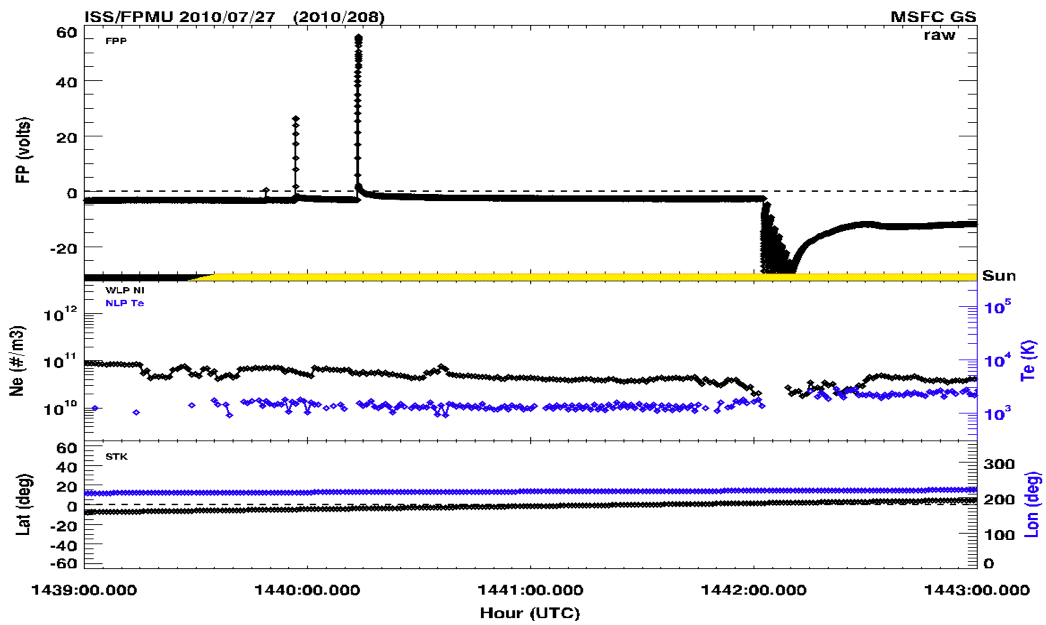

Figure 7.6-4. Positive Charging Events

Example of the positive charging events including the largest observed to date reaching approximately +55V.

Table 7.6-1. Charging Events ≥ 0 and ≤ –45V

Study, location	All Events	Events < -45V	Events > 0V
Boeing, starboard	2164	8	50
Boeing, port	2164	27	77
Boeing, center	2164	1	0
Wright et al., FPMU starboard	7	7	0
Sunlight unshunt, FPMU port	289	288	0
Positive transients	21	---	21

The NESC team emphasizes that Figure 7.6-3 does not represent a complete record of all charging on the ISS or even a carefully designed statistical study of ISS charging using a subset of eclipse exit charging data. The ISS potentials are available only when FPMU is operating and data are available through live telemetry downlink. The period starting 2007/188 through the end of 2013/105 represents approximately 33,117 ISS orbits (based on orbit numbers between the first two-line element set on 2007/188 and the first two-line element set on 2013/106). Only 2,171 eclipse exit charging events are included in the study from this period, which is approximately 6.6 percent of the orbits during the study period.

FPMU operation periods are selected for the engineering purpose they support including PCU operation verification, PIM3.0 charging model studies, plasma hazard analysis for EVA, verifying charging contributions due to visiting vehicles, payload science support, international ionosphere World Day periods, and space weather charging studies. No attempt was made to optimally distribute the FPMU operations to best sample the widest range of eclipse exit conditions in order to obtain a statistically unbiased set of charging data.

Figure 7.6-5 is the first example of auroral charging observed on ISS. The event was captured while the FPMU was running in support of Space Transportation System-123 mission activities at the ISS and automated transfer vehicle docking operations. This charging event cannot be due to solar array electrical current collection because the arrays are not biased at night. Night charging events on the ISS typically are observed at high latitudes during geomagnetic storms consistent with an auroral electron source for the charging currents.

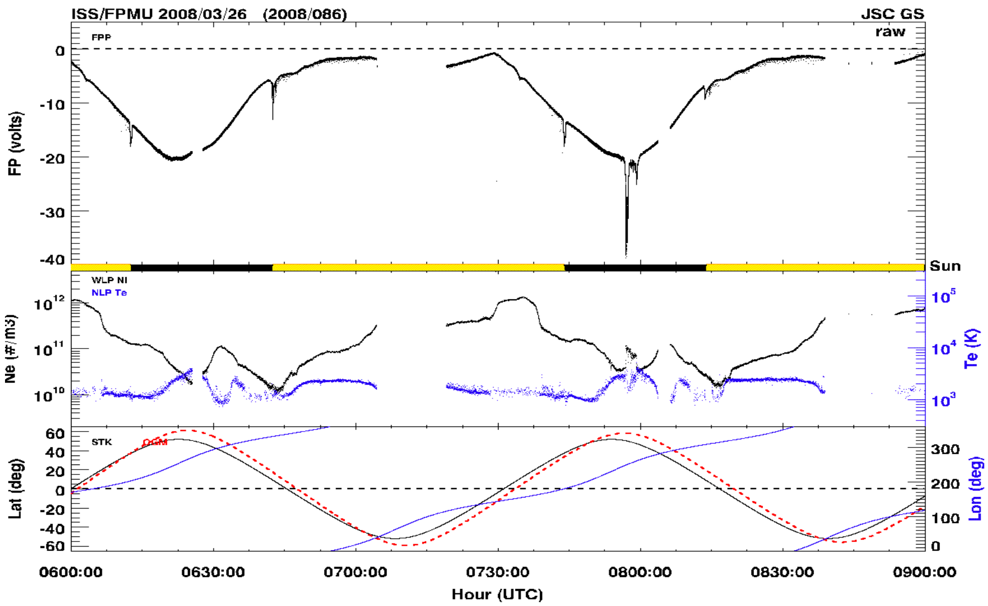

Figure 7.6-5. ISS Auroral Charging

Two ISS orbits showing short periods of solar array charging at eclipse exit and entry superimposed on the **v x B • L** potential oscillation due to the motion of ISS across the Earth's magnetic field. The -37V charging peak just before 08:00 UT is auroral charging at high northern latitudes in the middle of the night. This was the first and to date the largest auroral charging event observed on ISS.

Auroral charging of the ISS vehicle chassis is well-controlled by the PCUs since they are capable of discharging currents up to 10 amps while extreme auroral electrical current densities are typically on the order of 10^{-5} ampere per meter-squared $(A/m)^2$ to 10^{-4} A/m^2 [Cho, et al., 2012]. Electrical current collection from the most extreme auroral conditions should not exceed the capability of the PCUs to discharge the charging current because most of ISS is covered by insulating materials with a relative small area of conductor exposed to the space environment. For this reason, auroral contributions to the ISS frame charging have never been considered a risk for EVA as long as the PCUs are operating.

However, the situation is quite different if the plasma hazard forecast process is used instead of the PCUs to protect the crew from arcing hazards during EVA because auroral charging cannot be predicted using the IRI model and PIM3.0 analysis. IRI is a climatology model which only treats the low energy (~0.1 eV) charged particles that comprise the bulk of the ionosphere plasma, but does not provide information on the currents of high energy (~1000s to 10,000s eV) electrons responsible for auroral charging. Even if the auroral particle flux information was available, the PIM3.0 does not include a module for incorporating the contributions of auroral currents to ISS charging. A decision to discontinue PCU use for protecting EVA astronauts from arcing hazards in favor of the plasma hazard forecast process will leave the crew exposed to negative charging hazards due to the ISS frame charging by the aurora.

Figure 7.6-5 is not only the first auroral charging event observed on the ISS, but is also the largest. The ISS potential increase due to the auroral electron current is more negative by about 17V than the background −20V due to $\mathbf{v} \times \mathbf{B} \bullet \mathbf{L}$. In this case, the net charge at the location of the FPMU where the charging was measured is −37V, which does not exceed the −45.5V limit. However, a similar −17V charging event would result in violations of the −45.5V safety limit for any part of the ISS structure with a potential more negative than −28V. Such a violation might occur, for example, when the ISS exits eclipse at high latitudes where aurora is present such that auroral charging is coincident with the eclipse exit charging. It can be estimated what kind of conditions might lead to these safety violations by consulting the data set used to generate Figure 7.6-3 to see how often charging events with potentials of −28V or more have been observed. There are 55 eclipse exit charging events with negative potentials more negative than −28V at the ISS centerline; 444 more negative than −28V at the ISS port Truss tip and 760 more negative than −28V at the ISS starboard Truss tip. Each of these events would result in potentials on the ISS reaching or exceeding the −45V safety limit. *No analysis has been presented by the ISSP to evaluate the risk trade involved in discontinuing the use of PCUs, which currently control this risk and using the plasma hazard forecast process that is incapable of predicting auroral charging threats.*

While −17V was used in the preceding discussion, there is no reason at this time to believe that auroral charging could not result in higher potentials. Sampling of auroral charging by FPMU has not been extensive due a number of factors. First, FPMU is operating only in campaign mode for limited amounts of time so auroral events may be missed. There has been some effort in recent years to target FPMU operations to capture auroral charging data [Minow, et al., 2010, 2012; Minow and Parker, 2013], but there are still geomagnetic storm periods that are missed due to constraints on operation of the instrument. Second, there is a sampling bias due to the position of an ISS orbit relative to the location of the aurora. Even during geomagnetic storm periods when aurora moves closer to the equator, the ISS may not encounter the aurora because there is a local time dependence on the maximum magnetic latitude along the orbit where aurora is more likely to be encountered. If the highest magnetic latitudes along the orbit are not at the right longitude, then the ISS is unlikely to encounter strong auroral electron particle flux regardless of the strength of the aurora. Finally, auroral activity sampled since FPMU started operations on the ISS has not been that strong because FPMU started operations in late 2006 as the last solar cycle was ending, through the geomagnetic quiet period between the previous and current solar cycle, and through the current relatively low activity solar cycle. The result is that only nine periods during geomagnetic storms with auroral charging have been observed through April 2013 [Minow and Parker, 2013] with one or two additional periods observed later in 2013.

References:

1. Wright, Jr., K.H.; Swenson, C.; D. Thompson, D.; A. Barjatya, A.; S. L. Koontz, S.L.; T. Schneider, T.; Vaughn, J.; Minow, J.; Craven, P.; Coffey, V.; Parker, L.; and Bui, T. (2007): "Initial results from the Floating Potential Measurement Unit aboard the International Space Station," *10th Spacecraft Charging and Technology Conference*, Biarritz, France, June 18-21, 2007.
2. Craven, P.D; Wright, Jr., K.H.; Minow, J.I.; Coffey, V.N.; Schneider, T.A.; J.A. Vaughn, Ferguson, D.C.; and Parker, L.N. (2009): Survey of International Space Station Charging Events, AIAA-2009-0119, *47th AIAA Aerospace Sciences Meeting and Exhibit*, Orlando, Florida, January 5-8, 2009.
3. Minow, J.I.; Wright, Jr., J.H.; Chandler, M.O.; Coffey, V.N.; Craven, P.D.; Schneider, T.A.; Parker, L.N.; Ferguson, D.C.; Koontz, S.L.; and Alred, J.W. (2010): Summary of 2006 to 2010 FPMU Measurements of International Space Station Frame Potential Variations, *11th Spacecraft Charging Technology Conference*, Albuquerque, New Mexico, 20 – 24 September 2010.
4. Boeing (2013): *PIMVar1_results.xls* file, 2013
5. Wright, et al. (2009): Wright, K.H., FPMURapidChargingEvents_KHW_2009Mar02.xls file, 2009.
6. Cho, M., K. Saito, and T. Hamanaga (2012): "Data Analysis of the Polar Plasma Environment for Spacecraft Charging Analysis," *Acta Astronautica*, 81, 160-173, 2012.
7. Minow, J.I.; Pettit, D.R.; and Hartman, W.A. (2012): "Space Weather Monitoring for ISS Space Environments Engineering and Crew Auroral Observations," Abstract IN31D-05 presented at *2012 Fall Meeting, AGU*, San Francisco, California, December 3-7, 2012.
8. Minow, J. I., and L.N Parker (2013): "Space Weather Monitoring for ISS Geomagnetic Storm Studies," *Space Weather Workshop (invited)*, Boulder, Colorado, 16-19 April, 2013.

7.7 Estimate of Likelihood of Auroral Charging for ISS

As discussed in previous inputs to the ISS EVA Charging Study, the aurora have been observed to cause charging of bodies in low altitude orbit from −100 to −2,000V. Such charging events are relatively infrequent, as discussed below. However, the events are typically of short duration (e.g., ~10 seconds to 1 minute typically) and up to 3 minutes on one occasion (Minow, private communication). Solar lighting, seasonal variations in the ionospheric density, geomagnetic activity, and plasma wake shadowing are known to contribute to the event likelihood. For EVAs, the main requirements are the presence of the ISS in the auroral zone, the encounter with an auroral arc, and the shadowing (i.e., from sunlight and the ionospheric plasma) of the astronaut. One method to estimate the probability of the astronaut experiencing an auroral charging event is a Monte Carlo simulation taking into account these variable conditions. However, for the purposes of this assessment, such a detailed analysis is not appropriate. Rather, a first order estimate on the upper limit of the hazard was derived.

Upper Bound on Auroral Charging Hazard

As shown in Figure 7.7-1 [Evans, 2012], the auroral zone forms a roughly ellipsoidal pattern around the Earth's magnetic poles oriented in local time. The maximum probability of encountering an auroral arc (assumed here to occur in the form of roughly longitudinal arcs ~60 km in latitudinal thickness) is 0.01 (for a 1-degree × 8-arc minute bin in Figure 7.7-1) near 65 degrees geomagnetic latitude and 21 hours local time. The equatorward extension of the auroral zone is ~60 degree-geomagnetic. This corresponds to geographic latitude of ~49 degrees as the Earth's magnetic field is inclined ~11 degrees to the geographic pole. Thus, the ISS needs to be both poleward of ~49 degree-geographic latitude and approximately in the longitude sectors near ~70 degrees W (North Pole) and ~110 degrees E (South Pole). This "auroral charging" region, in geomagnetic coordinates, is marked by the red ellipse in Figure 7.7-1. Figure 7.7-2 [Anderson, 2005] shows the locations of observed Defense Meteorological Satellite Program (DMSP) auroral charging events superimposed on the ISS orbit (Note: the DMSP data are skewed because of various data collection and temporal selection issues) in geographic coordinates—the blue rectangles mark the approximate regions of ISS charging. A simple estimate of the ISS orbit indicates that it has a probability of ~0.16 to 0.18 of being poleward of 49 degrees for a given orbit. A similar analysis gives a fractional probability of ~0.13 for the ISS to be within the longitude range of the auroral zone. Since the two events are independent of each other, the probability of being in the auroral charging region is given by the product of their respective probabilities. That is, the ISS will likely "on the average" encounter the lower edge of the auroral charging zone with a probability, P_E, of (0.13 × 0.16 =) ~0.02 during an orbit. Further, Evans estimates that at least one 10-second duration active auroral arc will be encountered with a probability of 0.1 for a single orbit crossing the auroral zone [Evans, 2012].

Since the ISS skirts the equatorward edge of the auroral zone rather than passing through it, it is assumed that a more conservative estimate of the probability, P_{AC}, of encountering a 10-second duration arc would be between 0.0001 to 0.001 for a single ISS passage through the auroral zone based on Figure 7.7-1.

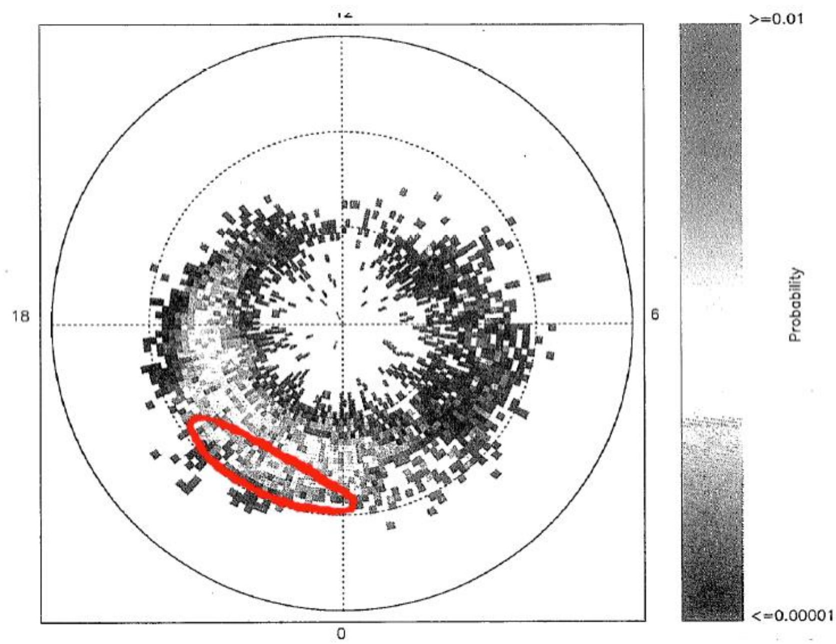

Figure 7.7-1. Absolute probability of encountering a large energy flux event/aurora as a function of corrected geomagnetic latitude and local time for a satellite. Latitude scale is from 45 to 90 degrees magnetic [Evans, 2012]. The red ellipse marks the approximate region where one would expect to see ISS charging.

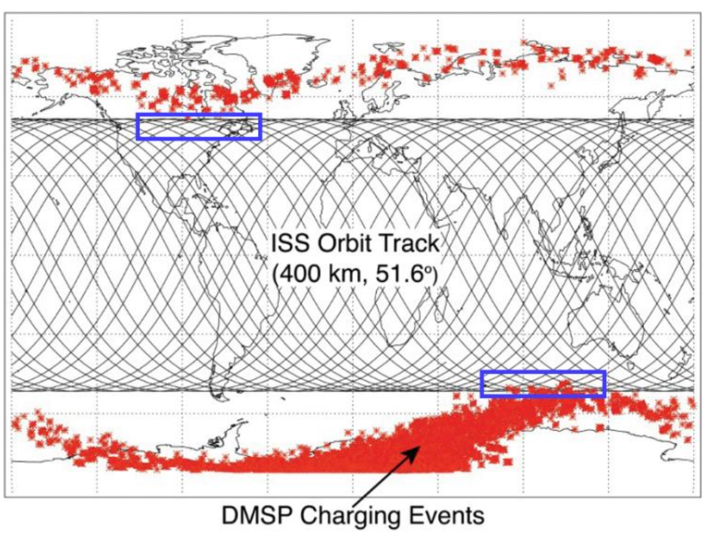

Figure 7.7-2. The ISS orbit track over 24 hours and the locations (red) of DMSP charging events of less than -100V [Anderson, 2005]. The rectangles mark the approximate regions where one would expect to see ISS charging.

If an EVA were ~6 hours, then that would be ~4 orbits. Assuming that the ISS will encounter the auroral zone twice (North or South) during a single orbit, the total probability, P_T, for 4 orbits would be given by $P_T = P_E*(1-(1-P_{AC})^{2*4}) \sim 0.02*2*4*P_{AC}$ for a probability of $P_T \sim 1.6 \times 10^{-5}$ to

1.6×10^{-4} for an arbitrary 6-hour EVA. Mitigating this concern, however, would be the previously mentioned issues of the astronaut being in both sunlight and plasma shadows. The solar wind conditions can be used to give up to a 40-minute warning of pending auroral activity or the use of Kp (or even "looking out the window" to see if aurora are in progress) to either terminate or abort an EVA further limiting the threat of auroral charging.

Conclusion

While it is strongly encouraged to carry out a much more thorough "Monte Carlo" analysis of the likelihood of encountering a 10-second duration auroral arc, the preceding estimates put an upper bound on the probability of 1.6×10^{-5} to 1.6×10^{-4} for a 6-hour EVA. Seasonal, solar cycle, and "shadowing" issues will further significantly change the estimate—the latter requirement for "shadowing" will greatly reduce the number, but currently there is no way to estimate that factor as it is "mission-dependent." Finally, terminating or avoiding EVAs based on forecasting or monitoring of auroral conditions could be used to further limit the concern of auroral charging.

References:

1. Evans, D. S. (2012): "A Study of Intense Auroral Electron Precipitation Events," *Space Environments Laboratory*, NOAA, Boulder, Colorado, personal communication, 2012.
2. Anderson, P. (2005): "Spacecraft Charging Hazards In Low-Earth Orbit," *9th Spacecraft Charging Technology Conference*, 2005.

7.8 PCU Capability to Maintain the ISS Near to Space Plasma Potential

7.8.1 PCU IV Characteristic versus FP Mitigation

The PCUs make EVA safer for the astronaut under negative conditions including rapid charging events and frame charging due to aurora. The discussion below shows that the PCU has the ability to maintain the ISS chassis potential within 15V of the local space plasma for all conceivable conditions because the plasma contactor can emit electron currents two orders of magnitude greater than the largest emission currents observed to date on the ISS. The PCU is capable of emitting currents greater than the sum of all possible plasma currents to the station, an extreme "worst-on-worst" upper bound. The PCU is capable of controlling the ISS potential for all planned future ISS configurations.

$$A_{cell} := 0.08\ m \cdot 0.08\ m = 0.006\ m^2$$

$$A_{panel} := 200 \cdot A_{cell} = 1.28\ m^2$$

$$A_{blanket} := 82 \cdot A_{panel} = 105\ m^2$$
$$A_{wing} := 2\ A_{blanket} = 210\ m^2$$

$$A_{array} := 8 \cdot A_{wing} = 1679\ m^2$$

The maximum electron current that the ISS could possibly collect is when all the array surfaces were facing the ram in the highest density ionosphere and the total array solar cell area were collecting as if it were entirely exposed conductors. This is an extreme upper bound because the solar cells top surfaces are insulating cover glass. The solar array has eight wings, with each wing having two flexible blankets with solar cells. The blankets consist of 82 live panels with 200 8-cm × 8-cm cells. Thus, the mathematical upper bound on the electron collecting area is less than 1700 m^2.

The electron thermal current, j_{th}, is a function of the plasma electron temperature, T, and density, n:

$$j_{th}(n,T) := e_{charge} \cdot n \cdot \sqrt{\frac{e_{charge} \cdot T}{2 \cdot \pi \cdot m_e}}$$

where m_e is the electron mass and e_{charge} is the charge on an electron. The electron current collected in worst-case ionosphere environment is around 20 ampere (A).

$$n_e := 1 \cdot 10^{12}\ m^{-3}$$
$$T_e := 0.2\ V$$
$$j := j_{th}(n_e, T_e) = 0.012\ \frac{A}{m^2}$$
$$I_{array} := j \cdot A_{array} = 20\ A$$

This is an unrealistically high worst (maximum collecting area) on worst (maximum electron current density) upper bound on the electron current. This upper bound is almost 40 times larger than the largest PCU currents observed to date, 0.575 A PCU 1 + PCU 2, measured on orbit [Koontz, 2013 private communication].

Prior to flight, the plasma contactor hollow cathode was subject to a 28,000-hour life test in a vacuum chamber [Sarver-Verhey, 1997]. The test was conducted at 12A emission current. As shown in Figure 7.8-1, the PCU I-V trace is essentially vertical at 10A. Hollow cathodes of essentially the same design are qualified for and routinely run in electric propulsion thrusters at more than 13A continuous emission current. For brief periods, several minutes at a time, the PCU hollow cathode is able to emit more than 20A without damage (Goebel[2]).

2 Goebel, Dr. Dan, JPL Hollow Cathode Expert.

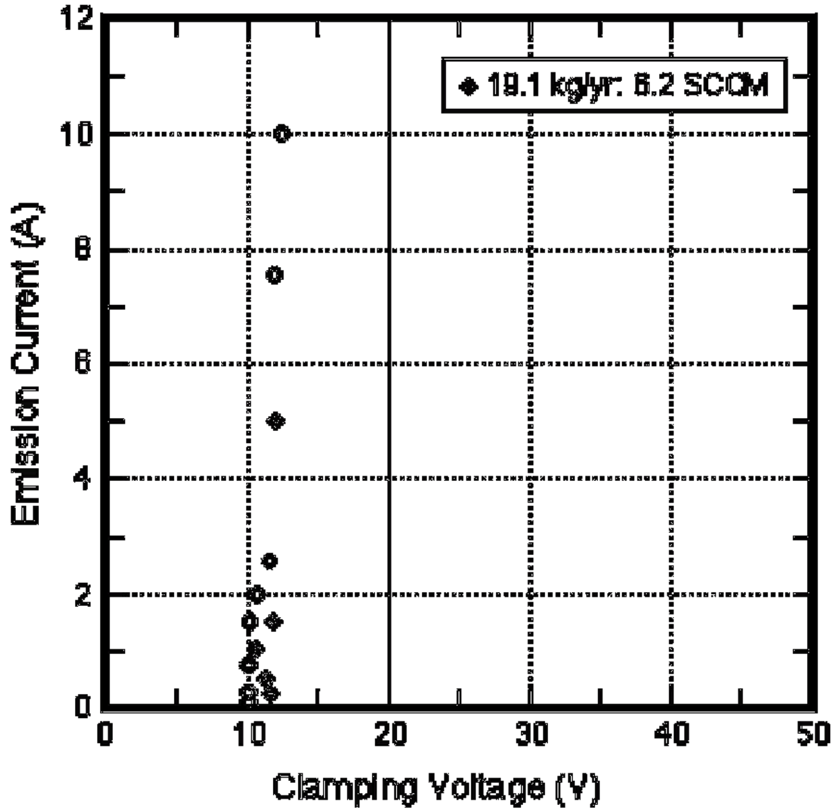

Figure 7.8-1. Plasma Contactor Emission Current Measured in a Ground Test Chamber as a Function of Voltage

The NESC team's conclusion is that PCU is capable of emitting orders of magnitude greater electron currents than has been needed to date on the ISS and that the device is capable of handling the even worst-case upper bound electron currents from worst-case environments.

References:

1. Koontz, Steve (2013): "PCU_emission_currents_2010_through_2013.xlsx," private communication.
2. Sarver-Verhey, T.R. (1997): "28,000 Hour Xenon Hollow Cathode Life Test Results," IEPC-97-168, *25th International Electric Propulsion Conference*, Cleveland, Ohio, August 24-28, 1997.

7.8.2 PCU Operational Life

The on-orbit PCUs both satisfy the two necessary conditions for long life. First, both PCUs have enough xenon to last well past 2028. The chart in Figure 7.8-2 from "Plasma Contactor Unit (PCU) – Status," [Kaminski and Scudder, 2013] was used to estimate that each EVA uses about 65 gram (gm) of xenon.

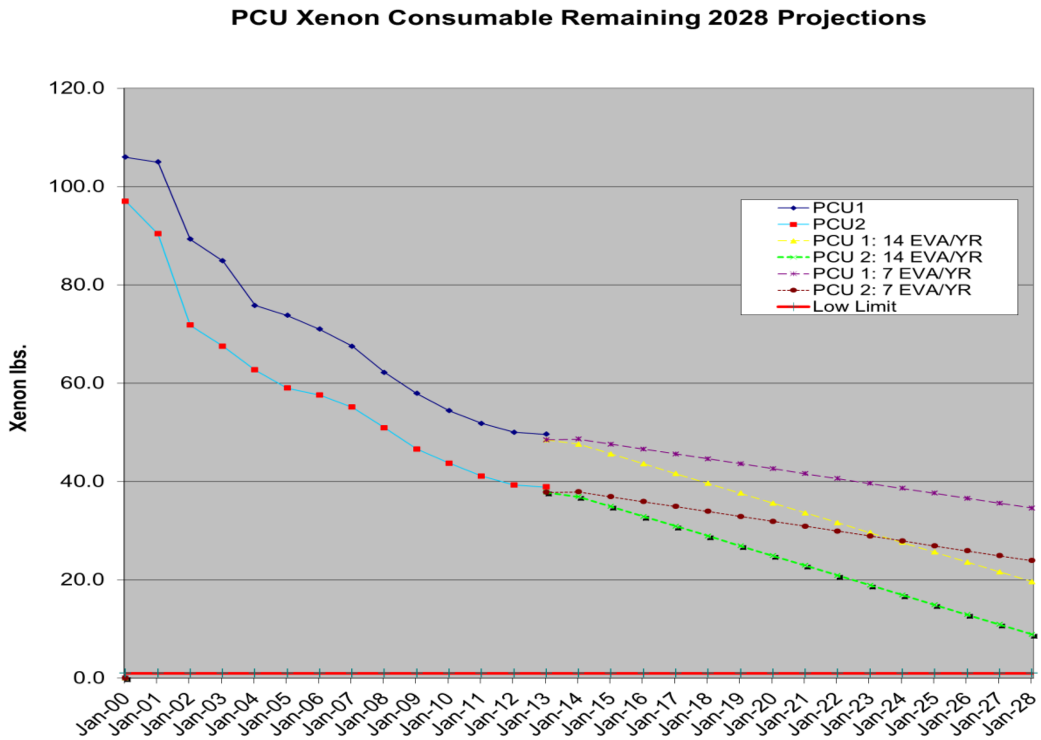

Figure 7.8-2. Xenon Usage Projections

Kaminski and Scudder's lowest estimate of remaining xenon is that PCU2 may have 37 pounds remaining in the tank, about a pound less than shown in Figure 7.8-2. Based on the charts in that presentation and the worst-case assumption of 14 EVAs per year, the remaining xenon will last an additional 18 years, or through 2031. In the calculation below, the xenon mass used for an EVA, M_{EVA}, is estimated from the slope in Figure 7.8-2. M_{PCU2} is the estimated mass of xenon remaining in the PCU2 tank.

$$M_{EVA} := \frac{20\ \mathbf{lb}}{10 \cdot 14} = 0.065\ \mathbf{kg}$$

$$M_{PCU2} := 36.93\ \mathbf{lb}$$

$$\frac{M_{PCU2}}{\frac{14}{\mathbf{yr}} \cdot M_{EVA}} = 18\ \mathbf{yr}$$

The second requirement is that the PCU hardware, in particular the hollow cathode assembly, has sufficient life to process the xenon remaining in the tank. The low side of the nominal xenon flow rate is 6 standard cubic centimeters per minute. The lowest rate can be chosen because it requires the longest hollow cathode life.

$$m_{dot} := 6.0 \frac{cm^3}{min} Loschmidt \cdot m_{Xe} = 0.6 \frac{mg}{s}$$

From this, calculate the total time per EVA that the plasma contactor is operated.

$$t_{EVA} := \frac{M_{EVA}}{m_{dot}} = 31 \; hr$$

From Figure 7.8-2, it is estimated the PCU1 was loaded with 48 kilograms of xenon. The PCU would have to operate for 22,000 hours to process that much xenon.

$$\frac{48 \; kg}{m_{dot}} = 22597 \; hr$$

The plasma contactor hollow cathode assembly was qualified prior to flight with a 28,000-hour life test in a vacuum chamber [Sarver-Verhey, 1997]. Since then, similar hollow cathode assemblies have operated for long periods without any difficulty. The NASA Solar Technology Application Readiness (NSTAR) ion thruster has two similar cathodes. The NSTAR Extended Life Test was run for 30,000 hours before ending due to programmatic constraints [Sengupta, et al., 2004]. During the Deep Space 1 flight mission, the NSTAR thruster accumulated 16,265 hours before the mission ended [Rayman, 2003]. The neutralizer hollow cathode used on the NASA Evolutionary Xenon Thruster (NEXT) ion thruster is the same design as the ISS PCU. The NEXT thruster recently successfully completed a 48,000-hour life test [NASA, 2013b]. This is more than twice the worst-case required hollow cathode life.

References:

1. Kaminski, R.; and Scudder, M. (2013): *Boeing ISS EPS*, September 2013.
2. Sarver-Verhey, T.R. (1997): “28,000 Hour Xenon Hollow Cathode Life Test Results,” IEPC-97-168, *25th International Electric Propulsion Conference*, Cleveland, Ohio, August 24-28, 1997.
3. Sengupta A.; Brophy J.R.; Anderson J.R.; and Garner C. (2004): “An Overview of the Results from the 30,000 Hour Life Test of the Deep Space 1 Flight Spare Ion Engine,” AIAA Paper 2004-3608, *40th Joint Propulsion Conference*, Ft. Lauderdale, Florida, July 11-14, 2004.
4. Rayman, M.D. (2003): “The Successful Conclusion Of The Deep Space 1 Mission: Important Results Without a Flashy Title,” *Space Technology 23*, Nos. 2-3, p. 185, 2003.
5. NASA (2013b): Press Release 13-193 “NASA Thruster Achieves World-Record 5+ Years of Operation.” June 24, 2013.

7.9 EMU Exterior Metal Parts

This section summarizes the EMU (U.S. suit) exterior metal parts that may pose an entry point into the astronaut’s body either by direct contact with a charged metal surface (of the ISS) or a plasma contact so that two of them can cause or permit electrical current flow in the astronaut’s body.

Table 7.9-1 lists the name, material, coating/covering, isolation ohms, probability of failure and comments for every entry point. The table title permits listing a material (i.e., stainless steel or Al) and a coating (e.g., anodize or paint or uncoated stainless steel), but that information is difficult to find and is not listed here.

It can be seen in Section 7.10 that the specific materials are not used in the calculations and they are not listed in Table 7.9-1.

Table 7.9-1 contains word descriptions of the relative importance of the various items listed. Refer to Figures 6.3-9 and 6.3-10 to illustrate the listed entry points. “Covering flap” means that the suit material covers the named metal, and there will be little or no plasma contact. Superscripts refer to the references presented after the table.

The NESC team decided to use the neck ring as the plasma contact entry and the waist ring as the ISS conductive entry to provide a current path through the thorax of the astronaut for worst-case calculations. The NESC team considered that the *International Space Station (ISS) Probabilistic Risk Assessment (PRA) EVA Shock Update and Summary* has assumed contact with all possible external metal contact points [Duncan, 2013]. These have all been covered with flaps of material as can be seen in the various photos of the EMU. The contact point material (anodize or paint or stainless steel) does not matter.

- Isolation of MMWS Components:
  - Implementation to reduce electrical current paths
- Isolation of interface receptacles using non-conductive materials:
  - Kapton® film acts as a dielectric membrane between Al baseplate and stainless steel receptacles
  - Hard anodized washers are used to isolate conductive paths through fasteners
- Testing and validation:
  - Isolation checks
  - Mechanical stress test

Table 7.9-1. EMU Metal Entry Points Summary

#	Name	Material (Coating & Covering)	ISS Contact? Per NESC team usage	Pfail[2] (Ranking for ISS contact)	Plasma Contact?	Comments, References and NESC team action
1	Scye Bearing[1] SB[2]	covering flap	Less likely than waist bearing	0.00000 (8, 11)		
2	Arm Bearing[1] AB[2]	covering flap	Less likely than waist bearing	0.00025 (5)		
3	Wrist Bearing[1] (or Wrist Ring)	covering flap	Less likely than waist bearing	0.006 (1)		
4	Waist Bearing WB[2]/ D-Rings[1]	covering flap		0.003 (4)	Considered most likely as plasma contact	(is sometimes "waist ring", or WR)
5	Thigh Disconnect[1]TD[2]	covering flap	Less likely than waist bearing	0.005 (2 & 3)		
6	Ankle Disconnect[1]AD[2]	covering flap	Less likely than waist bearing	0.001 (6 & 7)		
7	Body Seal Closure-(BSC)/MMWS Connection[1]	covering flap	BSC equally likely to waist bearing	0.001 (6 & 7)	Considered most likely as plasma contact	MMWS isolated[1]
8	Neck Ring[1]NR[2]		Less likely than waist bearing	0.00000 (8, 11)		Reference 2 states probability of ISS contact is 0.00000; and plasma contact to NR lower than BSC or WR.
9	Helmet Purge Valve[1]HPV[2]	covered with white		0.00000 (8, 11)		No outside exposure
10	CCA[3]	no outside exposure	N/A	0.00000 (8, 11)		No outside exposure
11	*OBS/DCM[2]	insulated and electrically isolated	N/A	0.005 (2 & 3)		>50 megohms per Ref [3]
12	(not EMU) Any ISS damaged anodize[2]	Most of the ISS exterior metal has been anodized	Consider only direct contact for EMC/ astronaut hazard assessment	0.01 (rank is high)	N/A	One part of EMU must touch this for Damage probability

#	Name	Material (Coating & Covering)	ISS Contact? Per NESC team usage	Pfail[2] (Ranking for ISS contact)	Plasma Contact?	Comments, References and NESC team action
13	(not EMU) Any ISS exposed stainless steel	Lots of bits and pieces (nuts & bolts; solar array tensioners and other unlisted items.	Consider only direct contact for EMC/ astronaut hazard assessment	0.01 (rank is high)	N/A	One part of EMU must touch this for damage probability

1. ISS-NCR-232F (2012): *Lack of Two-fault Tolerance to EVA Crew Shock in the Low Earth Orbit Plasma Environment*, 1/31/2012, Boeing ISS System Safety, Joseph E. Thomas, originator. Pages have Tracking Number: (blank), "International Space Station Safety Noncompliance Report (NCR)," Date: 1/26/12.
2. Duncan, G. (2013): Document DRD-MAPI-SA-06-ISSPRA-12-56, EVA Shock Update and Summary, International Space Station (ISS) Probabilistic Risk Assessment (PRA) Trade Study – Long Form, ISS-PRA-12-56 (Probability Risk Assessment Doc), Prepared by Gary Duncan, dated May 17, 2013.
3. Castillo, M.; PPT "Modular Baseplate Assembly/Body Restraint Tether/Handrail Electrical Continuity Test", ONE EVA, 05/04/10.

The Material column contents are only outlined as rough descriptions of the coating and covering. The probability of failure is shown in the Pfail column as contained in ISS-PRA-12-56.

*OBS/DCM (Display and Control Module) is located above the BSC with the MMWS.

Figure 7.9-1 shows the communications carrier assembly (CCA) [Duncan, page 7, Figure 2, 2013]. The CCA is a fabric cap worn by the astronauts with microphones and speakers for use with the radio. It allows hands-free radio communications within the suit. It seems to have no external connections, but the ISS-PRA-12-56 implies that there is a connector that is exposed on the outside of the EMU. The CCA probability of contact with the ISS chassis is rated in the ISS-PRA-12-56 as 0.00000. Figure 7.9-1 also shows visible wrist rings before attaching gloves.

Photo Courtesy NASA

Figure 7.9-1. EMU Photo. Note CCA –a cap with microphone and speakers. Note visible wrist rings before attaching gloves.

Figure 7.9-2 is another EMU photo that also shows the exposed wrist ring before the covering flap is positioned over the ring. Note on the right that the covering flap leaves no exposed wrist ring for contact with space plasma; other details can also be seen.

Figure 7.9-3 is a photo of a suited astronaut. Additional EMU pictures to support this section are included in Appendix E.

Photo Courtesy NASA

Figure 7.9-2. EMU Photo

Figure 7.9-3. Suited astronaut: EMU upper part (picture source unknown). Some details of wrist, EMU tether lower right and equipment/tool tether (right) shown.

Reference:

1. Duncan, G. (2013): Document DRD-MAPI-SA-06-ISSPRA-12-56, EVA Shock Update and Summary, International Space Station (ISS) Probabilistic Risk Assessment (PRA) Trade Study – Long Form, ISS-PRA-12-56 (Probability Risk Assessment Doc), Prepared by Gary Duncan, dated May 17, 2013.

7.10 Reassessment of the Positive Voltage EVA Hazard

The upper bound electron collection currents that could flow through an astronaut as a result of low positive potentials are less than 1 mA. This is an order of magnitude lower than the lowest currents in ISS-NCR-232F [Kramer, et al., 2010], and may not be hazardous.

The changes to the EMU outlined in the "NESC_ISS_Shock_EVA_Actions.pptx" (provided in Appendix D) have eliminated almost all electrical current paths for electrons collected from the ionosphere to flow through the astronaut's torso to the ISS structure ground [Roeschel, 2013]. A single, highly improbable electrical current path has been identified. Maximum currents through this path for both solar max and solar min are shown to be less than 1 mA. Based on these calculations, it is suggested revisiting the question of whether plasma currents from low positive voltages are an EVA hazard. The analysis does not consider whether a hazard exists when there are large negative potentials on the ISS and the plasma contactor is not operating and merely assumes these conditions for conservatism.

Analysis

Under normal conditions, since the astronaut's tether has an insulating segment, there is no electrical contact between the astronaut and potentials on the ISS [Roeschel, 2013]. However, in the unlikely case that the tether is in electrical contact with a ring on the EMU, then electrical current could flow through the astronaut to another anodized ring exposed to the plasma and back through the plasma, as shown in Figure 7.10-1.

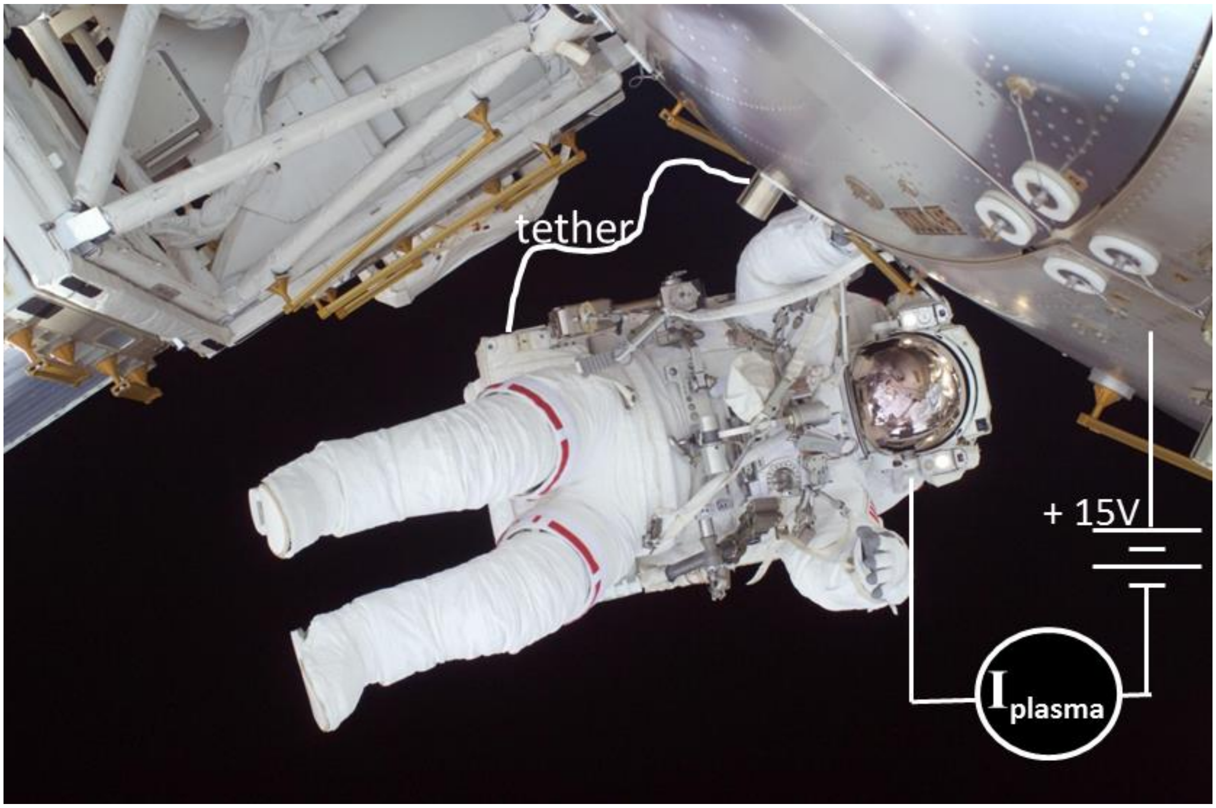

Figure 7.10-1. Circuit where the Astronaut is ~15V Positive with Respect to the Surrounding Plasma

This requires physical contact of the bare metal tether with a suit ring whose fabric cover has been inadvertently displaced (see Figure 7.10-2) on the stainless steel bearing ring, not an anodized ring. Electron current can be collected when the potentials on the EMU are positive with respect to the ionosphere plasma, such as those possible due to the station's motion across the Earth's magnetic field when the plasma contactor is operational. Following Kramer, et al., the extreme worst-case positive potentials possible in this scenario are the order of approximately +15V, and such potentials can only occur outboard of the SARJ [Kramer, et al., 2010].

Figure 7.10-2. Example of an exposed section of the stainless steel wrist bearing ring directly above the blue anodized ring [Roeschel, 2013]. Normally both rings are covered by suit fabric.

Electrically, the circuit is represented schematically in Figure 7.10-3. Positive potential generated at the end of the truss by the ISS's orbital motion is carried to the suit by the tether contacting the waist ring. This positive potential goes through the astronaut's torso and appears on the exposed, anodized neck ring. This scenario also assumes there are flaws in the anodization on the interior of the suit, and electrical current flows through sweat-soaked garments through the torso, not around it. Calculations below exclude electrical current collection by modular base plate because the data presented by Castillo (provided in Appendix D) showed it was electrically isolated from the rest of the EMU.

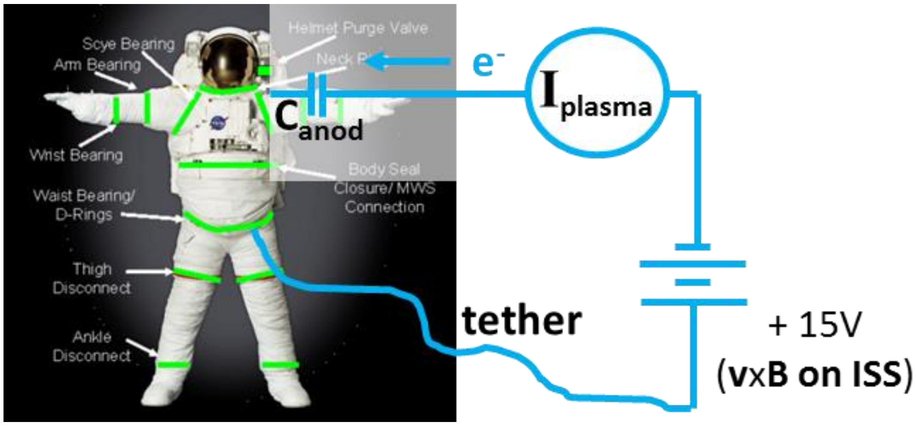

Figure 7.10-3. Electrical equivalent circuit. The only metal surface always exposed to the ionosphere is the neck ring, which has an insulating coating. (EMU figure from ISS-NCR-232F).

The electron current that flows is limited by the electron current collected from the ionosphere by the exposed section of the EMU neck ring. To estimate the collection, approximate the exposed area of the ring as a strip 1-inch wide by 1-foot long.

$$A_{ring} := \frac{1}{12}\, ft^2 = 0.008\ m^2$$

The simplest estimate of the current an object can collect from a plasma is to assume that every electron that conservation of angular momentum would not prevent from being collected is collected. This an upper bound, called "Orbit Limited Collection" to the actual currents collected by complex objects in a dense plasma where potentials on nearby dielectric materials, shadowing by other objects, and space charge effects can dramatically limit the current. For symmetrical conductors floating in space, three different expressions, shown in Figure 7.10-4, can be used to estimate the orbit limited upper bound current depending on the relative dimensions of the object. In the figure, the abscissa is the potential on the object divided by the electron temperature and ordinate in the plot labeled "Current" is the current density to the object divided by the electron thermal current density. For a long, thin object (e.g., the neck ring), the cylindrical probe approximation is appropriate.

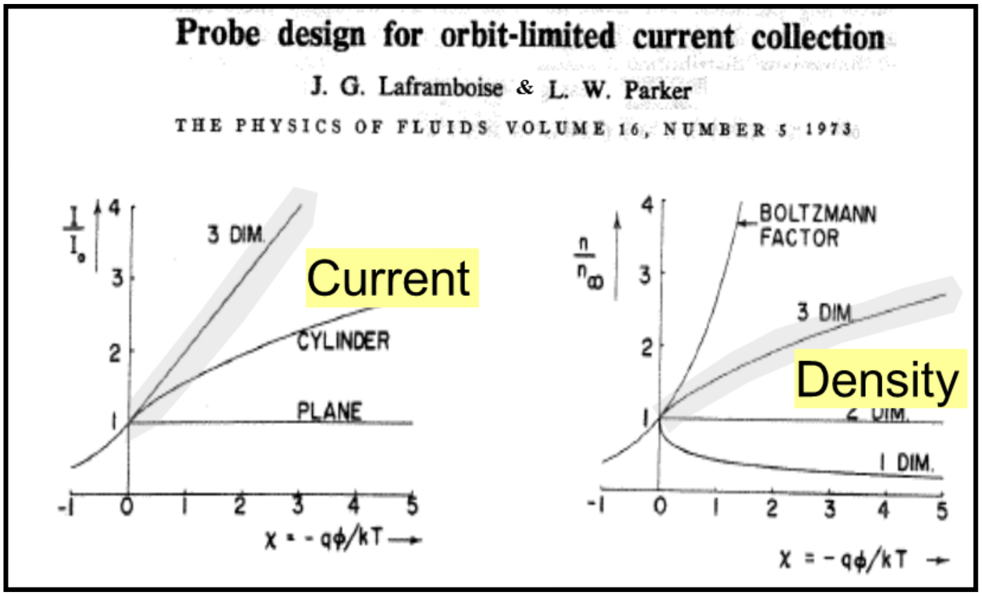

Figure 7.10-4. Plasma Current Collection for Spherical (3-DIM), Cylindrical, and Planar Probes [Hamilton and Kramer, 2007]

Following J.E. Allen, “Probe Theory – The Orbit Motion Approach,” Physical Scripta. Vol. 45, 497-503, 1992, the collected current in terms of the one-sided electron thermal current density, the area of the collecting surface, and the applied dimensionless potential can be written [Allen, 1992].

$$I_{cylinder} = 2\pi\, n\, r_p\, l\, e \left(\frac{kT}{2\pi\, m}\right)^{1/2} \frac{2}{\sqrt{\pi}} \left(1 + \frac{eV_p}{kT}\right)^{1/2}$$

$$= j_{th} A_{cylinder} \frac{2}{\sqrt{\pi}} (1+\chi)^{1/2} \qquad \chi \equiv \frac{eV_p}{kT}$$

where the one-sided electron thermal current is defined as

$$j_{th}(n,T) := e_{charge} \cdot n \cdot \sqrt{\frac{e_{charge} \cdot T}{2 \cdot \pi \cdot m_e}}$$

Fortunately, the ISS FPMU [Wright, et al., 2008] has a cylindrical probe, narrow-sweep langmuir probe (NLP), with dimensions similar to that of an anodized ring. One way to test the cylindrical formula’s applicability is to compare the calculated current using it with the actual electron current measured by the NLP.

The NLP, shown in Figure 7.10-5, is one of the instruments on the ISS FPMU.

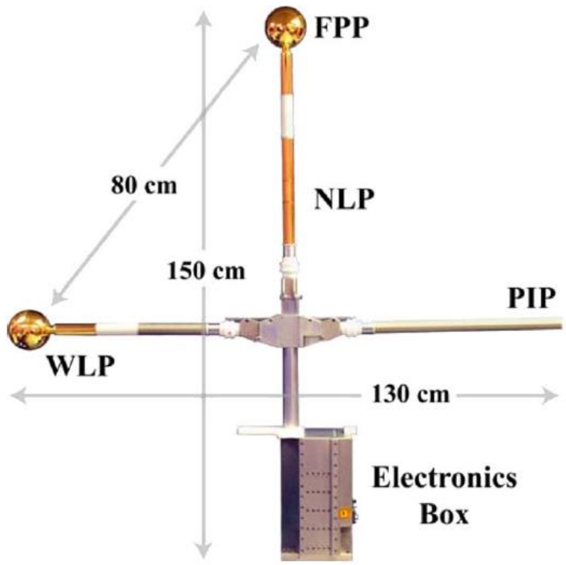

Figure 7.10-5. Diagram of FPMU in its Deployed State with Indicated Dimensions [Wright, et al., 2008]

The NLP is a gold-plated cylinder with a radius of 1.43 cm and length of 5.08 cm. Its area is 0.005 m^2, a little over half the team's estimate of the exposed anodized area of the neck ring. An electron current collection curve is shown in Figure 7.10-6.

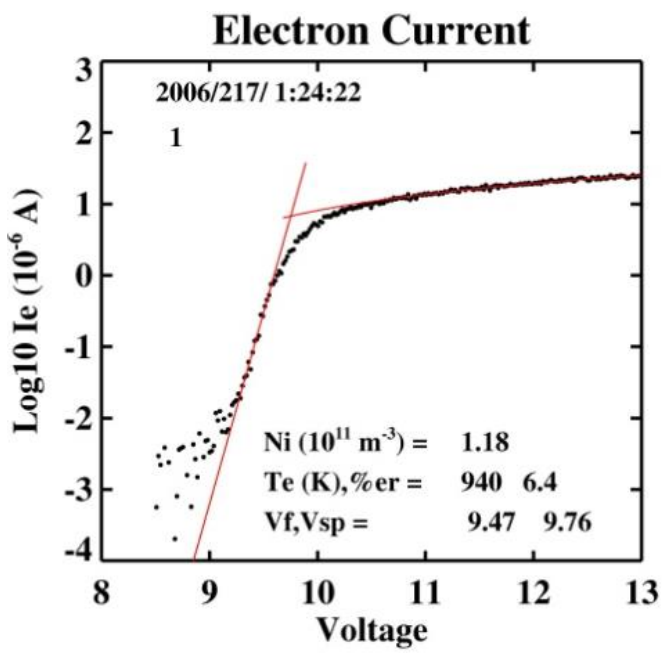

Figure 7.10-6. An NLP Electron Current as a Function of Voltage [Wright, et al., 2008]

Using the parameters in the figure and the cylindrical orbit limited collection formula the electron collection at the highest potential is 31 (microampere) μA about 50 percent higher than the 20 μA measured current shown in Figure 7.10-6.

$$n := 1.18 \cdot 10^{11}\ m^{-3} \qquad T_e := \frac{940}{11604}\ V$$

$$j_{th}(n, T_e) = (9.003 \cdot 10^{-4})\ \frac{A}{m^2}$$

$$\phi := (13 - 9.47)\ V = 3.53\ V$$

$$A_{probe} := 2\ \pi \cdot (1.43\ cm) \cdot 5.08\ cm = (4.564 \cdot 10^{-3})\ m^2$$

$$I_{probe} := A_{probe} \cdot j_{th}(n, T_e) \cdot \frac{2}{\sqrt{\pi}} \left(1 + \frac{\phi}{T_e}\right)^{\frac{1}{2}} = 31\ \mu A$$

As expected, the current to the probe, I_{probe}, calculated using orbit limited theory is larger than the measured probe current because orbit limited theory, as discussed above is an upper bound. More accurate formulations that take into account the effect space charge (finite Debye length) would reduce the calculated current.

Using worst-case solar max plasma environment and worst-case **v × B • L** potential from in ISS-NCR-232F (Attachment 8), the upper bound, orbit-limited collection current is less than 1 mA.

$$n := 10^{12}\ m^{-3} \qquad T_e := 0.1\ V$$

$$\phi := 15\ V \qquad A_{ring} := \frac{1}{12}\ ft^2 = 0.008\ m^2$$

$$I_{ring} := A_{ring} \cdot j_{th}(n, T_e) \cdot \frac{2}{\sqrt{\pi}} \left(1 + \frac{\phi}{T_e}\right)^{\frac{1}{2}} = 0.91\ mA$$

The currents listed in ISS-NCR-232F/Attachment 8 for these conditions are as much as 50 times greater than this upper bound value (see Figure 7.10-7).

Modified-MMWS Maximum Currents				
V=15volts		T_e=0.1eV		$n_e=1\times10^{12} m^{-3}$
		Collect Electrons		
		A 0.3m²	B 0.031m²	C 0.3m²
Contact Structure Ground	A	×	5.2mA	20.1mA
	B	45.4mA	×	21.4mA
	C	20.1mA	4.7mA	×

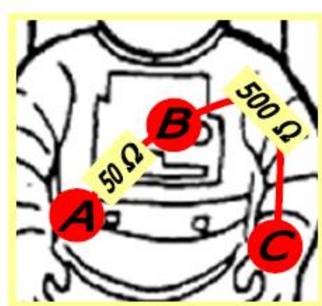

Figure 7.10-7. EMU Currents Post MMWS Modification [ISS-NCR-232F, Attachment 8, 2012]

Discussion

The calculation above gives very much lower electrical current values than used in ISS-NCR-232F for the particular case of the plasma contactor operating, the station experiencing a maximum **v × B • L** potential, and the astronaut at the extreme end of the truss. The calculated current, while significantly low, is probably an extreme overestimate because it is for a conducting cylinder sticking out in a plasma without any surrounding dielectrics to impede electron collection.

As is pointed out by Kramer, et al., 2008, because of surrounding dielectrics, the ISS solar array does not collect like the simple, orbit-limited theory. The ISS solar arrays collect much less electrical current than the model above would have predicted. For the solar array, the dielectrics reduced the electrical current by more than an order of magnitude. It can be expected dielectric on the suit as the same order of reduction in EMU currents compared with the upper bound calculated above.

Another issue is the duration of the current. The value above is for the peak electrical current to the neck ring surface. Since the outer surface of the neck ring is insulating, it acts as a capacitor (Figure 7.10-3). In the calculation below, it can be assumed the coating is thin anodization. This is a worst-case for the charging time because it was assumed that a very thin coating and anodization has a very high dielectric constant.

$$d_{anod} = \left(1.27 \cdot 10^{-5}\right)\ m$$
$$\kappa = 6.7$$
$$C_{anod} := \frac{\kappa \cdot \varepsilon_0}{d_{anod}} = \left(4.671 \cdot 10^{-6}\right)\ \frac{F}{m^2}$$

The collected current reduces the voltage that is seen by the plasma. For the values above the timescale for the current to flow is less than one millisecond. Over that timescale, the average current is about half the calculated peak current.

$$\frac{\phi}{\left(\dfrac{I_{ring}}{C_{anod} \cdot A_{ring}}\right)} = 0.9\ ms$$

With respect to DC collection on the EMU, two factors combine that virtually eliminate any hazard from this type of collection. First, applying the appropriate plasma models (as discussed above) significantly reduces calculated current collection. Second, the electrical isolation of the MMWS (i.e., tool belt) radically reduces the area of exposed bare metal on the EMU. The reduction in collection areas is described in “NESC_ISS_Shock_EVA_Actions.pptx” (provided in Appendix D) [Roeschel, 2013]. Combining realistic current collection scenarios with a very small area of exposed bare metal on the EMU will result in an extremely small DC current collected by the EMU.

The accuracy of the analysis above includes many assumptions and approximations. It is beyond the scope of this task to perform a more accurate and detailed investigation. However, the above analysis shows that even a calculation that assumes that the neck ring collects like a cylinder floating in the ionosphere, rather than a sphere, marginalizes any astronaut hazard due to **v × B • L**-induced positive potentials when the PCU is operating. Accounting for the nearby dielectric suit surfaces and the actual EMU geometry will further reduce the currents collected. A more thorough investigation is warranted and will surely reduce the potential hazard from positive current collection.

References:

1. Kramer, L.; Hamilton, D.; Mikatarian R.; Thomas J.; and Koontz, S. (2010): "Positive Voltage Hazard to EMU Crewman from Currents through Plasma," *Proc. 4th IAASS Conference 'Making Safety Matter,* Huntsville, Alabama, USA, 19–21 May 2010 (ESA SP-680, September 2010).
2. Roeschel, E. (2013): "NESC_ISS_Shock_EVA_Actions.pptx," 6-25-13.
3. Hamilton, D. and Kramer, L. (2007): "Simple Transient Circuit Simulation of EMU Touching Solar Array (Bird on a Wire….NOT!!!!)," page 37, August 29, 2007.
4. Allen, J.E. (1992): "Probe Theory – The Orbit Motion Approach," *Physical Scripta*. Vol. 45, 497-503, 1992.
5. Wright, et al. (2008): "Charging of the ISS as Observed by the FPMU: Initial Results," *IEEE Transactions on Plasma Science,* Vol. 36, No. 5, October 2008.
6. ISS-NCR-232F (2012): Lack of Two-fault Tolerance to EVA Crew Shock in the Low Earth Orbit Plasma Environment, 1/31/2012, Boeing ISS System Safety, Joseph E. Thomas, originator. Pages have Tracking Number: (blank), "International Space Station Safety Noncompliance Report (NCR)." Date: 1/26/12.

7.11 Features of the Current Path from the ISS-EMU-Plasma Circuit versus the Shock Hazard

7.11.1 Electrical Current Path from the ISS through the Astronaut to the Plasma through Multiple Layers of Insulation

The identified hazard is the possible flow of electrical current through an astronaut's torso. The voltage that drives the electrical current is the difference between the ISS chassis at the location of the astronaut and the potential of the ambient ionosphere. If the PCU is not operating, this potential difference can be driven by a combination of the orbital motion of the station through the Earth's magnetic field (**v × B • L**) and by the exposed electrical potentials on the ISS 160V solar arrays. The NESC team found that there are several specific features of the EVA suit – tether – tool system, each designed to interrupt the circuit. For electrical current to flow through an astronaut requires a simultaneous failure of several of these features. Below, the electrical circuit current path from the station is followed through the astronaut to the ambient ionosphere and identifies the four or five features in series that are designed to stop electrical current flow.

The astronaut is attached to the ISS by an 85-foot safety tether. One end of this conducting tether is clipped to rings on the ISS. It is the NESC team's understanding that the tether attachment point rings have an insulating anodized coating. This is the first break in the circuit.

The end of the tether attached to the astronaut has several inches of non-conducting fabric specifically designed to insulate the astronaut from the ISS potential as shown in Figure 7.11-1 (all photos from Eduardo Roeschel, "NESC_ISS_Shock_EVA_Actions.pptx."). See Appendix D.1 [Roeschel, 2013].

Figure 7.11-1. Safety Tether showing the Insulating Fabric Section at the End

The tether is attached to the waist ring on the EMU, as shown in Figure 7.11-2. Notice the fabric end of the tether connecting to the EMU waist ring.

Figure 7.11-2. EMU showing the Fabric section of the Safety Tether and how all the Anodized Rings are Covered by the Suit Fabric

The EMU suit has waist, elbow, and wrist rings made of anodized Al and bearing rings of stainless steel. For the tether to transmit the station potential to the astronaut, the conducting tether would have to contact one of the stainless steel bearing rings where the covering fabric has been moved. The tether contacting the MMWS base plate is not a hazard, since the MMWS base plate is electrically isolated from the rest of the EMU.

An alternative path is for an EMU ring to make direct electrical contact with the ISS. In order for this to occur, the fabric cover must be moved, the stainless steel bearing ring has to either contact the ISS at a location where the anodization has been removed, or there is an exposed stainless steel fastener. See Section 7.9.

This still would not complete the circuit. If the sequence of events above were all to occur simultaneously, the ISS potential would be on a suit ring. There is a high probability that the astronaut's perspiration would support a conducting path to the astronaut's torso. Perspiration could then also make a conducting path to the neck ring.

For negative ISS potentials, the circuit is then completed by ions from the ionosphere accumulating on the exterior insulating neck ring surface, charging it to the local ionosphere potential (see Figure 6.3-7d). The hazard comes from currents that would flow from a breakdown across that insulating surface (see Figure 6.3-7e).

For the positive potentials, the electrical current path is by electron collection on the insulating surface of the neck ring. As shown in Section 7.10 of this report, the magnitude of this path is limited to less than 1 mA for 1 ms.

In summary, to generate an arc that is hazardous to an astronaut, the station has to be at high negative potential and there must be a complete electrical circuit current path from the ISS chassis through the astronaut to the ionosphere to exist long enough for an arc to occur. To establish the electrical circuit associated with the negative charging hazard requires the following events to happen simultaneously during an EVA:

1. at a location on the ISS where the anodized layer has worn through;
2. the tether clip contacts the attachment ring;
3. the conducting tether ahead of the insulating fabric section is in contact with a suit ring;
4. where the fabric cover has pulled back;
5. the ring is made of stainless steel, not anodized Al;
6. there is enough perspiration for a low resistance path;
7. the astronaut is in contact with the neck ring.

The circuit parts (items 1 through 7) are shown schematically in Figure 7.11-3. The probabilities are gross estimates. The "ISS Not Anodized" and "Contact Neck Ring" are based on the NESC team's interpretation of DRD-MAPI-SA-06-ISSPRA-12-56 [ISS-PRA-12-56, 2013]. The purpose of Figure 7.11-3 is to show how many insulation failures must occur simultaneously in-series to establish the negative charging hazard circuit.

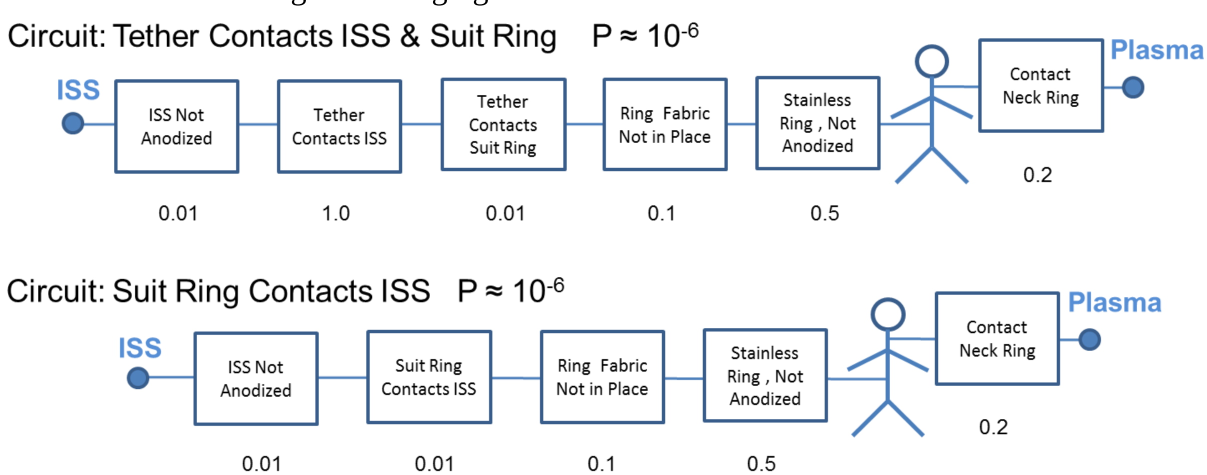

Figure 7.11-3. Circuit Paths from ISS Chassis Ground to the Astronaut Inside the EMU

References:

1. Roeschel, E. (2013): "NESC_ISS_Shock_EVA_Actions.pptx" 6-25-13.
2. Duncan, G. (2013): Document DRD-MAPI-SA-06-ISSPRA-12-56, EVA Shock Update and Summary, International Space Station (ISS) Probabilistic Risk Assessment (PRA) Trade Study – Long Form, ISS-PRA-12-56 (Probability Risk Assessment Doc), Prepared by Gary Duncan, dated May 17, 2013.

7.11.2 Effects of Coincidental EMU Insulation Failures

The NESC team reviewed the "Shock to EVA Crewman due to Negative ISS Potential" in DRD-MAPI-SA-06-ISSPRA-12-56. The hazard consist of the joint probability that the ISS chassis ground is at a potential more negative than –45V with respect to the local ionosphere and that there is a circuit path that connects the astronaut to the ISS chassis ground.

Potentials more negative than –45V can only occur when no PCU is operating. In ISS-PRA-12-56, it is estimated that with the PCU off, the probability of a "negative potential situational condition factor" occurring during an EVA is 0.0137. In Figure 7.11-3, the NESC team estimated the probability of a complete circuit from ISS ground to the astronaut within the EMU as 10^{-6}. This low value comes from the EMU modifications designed to prevent the shock hazard as described in Roeschel, "NESC_ISS_Shock_EVA_Actions.pptx."

As discussed in Section 7.13.1, the probabilities in Figure 7.11-3 are crude estimates for illustrating the point that many insulation failures must occur simultaneously. The combined probability of the negative charging (0.0137) environment occurring and the circuit closure (10^{-6}) is about 1 in 10 million, a much lower probability reported in ISS-PRA-12-56:

> "The probability of the negative shock hazard is about 1 in 250,000."

7.12 Shunt Array FDIR

7.12.1 FDIR Operation

FDIR algorithms are used in the ISS system to detect that a fault condition has occurred, confine the fault, and execute a recovery process (ISS EPS TM 21109) [Anon., 2004]. The array shunt FDIR is enabled, as a third shock hazard control, after the two PCUs are verified to be in discharge mode prior to the start of an EVA. The PCU will remain in this mode as long as the anode current is greater than 0.5A. Below 0.5A, the PCU returns to its startup routine. Five parameters are monitored for the PCUs: (1) plasma current, (2) anode voltage, (3) cathode heater voltage, (4) tank and tube temperature, and (5) tank and tube pressure. The PCU has its own FDIR, which reacts to the loss of or low discharge consequently setting the corresponding fault indicators.

When enabled, the array shunt FDIR will monitor the PCU fault indicators. In the event of one PCU failure during or prior to an EVA (Plasma Hazard Mitigation during EVA, B9-908), the FDIR will shunt all active solar arrays. The EVA might continue with no more than two arrays unshunted while oriented less than 105 degrees from the velocity vector. These allowed arrays are determined as part of the pre-planning FP analysis. Subsequently, in order to maintain ISS power balance, arrays will be unshunted when needed, but after the panel is oriented more than 105 degrees from the velocity vector. To remain power positive, the unshunting must occur on the order of 10s of minutes after the FDIR response.

It is undesirable to keep the arrays shunted because extended battery discharge will occur on the order of 1 hour, which shortens the cell life. As of 2004, it takes an average of 51 minutes of battery discharge (all arrays shunted) to deplete down to the maximum design depth-of-discharge of 35 percent [Dong, 2004; Dalton, 2004] (calculated from information in these references). The ISS battery capacity total is 192 kilowatt hours (kWh), with 24 batteries at 8 kWh each[3,4] [Boeing, 2009; Space Systems/Loral, 1998]. One battery consists of two orbital replacement units (ORU) electrically in series. See Figure 7.12-1.

NiH_2 Battery ORU
©2007 Space Systems Loral

Figure 7.12-1. ISS NiH_2 Battery ORU

The FDIR was activated 3 times since it has been in use. The validation of the array shunting FDIR seems to have been limited. Below is a summary of the three on-orbit events:

(1) 2006/348:19:50 – In preparation for 12A.1 EVA 2 the FDIR was inadvertently actuated during a Node1 multiplexer/demultiplexer (MDM) transition. 2 of 3 deployed arrays shunted, 1 did not; root cause of arrays not shunting isolated to a timing issue between MDMs. (The software timing error was analyzed and fixed under SCR 35596.)

(2) 2006/348:22:56 – During 12A.1 EVA 2, PCU1 was intentionally commanded to "standby" for assembly operations. PCU not in "discharge" mode is one of the triggers to shunt the solar arrays. All arrays were shunted by the FDIR.

(3) 2006/350:22:38 – During 12A.1 EVA 3, PCU2 was intentionally commanded to "standby" for assembly operations. All arrays were shunted by the FDIR.

---

[3] http://www.boeing.com/assets/pdf/defense-space/space/spacestation/components/docs/S6.pdf

[4] http://sslmda.com/downloads/products/ispacest.pdf

References:

1. Anon. (2004): ISS Electrical Power Systems Training Manual, ISS EPS TM 21109, Mission Operations Directorate, Space Flight Training Division, NASA Johnson Space Center, 2004.
2. Dong, S., et al. (2004): *International Space Station Nickel-Hydrogen Extended Battery Discharge Model Analysis*, 2004.
3. Dalton, Mark P. (2004): *International Space Station Nickel-Hydrogen Batteries Approached 3-Year On-Orbit*, 2004.
4. Boeing (2009): "Discovery to Transport Last U.S., Boeing-built Starboard Truss Segment to Space Station," January 2009. http://www.boeing.com/assets/pdf/defense-space/space/spacestation/components/docs/S6.pdf
5. Space Systems/Loral (1998): http://sslmda.com/downloads/products/ispacest.pdf

7.12.2 Risks for High Negative Potential Peaks

The array off pointing prior to unshunting is performed to reduce the RAM electrical current collection. However, the magnitude of the rapid charging event created during the unshunting (even in wake) has not been characterized.

The use of the FDIR presents risks for high negative potential peaks of short duration if, during required power restoration following the FDIR, any array is unshunted in sunlight. The results of on-orbit experiments conducted in 2010 on days 155 and 205 through 212 revealed large negative potentials, up to –95V, when an array was unshunted in daylight while facing in the RAM direction with PCUs off. The duration of the peaks observed was approximately 10 ms. During the experiments, all eight arrays were forced to remain shunted via ground commanding as the station entered insolation. Approximately 3 minutes into insolation, the arrays were commanded to unshunt one at a time. FP data from the FPMU was recorded, as shown in Figure 7.12-2. These potential peaks were present each time the commanded unshunt was performed, with minor variations in peak potential and peak duration. The experiments were limited to unshunting arrays in daylight at the beginning of the orbital day with the arrays facing in the RAM direction and PCUs off. More experimentation should be done to determine the nature of potential peaks at other times during the daylight portion of the orbit, at various array angles, and with PCUs on and off. Characterization of potential peaks with arrays pointing at >105 degrees from RAM is particularly important because it is the minimum pointing angle required during post-FDIR power recovery. Currently, there is no other data to support potential peaks when unshunting at >105 degrees. The FDIR is not a good hazard control strategy considering it could cause charging in excess of the defined hazard limit. It is unknown if these potential peaks are a hazard considering their short duration (~10 ms) because the defined hazard limit does not specify a time duration.

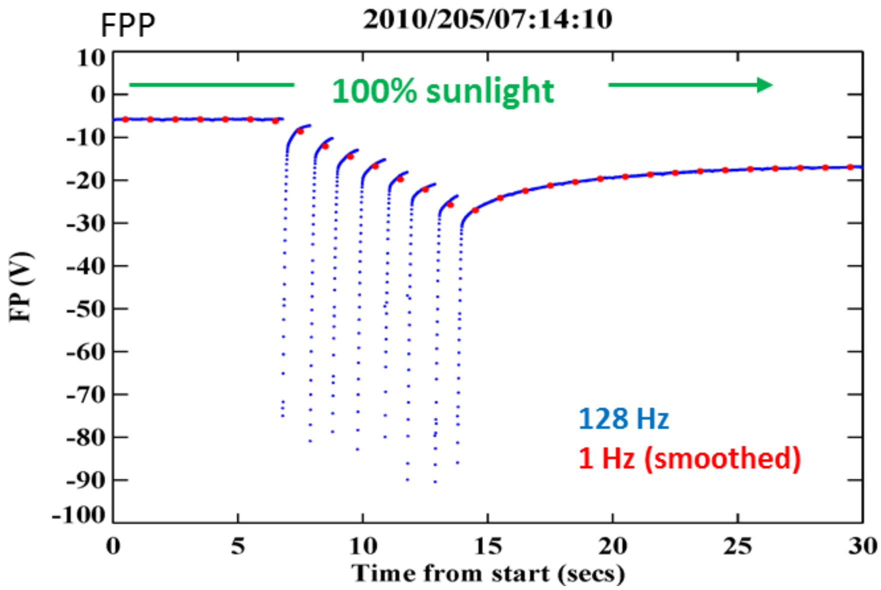

Figure 7.12-2. FP Data from the FPMU

7.13 The Negative FP Limit

EMU Limit

The latest version of the Hazard Report (ISS-EVA-312-AC) and the NCR (ISS-NCR-232G) do not explicitly state a requirement for the FP limit of the EMU. A review of past NCRs and EMU documentation by the NESC team indicates that the EVA Office adopted –40V as the FP limit for the EMU in 2002. The adoption of the –40V level for the EMU appears to have occurred as a result of testing in 2001 at MSFC. Specifically, in 2001, a set of arc tests on EMU samples was performed. A statistical analysis of 10 samples was performed. These data were presented in an American Institute of Aeronautics and Astronautics (AIAA) conference paper in January 2002 [Schneider, 2002]. The statistical analysis indicated a median arc voltage value of –74V with a standard deviation (σ) of 8.1V. In April 2002, the statistical summary was presented by Hamilton Sundstrand (the EMU manufacturer) to an ISS/EVA panel [Gworek, 2002]. In that presentation, it was noted that –40V represented 4.2 standard deviations (4.2σ) from the median arc voltage. According to the presentation, the 4.2σ value represented a 0.01-percent chance of arcing at –40V.

ISS Vehicle Limit

The negative FP limit associated with the ISS vehicle was established to be –40V after a limited number of arcing tests in 1991 described in Section 7.13.1. However, per the ISS-NCR-232G, Block 13: *"The largest accepted charging violation is –45.5V."* This safety margin reduction is justified, in the same NCR: *"At the 1/14/09 SRP, a risk acceptance point of –45.5V was agreed upon by the Panel as a final non-negotiable limit for the negative potential. It was believed that the risk of increase in voltage was within the realm of engineering judgment acceptance."*

The ISS-NCR-232F/G document accepts an increased risk associated with an EMU possibly encountering a section of ISS charged to –45.5V for scenarios involving a PCU failure as described by the following statement:

> *"In order to stay within previously accepted charging exceedances, OCAD #1 00006 specifies that only pairs of arrays which result in charging levels lower in magnitude than –45.5V, per attachment 1, may be excluded from shunting and allowed to autotrack following a PCU failure."*

References:

1. Schneider, T.A.; Carruth, M.R., Jr.; and Hansen, H.J. (2012): "Minimum Arc Threshold Voltage Experiments on Extravehicular Mobility Unit Samples," AIAA Paper 2002-1040, *40th AIAA Aerospace Sciences Meeting and Exhibit*, Reno, NV, January 14-17, 2002.
2. Gworek, P.; and Hansen, H. (2002): "EMU – Plasma Arc Update", Presentation to *CCB, Hamilton Sundstrand Space Systems International, Inc.*, April 3, 2002.

7.13.1 Origin of the –40V ISS Charging Limit

The ISS, like many spacecraft, uses Al metal in the construction of most of its structural components – due to the lightweight nature of Al. To avoid corrosion issues, Al is anodized. The anodizing process creates an oxide layer on the Al surface, which protects it from corrosion. The oxide layer is a dielectric layer (i.e., electrically insulating). In the case of ISS, the MMOD shields form the outer shell of the spacecraft and are in contact with the ionosphere plasma environment. The MMOD shields are made of Al metal and are anodized. In fact, a special anodization process was used to protect the MMOD shields on the ISS, which represent a large fraction of the vehicle's surface area. The special anodized coating was needed to obtain thermo-optical characteristics, which would keep the MMOD shields relatively cool compared to standard anodized Al components. The special anodizing process used on the ISS MMOD shields resulted in an extremely thin anodization (oxide) layer, with thickness on the order of 1.3 microns.

Early in the design process for the ISS, a solar array power system was adopted which operates at 160V. The power system also employs the standard negative ground scheme, whereby the negative terminal of the power system is attached to spacecraft chassis (i.e., the Al metal hull), which includes the MMOD shields. Recognizing that the 160V solar arrays would interact with the ionosphere plasma, NASA personnel in the field of spacecraft charging predicted that the ISS vehicle would experience negative charging on the Al metal hull, followed by positive ion collection on the RAM facing anodization layers. The result would be a large electric field developing across a very thin dielectric layer. In the event the electric field exceeded the dielectric strength of the anodization (oxide) layer, an electrical discharge (arc) would form and damage the anodization layer. In a related scenario, if a micrometeoroid particle were to impact a charged anodization layer, it could precipitate an arc.

Therefore, in the 1990 to 1991 time period, M. Ralph Carruth Jr., and Mr. Jason Vaughn, from MSFC, conducted a test campaign to determine if an arc would be generated on a negatively-charged anodized Al plate immersed in a plasma environment in the event that the anodized layer was struck by a micrometeoroid particle. The tests sought to determine if there was a lower charging limit such that an arc would not be generated in the event of a particle strike.

All of the tests were conducted at Auburn University using a “hypervelocity gun” as a source of fast micrometeoroid particles. The tests were very time consuming to set up and execute. A plasma comparable to the ionosphere plasma had to be created and maintained at high vacuum, an anodized sample had to be charged to a specific voltage, and the high energy hypervelocity gun had to be successfully fired during the time window when the plasma and charging conditions were as desired.

The complexity and long set up times associated with the Carruth and Vaughn test led to only a limited number of successful shots. Details about this test campaign appear to be captured in the following reference: “Minutes from the Joint Meeting of the Electrical Grounding Tiger Team and the Electrical Power System Working Group for Development of the Decision Package for SSF Electrical Grounding,” Fairview Park, OH, August 5-7, 1991, (Carruth and Vaughn), pp. 172-181. Unfortunately, this reference appears to have had only a limited distribution and, unfortunately, the NESC team has not found a copy of this report.

Fortunately, both Carruth and Vaughn still work at MSFC and can be consulted about their recollection of the test campaign. According to Mr. Vaughn in a December 3, 2013, e-mail to Todd Schneider:

> *What I remember was we ran several tests with single MMOD shots at each level. We started at –150V and went down in steps of –25V. We definitely saw an arc at –75V, but it did not appear to be a full discharge of the cap [capacitor]. With one shot at –50V, we did not produce an arc. Because we did not see an arc at –50V, we asked for more resources to generate more data and better statistics at –50V. However, at that time in the investigation and all the data pointing to needing a PC [plasma contactor], the program management decided to solve the problem with the addition of the PC [plasma contactor].*

From past discussions between Carruth and Schneider during ISS Plasma Charging Tiger Team activities in 2000, the ISSP (in 1991) asked Carruth to recommend a safe charging level for anodized ISS structural elements. Based on the limited data at –50V, Carruth recommended adopting a 10V margin and suggested –40V.

The origin of the ISS –40V limit, therefore, is based on the work of Carruth and Vaughn in the early 1990s to determine a voltage whereby a charged section of the ISS MMOD shield would not arc in the event that section was struck by a micrometeoroid particle.

In parallel with the work at MSFC to investigate arc initiation was an effort to determine the expected vehicle charging levels due to the interaction between the high voltage solar arrays and the ionosphere plasma environment. In 1991, at the Lewis Research Center (LeRC) – later renamed Glenn Research Center – Carolyn Purvis, Dale Ferguson, and David Snyder made measurements of the current collection of ISS solar array (or photo-voltaic array) panels in a representative ionosphere plasma. Their measurements showed that the ISS solar arrays were capable of collecting large electron currents from the ionosphere plasma, which pointed toward ISS vehicle charging levels that could reach –140V.

Recognizing the need to limit ISS vehicle charging in order to minimize arcing on anodized surfaces, the LeRC team developed an active charge control system. Michael Patterson (LeRC) used the setup built by Purvis, Ferguson, and Snyder to demonstrate that a hollow cathode device could be deployed on ISS, which would actively control/limit the charging on the ISS chassis to –40V. The hollow cathode system demonstrated by Patterson became known as the PCU and formal implementation of the PCU was approved in April 1992 [Moorehead, 1992].

At the time the –40V limit was established, the primary concern about the ISS spacecraft charging was related to the potential damage that an arc could do to the anodization layer on a MMOD shield. If enough arcs occurred on the MMOD shields, the thermo-optical properties of the anodization layer on the MMOD shield could be significantly altered, which would result in taxing the ISS cooling systems. In other words, in the 1990s the problem associated with arcing on ISS was a vehicle-level problem, and not a personnel safety problem.

Reference:

1. Moorehead, R.W., Deputy Director (1992): *Space Station Freedom Program and Operations, communication to Work Packages 1-4 Directors*, dated April 3, 1992.

7.13.2 Plasma Safety Hazard Identification and Risk Acceptance at –45.5V Charging Levels

In September of 2000, Schneider and Carruth, conducted a test (at MSFC) to determine if components of the EMU would arc if they were charged in the presence of a plasma environment. This test was triggered by the work of members in the ISS PCU Tiger Team, who recognized that it might be possible for the EMU to become charged to the same potential as the ISS vehicle metal chassis. The results of the test by Schneider and Carruth showed that EMU components (e.g., the display and control module) could indeed arc. In fact, an arc at –68V was recorded for an anodized component of the display and control module in the MSFC plasma test chamber.

Thus, a shift occurred in the ISS spacecraft charging community from concern about arc damage on the ISS vehicle to a possible electrical safety hazard for an astronaut conducting a spacewalk wearing an EMU.

In the 2000 to 2001 time period, studies by the EMU suit manufacturer Hamilton Sundstrand and NASA's EVA teams confirmed that electrical pathways did exist which would allow for the EMU suit to reach the same charging level as the ISS vehicle. So, if the ISS vehicle was experiencing charge levels of –80V, then it would be possible for the EMU to also charge to –80V. Since the EMU did contain anodized components exposed to the ionosphere plasma, the possibility existed that electrical discharges (arcs) could develop on those EMU components via dielectric breakdown. Unfortunately, since the astronaut is in contact with metal components inside the EMU, due to conduction via the perspiration-soaked cooling garment covering their bodies, there is a possible safety concern that emerges since the astronaut's body is part of an electrical circuit in which an arc is occurring. That is, an electrical shock hazard could becreated for an astronaut inside an electrically charged EMU suit.

To help in determining the safe operating limits for EMU charging, Harold Hansen (Hamilton Sundstrand) and Todd Schneider (NASA/MSFC) conducted an arcing test in 2001 using anodized Al samples prepared using the same processes as EMU components. The full test description and results can be found in Schneider, et al., 2002.

The 2001 test by Hansen and Schneider showed that within the limitation of a dataset that included only 10 samples, a statistical fit to the data indicated that –40V represented a 0.01-percent probability of generating an arc on an anodized EMU component. Using the test results, combined with the previously defined vehicle limit, it appears that in 2002 the EVA Safety teams adopted –40V as the safe limit for EMU charging. This limit was then applied to the creation of EVA reports and hazard documents.

As the EMU plasma shock hazard represented a possibly catastrophic hazard for the astronaut, it was mandated that a two-fault tolerant safety system be used to protect the astronaut on EVA from the plasma charging hazard. To meet this two-fault tolerant requirement, two PCUs were operated during an EVA and solar arrays were shunted (i.e., power production from the array was stopped by shorting the output of the array). This ensured that the ISS charging would be more positive than –40V.

By 2007, a better understanding of the ISS spacecraft charging had emerged with the availability of measured vehicle charging data from the FPMU, which was deployed on the ISS in 2006. Using a modeling capability based on empirical data, the Boeing Company projected a scenario in which a –45.5V charging level could be reached on the ISS in the event that no active charge control device (e.g., PCU) was operating, but the solar arrays were producing power (i.e., not shunted). This marks the first time an exception was made to allow for a scenario in which an EVA astronaut might be exposed to charging levels exceeding the –40V charging limit. The exception is documented in the "ISS Safety Noncompliance Report," ISS-NCR-203 Rev. B, The Boeing Company/Space Exploration/International Space Station, September 19, 2007 [Boeing, 2007]. It should be noted that this NCR was intended only to cover the ISS build stage 10A (October 2007 to February 2008).

The exception documented in the ISS-NCR-203 Rev. B is actually a worst-case scenario in which two PCUs fail and solar array shunting is not allowed due to the need to maintain a minimum safe power level onboard the ISS. The -45.5V level is actually a model prediction using the Boeing Company's ISS charging model.

In 2009, using the ISS-NCR-203 Rev. B as a precedent, a SRP apparently agreed to once again accept the risk associated with an EVA continuing after predicted potentials could reach -45.5V. Recall that the following statement documents that decision:

> *"At the 1/14/09 SRP, a risk acceptance point of –45.5V was agreed upon by the Panel as a final non-negotiable limit for the negative potential. It was believed that the risk of increase in voltage was within the realm of engineering judgment acceptance."*

This statement appeared in ISS-NCR-232F, *"Lack of Two-fault Tolerance to EVA Crew Shock in the Low Earth Orbit Plasma Environment,"* The Boeing Company/Space Exploration/ International Space Station, Joseph E. Thomas (Document Originator), 1/26/2012, page 6 [Thomas, 2012].

It is important to distinguish between a risk acceptance of –45.5V and a safety limit of –40V. The risk acceptance does not change the established safety limit, rather it allows for an EVA to continue with only single-fault or zero-fault tolerant hazard controls and increased safety risks.

The –40V charging limit for both the vehicle and the EMU was based on test data. In the case of the vehicle, the test data focused on micrometeoroid impact induced arcing. In the case of the EMU, the testing was on dielectric breakdown of samples produced by Hamilton-Sundstrand, the vendor who constructed the EMU. Thus, it seems prudent that changes to the established charging limits, for either the vehicle or the EMU, would be accompanied by new test data that makes a compelling case.

Reference:

1. Boeing (2007): "ISS Safety Noncompliance Report," The Boeing Company/Space Exploration/International Space Station, ISS-NCR-203 Rev. B, September 19, 2007.
2. Thomas, J.E. (2012): *Lack of Two-fault Tolerance to EVA Crew Shock in the Low Earth Orbit Plasma Environment*, The Boeing Company/Space Exploration/ International Space Station, Joseph E. Thomas (Document Originator), ISS-NCR-232F, 1/26/2012.

7.14 Review of the ISS-NCR-232G: Lack of Two-fault Tolerance to EVA Crew Shock in the Low Earth Orbit Plasma Environment

The ISS-NCR-232G is the governing document to define the use of controls during EVAs, lack of three controls (two-fault tolerance), or failures of controls. In addition to the discrepancies in the control approach, as defined in Section 6 of this document, the NESC team agreed there are inconsistencies and other general statements to address in the reviewed documentation. For example:

- The document implies that independent Space Environment Scientists are in agreement with "*the environment will remain benign at least through Solar Cycle 25 which extends through -2030."* The NESC team does not agree this is widely accepted.
- There are obvious inconsistencies, relating to the ISS safe FP limits. Currently, both –40V and –45.5V are referenced. If –40V is the limit and the –45.5V includes the accepted risk, it needs to be explicitly stated. The tolerance of the calculations also needs to be taken into consideration.
- There is no safety limit specified for the positive potential (if considered a hazard) and electrical current collection.

- The use of the "short-term" expressions is misleading when referring to a 14-day forecast since a 1-day prior to forecast might be in order.
- There is no coherent list of all possible electrical current entry points into the astronaut via the EMU's external metal contact points, especially when also looking at the PRA-12-56.

Refer to Appendix C for the complete review of the ISS-NCR-232G.

7.15 Examination of ISS-PRA-12-56: PRA for Shock Hazard

At the request of the NESC team, a Jet Propulsion Laboratory (JPL) PRA expert briefly reviewed the information provided by the NESC team, the ISS-PRA-12-56 document. He recommended that the PRA material, as it exists, needs an in-depth review. This conclusion is based on the following observations:

- The event sequence diagrams, event trees, and fault trees (a) lack direct provenance to the experiential evidence used to derive and quantify them, and (b) need to be reviewed for completeness (i.e., determine whether any potentially risk significant events/phenomena are omitted).
- As much of the probabilistic data originally resulted from expert opinion, the data need to be either verified by comparison with physical data or physics-based models, or have the uncertainty assigned to the probabilities expanded to include variations among cognizant experts.
- The ISS PRA report describes a model and data, which were quantified using the Systems Analysis Programs for Hands-on Integrated Reliability Evaluations (SAPHIRE) software tool. The fidelity of the model and data to the physics of EVA shock need to be reviewed—the intent should be to perform a broad, "horizontal" review followed by selected "vertical" slices.
- It is not clear if the negative case considers the PCU "on" (study categorizes the PCU as a positive hazard contributor) or if the analysis takes into consideration the suit changes or if the changes reduced the hazard posed by the PCU.

7.15.1 Additional PRA Review

A review of the PRA documentation package provided [1, 2] revealed lapses in clarity and detail. The methodology and underlying assumptions provided are insufficient to enable duplication of the stated findings. In general, the document would benefit from an editorial review of its detailed content. However, several areas could potentially benefit from additional detail. In its present form, the PRA does not meet commonly held standards for technical rigor [3]. Selected examples follow in the interest of increasing the level of clarity and potential value of the presentation:

- Terminology and labeling between documents greatly reduces clarity of presentation ([1], page 8): "+Transient Capacitive Discharge Hazard" is referred to as "AC Shock" in PRA [1, page 14]. Similarly "+DC Hazard" is labeled "DC Shock" [1, page 13], etc. To find these details one would need to be quite familiar with the contents of the PRA. Use of a summary with common nomenclature between documents [1, 2] could greatly help the clarity of presentation. A variation on Table 1 of PRA [1] would be preferable to relying on text to convey findings. This would allow the reader to more readily inter-compare relevant magnitudes. Why are probabilities for a "single crew member" provided in [1, page 8, see "PRA Updates and Results"]? In other sections, mean probability for "two crew members" are stated. If there is a compelling reason why this is done it should be clearly stated, if not, if one should consider simplifying to a common case and language. This would improve readability of the text for decision makers. At best, the current narrative formats used in [1,2] are challenging to decipher and time consuming if one wished to compare in detail.

- Clarity ([1], page 8): The term "baseline" needs to be clearly defined. See comment below regarding "baseline" definition used in PRA.
- Documentation of methodology ([2], page 11-12): Contact probabilities (Table 3-4) justification largely unstated – some appear larger than one might expect given present of insulating material. Have these tables been updated to reflect suit modification? Text presently states: "…reliability data used to populate the events in model originally generated in 2008 using expert judgment…." Table 2 provides point estimate for "negative potential situational condition factor = 0.0137" – what is the uncertainty in this value? Stated uncertainties in contact probabilities all have "uncertainty 7 log normal"—unclear what this means here – is this the standard deviation, error factors [7, pages 78-79], or other? Unclear why all uncertainties have the same magnitude.

  Comment: At a minimum, it would appear to be of value to reveal these inputs, document rationale, and where the possible link to physical measurement is (e.g., contact probability of anodized-anodized Al surface ~ 0.01, etc.). Unclear from documentation provided and hard to tell if values represent "opinion" or physical observation. Similar comments hold for the uncertainties used in simulations.
- A contact probability of zero is equivalent to "not credible" [2]. Inclusion in this form merely tends to complicate model topology and distract from clarity of presentation. Reader is left pondering why such events are present beyond indicating that they have been considered.

  Comment: The results presented in the document cannot be uniquely reproduced from the explanation provided. Would be of value to compute and explicitly document product of values leading to max-min probabilities. Such a crosscheck would bound the expected order of magnitude and validate of the detailed simulation described [2, pages 16-62]. Such an exercise could potentially lend physical insight and credibility to the modeled results.
- Unclear [2, Figures 6-8]: 2- versus 1-Crew probabilities appear to scale with exposure time. This makes physical sense, however, inclusion merely graphically confuse data presentation. Why is this information detail desirable to present? If it is – maybe of value clearly state desired conclusion.

- Unclear [2]: "…for a shock hazard, several events must occur simultaneously…" latter stated "…model does not depend on chronological sequence of events…." Observation if "simultaneous" – how could sequence matter within such a logical framework? Given the underlying circuit topology assumed, the threat must occur at the same time a path is present.
- Acronym "OBS" does not appear to be defined – from context reader might assume "Operational Bioinstrumentation System." Similarly, acronym "CCA" does not appear to be defined – from context – appears to be an electrical connector interface or similar. Recommend checking documents [1,2] for definition of all acronyms.
- Unclear [2]: "The risk of loss of crew (LOC) for a single EVA, but the baseline ISS PRA EVA model is presented for comparison only; it should be noted that the EVA shock hazard is the probability an EVA crew would experience a shock and imply LOC…." Unclear why stated "baseline" is relevant if suit modification has occurred and in use? Why would one not treat the modified suit as the baseline and merely state improvement over prior art in passing? Alternatively, need to provide context and logic for stated baseline.
- Executive Summary [2]: The potential is one parameter of interest here – the magnitude of the electrical current that can be sourced by the threat is the other – would be of value to briefly discuss both aspects.
- Typesetting ([1], page 6-7): "…These five events are discussed individually below." Six items are enumerated. Document could benefit from careful editorial review.

References:

1. ISS-NCR-232G (2013): *Lack of Two-fault Tolerance to EVA Crew Shock in the Low Earth Orbit Plasma Environment*, NCR-20264-R7, 18 September 2013.
2. Schmidl, D. (2013a): *EVA Shock Update and Summary PRA Report ISSPRA-12-56*, NASA JSC, May 7, 2013, DRD-MAPI-SA-06-ISSPRA-12-56.
3. Stamatelatos, M. and Dezfuli, H. (2011) *Probabilistic Risk Assessment Procedures Guide for NASA Managers and Practitioners*, Second Edition, 2011, NASA/SP-2011-3421.
4. Smith, C.L. and Wood S.T. (2011a): "Systems Analysis Program for Hands-on Integrated Reliability Evaluations (SAPHIRE) Version 8, Volume 1: Overview and Summary," 2011, United States Nuclear Regulatory Commission, NUREG/CR-7039, Vol. 1.
5. Smith, C.L. and Wood S.T. (2011b): "Systems Analysis Program for Hands-on Integrated Reliability Evaluations (SAPHIRE) Version 8, Volume 1: Technical Reference," 2011, United States Nuclear Regulatory Commission, NUREG/CR-7039, Vol. 2.

8.0 Findings, Observations, and NESC Recommendations

8.1 Findings

The following findings were identified:

F-1. There are numerous shortcomings in the space weather forecast planning used on the ISS that limits its use for 14-day (or any) forecasting:

- Ne and Te "forecast" is a simple persistence of condition methods based on the assumption that conditions in 14 days will be same as on day the FPMU measurements are obtained.
- Validation of Ne and Te environment forecast is based on data from two limited time periods.
- IRI model used to project measured data into future is a monthly average climatology model incapable of predicting the full range of environments responsible for ISS charging.
- No complete verification of ability to predict ISS potentials 14 days in advance has been demonstrated.
- Plasma hazard assessment report does not include information on current state of geomagnetic activity—no documented plans to deal with FPMU data obtained during disturbed periods when reference data may under represent the charging environment present in 14 days at the time of EVA.
- Assumption that solar activity will remain benign through next solar cycle into ~2030 has no basis in current ability of solar physics community to predict future solar activity.

F-2. The FPMU is an integral part of the proposed forecast process; however, there is no explicit contingency procedure when FPMU data is not available.

- FPMU data are critical since Ne and Te values from the IRI statistical model are constrained by FPMU measurements in determining which set of IRI values are used as inputs to the PIM3.0 charging model calculations for the plasma hazard forecast approach.
- A spare FPMU unit is available on board the ISS, but will require an EVA to replace a failed unit.

F-3. Comparisons between calculations of the ISS potentials by PIM3.0 using the actual ionospheric environment with the real-time FPMU measurements has identified deficiencies. Potentials more negative than –45V have been measured on the ISS. The ionosphere forecast and PIM3.0 models are not capable of predicting these large potentials (see Figure 7.6-3).

Limitations and sources of error in the PIM:

- Analytical approximations used in the numerical solutions for the potential barriers in the gaps between solar cells (solar array electrical current collection model).

- Assumption that every solar cell collects the same electrical current.
- Uncertainties in FPMU Ne and Te input data (due to FPMU data reduction errors).
- Timing of FPMU data chosen for PIM3.0 input relative to charging peak.
- Errors in knowledge of solar array angles, ISS flight attitude, and ISS velocity.
- Variations in ion collection area (free parameter adjusted to obtain best results).
- Use of static (equilibrium) charging algorithm cannot predict rapid charging events.
- Use of single capacitance in time-dependent charging algorithms oversimplifies the physics of the ISS charging and fails to model fast transient charging.
- The IRI and PIM3.0 models do not contain the appropriate physics to predict auroral charging.

F-4. The proposed usage of PIM3.0 puts this model in the critical path to EVA, yet fails to meet the NASA modeling standards imposed after the Columbia tragedy.

- The CAIB report and NASA's response to it emphasizes that various aspects of ensuring credibility of modeling results gets conveyed to critical decision makers relying on those results.
- PIM3.0 fails to meet the minimum requirements:
  - The limitations of the PIM3.0 are not explicitly known by the decision makers.
  - User's manual and parameter definitions for the PIM3.0 code are not available.
  - The configuration files for the use of PIM3.0 are not documented in the pre-planning proposed procedure. These will constrain how the model is used every time.
  - The model has not been independently peer reviewed.
  - There is no process identified to update PIM3.0 to include physical changes to the station configuration.
  - There is no clearly documented validation, verification, or certification process.
- This model should not be in the critical path if it lacks the pedigree associated with above mentioned standards.

F-5. The PCU maintains the ISS near to space plasma potential, even under poorly characterized charging events like rapid charging events.

- Under the worst-case conditions, the PCU has the capability of sourcing enough electrical current to keep the ISS close to the plasma potential.
- The PCU has demonstrated emission to 10 A in ground testing. (See Figure 7.8-1.)
- The largest PCUs electrical current measured on orbit is 0.575 A.

F-6. The added positive potential caused by operating the PCUs introduces negligible additional electrical current collection in the EMU in light of the recent EMU electrical isolation modifications, even outboard of the SARJ.

- An analysis was performed by the NESC team of plasma current collection by the EMU due to positive ISS potentials with the PCU on.
- Electron plasma currents have been recalculated accounting for modifications to the EMU including those that isolate equipment.
    - Currently, there is no DC condition due to the isolation of the MMWS since it is no longer an exposed conducting path.
- The NESC team calculation used the orbit-limited cylindrical electrical current collection model, which is more applicable than the more conservative orbit-limited spherical electrical current collection model.
- An analysis performed by the NESC team showed that the previous calculations of thorax electrical current levels used to determine that low positive potentials are a hazard, were more than an order of magnitude too large.
- Electrical isolation of the MMWS has greatly reduced the probability of any potential hazard due to DC conditions.

F-7. The PCU has adequate supply of xenon gas and the hardware (hollow cathode) has demonstrated life in space to support its use at the ISS past 2028.

- Both PCUs satisfy the two necessary conditions for long life:
    - There is enough propellant to run the PCUs past 2031.
- No PCU hardware component has been identified to limit the operational life shorter than 2024.
- In flight hollow cathode experience, DS1, demonstrated >16,000 hours (Test Readiness Level 9). Currently on the Dawn spacecraft, the three thrusters and their hollow cathodes have a combined >35,000 hours of operation.

F-8. The modified suit acts as a hazard control by disrupting the electrical current path from the ISS through the astronaut to the plasma through multiple layers of insulation.

- There are several specific features of the EVA suit – tether – tool system each designed to interrupt the circuit.

– For electrical current to flow through an astronaut requires a simultaneous failure of several of these features.

F-9. The low likelihood of occurrence of coincidental EMU insulation failures in the ISS-EMU-plasma circuit necessary for electrical current flow through the astronaut torso supports its use as a control.

– The FP as a known hazard is controlled by the insulated EMU-tool system as supported by the calculated low probability of a shock hazard, which considers the environment and the electrical current path.

– The NESC team's preliminary estimates from the circuit path probability suggest that the suit insulation reduces the probability of shock hazard to less than 1 in 10^7.

F-10. The array shunting FDIR has not been validated and its use presents risks.

– There is a risk for high negative peaks (of short duration) when an array segment is unshunted in daylight after a FDIR response.

- Solar array unshunting can occur during EVA. Present flight rules provide no guidance when to unshunt arrays.
- The peak magnitude of rapid charging events due to unshunting the array in wake (>105 degrees from RAM) is not known.
- Presents a potential risk to the ISS power balance.
    - To remain power-positive, unshunting must occur on the order of 10s of minutes after FDIR's response.

– The array shunting FDIR is considered a complicated algorithm potentially causing steady state power level issues as well as unknown and unexpected rapid charging events.

F-11. Use of the low-risk active hazard controls (e.g., PCUs) becomes optional in the ISS NCR-232G guidelines and depends on results from a "short-term plasma forecast" assessment issued prior to a planned EVA. The need for active hazard controls therefore depends on the ability of the higher risk "short-term plasma forecast" method to reliablypredict ISS floating potential prior to an EVA.

– Reliability of the "short-term plasma forecast" (as described in the ISS-NCR-232G) is based on the assumption that low solar activity and benign charging conditions will continue for the balance of the current Solar Cycle 24 and all of Solar Cycle 25, allowing the persistence of plasma environments over time to characterize charging hazards.

F-12. Discontinuing the use of PCUs in favor of the forecast is not the lowest risk option for mitigating EVA shock hazard.

– Data shows PCUs fully capable of controlling any potential hazard. They are designed to be reliable and have the xenon needed to continue past 2028.

– The forecast cannot predict all the observed types of ISS charging.

F-13. There is no written documentation provided as to what is considered a safe voltage level with respect to arc generation on an EMU suit. The value of –40V is referenced as a vehicle requirement.

– While the –40V level appears to be used in safety assessments related to the EMU, no specific voltage requirement can be found which applies directly to the EMU.
– The current Hazard Report (ISS-EVA-0312-AC) does not provide a negative voltage level (with respect to the ionosphere plasma) which constitutes a safe operating limit for the EMU – in order to avoid arc generation.
– ISS-NCR-232F and ISS-NCR-232G discuss operation of the ISS vehicle with respect to a –40V required limit; however, these reports do not provide any specific references to safe voltage limits for the EMU suit.

F-14. There is no written documentation provided which justifies the "risk acceptance point" of –45.5V for the ISS vehicle charging with respect to the ionosphere plasma. Furthermore, no information is provided as to the application to the EMU suit of this increased risk level.

– While it is made clear in ISS-NCR-232G that the –45.5V level was established at the "1/14/09 SRP," no information is provided as to how much additional risk for arcing occurs when an EMU is charged to –45.5V as compared to –40V.
– Page 6 of ISS-NCR-232G contains the following statement:
"*At the 1/14/09 SRP, a risk acceptance point of –45.5V was agreed upon by the Panel as a final non-negotiable limit for the negative potential. It was believed that the risk of increase in voltage was within the realm of engineering judgment acceptance*."

– No information about the rationale used to support the –45.5V decision was found in all of the documentation reviewed by this NESC assessment team – including official, unofficial, and background reports and presentations.

F-15. There are inconsistencies between the released documented processes (e.g., in the ISS-NCR-232G) and what is conveyed by the ISS Space Environment Community verbally or via email.

8.2 Observations

O-1. This assessment does not include scattered plots with the full set of ISS charging events nor sensitivity analysis of the floating potential calculations since there was limited information available on the PIM3.0 code.

O-2. The limited information on the PIM3.0 restricted the ability to assess the code's physics and capabilities.

O-3. The NESC team did not evaluate the EMU systems (i.e., electrical systems, instruments) to understand their susceptibility to the study's hazards.

O-4. The analysis in this assessment focused on the current ISS configuration and did not attempt to address the effects of proposed configuration changes, such as future Russian solar arrays.

8.3 NESC Recommendations

The following NESC recommendations were identified and directed towards the ISS Environments and EVA Safety teams unless otherwise identified:

R-1. The ISS-NCR-232G approach should be revised. The NESC team disagrees with the use of shock hazard forecasting based on environments and modeling to eliminate the PCU usage. ***(F-1, F-3, F-11, F-12)***

R-2. Both PCUs should be operated in discharge during the entire EVA regardless of pre-EVA hazard severity measurements, short-term ionospheric environment forecasts, or location of the EVA. ***(F-5, F-6, F-7, F-12)***

- This provides two of the required three controls to achieve two-fault tolerance.

R-3. Evaluate the use of the low probability of the ISS crew contact circuit path (per PRA and EMU modifications) as the basis for the third control to achieve two-fault tolerance instead of the FDIR. ***(F-8, F-9, F-10)***

- This includes revising the PRA per preliminary analysis demonstrated in this assessment.

R-4. Reassess the severity of the positive potential hazard based on changes to the EMU configuration and the analysis provided in this report. ***(F-6, F-8, F-11)***

- EMU "positive shock hazard" is the result of making unrealistic assumptions about plasma collection that model the EMU as a bare metal sphere floating in space connected with a wire to the ISS chassis ground, then claim that the actual configuration of the "EMU cannot be used as a hazard control" for this contrived "hazard."
- If the floating positive potential is demonstrated and accepted as not a threat then YVV orientation as a control should be discontinued.

R-5. Perform a quantitative analysis to determine whether the rapid charging events exceeding –45V constitutes a threat to crew during EVA. ***(F-3, F-10)***

R-6. If the ISSP continues to use the 14-day forecast and PIM3.0 process, described in ISS-NCR-232G, for EVA hazard control planning, then it is recommended to address the issues described below. ***(F-1, F-2, F-3, F-4, F-11, F-12)***

- The PIM3.0 code is an engineering tool and would need to be updated to meet the NASA software standards (NASA-STD-7009) if it is to be used for EVA safety critical decisions.
- PIM3.0 code should be peer reviewed, documented, and a user's guide provided.
- The PIM3.0 input file should be documented to generate plasma hazard assessments in both the shock hazard control guidelines and plasma hazard assessments to assure configuration control when using the model.
- FP calculations should have error values assigned to them.
- The PIM3.0 should be updated to incorporate algorithms for simulating all measured data including rapid charging events if these are determined to be a hazard (R-5).
- Verify the ionosphere environment statistics derived from the IRI-2001 model are applicable to the IRI-2011 model.
- Forecasting based on persistence of ionospheric conditions is useful for long-term (14 days) solar array configuration pre-planning, but this could also be accomplished using statistical models for range of expected conditions (including worst-case)
- Alternative sources of ionospheric Ne and Te data (e.g., COSMIC Ne profiles, ionosonde Ne values, and GAIM model Ne and Te output) are available for use as contingency option for characterizing environment should FPMU data not be available.

R-7. The ISSP should complete a systematic study of all available FPMU data. This study should include information on the magnitude of charging events, changes in potential, rise and decay times, statistical ranges, and other details as required to fully characterize the charging events. ***(F-1, F-2, F-3, F-10)***

- A yearly review of space weather status and the latest ISS measurements is recommended.

R-8. Develop procedures for terminating or avoiding EVA in the wake of the ISS during severe auroral events (e.g., capable of generating frame and surface potentials* in excess of –100 to –1000V). ***(F-1, F-3)***

- Demonstrate the threat by independently verifying the effects of extreme auroral charging effects on the EMU. Ground tests have shown surface discharges on suit materials in simulated auroral conditions, but no tests have been done to determine if these will affect the EMU.
- Evaluate auroral charging effects during an EVA with PCUs turned on since the PCUs might not offer protection against these rare, but extreme, events in the ISS wake.
  - Recommend monitoring geomagnetic indices (e.g., Kp or similar indices) and coronal mass ejections (CME) in real-time (at least 1 to 2 hours ahead of EVA). If likelihood of severe auroral activity at the ISS, delay or terminate EVA.

- Conduct a thorough statistical analysis of likelihood of severe auroral arc at the ISS during EVA.

*PCUs mitigate the ISS frame charging, but will not reduce potentials on insulating surfaces

R-9. Documentation related to EVA shock hazard control needs to be updated to be clear and specific in the following subjects. ***(F-11, F-12, F-13, F-14, F-15)***

1) PCU utilization
2) Disable FDIR
3) Marginalization of positive hazard
4) PRA
5) EMU tools isolation
6) Elimination of YVV

- The ISS-NCR-232G document should be updated to correct inconsistencies, missing references, and other general statements.
- A complete document review is provided in Appendix C of this report.

9.0 Alternate Viewpoint

There were no alternate viewpoints identified during the course of this assessment by the NESC team or the NRB quorum.

10.0 Other Deliverables

No unique hardware, software, or data packages, outside those contained in this report, were disseminated to other parties outside this assessment.

11.0 Lessons Learned

No applicable lessons learned were identified for entry into the NASA Lessons Learned Information System (LLIS) as a result of this assessment.

12.0 Recommendations for NASA Standards and Specifications

No recommendations for NASA standards and specifications were identified as a result of this assessment.

13.0 Definition of Terms

Corrective Actions — Changes to design processes, work instructions, workmanship practices, training, inspections, tests, procedures, specifications, drawings, tools, equipment, facilities, resources, or material that result in preventing, minimizing, or limiting the potential for recurrence of a problem.

Finding	A relevant factual conclusion and/or issue that is within the assessment scope and that the team has rigorously based on data from their independent analyses, tests, inspections, and/or reviews of technical documentation.
Lessons Learned	Knowledge, understanding, or conclusive insight gained by experience that may benefit other current or future NASA programs and projects. The experience may be positive, as in a successful test or mission, or negative, as in a mishap or failure.
Observation	A noteworthy fact, issue, and/or risk, which may not be directly within the assessment scope, but could generate a separate issue or concern if not addressed. Alternatively, an observation can be a positive acknowledgement of a Center/Program/Project/Organization's operational structure, tools, and/or support provided.
Problem	The subject of the independent technical assessment.
Proximate Cause	The event(s) that occurred, including any condition(s) that existed immediately before the undesired outcome, directly resulted in its occurrence and, if eliminated or modified, would have prevented the undesired outcome.
Recommendation	A proposed measurable stakeholder action directly supported by specific Finding(s) and/or Observation(s) that will correct or mitigate an identified issue or risk.
Root Cause	One of multiple factors (events, conditions, or organizational factors) that contributed to or created the proximate cause and subsequent undesired outcome and, if eliminated or modified, would have prevented the undesired outcome. Typically, multiple root causes contribute to an undesired outcome.
Supporting Narrative	A paragraph, or section, in an NESC final report that provides the detailed explanation of a succinctly worded finding or observation. For example, the logical deduction that led to a finding or observation; descriptions of assumptions, exceptions, clarifications, and boundary conditions. Avoid squeezing all of this information into a finding or observation.

13.1 ISS PCU Report Definition of Terms

Aurora

Transient displays of light, often displaying as moving curtains and rays, at high latitudes associated with geomagnetic disturbances.

Auroral region

Oval-shaped, high-latitude zone centered on the geomagnetic pole, in which aurora are most visible.

Auroral activity

Usually refers to visible aurora and the particles that create them, but may also refer to electrical currents that flow in the auroral region. One measure of auroral activity is hemispheric power.

Auroral boundary

The high and low latitude edges of the auroral zone, typically 72 degrees (poleward) and 62 degrees (equatorward).

Auroral precipitation

Ionized particles that fall, or are accelerated, into Earth's atmosphere to create the aurora and aid in the flow of electrical current.

Coronal Mass Ejection

An eruption in the outer solar atmosphere that sends billions of tons of magnetized plasma clouds into interplanetary space. When traveling at high speeds these ejections create shocks in the solar wind. Earth-intercept of a CME is often followed by a geomagnetic storm.

Electron volt (eV)

A small unit of energy that is associated with a particle of a single charge, such as an electron or proton, moving through an electric potential of 1V. It is equivalent to 1.602x10^-19 J. Highly energized particles may have energies of mega electron volts (MeV) or beyond.

Energetic charged particles

Charged particles such as energetic electrons and energetic protons, and sometimes heavier ions, that have high enough energies to be moving at a significant fraction of the speed of light – at least 1 percent of the speed of light. These energetic particles can cause ionizing radiation damage spacecraft components and biological materials, such as DNA.

Energetic electrons

Electrons that are traveling much faster than ambient electrons in the space plasma and have the potential for causing ionizing radiation damage to spacecraft and astronauts. Glossary/energetic electrons

Energetic Protons

Protons that are traveling much faster than typical protons in the space plasma and have the potential for causing radiation damage to spacecraft and astronauts. Glossary/energetic protons

Geomagnetic Kp Index

The Kp-index is an indicator of the geomagnetic disturbance level in Earth's mid- and high-latitude magnetic field compared to a quiet day.

Geomagnetic Storm/Space Weather Storm in the Earth's Magnetosphere

Disturbances/Changes in Earth's magnetic field due to changes in solar wind conditions typically lasting 3 to 6 days.

Kp Index

The Kp index indicates the magnitude of geomagnetic disturbance on a 0 to 9 scale, with zero being very quiet and 9 indicating a major geomagnetic storm. The index has a 3-hour cadence. Higher values of Kp are associated with geomagnetic storming, the appearance of auroral lights at lower than normal latitudes, and stronger linkages between Earth's upper atmosphere and magnetosphere. See also the "Kp Indices" Cygnet wiki page.

Magnetosphere

The region of space dominated by the magnetic field of a star or planet. Earth's magnetosphere takes on a tear-drop shape under the influence of the flowing solar wind.

Plasma

Plasma is a distinct phase of matter, separate from the traditional solids, liquids, and gases. It is a collection of charged particles that respond strongly and collectively to electromagnetic fields, taking the form of gas-like clouds. Since the particles in plasma are electrically charged (generally by being stripped of electrons), it is frequently described as an "ionized gas." (http://physics.about.com/od/glossary/g/plasma.htm)

Space Weather

Describes the variable conditions in space, due to solar activity and the solar wind.

14.0 Acronyms List

A	Ampere
A/m^2	Ampere per meter
AIAA	American Institute of Aeronautics and Astronautics
Al	Aluminum
B	Magnetic Field Strength
BRT	Body Restraint Tether
BSC	Body Seal Closure
C_{CG}	Capacitance of Solar Array Cover Glass
C_{EMU}	Capacitance of EMU Insulating Coating
C_{ISS}	Capacitance of ISS Anodization
CAIB	Columbia Accident Investigation Board
CCA	Communications Carrier Assembly
CME	Coronal Mass Ejection
DC	Direct Current
DCM	Display and Control Module
DMSP	Defense Meteorological Satellite Program
EMU	Extravehicular Mobility Unit
EPS	Electrical Power System
EVA	Extravehicular Activity
FDIR	Fault Detection, Isolation, and Recovery
FP	Floating Potential
FPMU	Floating Potential Measurement Unit (operational on ISS from August 2006 to present)
GAIM	Global Assimilation of Ionospheric Measurements (ionosphere model)
gm	gram
GMT	Greenwich Mean Time
IGRF	International Geomagnetic Reference Field
IRI	International Reference Ionosphere (ionosphere model)
ISS	International Space Station
ISSP	ISS Program
j_{th}	Electron Thermal Current
JPL	Jet Propulsion Laboratory
JSC	Johnson Space Center
KSC	Kennedy Space Center
kWh	Kilowatt Hours
L	Length of Conductor
LCVG	Liquid Cooling and Ventilation Garment
LaRC	Langley Research Center
LeRC	Lewis Research Center
LOC	Loss of Crew

M&S	Modeling and Simulation
mA	Milliampere
MDM	Multiplexer/Demultiplexer
m_e	Electron Mass
MMOD	Micrometeoroid Orbital Debris
MMWS	Modular Mini Workstation
mm	Millimeter
ms	Microsecond
msec	Millisecond
MSFC	Marshall Space Flight Center
n	Density
NCE	NESC Chief Engineer
NCR	Noncompliance Report
NESC	NASA Engineering and Safety Center
NEXT	NASA Evolutionary Xenon Thruster
NLP	Narrow-sweep Langmuir Probe (component of FPMU suite of plasma instruments)
NOAA	National Oceanic and Atmospheric Administration
NRB	NESC Review Board
NSTAR	NASA Solar Technology Application Readiness
O	Oxygen
OBS	Operational Bioinstrumentation System
ORU	Orbital Replacement Unit
P_T	Total Probability
PCU	Plasma Contactor Unit
PIM	Plasma Interaction Model (Boeing/SAIC ISS charging model)
PRA	Probabilistic Risk Assessment
rad	Radiation Absorbed Dose
SAIC	Science Applications International Corporation
SAPHIRE	Systems Analysis Programs for Hands-on Integrated Reliability Evaluations
SARJ	Solar Alpha Rotary Joint
SRP	Safety Review Panel
SSP	Space Shuttle Program
SWPC	Space Weather Prediction Center (NOAA, source for space environment data)
T	Temperature
TDT	Technical Discipline Team
TVCIC	Television Camera Interface Converter
U.S.	United States
v	Spacecraft Velocity Vector
V	Volt
$\mathbf{v} \times \mathbf{B} \bullet \mathbf{L}$	Vector cross product of velocity and magnetic field

WLP	Wide-sweep Langmuir Probe (component of FPMU suite of plasma instruments)
YVV	Y-axis in the Velocity Vector

σ	Sigma
e	Electron charge
ε0	Permittivity of free space
kB	Boltzmann's constant
λD	Debye length
Ne	Electron density
Te	Electron temperature
Vf	Floating potential
Vp	Plasma potential
µA	Microampere

15.0 References

1. Allen, J.E. (1992): "Probe Theory – The Orbit Motion Approach," *Physical Scripta*. Vol. 45, 497-503, 1992.
2. Anderson, P. (2005): "Spacecraft Charging Hazards In Low-Earth Orbit," *9th Spacecraft Charging Technology Conference*, 2005.
3. Anon. (2004): ISS Electrical Power Systems Training Manual, ISS EPS TM 21109, Mission Operations Directorate, Space Flight Training Division, NASA Johnson Space Center, 2004.
4. Anthes, R. A. (2011): "Exploring Earth's atmosphere with radio occultation: Contributions to weather, climate and space weather," *Atmos. Meas. Tech.*, 4, 1077–1103, doi:10.5194/amt-4-1077-2011.
5. Biesecker, D.; Balch, C.; and McIntosh, S. (2013): "Where is Solar Cycle 24? Did it happen already? Is There More to Come?," Presented at the *NOAA 2013 Space Weather Workshop*, Boulder, Colorado, 16-19 April 2013.
6. Boeing (2007): "ISS Safety Noncompliance Report," The Boeing Company/Space Exploration/International Space Station, ISS-NCR-203 Rev. B, September 19, 2007.
7. Boeing (2009): "Discovery to Transport Last U.S., Boeing-built Starboard Truss Segment to Space Station," January 2009. http://www.boeing.com/assets/pdf/defense-space/space/spacestation/components/docs/S6.pdf
8. Boeing (2013): *PIMVar1_results.xls* file, 2013a.
9. CAIB (2003): *Columbia Accident Investigation Board, Volume 1*, August 2003.
10. Carruth, Jr., M.R., et al. (2001): "ISS and Space Environment Interactions without Operating Plasma Contactor," AIAA-2001-401, *Aerospace Sciences Meeting and Exhibit, 39th*, Reno, Nevada, January 9-11, 2001.
11. Castillo, M. (2010): *Modular Baseplate Assembly/Body Restraint Tether/Handrail Electrical Continuity Test*, dtd. 05/04/10.

12. Cho, M., K. Saito, and T. Hamanaga (2012): "Data Analysis of the Polar Plasma Environment for Spacecraft Charging Analysis," *Acta Astronautica*, 81, 160-173, 2012.
13. Craven, P.D; Wright, Jr., K.H.; Minow, J.I.; Coffey, V.N.; Schneider, T.A.; J.A. Vaughn, Ferguson, D.C.; and Parker, L.N. (2009): Survey of International Space Station Charging Events, AIAA-2009-0119, *47th AIAA Aerospace Sciences Meeting and Exhibit*, Orlando, Florida, January 5-8, 2009.
14. Dalton, Mark P. (2004): *International Space Station Nickel-Hydrogen Batteries Approached 3-Year On-Orbit*, 2004.
15. Dong, S., et al. (2004): *International Space Station Nickel-Hydrogen Extended Battery Discharge Model Analysis*, 2004.
16. Duncan, G. (2013): Document DRD-MAPI-SA-06-ISSPRA-12-56, EVA Shock Update and Summary, International Space Station (ISS) Probabilistic Risk Assessment (PRA) Trade Study - Long Form, ISS-PRA-12-56 (Probability Risk Assessment Doc), Prepared by Gary Duncan, dated May 17, 2013.
17. Evans, D. S. (2012): "A Study of Intense Auroral Electron Precipitation Events," *Space Environments Laboratory*, NOAA, Boulder, Colorado, personal communication, 2012.
18. Gworek, P.; and Hansen, H. (2002): "EMU - Plasma Arc Update", Presentation to *CCB, Hamilton Sundstrand Space Systems International, Inc.*, April 3, 2002.
19. Hamilton, D. and Kramer, L. (2007): "Simple Transient Circuit Simulation of EMU Touching Solar Array (Bird on a Wire….NOT!!!!)," page 37, August 29, 2007.
20. Hartman, D. (2013a): *Plasma Hazard Relief Assessment for US EVA 22*, ISS-HOU-ENV-WAH-130032, 25 June 2013.
21. Hartman, D. (2013b): *Plasma Hazard Relief Assessment for US EVA 23*, ISS-HOU-ENV-WAH-130035, 2 July 2013.
22. Hartman, D. (2013c): *Extension of Plasma Forecasting, Boeing Space Environments*, 2013.
23. ISS-EVA-312-AC (2012): *Electric Shock to EVA Crew Resulting from EMU Arcing in Plasma*, 1/26/2012.
24. ISS-NCR-232F (2012): *Lack of Two-fault Tolerance to EVA Crew Shock in the Low Earth Orbit Plasma Environment*, 1/31/2012.
25. ISS-NCR-232G (2013): *Lack of Two-fault Tolerance to EVA Crew Shock in the Low Earth Orbit Plasma Environment*, NCR-20264-R7, 18 September 2013.
26. Kaminski, R.; and Scudder, M. (2013): *Boeing ISS EPS*, September 2013.
27. Koontz, Steve (2013): "PCU_emission_currents_2010_through_2013.xlsx," private communication.
28. Kramer, L.; Hamilton, D.; Mikatarian R.; Thomas J.; and Koontz, S. (2010): "Positive Voltage Hazard to EMU Crewman from Currents through Plasma," *Proc. 4th IAASS Conference 'Making Safety Matter'*, Huntsville, Alabama, USA, 19–21 May 2010 (ESA SP-680, September 2010).
29. Kichak, R., E. Young, C. Pandipati, and R. Cooke, International Space Station (ISS) External Television (TV) Camera Shutdown Investigation, NASA TM-2009-215572, NESC-RP-06-49/06-001-E, February 2009.

30. Mikatarian, R. (2010): *Operation of the FPMU to Support Plasma Hazard Assessments, FINAL-ShortVer-2010-04-13-SSPCB-FPMU-Requirements-revK.pdf*, April 13, 2010.
31. Mikatarian, R.; Schmidl, D.; Hartman, D.; Kramer, L. (2013): *Plasma NCR 232 Update*, SSPCB, Boeing Space Environments, October 1, 2013. *Initial Draft: July 2013.*
32. Minow, J. I., and L.N Parker (2013): "Space Weather Monitoring for ISS Geomagnetic Storm Studies," *Space Weather Workshop (invited)*, Boulder, Colorado, 16-19 April, 2013.
33. Minow, J.I. (2004): "Development and Implementation of an Empirical Ionosphere Variability Model," *Adv. in Space Res.*, 33, 887-892, 2004.
34. Minow, J.I.; Pettit, D.R.; and Hartman, W.A. (2012): "Space Weather Monitoring for ISS Space Environments Engineering and Crew Auroral Observations," Abstract IN31D-05 presented at *2012 Fall Meeting, AGU*, San Francisco, California, December 3-7, 2012.
35. Minow, J.I.; Wright, Jr., J.H.; Chandler, M.O.; Coffey, V.N.; Craven, P.D.; Schneider, T.A.; Parker, L.N.; Ferguson, D.C.; Koontz, S.L.; and Alred, J.W. (2010): Summary of 2006 to 2010 FPMU Measurements of International Space Station Frame Potential Variations, *11th Spacecraft Charging Technology Conference*, Albuquerque, New Mexico, 20 - 24 September 2010.
36. Moorehead, R.W., Deputy Director (1992): *Space Station Freedom Program and Operations, communication to Work Packages 1-4 Directors*, dated April 3, 1992.
37. NASA (2004): *A Renewed Commitment to Excellence: An Assessment of the NASA Agency-wide Applicability of the Columbia Accident Investigation Board Report*, PB2005-100968, January 2004.
38. NASA (2009): *Assessment of International Space Station (ISS) Program Plasma Contactor Unit (PCU) Utilization*, NESC Report NESC-RP- 07-054, May 14, 2009.
39. NASA (2013a): NASA-STD-7009 Standard for Models and Simulations, July 10, 2013.
40. NASA (2013b): Press Release 13-193 "NASA Thruster Achieves World-Record 5+ Years of Operation." June 24, 2013.
41. NOAA (2014), Space Weather Prediction Center, URL: http://www.swpc.noaa.gov/ftpdir/lists/iono_day/README, accessed 21 May 2014.
42. Pesnell, W.D. (2008): "Predictions of Solar Cycle 24," *Solar Phys.*, 252, 209-220, 2008.
43. Pesnell, W.D. (2012): "Solar Cycle Predictions (Invited Review)," *Solar Phys.*, 281, 507-532, 2012.
44. Rayman, M.D. (2003): "The Successful Conclusion Of The Deep Space 1 Mission: Important Results Without a Flashy Title," *Space Technology 23*, Nos. 2-3, p. 185, 2003.
45. Rocken, C., Kuo, Y.H.; Schreiner, W.; Hunt, D.; Sokolovskiy, S.; and McCormick, C. (2000): "COSMIC system description," *Terr. Atmos. Oceanic Sci.*, 11, 21–52.
46. Roeschel, E. (2013): "NESC_ISS_Shock_EVA_Actions.pptx" 6-25-13.
47. Sarver-Verhey, T.R. (1997): "28,000 Hour Xenon Hollow Cathode Life Test Results," IEPC-97-168, *25th International Electric Propulsion Conference*, Cleveland, Ohio, August 24-28, 1997.
48. Schmidl, D. (2013a): *EVA Shock Update and Summary PRA Report ISSPRA-12-56*, NASA JSC, May 7, 2013, DRD-MAPI-SA-06-ISSPRA-12-56.

49. Schmidl, D. (2013b): *Plasma Hazard Relief Assessment for US EVA 21*, ISS-HOU-ENV-WDS-110018, 10 May 2013.
50. Schneider, T.A.; Carruth, M.R., Jr.; and Hansen, H.J. (2012): "Minimum Arc Threshold Voltage Experiments on Extravehicular Mobility Unit Samples," AIAA Paper 2002-1040, *40th AIAA Aerospace Sciences Meeting and Exhibit*, Reno, NV, January 14-17, 2002.
51. Schreiner, W.; Rocken, C.; Sokolovskiy, S.; Syndergaard, S.; and Hunt, D. (2007): Estimates of the Precision of GPS Radio Occultations from the COSMIC/ FORMOSAT-3 Mission, *Geophys. Res. Lett*., 34, L04808,doi:10.1029/2006GL027557.
52. Sengupta A.; Brophy J.R.; Anderson J.R.; and Garner C. (2004): "An Overview of the Results from the 30,000 Hour Life Test of the Deep Space 1 Flight Spare Ion Engine," AIAA Paper 2004-3608, *40th Joint Propulsion Conference,* Ft. Lauderdale, Florida, July 11-14, 2004.
53. Smith, C.L. and Wood S.T. (2011a): "Systems Analysis Program for Hands-on Integrated Reliability Evaluations (SAPHIRE) Version 8, Volume 1: Overview and Summary," 2011, United States Nuclear Regulatory Commission, NUREG/CR-7039, Vol. 1.
54. Smith, C.L. and Wood S.T. (2011b): "Systems Analysis Program for Hands-on Integrated Reliability Evaluations (SAPHIRE) Version 8, Volume 1: Technical Reference," 2011, United States Nuclear Regulatory Commission, NUREG/CR-7039, Vol. 2.
55. Space Station Program Office (1994): *Space Station Ionizing Radiation Design Environment*, Revision C, 3, SSP 30512, June 1994.
56. Space Systems/Loral (1998): http://sslmda.com/downloads/products/ispacest.pdf
57. Stamatelatos, M. and Dezfuli, H. (2011) *Probabilistic Risk Assessment Procedures Guide for NASA Managers and Practitioners*, Second Edition, 2011, NASA/SP-2011-3421.
58. Swenson, C.; and D. Thompson (2002): "FPMU Systems Overview," presented at *FPMU CDR*, February 19-20, 2002.
59. Thomas, J.E. (2012): *Lack of Two-fault Tolerance to EVA Crew Shock in the Low Earth Orbit Plasma Environment*, The Boeing Company/Space Exploration/ International Space Station, Joseph E. Thomas (Document Originator), ISS-NCR-232F, 1/26/2012.
60. Utah State University (2002): SDL 2002, FPMU Limited-Life Items List, SDL/02-037, Space Dynamics Laboratory, Utah State University, 7 February 2002.
61. Wright, Jr., K.H.; Swenson, C.; D. Thompson, D.; A. Barjatya, A.; S. L. Koontz, S.L.; T. Schneider, T.; Vaughn, J.; Minow, J.; Craven, P.; Coffey,V.; Parker, L.; and Bui, T. (2007): "Initial results from the Floating Potential Measurement Unit aboard the International Space Station," *10th Spacecraft Charging and Technology Conference*, Biarritz, France, June 18-21, 2007.
62. Wright, et al. (2008): "Charging of the ISS as Observed by the FPMU: Initial Results," *IEEE Transactions on Plasma Science*, Vol. 36, No. 5, October 2008.
63. Wright, et al. (2009): Wright, K.H., FPMURapidChargingEvents_KHW_2009Mar02.xls file, 2009.

16.0 Appendices

Appendix A. Human Current Safety Limits

DC Current Effects (from IEC TS 60479-1)

6.1 Threshold of perception and threshold of reaction

These thresholds depend on several parameters, such as the contact area, the conditions of contact (dryness, wetness, pressure, temperature), the duration of current flow and on the physiological characteristics of the individual. Unlike a.c., only making and breaking of current is felt and no other sensation is noticed during the current flow at the level of the threshold of perception. Under conditions comparable to those applied in studies with a.c., the threshold of reaction was found to be about 2 mA.

Recommend using the threshold for startle reaction since this is for EVA.

Table 13 – Time/current zones for d.c. for hand to feet pathway – Summary of zones of Figure 22

Zones	Boundaries	Physiological effects
DC-1	Up to 2 mA curve a	Slight pricking sensation possible when making, breaking or rapidly altering current flow
DC-2	2 mA up to curve b	Involuntary muscular contractions likely especially when making, breaking or rapidly altering current flow but usually no harmful electrical physiological effects
DC-3	Curve b and above	Strong involuntary muscular reactions and reversible disturbances of formation and conduction of impulses in the heart may occur, increasing with current magnitude and time. Usually no organic damage to be expected
DC-4 [1]	Above curve c_1	Patho-physiological effects may occur such as cardiac arrest, breathing arrest, and burns or other cellular damage. Probability of ventricular fibrillation increasing with current magnitude and time
	c_1-c_2	DC-4.1 Probability of ventricular fibrillation increasing up to about 5 %
	c_2-c_3	DC-4.2 Probability of ventricular fibrillation up to about 50 %
	Beyond curve c_3	DC-4.3 Probability of ventricular fibrillation above 50 %

[1] For durations of current flow below 200 ms, ventricular fibrillation is only initiated within the vulnerable period if the relevant thresholds are surpassed. As regards ventricular fibrillation this figure relates to the effects of current which flows in the path left hand to feet and for upward current. For other current paths the heart current factor has to be considered.

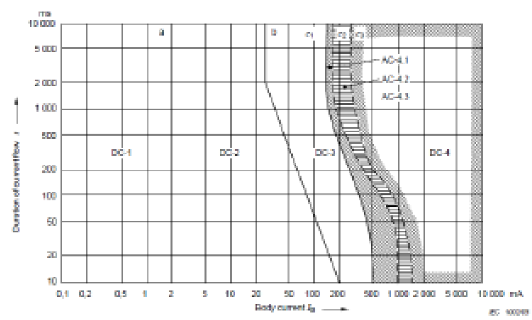

Figure 22 – Conventional time/current zones of effects of d.c. currents on persons for a longitudinal upward current path (for explanation see Table 13)

11/12/2013 Jack Rasbury/Wyle/SF

Appendix B. Overview of Plasma Shock Hazard to EVA Crew

Agenda

- ❑ Shock Hazard Limits
- ❑ Approaches to Defining Hazard Severity
- ❑ Conclusions

Note: This presentation summarizes work performed prior to sign-off of NCR-ISS-232.

Physiological Effects

Effect/feeling	Direct current (mA)		Alternating current (mA)			
			60 Hz		10,000 Hz	
	150 lb	115 lb	150 lb	115 lb	150 lb	115 lb
Slight sensation	1	0.6	0.4	0.3	7	5
Perception threshold	5.2	3.5	1.1	0.7	12	8
Shock not painful	9	6	1.8	1.2	17	11
Shock painful	62	41	9	6	55	37
Muscle clamps source	76	51	16	10.5	75	50
Respiratory arrest	170	109	30	19	180	95
>0.03-s vent. fibril.	1300	870	1000	670	1100	740
>3-s vent. fibril.	500	370	100	67	500	340
>5-s vent. fibril.	375	250	75	50	375	250
Cardiac arrest	--	--	4000	4000	--	--
Organs burn	--	--	5000	5000	--	--

Page No. 3

Jack Rasbury/281-212-1399

Safety Limits

Standard	Limit (mA)	Applies To
JSC-STD-8080 (Std. E-13)	0.001 to 0.1	Bioinstrumentation
JSC 20483 (Obsolete)	0.5 to 1	Bioinstrumentation
NASA-STD-3000 (Obsolete)	0.05 to 0.7 (Leakage) 9.6 to 40 (Let-Go)	Flight Equipment
NASA-STD-3001, Vol. 2	0.05 to 0.5 (Leakage) Defers to IEC 60479	Flight Equipment
IEC 60601-1	0.01 to 1	Medical Equipment
IEC 60950-1	0.25 to 3.5	IT Equipment
IEC 60479-1 IEC 60479-5	0.5 to 2 (Startle Reaction) 5 to 25 (Strong Muscular Reaction) 40 to 350 (Ventricular Fibrillation)	User Defined

The standards are sometimes difficult to interpret and apply.

To date, the IEC 60479 documents have been the most useful.

Page No. 4

Jack Rasbury/281-212-1399

Defining Hazard Severity - Approach 1

- ❑ Model the human body and calculate hazard currents
  - ❑ Work performed prior to ISS mission 15A

Page No. 5 Jack Rasbury/281-212-1399

Body Impedance

- Body impedance is determined by:
  - The contact locations (current pathway)
  - The contact surface area
  - Moisture or wounds on the skin
  - And other factors

Garment Resistance at Rings

Resistance of Garment Between Skin and Metal Contact Area

- Garment thickness, **d = 0.3 cm**
- Area of skin contact, **A = 100 cm2**
- Conductivity of sweat, σ = 0.005560 mhos/cm (from Licht, Stern and Shwachman)
- Resistivity of sweat, δ = 1/ σ = 180 ohm-cm
- Resistance = (δ * d)/A = 0.**54 ohms**
- For the skin contact area of 50 **cm2**, the resistance would be **9.83 ohms**.

Jan 15 15A SORR SLSD Shock Data

Douglas Hamilton Space Medicine JSC

- Internal impedance of the body is mostly resistive and concentrated at the joints
- Human transthoracic impedance can range from 25 to 100 ohms

Page No. 6

Jack Rasbury/281-212-1399

Hazard Currents (in mA) Broken Down By Tether and Mini-Workstation Only @ Solar Min

SOLAR MIN	Wrist	Lower Arm Ring	Body Seal Closure	Waist Ring	Upper Leg Ring	Ankle	
Body Seal Closure or Waist Ring	14.4	19.6	N/A	N/A	20.8	14.4	NASA STD 3000 Solar Min Tether and Mini-Workstation
Physiological Effect	1,2,3,4,5	1,2,3,4,5	N/A	N/A	1,2,3,4,5,6,7	1,2,3,4,5	
Body Seal Closure or Waist Ring	8.6	9.7	N/A	N/A	10.0	8.6	NASA STD 3000 Solar Min Tether only
Physiological Effect	1,2,3	1,2,3	N/A	N/A	1,2,3	1,2,3	
Body Seal Closure or Waist Ring	11.2	13.5	N/A	N/A	13.9	11.2	NASA STD 3000 Solar Min Mini-Workstation Only
Physiological Effect	1,2,3,4,5	1,2,3,4,5	N/A	N/A	1,2,3,4,5	1,2,3,4,5	
Body Seal Closure or Waist Ring	9.4	16.3	N/A	26.3	23.1	8.5	Freiberger Resistances using MWS and Tether at Solar Min
Physiological Effect	1,2,3	1,2,3,4,5	N/A	1,2,3,4,5,6,7	1,2,3,4,5,6,7	1,2,3	
Body Seal Closure	8.7	12.0	N/A	16.0	14.8	8.2	Freiberger Resistancesand only MWS at Solar Min
Physiological Effect	1,2,3	1,2,3,4,5	N/A	1,2,3,4,5	1,2,3,4,5	1,2,3	
Body Seal Closure	7.4	9.0	N/A	11.0	10.4	7.2	Freiberger Resistances and only Tether at Solar Min
Physiological Effect	1,2,3	1,2,3	N/A	1,2,3,4,5	1,2,3,4,5	1,2,3	
Waist Ring	9.2	15.9	N/A	N/A	23.9	8.8	Freiberger Resistances using MWS and Tether at Solar Min
Physiological Effect	1,2,3	1,2,3,4,5	N/A	N/A	1,2,3,4,5,6,7	1,2,3	
Waist Ring	8.6	11.8	16.0	N/A	15.1	8.3	Freiberger Resistances and only MWS at Solar Min
Physiological Effect	1,2,3	1,2,3,4,5	1,2,3,4,5	N/A	1,2,3,4,5	1,2,3	
Waist Ring	7.3	8.9	11.0	N/A	10.6	7.2	Freiberger Resistances and only Tether at Solar Min
Physiological Effect	1,2,3	1,2,3	1,2,3,4,5	N/A	1,2,3,4,5	1,2,3	

Physiological Effect	
1	Trauma Secondary to Simultaneous Involuntary Flexor and Extensor Muscle Contractions
2	Simultaneous Stimulation of Central and Peripheral Sensory and Motor Nerve Bundles.
3	Activate Autonomic Nerve Plexus Causing Nausea and Vomiting
4	Stimulate Spinal Spastic Motor Reflexes Involving Motor Neurons Inferior to the Spinal location of the Sensory Nerve Path.
5	Significant Startle Response with Involuntary Limb Retraction
6	Cardiac Stimulation
7	Minimum Cardiac Fibrillation Thresholds

3 metal collection areas 0.33=Tether, 0.49=MWS and 0.83 Total Area (in square meters.)
2 densities for solar min: $2x10^{11}$ and solar max $1x10^{12}$ m^{-3}.

Jan 22 15A Tiger team

2009, Douglas Hamilton

Hazard Currents (in mA)
Broken Down By Tether and Mini-Workstation Only @ Solar Max

SOLAR MAX	Wrist	Lower Arm Ring	Body Seal Closure	Waist Ring	Upper Leg Ring	Ankle	
Body Seal Closure or Waist Ring	21.2	37.6	N/A	N/A	43.8	21.2	NASA STD 3000 Solar Max Tether and Mini-Workstation
Physiological Effect	1,2,3,4,5,6,7	1,2,3,4,5,6,7	N/A	N/A	1,2,3,4,5,6,7	1,2,3,4,5,6,7	
Body Seal Closure or Waist Ring	19.0	31.8	N/A	N/A	36.4	19.0	NASA STD 3000 Solar Max Tether Only
Physiological Effect	1,2,3,4,5	1,2,3,4,5,6,7	N/A	N/A	1,2,3,4,5,6,7	1,2,3,4,5	
Body Seal Closure or Waist Ring	17.0	26.8	N/A	N/A	30.2	17.0	NASA STD 3000 Solar Max Mini-Workstation Only
Physiological Effect	1,2,3,4,5	1,2,3,4,5,6,7	N/A	N/A	1,2,3,4,5,6,7	1,2,3,4,5	
Body Seal Closure	13.2	25.7	N/A	198.5	65.0	12.1	Freiberger Resistances using MWS and Tether at Solar Max
Physiological Effect	1,2,3,4,5	1,2,3,4,5,6,7	N/A	1,2,3,4,5,6,7	1,2,3,4,5,6,7	1,2,3,4,5	
Body Seal Closure	11.7	19.8	N/A	100.1	41.3	10.9	Freiberger Resistances and only MWS at Solar Max
Physiological Effect	1,2,3,4,5	1,2,3,4,5	N/A	1,2,3,4,5,6,7	1,2,3,4,5,6,7	1,2,3,4,5	
Body Seal Closure	12.5	22.6	N/A	140.7	51.9	11.6	Freiberger Resistances and only Tether at Solar Max
Physiological Effect	1,2,3,4,5	1,2,3,4,5,6,7	N/A	1,2,3,4,5,6,7	1,2,3,4,5,6,7	1,2,3,4,5	
Waist Ring	13.0	24.6	198.5	N/A	77.9	12.4	Freiberger Resistances using MWS and Tether at Solar Max
Physiological Effect	1,2,3,4,5	1,2,3,4,5,6,7	1,2,3,4,5,6,7	N/A	1,2,3,4,5,6,7	1,2,3,4,5	
Waist Ring	11.5	19.1	100.1	N/A	47.7	11.1	Freiberger Resistances and only MWS at Solar Max
Physiological Effect	1,2,3,4,5	1,2,3,4,5	1,2,3,4,5,6,7	N/A	1,2,3,4,5,6,7	1,2,3,4,5	
Waist Ring	12.3	21.7	140.7	N/A	61.0	11.8	Freiberger Resistances and only Tether at Solar Max
Physiological Effect	1,2,3,4,5	1,2,3,4,5,6,7	1,2,3,4,5,6,7	N/A	1,2,3,4,5,6,7	1,2,3,4,5	

Physiological Effect	
1	Trauma Secondary to Simultaneous Involuntary Flexor and Extensor Muscle Contractions
2	Simultaneous Stimulation of Central and Peripheral Sensory and Motor Nerve Bundles.
3	Activate Autonomic Nerve Plexus Causing Nausea and Vomiting
4	Stimulate Spinal Spastic Motor Reflexes Involving Motor Neurons Inferior to the Spinal location of the Sensory Nerve Path.
5	Significant Startle Response with Involuntary Limb Retraction
6	Cardiac Stimulation
7	Minimum Cardiac Fibrillation Thresholds

3 metal collection areas 0.33=Tether, 0.49=MWS and 0.83 Total Area (in square meters.)
2 densities for solar min: $2x10^{11}$ and solar max $1x10^{12}$ m^{-3}.

Jan 22 15A Tiger team

2009, Douglas Hamilton

SLSD Conclusions Prior to ISS Mission 15A

- 15A Hazard Currents could:
  - Cause Trauma Secondary to Simultaneous Involuntary Flexor and Extensor Muscle Contractions
  - Cause Simultaneous Stimulation of Central and Peripheral Sensory and Motor Nerve Bundles.
  - Activate Autonomic Nerve Plexus Causing Nausea and Vomiting
  - Stimulate Spinal Spastic Motor Reflexes Involving Motor Neurons Inferior to the Spinal location of the Sensory Nerve Path.
  - Cause Significant Startle Response with Involuntary Limb Retraction
  - Cause Cardiac Stimulation
  - Reach Minimum Cardiac Fibrillation Thresholds

2009, Douglas Hamilton

Page No. 9

Jack Rasbury/281-212-1399

Defining Hazard Severity - Approach 2

- 3D Computational Modeling
  - Represents hazard prior to MMWS and OBS mods

Page No. 10 Jack Rasbury/281-212-1399

Naval Health Research Center Detachment Directed Energy Bio-effects Laboratory Pilot Study

Finite Difference Time Domain Model

The first computational model, calculates the distribution of electric fields.

Spatially Extended Nonlinear Node Model

The second computational model, the Spatially Extended Nonlinear Node model, was used to establish action potential thresholds for neurons of different diameters

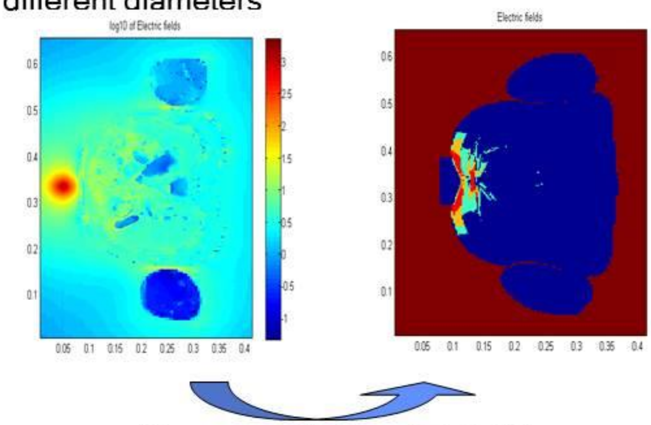

Convert calculated E-fields into Nerve Action Potentials

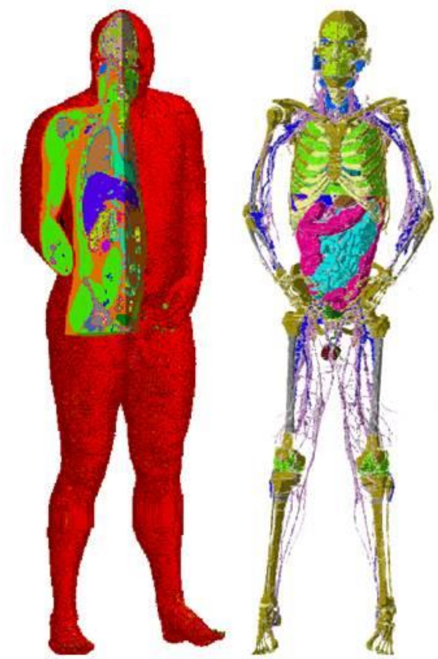

Brooks Man anatomical model with a cutout (left image) and with skin, fat and muscles removed (right image).
2011, Douglas Hamilton

Shock Hazard Path in EVA Suit

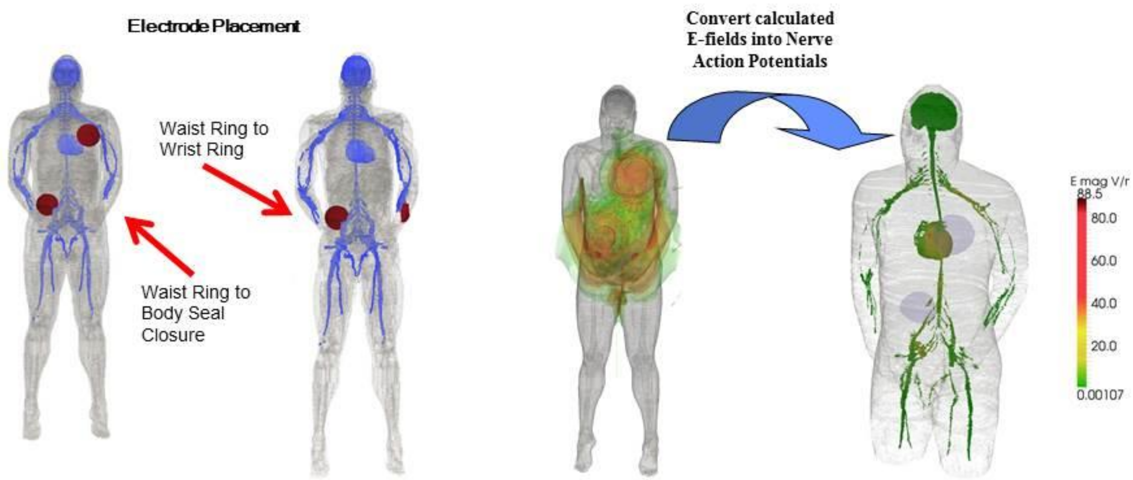

- The peak current induced by a 15 volt contact was:
  - 18.3 mA for the chest-to-hip current path
  - 15.5 mA for the wrist-to-hip current path

2011, Douglas Hamilton

SLSD Conclusions Prior to MMWS/OBS Mods

- If only the large nerve trunks are considered, it is clear that a 15 volt electrical shock to the wrist is likely to cause involuntary left upper extremity movement mediated by motor nerve stimulation of median, ulnar or radial nerves.
- Involuntary motor response in the entire body could be triggered by direct stimulation of left upper extremity sensory nerves which may trigger a spinal reflex.
- Neuromuscular response resulting from direct stimulation of a major nerve trunk is unlikely for a15 volt electrical shock if the electrode path is from the waist to anterior chest.
- The possibility of a startle reaction due to direct excitation of cutaneous receptors is large because the induced current was in excess of 18 milliamps.

Page No. 13 Jack Rasbury/281-212-1399

Comparison to IEC 60479-5

DC Voltage Effects

TR 60479-5 © IEC:2007 – 19 –

Table 2d – Startle reaction for direct current

Startle reaction Current threshold	mA	DC touch voltage thresholds for long duration V								
		Saltwater-wet			Water-wet			Dry		
		Large contact	Medium contact	Small contact	Large contact	Medium contact	Small contact	Large contact	Medium contact	Small contact
Hand-to-hand	2	2	4	12	3	12	56	7	23	78
Both-hands-to-feet	2	1	2	6	2	7	35	4	15	59
Hand-to-seat	2	1	2	6	1	6	28	3	12	39

Table 2e – Strong muscular reaction for direct current

Strong muscular effects Current threshold	mA	DC touch voltage thresholds for long duration V								
		Saltwater-wet			Water-wet			Dry		
		Large contact	Medium contact	Small contact	Large contact	Medium contact	Small contact	Large contact	Medium contact	Small contact
Hand-to-hand	25	24	44	112	29	81	156	43	89	156
Both-hands-to-feet	25	13	23	63	16	51	133	26	67	133
Hand-to-seat	25	12	22	56	15	41	78	21	45	78

AC Voltage Effects

Table 2a – Startle reaction for alternating current 50/60 Hz

Startle reaction Current threshold	mA	AC touch voltage thresholds for long duration V								
		Saltwater-wet			Water-wet			Dry		
		Large contact	Medium contact	Small contact	Large contact	Medium contact	Small contact	Large contact	Medium contact	Small contact
Hand-to-hand	0,5	1	1	3	1	4	21	2	9	40
Both-hands-to-feet	0,5	0,3	1	2	0,4	3	13	1	5	23
Hand-to-seat	0,5	0,3	0,5	2	0,4	2	11	1	4	20

Table 2b – Strong muscular reaction for alternating current 50/60 Hz

Muscular effects Current threshold	mA	AC touch voltage thresholds for long duration V								
		Saltwater-wet			Water-wet			Dry		
		Large contact	Medium contact	Small contact	Large contact	Medium contact	Small contact	Large contact	Medium contact	Small contact
Hand-to-hand	5	5	9	27	7	25	93	11	40	104
Both-hands-to-feet	10	5	9	27	7	25	93	11	40	104
Hand-to-seat	5	3	5	13	3	13	46	6	20	52

Jack Rasbury/281-212-1399

Appendix C. ISS-NCR-232G Review

REVIEWER/Date: Albert Whittlesey, JPL, 2/13/14,
member of NESC ISS Plasma Contactor Unit (PCU) Utilization Plan Assessment Team (shortened to "NESC Team," or usually "The Team" in this review).

COMMENTS TO:

REPORT NUMBER: ISS-NCR-232G

REPORT TITLE: Lack of Two-fault Tolerance to EVA Crew Shock in the Low Earth Orbit Plasma Environment

REPORT AUTHOR: The Boeing Company Space Exploration International Space Station,

DATE OF ISSUE: Sept. 27, 2013, signed by Scott I. Wolf

Background/Introduction:

Block 12: Section A. Applicable Requirement:
SSP 410001 System Specification for ISS
Paragraph 3.3.6.1.1.1 1 Catastrophic Hazard
The on-orbit Space Station shall be designed such that no two failures, or two operator errors (see 6.1), or one of each can result in a disabling or fatal personnel injury, or loss of one of the following: Orbiter or ISS.
SSP 41162 Safety Requirements for ISS
Paragraph 3.3.6.1.1.1 1 Catastrophic Hazards
The USOS shall be designed such that no two failures, or two operator errors (see 6.1), or one of each can result in a disabling or fatal personnel injury, or loss of the Orbiter or ISS.

No comment.

Block 13: Section B. Description of noncompliance: (specify how the design or operation does not meet the safety requirements):

NEGATIVE POTENTIALS, Cause 1.

I have difficulty reading and interpreting the cases involved and how to read and understand Attachment 1 as it supports the text in this Block/Section. In spite of that, I make the following observations.

1. The second row of numbers is 38.8, 29.7, 25.7, and 33.5

From looking at Attachment 1, it looks like the second number should be 29.8:
33.8, 29.8, 25.7, and 33.5
It does not matter in a technical sense but it hinders my understanding of what I should be reading as support for the text.

2. Why are the two numbers 40.8 and 40.7 highlighted in red? It can't be because they exceed the 45.5V requirement. I think it is because they are between 40 and 45.5V, as noted in attachment 1. I think a yellow background highlight of the numbers would have been more meaningful. Also see "Block 15: Section D, paragraph 10: "At the 1/14/09 SRP, a risk acceptance point of -45.5V was agreed upon by the Panel as a final non-negotiable limit for the negative potential." There appears to be an inconsistency between -40V and -45.5V as a hazard limit. Which is correct?

3. "*The largest accepted charging violation is -45.5V*."

Is it permissible to have a waiver based on a prior waiver? In that case, the 40.8 and 40.7V would be permissible on a waiver basis.

4. Apparently the numbers shown in Attachment 1 were generated by PIM3.0. The NESC Team has difficulties with PIM3.0, based on the lack of documentation of the code itself, and the input parameters used for any given use of the code. I don't know if the numbers in attachment 1 are adequately thus documented in the attachment 1 reference, EID684-13598, Rev. B (not examined).

POSITIVE POTENTIALS, Causes 2 & 3.

1. Attachment 2 notes that ISS potentials near the truss extremities can reach +11.9V per EID684-15543. The two paragraphs note that these voltages could "create a shock hazard," and there are "no certified controls to protect against this hazard." Furthermore, this section states that "The EMU is not designed or certified to insulate against electric shock per hazard report EMU-018." Specifically, the "most likely path is between the Modular Mini Workstation (MMWS) and the Display and Control Module (DCM). We have been told repeatedly that most of the EMU metallic parts visible on the surface of the EMU are now carefully covered before and EVA and thus cannot be a current contact point. Additionally, the MMWS is isolated as a possible current flow path into the astronaut (see Attachment 5 as an example). As the team understands it, the only metallic outer path into the astronaut either from a galvanic contact or from a plasma connection is the (anodized) neck ring or

other parts of the headgear, none of which permit a current path through the thorax of the astronaut, which is the most sensitive path for shock hazard.
2. "Bird on a Wire" (Kramer, 2007) uses certain curves to estimate the possible plasma current into exterior metal parts of the EMU (pages 37-38). The Team has examined these curves and found that alternate conservative estimation equations to estimate thorax current are more appropriate and have been validated by the FPMU, that substantially reduce the estimated currents from a neck ring and the current thus calculated current no longer exceeds the applicable safety limits (Katz, et al., 2013), even when positive voltages are as high as 15V (calculated only to +15V, but the positive voltage can be higher and still be safe).

Block 14: Section C, Reason requirement cannot be fulfilled:

NEGATIVE POTENTIALS, Cause 1.

See above for rationale why -40V can be exceeded.

POSITIVE POTENTIALS, Causes 2 & 3).

See above for rationale why Positive potentials will not be a problem.

Block 15: Section D Acceptance Rationale

NEGATIVE POTENTIALS, Cause 1.

1. The present depressed Solar Cycle 24 is limiting charging levels on ISS due to the hotter electrons collecting on the solar array cover glass and producing a potential barrier. This barrier prevents electrons from collecting in the solar array gaps and charging the ISS. The Space Environments community has concluded that, based on the downward trend of recent Solar Cycles, the environment will remain benign at least through Solar Cycle 25, which extends through 2030. FPMU measurements since 2007 have indicated no ISS charging in excess of -45V.

Prior attempts to predict the magnitude of any given solar cycle have failed sometimes to a great degree. Basing future estimates of the future charging of the ISS on this basis is folly.

In any given solar cycle regardless of how strong it is, can have one or more large sunspots that can create huge ISS charging events, even if the cycle itself if generally low.

Making environmental ISS potential predictions on this basis for another 17 years is quite unwise.

> 2. *The ISS floating potential will be verified by a "short-term plasma forecast," issued 14 days prior to a planned EVA. For the negative potential hazard for EVAs that are conducted entirely in-board of the SARJ. PCUs can be placed in discharge even though the ISS charging environment in the current depressed solar cycle does not require it. Because the PCUs are optional, enabling the autoshunt FDIR is not required.*

Assuming that the environment will be the same 14 days from what is today, although generally true, is not adequately true to always use that estimate as gospel for the actual day of a planned EMU. The Team agrees that a FDIR is not an appropriate control (but for other reasons).

> 3. *The "short-term plasma forecast" assessments: (1) utilize planned EVA solar array positions, vehicle attitude, etc. (2) use "short-term" in-situ ionospheric FPMU measured plasma properties to assess present state of ionosphere (e.g., to determine if it is a nominal or* **+1-** *1 or 2σ environment as compared to the International Reference Ionosphere II AI\ model\, and (3) are based on the assumption that the ionosphere will not undergo significant changes over a period of a few weeks (assumption confirmed with considerable FPMU data). In addition, the forecasting process includes space weather solar events (i.e., enhanced solar activity, CMEs, severe solar flares) and are addressed/monitored in real time.*

This section does not include a reference as to where this forecast process is documented.

Utilizing the estimate that the ionosphere will not undergo significant changes over a period of a few weeks has not yet been verified to be a true assumption. The only way to properly verify the ISS state of charge on the day of the EVA is to use the FPMU. The forecasting process uses the data inputs as described above and then computes the ISS potentials based on a computer code called "PIM3.0." PIM3.0 has been shown to have unexplained differences that are far beyond the 1 or 2σ variance when the calculated potentials are compared to the FPMU measurements. At present, the PIM3.0 code as not been adequately validated (NASA coding standards for its use as a personnel hazard protection).

> 4. *It should be noted that certain events that occur after the forecast is issued may invalidate the "short-term forecast" (e.g., the solar array plan changes, reboosts. Debris Avoidance Maneuvers). Also, if an event occurred that was not anticipated after the forecast was issued. The "short-term plasma forecast" would be declared Invalid. Reference Flight Rule 89-908 Plasma Hazard Mitigation During EVA.*

The team agrees with this statement. The prior concerns still apply.

Paragraphs 5-9 in this section deal with "short-term" (meaning on the order of 14 days) "forecast predicts" (meaning calculations of today's ISS charging potentials). They suggest that for extraordinary circumstances raising the ISS potentials above those deemed acceptable, turning on the PCUs and executing the "autoshunt function" (meaning FDIR?) will be used to control ISS potentials. The team agrees that turning on the PCUs is appropriate but disagrees that the FDIR is th*e* appropriate third control for controlling ISS potentials to less than hazardous potentials.

Paragraph 10, stating that -45.5V has been accepted as a non-negotiable risk has been earlier noted that it is not consistent with an earlier implication that -40V is still the limit for non-hazardous ISS potentials.

Paragraph 11, the probabilistic risk assessment summary, is based on ISSPRA-12-56 and summary probability numbers are shown in Attachment 3. A PRA expert has examined -12-56 at the request of The team and notes that at best, the -12-56 PRA is not adequately documented to determine whether its results are consistent with input assumptions, nor is there enough detail/transparency to verify the accuracy of the stated outcome probabilities.

DC POSITIVE POTENTIALS, Cause 2.

Placing the PCUs In discharge produces positive potential hazard in+ 10 to+ 12V range outboard of SAAJ (i.e., catastrophic hazard). Without PCUs in discharge potential at the truss, tips may experience only + 1 to +2 volts.

The team has examined the basis for report's statement of "catastrophic hazard." The team has used newer plasma physics equations as reported separately in this report showing that more exact equations sometimes called "2D," still with generous margins, show much lower possible plasma accumulation currents than were reported in "Positive Voltage Hazard...." (Kramer et al., Sept 2010). With as much as +15V potential on the ISS structure, the astronaut's EMU currents will be much less than the Kramer calculations show for 3V, and are nominally safe by the hazard curves of "Bird on a Wire" by Hamilton and Kramer, August 29, 2007, slides 11-17.

For the positive potential hazard, the PCUs will not be put into discharge for all EVAs out-board of the SARJ. The short-term forecast will be utilized to verify the ISS floating potential environment and in the event of hazardous charging levels that necessitate PCU use during the EVA. ISS will be maneuvered to a YVV attitude which eliminates the hazard. If YVV is undesirable for technical reasons or there is insufficient time to change ISS attitude and there is significant programmatic risk in delaying the EVA, the rationale below can be utilized:

The team disagrees with the rule to not put the PCUs into discharge. The team, by contrast, believes that the best policy is to put the PCUs into discharge during the full EVA. The team recommends that the "short-term forecast" is OK for initial planning, but needs supplemental ISS charging determinations as the EVA nears and during EVA.

In order for the circuit to be completed, several events must occur simultaneously: (1) The EVA crewmember must be at a positively charged location on the ISS truss; (2) The EMU must make galvanic contact with ISS; (3) The exposed bare metal of the EMU must be collecting charge from the ionosphere; (4) The crew must make galvanic contact with bare metal in the EMU interior; and (5) The overall circuit impedance must be low enough to allow a harmful current level. These five events are discussed individually below. {with AW's comment about each}

1) *The VxB.L potential is only at outboard locations and varies with the orbit.*

The team agrees.

2) The medical team assessed possible locations of electric shock on January 12-13, 2009, with a number of points of possible galvanic contact. They are shown in attachment 4.

The NESC team has been led to believe that very few, if any, of the stated possible locations of possible galvanic contact exist after suit modifications. The team supposedly has been provided with up-to-date information which is odd, since the NCR -232G is dated Sept 17, 2013. This discrepancy needs investigation.

A Probabilistic Risk Assessment (PRA) (ISSPRA-12-56, May 7, 2013) was performed with the suspect metallic contact regions included as part of the relatively risk-ratings (before and after MMWS modification) shown in that document.

The team, again, believes that the galvanic contact regions assumed in the PRA are inappropriate and outdated and the PRA at the very least needs redoing with new assumptions. Additionally, the team had the -12-56 report reviewed by a PRA expert, who found its contents to be unreviewable due to lack of completeness. For human safety ratings, one would expect better.

3) 232G suggests that the Body Seal Closure, the Mini Workstation, the Body Restraint Tether, and the waist ring, all of which total collecting area sums to 0.8 m^2.

The team again finds this a large area, more closely fit by 0.3 m^2.

4) 232G assumes good galvanic contact inside the suit to the astronaut by sweat-soaked undergarments and LCVG.

The team agrees.

5) 232G notes that the magnitude of current through a crewmember body depends on the body impedance.

The team agrees, and believes this is built into the safety limit curves in various locations.

6) 232G notes that the MMWS has been modified to isolate the MGA and swings from the baseplate, but only suggests "a significant reduction in the current level .....” See attachment 5 for isolation modifications and Attachment 6 for the pre- and post-modification current levels.

The team notes that the -232G is not very clear, is difficult to read, and thus is subject to uncertainties. For one example, 3) above notes that a total collecting area was calculated to be 0.8 m^2, but the Tables in Attachment 6 have at most 0.3 m^2 collecting areas in the tables, even for "before MMWS modification.” As another example, Attachment 4 has a diagram of "External EMU Metal Surfaces" that is not compatible with the separate text in the PRA -12-56 (which has at least two additional possible external ISS contacts: CCA Connector?-what is this?; and OBS/DCM). As a third example, we are told numerous times that the EMU has had numerous modifications, and yet in Attachment 5, only the two MMWS components are described. The report would have been better served if each of the 9 external contact points in -232G Attachment 4 (11 external contact points used in the PRA -12-56 Table 3) had been listed in a table, showing the original non-isolated condition, and the post-isolation condition and what the improvement was (ohms before and ohms after), and when it was implemented.

TRANSIENT CAPACITIVE DISCHARGE POSITIVE POTENTIALS, Cause 3. *The likelihood of manifesting the +transient capacitive discharge current is comparable to that of the +DC current. Likewise, the MMWS modifications provide mitigation for this hazard as well as the +DC hazard by removing the largest and most likely contact point from the capacitance circuit. Further mitigation of this hazard in the Assembly Complete ISS configuration can be provided by taping the Operational Bioinstrumentation System (OBS) connections inside the EMU with Kaplan to electrically isolate the crewmember from the EMU single-point ground (Ref. CR EVA-01168).*

The team has not heard specifically if the OBS connector inside the EMC is normally taped with Kaplan (sic) (?Kapton®). The team has been told that all possible galvanic connections on the outer surface of the EMU are covered with fabric flaps or are taped (with the possible exception of the neck ring or other head area connections). The team has not seen a specific list of regions that are non-compliant to the general claim of "no galvanic connections from outside the EMU to the astronaut.”

PRA Updates and Results

The P6 lEA battery R&R task performed on Flights 2J/A and ULF4 represents a "worst-case" EVA from an exposure standpoint. The TCS jumper installations, venting and refill of the P6 PVTCS radiator on Flight ULF6 represent a comparable level of exposure. For analysis purposes, it was estimated that approx. 80% of such an EVA would be spent outboard of the P1/P3 interface, i.e., 5:12 of a 6:30 EVA duration. This is reflected in the PRA calculations (Ref. ISSPRA-12-56). See Attachment 3 for the PRA event flow model and PRA results.

The team has not examined this situation and cannot comment.

The PRA was updated to account for the +transient capacitive discharge hazard as well as the mitigation provided by modifications made to the Modular Mini Workstation (MMWS) to electrically isolate it from the Baseplate/BSC. For the Assembly Complete ISS configuration, the PRA also modeled the mitigation provided by isolating the OBS connections inside the EMU to prevent contact with the crewmember. The results of the updated PRA are as follows (numbers are rounded):

+Transient Capacitive Discharge Hazard

(A) The mean probability of a shock event for 1 crew member on a single EVA is 5.11 E-05 (1-in-19.573).
(B) The mean probability of a shock event for 1 crew member on a single EVA with the OBS isolated is 7.00E-07 (1-in-1.428.367).
+DC Hazard
(C) The mean probability of a shock event for 1 crew member on a single EVA is 4.75E-05 (1-in-21,075).
(D) The mean probability of a shock event for 1 crew member on a single EVA with the OBS isolated is 6.63E-07 (1-in-1 .509,206).

The Baseline EVA Risk from all other hazard causes for 2 crew members on a single EVA is 3.86E-05 (1-in-25.920).

The team obtained the services of a senior person with excellent PRA credentials and asked that person to review the -12-56 PRA.

That PRA expert did not have the time to adequately read and verify the total product. In fact, The team was only given a brief summary of the appearance of the document as it appeared to him. That report is provided in another section of The team's report (of which this section is a part). The summary was that it was difficult to properly track and validate the report's contents. However, it did not appear to provide total auditable verification of the results reported (numeric probabilities and error bars of the occurrence of various events). Numeric outputs of the PRA -12-56 are copied into the probabilities locate immediately above this paragraph.

Further, not to quote the PRA expert, but if the team or the ISS wishes to use this PRA (and -232G quotes the PRA extensively to support its conclusions), then the PRA -12-56 should also have a good peer review to validate its assumptions (including basic probability assumptions) and proper use of the specific PRA computer code recognized by the Team's PRA expert).

In conclusion, while there are multiple current paths through the EMU/crewmember that can result in catastrophic effects if the circuit is established, modifications to external conductive EMU equipment have reduced the current associated with the +DC and +transient capacitive discharge hazards

The likelihood of occurrence is comparable to other previously accepted risks.

This conclusion, although weakly stated, is the same one reached by the team: a re-assessment of the risk during an EVA is much reduced because of the changed EMU suit design to isolate most of the possible current attachment paths into the body of the astronaut, and by comparison to other previously accepted risks.

The team's additional recommendations to operate the PCUs during an EVA (two hazard controls); and not use the EVA shunt FDIR logic (possible hazardous FDIR responses in some situations); and to treat the EMU's isolation modifications as a third hazard control, all are compatible with the -232G conclusion above.

Appendix D. Tools and EMU Hardware Presentation

D.1 **NESC_ISS_Shock_EVA_Actions**

D.2 **Modular Baseplate Assembly/Body Restraint Tether/Handrail Electrical Continuity Test**

D.1 NESC_ISS_Shock_EVA_Actions

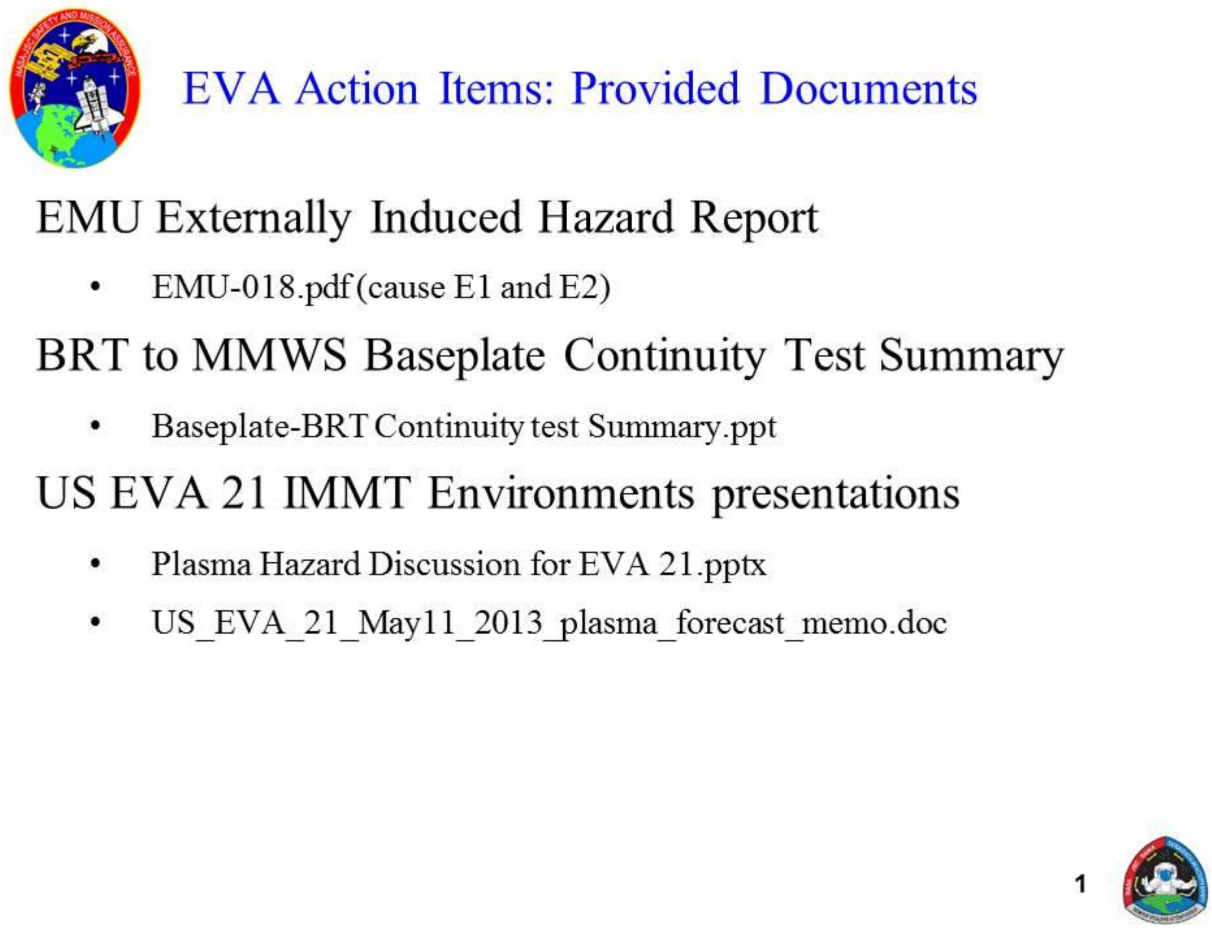

EVA Action Response: Tools and EMU hardware

MMWS Base Plate:

- Was a resistance requirement added?
  - Yes, req 3.1.5.6 was added to the CARD "For the -305 configuration modular baseplate, no conductive path shall exist between the baseplate and both the pivot latch receptacles and the tether ring.
  - This requirement is verified at Pre-Delivery Acceptance, Pre-Installation Acceptance and Qual via ohm meter.
- Number of on-orbit units: 3
- Number of ground spare units: TBD

BRT:

- Was the BRT isolated?
  - No, the project concluded, via test, there is no continuity through the BRT to the MMWS Baseplate. (Summary presentation "Baseplate-BRT Continuity test Summary.ppt")

EMU:

- Are the EMU connector and sizing rings coated?
  - Yes, all aluminum parts are clear anodized.

2

EVA Action Items: Pictures

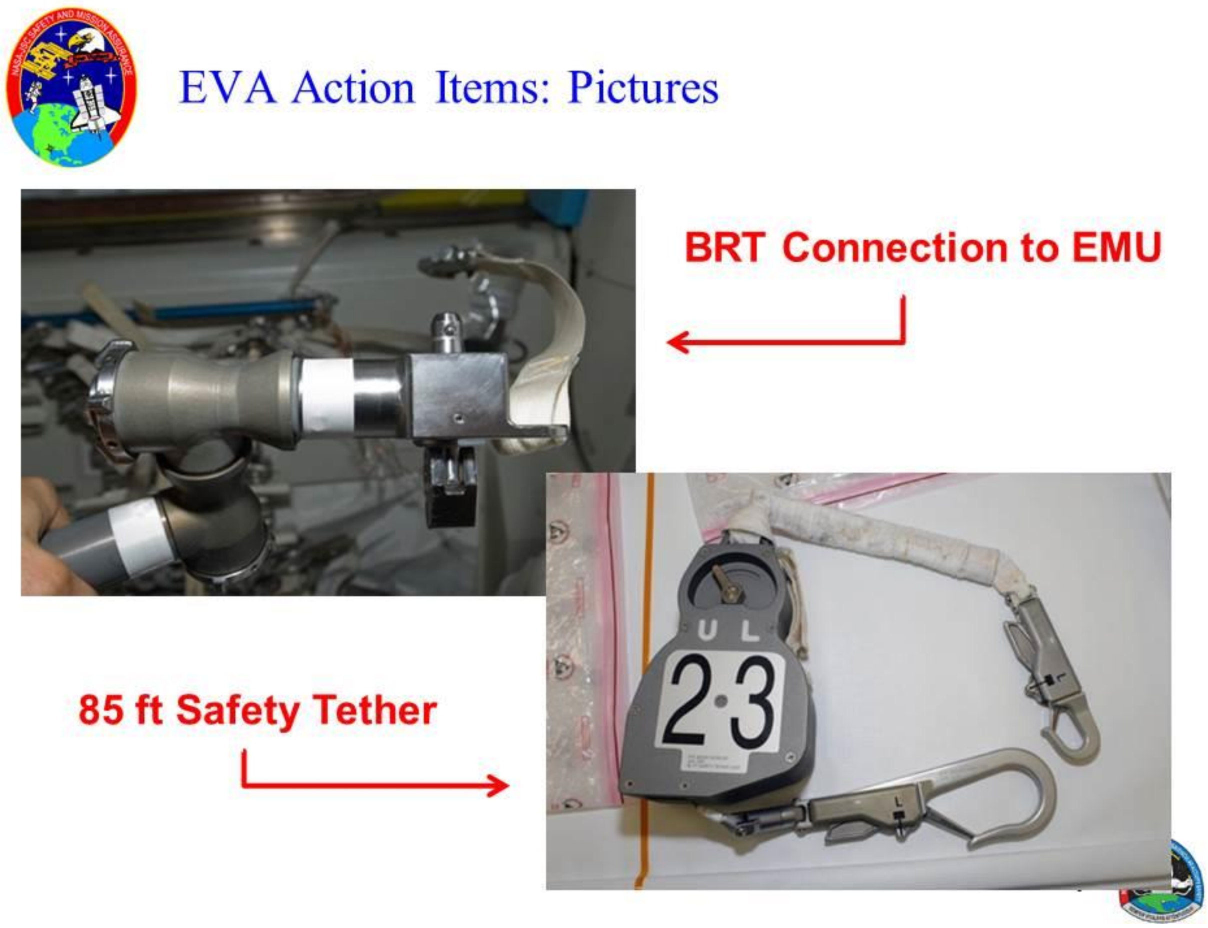
EVA Action Items: Pictures
BRT Connection to EMU
85 ft Safety Tether

EVA Action Items: Pictures

EVA Action Items: Pictures

6

EVA Action Items: Pictures

D.2 Modular Baseplate Assembly/Body Restraint Tether/Handrail Electrical Continuity Test

ONE EVA

Modular Baseplate Assembly / Body Restraint Tether / Handrail

Electrical Continuity Test

ONE EVA – Miguel Castillo

Background

Sponsor:

- OneEVA

Description and History

- To assess the likelihood of further reducing the potential shock hazard to an EVA Crewmember created by exposure to a plasma charged environment, One EVA was tasked with performing an electrical continuity test on 3 tool assemblies
- The 3 tools stack-up was as follows:
  - ✓ Modular Baseplate Assembly (S/N: 1022)
  - ✓ Body Restraint Tether (BRT) (S/N: 1003)
  - ✓ Handrail
    - Tube Drop (no anodize layer)
    - Assembly (gold anodized)

Figure 1 – MMWS Tool Stack-up

Data

ONE EVA

❑ TPS 1011EV175

- Using a multi-meter, verify electrical continuity exists between the following components:
  - ✓ Baseplate Conical Housing to MUT/BRT Mounting Boss: Left: Yes / No Right: Yes / No
  - ✓ BRT Mounting Housing to End Effector (EE) Trigger: Yes / No
  - ✓ Handrail wineglass bottom to scratched Tube surface Yes / No
- Record electrical resistance of the following interfaces:
  - ✓ BRT Tapered Housing to Stainless Steel Trigger inside the EE Jaws → OL (Figure 2)
  - ✓ Modular Baseplate Tapered Housing to Trigger inside the BRT's EE Jaws → OL (Figure 3)
  - ✓ Modular Baseplate Tapered Housing to one of the Hardrail Tube Drop Ends→OL (Figure 4)
  - ✓ Modular Baseplate Tapered Housing to Hardrail Wine Glass bottom surface→OL (Figure 5)

Note: According to the Fluke Model 179 Multimeter's user's manual, when measuring resistance OL ≥ 50 MΩ

Note 2: When measuring continuity on the BRT, a resistance value was only observed when interfacing the Tapered Housing to the first Rotating Dial and when interfacing the Trigger to either of the two Depress Levers. Any other Stainless Steel surface inside of those components were non-conductive when measuring from either the Tapered Housing or the EE Trigger (Figures 6 - 9).

Page No. 3 ONE EVA – Electrical Continuity Test Miguel Castillo – 05/04/10

Pictures

ONE EVA

Figure 2 – BRT Housing to EE Trigger

Figure 3 – Baseplate Housing to EE Trigger

Figure 4 – Baseplate to un-anodized Handrail

Figure 5 – Baseplate to anodized Handrail

Page No. 4 ONE EVA – Electrical Continuity Test Miguel Castillo – 05/04/10

Pictures

ONE EVA

Figure 6 – BRT Housing to 1st Rotating Dial

Figure 7 – BRT Housing to 2nd Dial

Figure 8 – BRT 2nd Dial to EE Base

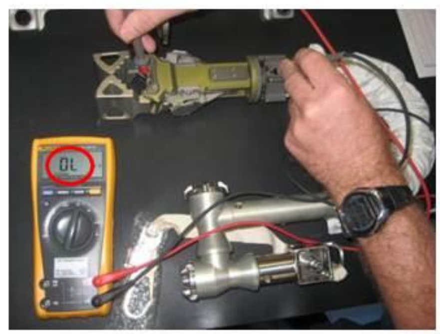

Figure 9 – BRT EE Base to EE Trigger

Page No. 5 ONE EVA – Electrical Continuity Test Miguel Castillo – 05/04/10

Conclusions and Recommendations

ONE EVA

Conclusion

- Electrical Conductivity test determined that in the BRT no continuity could be observed when attaching a multimeter between the tapered housing and the Trigger inside the End Effector Jaws
- Furthermore, no electrical resistance value of could be recorded when attaching the BRT to a Modular Baseplate and either an anodized or an un-anodized Handrail

Observations

- Although no resistance value could be recorded on this particular BRT, previous BRT design verifications have shown that a conductive path can be created between the various mechanisms inside the assembly, mainly by threading into Stainless Steel and anodized aluminum components

Page No. 6 ONE EVA – Electrical Continuity Test Miguel Castillo – 05/04/10

Appendix E. Additional EMU Pictures

EMU Overview and Sizing

February 3, 2006

1

EMU Sizing - Agenda

The purpose of this overview is to inform the reviewers of:

- Components of EMU
- Suit fitcheck process and the basics of an optimal suit fit

2

EMU - Overview

- **The EMU is the interface between the Crew Member and the EVA environment**
  - Provides a protective barrier against natural environment
  - Supplies oxygen for breathing and circulates water for cooling
- **Space Suit Assembly (SSA)** – anthropomorphic pressure vessel that encloses the crewmember
- **Life Support System (LSS)** – backpack containing consumables needed to sustain crewmember
- **Thermal Micrometeoroid Garment (TMG)** – Different layer garment covering EMU provides protection against radiation and micrometeoroids
- **Simplified Aid for EVA Rescue (SAFER)**- propulsive jetpack used for self rescue

3

EMU - Overview

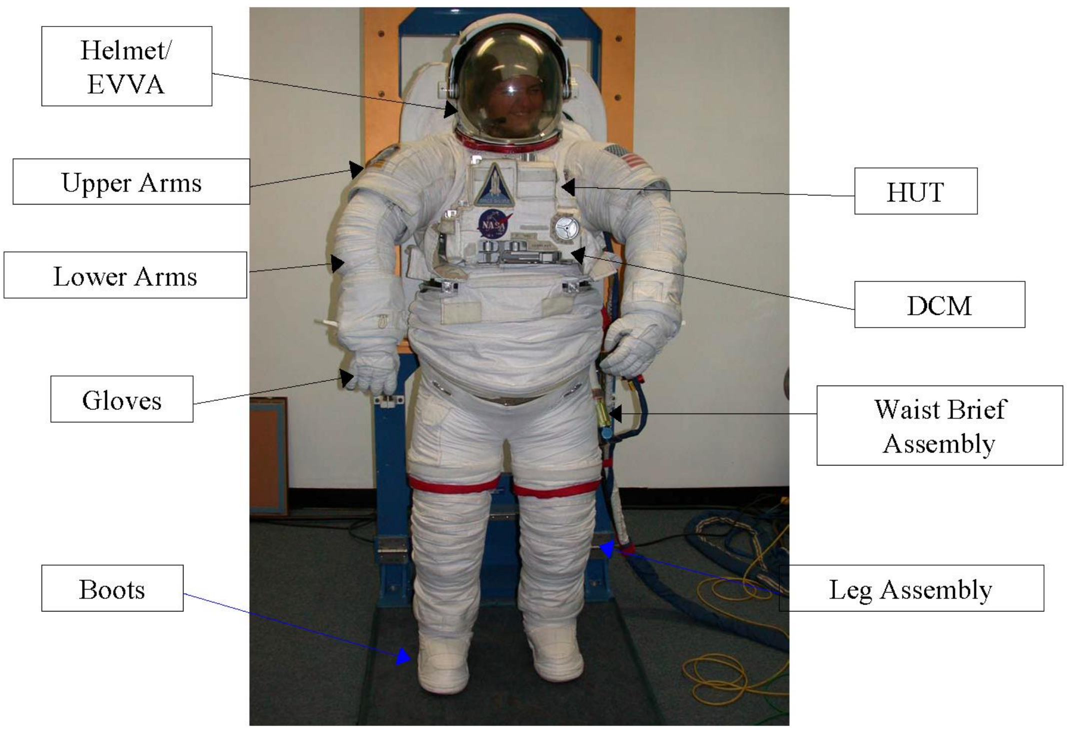

EMU- Helmet/ Extravehicular Visor Assembly (EVVA)

- Helmet Components:
  - Clear polycarbonate bubble
  - Neck ring
  - Ventilation pad
  - Helmet purge valve
- EVVA Components:
  - Protective visor
  - Gold visor
  - Sunshades
- One standard size

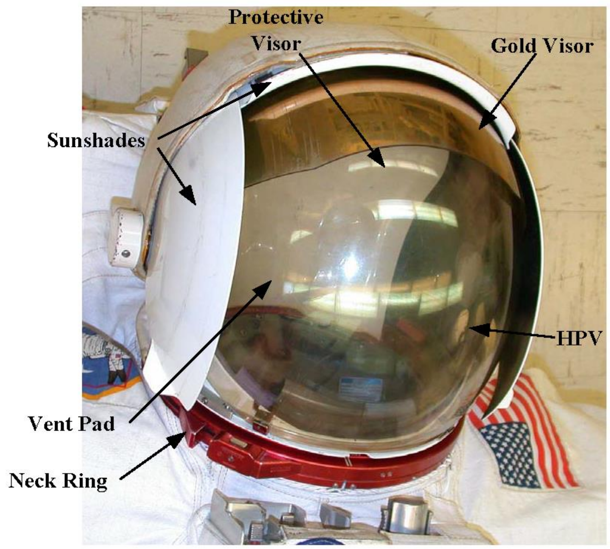

5

EMU-HUT

Planar HUT: rigid fiberglass structure surrounding the upper torso

- All other major components of the EMU are attached to the HUT
- Components:
  - Neck ring
  - Body Seal Closure (BSC)
  - Waterline and Vent Tube Assembly (WLVTA)
- Medium, Large, X-Large
- All sizes use standard 16" BSC
- On orbit replaceable unit (ORU)
- Scye bearings canted forward
- Shoulder movement is limited

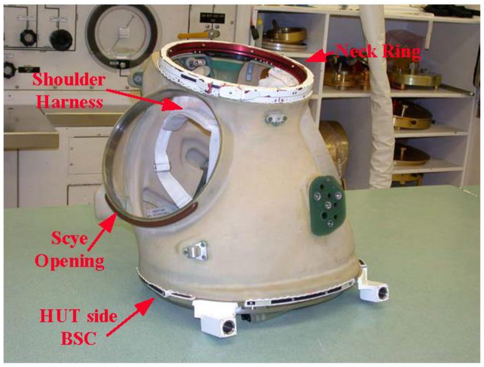

6

EMU – Arm Assembly

- Components:
  - Upper arm: allows shoulder mobility
  - Lower arm: allows elbow/wrist mobility
  - Sizing ring: 0.5" if required
- Nine sizes of lower arms
- Cam brackets provide additional adjustment

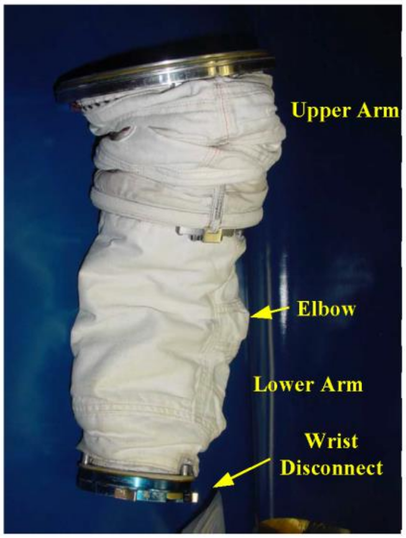

7

Short EMU sizing adjustment

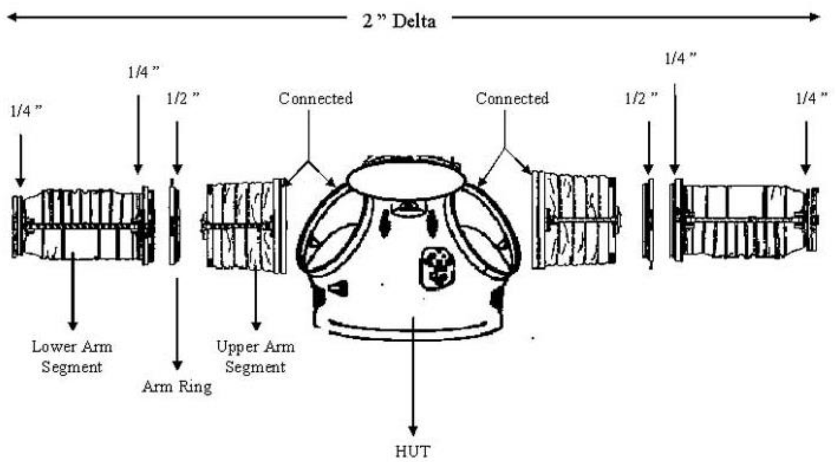

8

EMU Phase VI Gloves - Overview

- **Purpose:**
  - Acts as interface between the Crewmember and associated task
  - Provides protective barrier against natural environment
- **Components:**
  - Bladder
  - Restraint
  - TMG
  - Wrist Tether Strap
  - Wrist Disconnect

9

EMU – Phase VI Gloves

Phase VI Gloves

- Variety of existing and custom sizes
- Dual axis, two ring wrist gimbal design

Phase VI Glove

10

EMU Phase VI Gloves - Restraint

Palm Bar Strap

- Palm bar and palm plate prevent pressurized glove from ballooning out
- Tension adjusted via buckle on back of hand under glove TMG flap

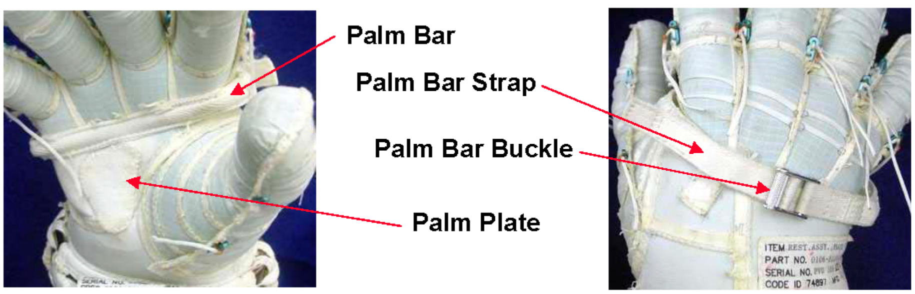

EMU – Lower Torso Assembly (LTA)

- Components:
  - Waist brief assembly
    Leg Assembly
    Boots
    Sizing rings (if required)
- Waist brief assembly: connects HUT to LTA via BSC
- Thigh sizing ring: 0.5"
- Leg sizing ring: 0.5", 1.0", or 1.5"
- Boots:
  - Limited sizing due to foot restraint
  - Heel has slot to fit in foot restraint

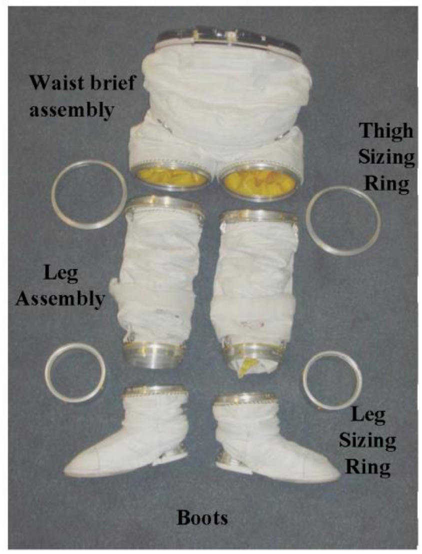

12

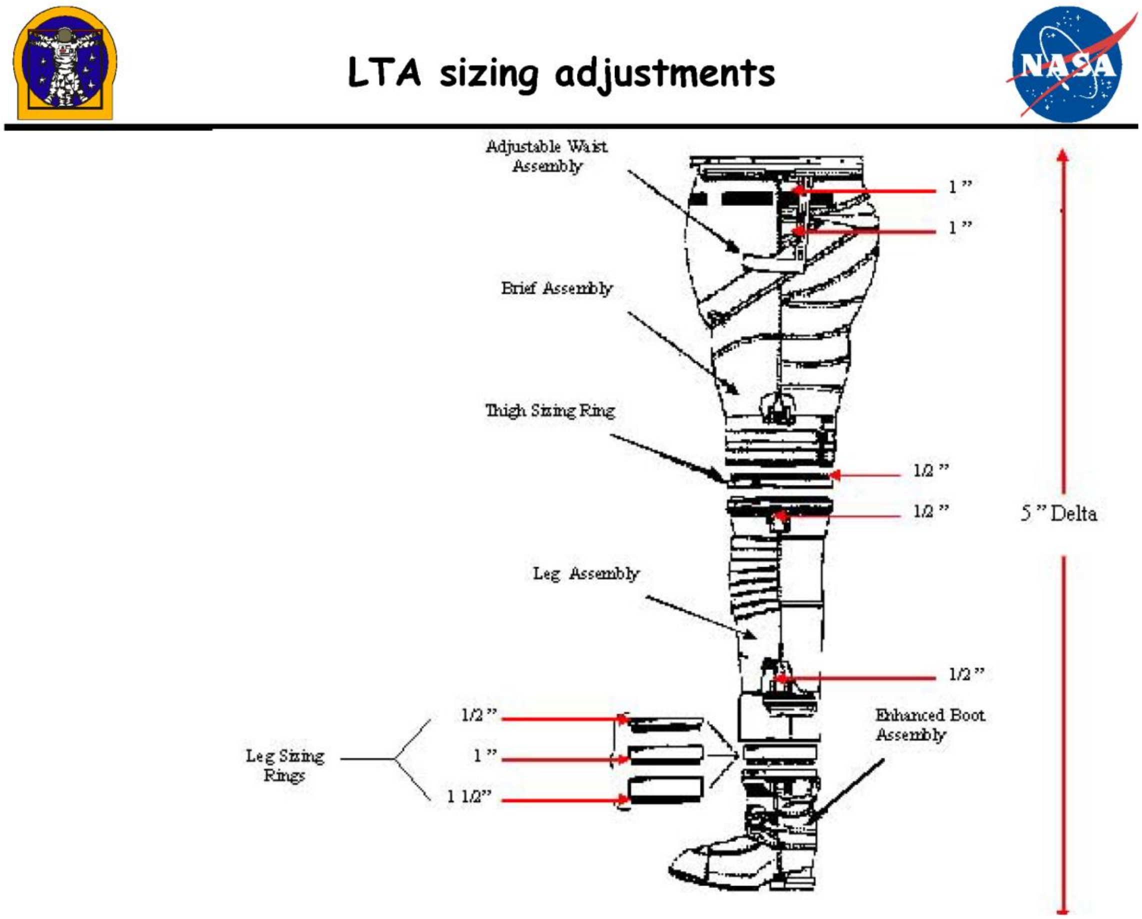
LTA sizing adjustments
Adjustable Waist Assembly
1 ”
1 ”
Brief Assembly
Thigh Sizing Ring
1/2 ”
1/2 ”
5 ” Delta
Leg Assembly
1/2 ”
Leg Sizing Rings
1/2 ”
1 ”
1 1/2”
Enhanced Boot Assembly

EMU-Waist Brief Assembly

- Two types of waists
  - Adjustable Waist: used for flight and provides resizing capability
  - Standard Waist: mostly used for NBL training and has 5 sizes
- Resizing involves manipulation of pins, axial restraints and webbing

14

EMU-Leg Assembly

- Encloses middle part of leg
- Four sizes of legs
- Two cam brackets offer additional sizing (0.5" x 2 = 1" total)
- Knee joint provides flexibility

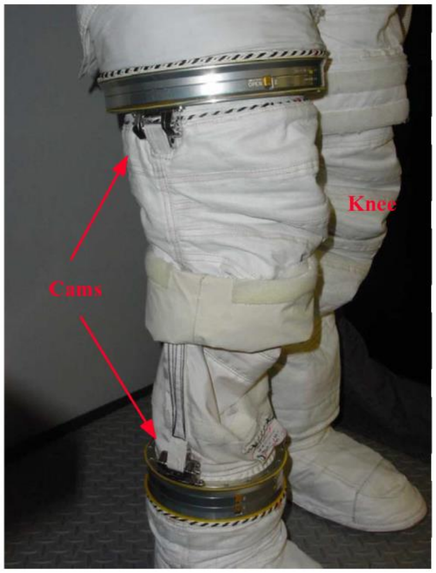

15

EMU-Boots

- Two sizes of boots
- Boot Sizing Inserts (BSI) with Toe Caps provide foot indexing within the boot and thermal protection.
- If BSI not worn, then thermal slipper sewn onto LCVG

16

EMU- Liquid Cooling Ventilation Garment (LCVG)

- Nylon cloth with clear and yellow tubing
- Liquid cooling tubes maintain desired body temperature
- Vent ducts at extremities send oxygen to primary life support system for conditioning
- Seven sizes with additional adjustments
- Comfort pads reduce pressure points or take up free volume in the EMU.

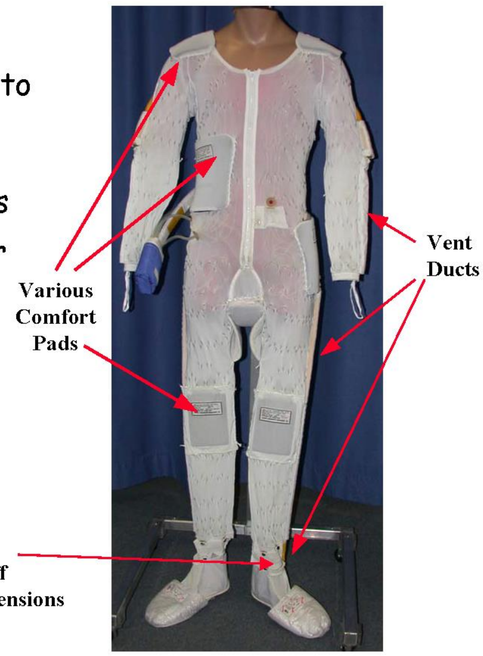

17

EMU- Communication Carrier Assembly (CCA)

- Components:
  - Crew Communications Electronics Module (CCEM)
  - Neck or Chin Strap
  - Sweat Band
  - Ear Cups.
- Six sizes CCAs
- CCEM contains the microphone booms
- Redundant mic booms and ear pieces

18

EMU- Disposable In-Suit Drink Bag (DIDB)

- Stores 32 oz drinkable water in the HUT
- Filled through the Station/Shuttle galley
- Contained in a restraint bag
- Twisting the bite valve can lead to leakage
- Straw may be repositioned

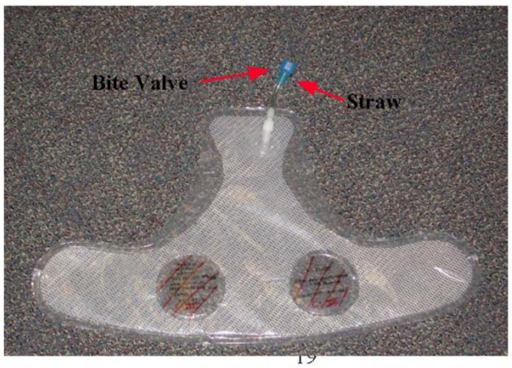

19

EMU-Ancillary Hardware

- **Comfort gloves:**
  - Worn under EMU gloves
  - Provides added comfort
  - Allows easier donning/doffing
  - Wicks away perspiration.

- **Thermal Comfort Undergarment (TCU):**
  - worn under the LCVG
  - undershirt and underpants
- **Maximum Absorbency Garment (MAG):**
  - super-absorbent undergarment worn during EVA

- **Crew Preference and Options Document:**
  - Valsalva, Fresnel Lens, Socks, Wristlet, sports bra, etc.

20

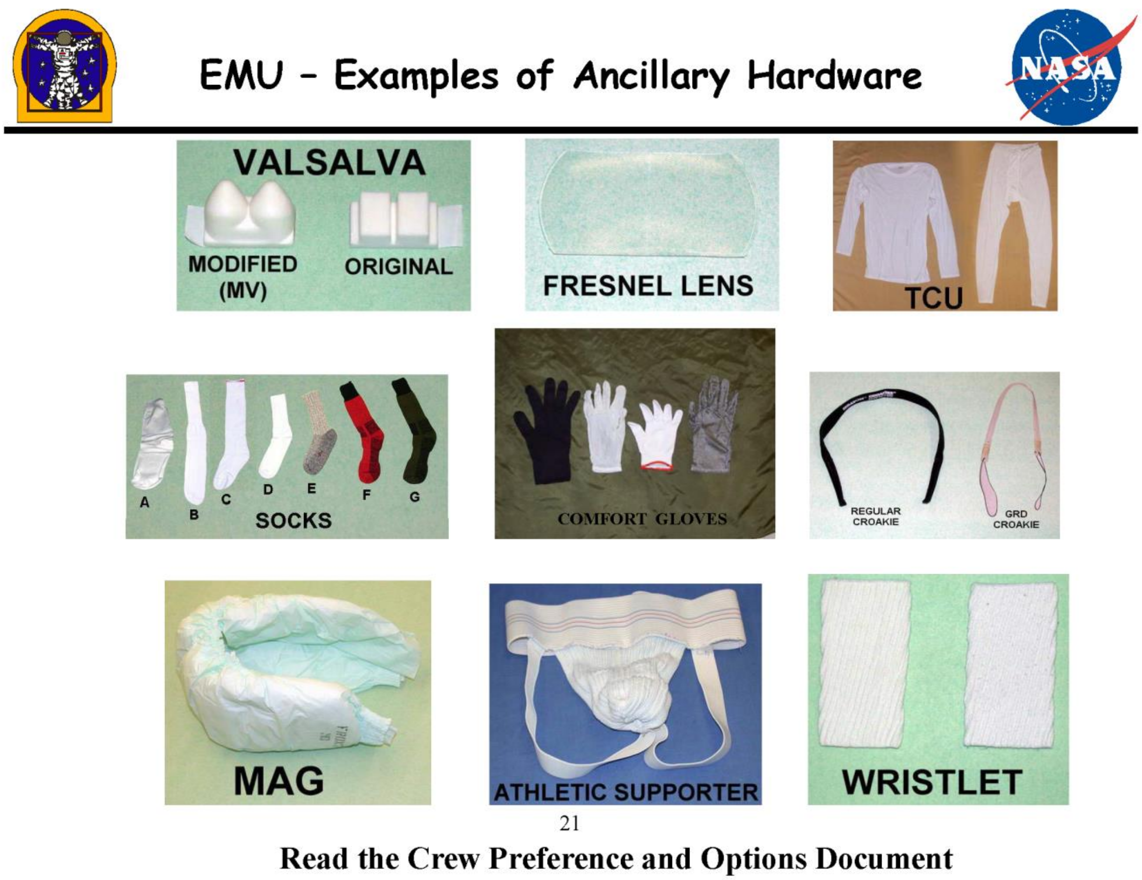

EMU – Examples of Ancillary Hardware
VALSALVA
MODIFIED (MV)
ORIGINAL
FRESNEL LENS
TCU
A B C D E F G
SOCKS
COMFORT GLOVES
REGULAR CROAKIE
GRD CROAKIE
MAG
ATHLETIC SUPPORTER
WRISTLET
21
Read the Crew Preference and Options Document

SAFER

- Provides contingency self rescue capability
- No redundancy
- Accommodates rescue when Orbiter is unavailable
- Utilizes GN2 thrusters
- Virtual reality lab provides 6 DOF training
- One time use only
- Evaluate SAFER reach in NBL

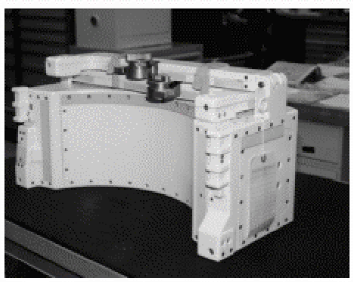

- **The purpose of this overview is to inform the reviewers of:**
  - Components of EMU
  - Suit fitcheck process/optimal suit fit

23

EMU – Fitcheck Process

- Proper fitcheck is critical!
  - ensures no long/short term physical impairments
  - ensures mission success

- Iterative process utilizing predicted sizing for initial fit and crewmember comments for recommended sizing
- Suit fit is evaluated in a 1-G fitcheck prior to an NBL qual evaluation
- After all suited events, post test summaries are distributed with suit fit comments

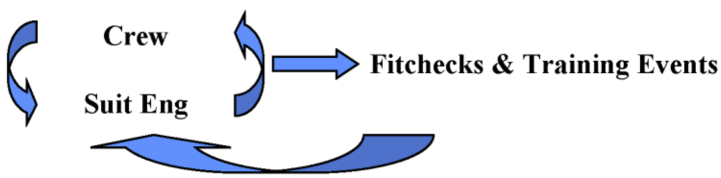

24

Fitcheck Process Flowchart

Measurements:
- Obtain anthropometric data (manually or laser device)
- Use anthros to predict possible EMU sizes

↓

Fitcheck:
- Evaluate unpressurized garments (MAG, TCU, LCVG)
- Discuss crew options
- Don/Doff HUT
- Don LTA
- Connect gloves
- Pressurize to 4.3 psi
- Evaluate reach limitations
- Evaluate contact areas and pressure points
- Be Proactive! Give fit comments to your suit engineer.

25

EMU Phase VI Gloves – Glove Fitcheck Process

Glove Fitcheck Process Flow Chart

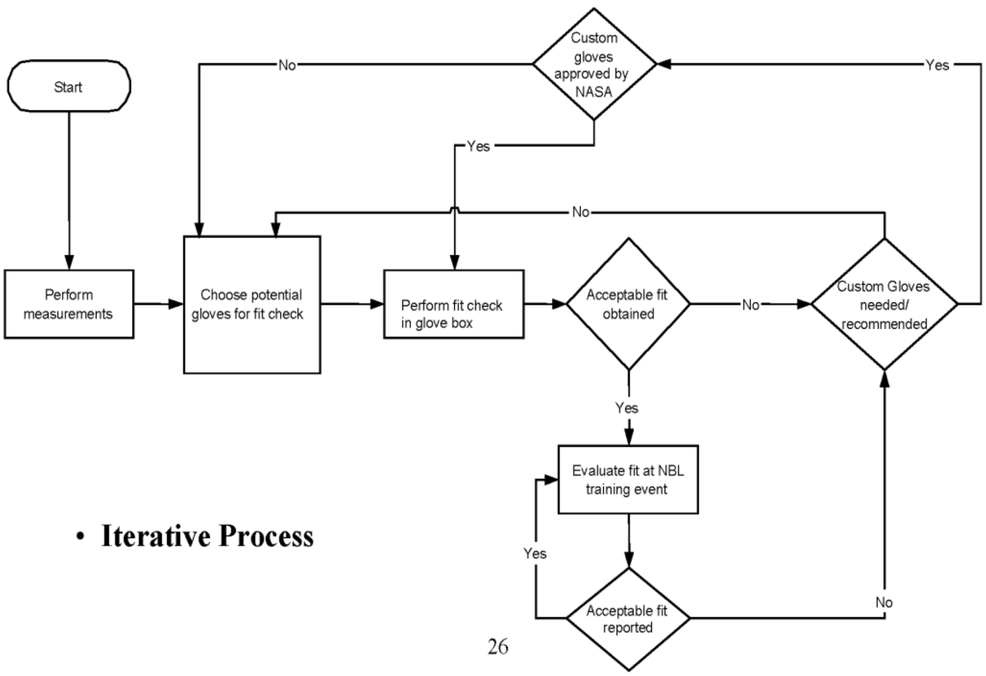

- **Iterative Process**

26

EMU – Post Fitcheck

- Evaluation suit fit during NBL and 1-G events
- Post Test Summaries document sizing issues
- Class I hardware evaluated in chamber runs, FFV
- 1" is added to the waist length for zero G spinal growth

27

ADDITIONAL US SPACECUIT PICTURES

http://spaceflight.nasa.gov/gallery/images/station/crew-32/html/iss032e024373.html

ISS032-E-024373 (30 Aug. 2012) --- NASA astronaut Sunita Williams, Expedition 32 flight engineer, attired in an Extravehicular Mobility Unit (EMU) spacesuit, is pictured in the Quest airlock of the International Space Station prior to a session of extravehicular activity (EVA).

ISS036-E-014724 (3 July 2013) --- NASA astronaut Chris Cassidy (left) and European Space Agency astronaut Luca Parmitano, both Expedition 36 flight engineers, attired in their Extravehicular Mobility Unit (EMU) spacesuits, participate in a "dry run" in the International Space Station's Quest airlock in preparation for the first of two sessions of extravehicular (EVA) scheduled for July 9 and July 16. NASA astronaut Karen Nyberg, flight engineer, assists Cassidy and Parmitano.

http://spaceflight.nasa.gov/gallery/images/station/crew-36/html/iss036e014724.html

How NASA Spacesuits Work: EMUs Explained (Infographic)
http://www.space.com/21987-how-nasa-spacesuits-work-infographic.html

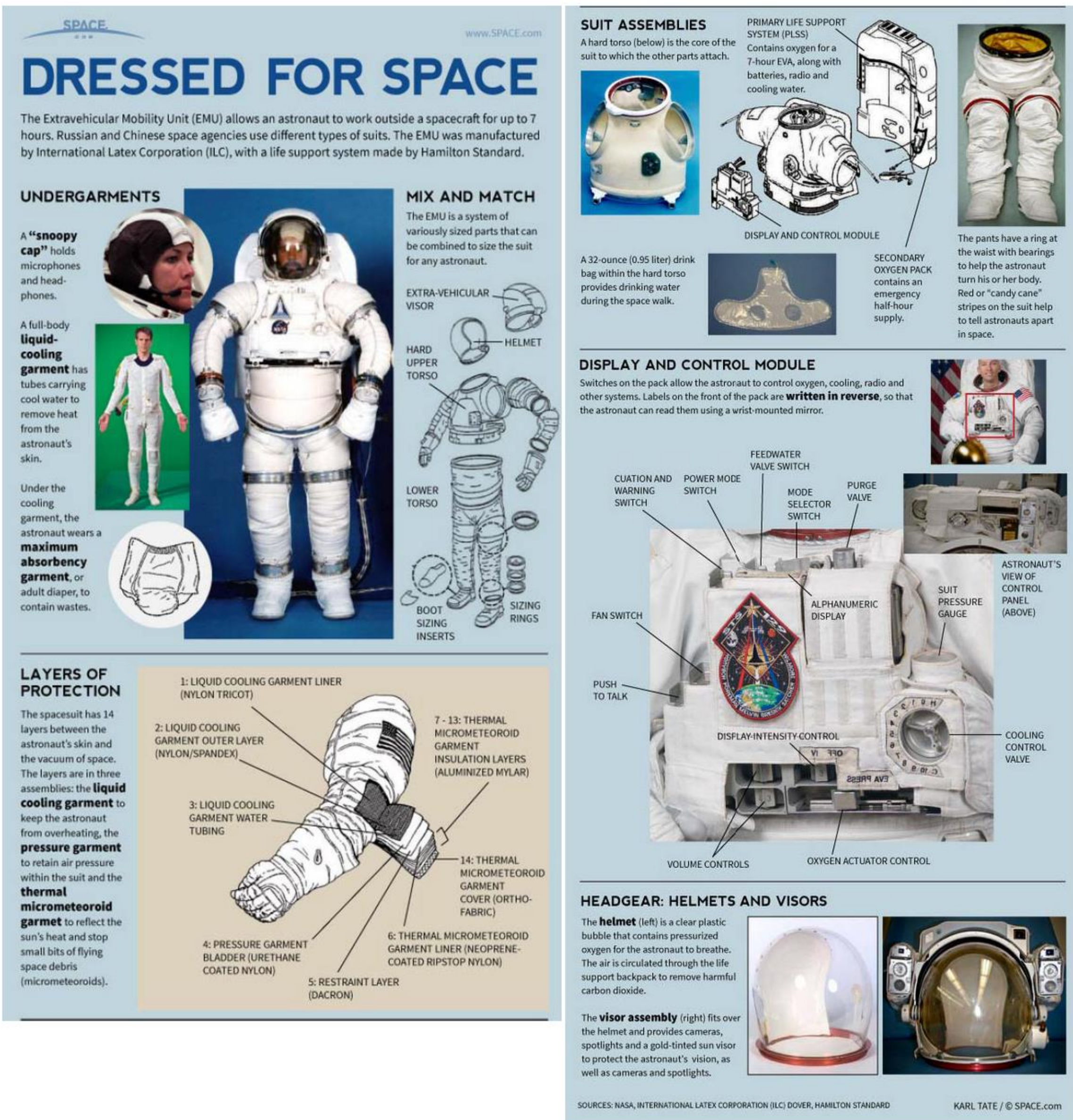

Appendix F. FDIR Reference Emails

Hernandez-Pelle, Amri I. (GSFC-5630)

From:	Scudder, Matthew P <matthew.p.scudder@boeing.com>
Sent:	Monday, August 05, 2013 7:04 PM
To:	Hernandez-Pelle, Amri I. (GSFC-5630); Iannello, Christopher J. {Chris} (KSC-C104); Galvez, Ronald M. (JSC-EP511)
Subject:	RE: ISS PCU Failure Array Shunt FDIR Algorithm
Attachments:	US_EVA_22.docx

All 8 power channels are independent so if even 1 array is shunted, that channel will be operating from batteries. ISS going to battery power is acceptable, as long as it is a relatively short duration. Operator initiated shutdown of ISS loads (referred to as power-downs) may occur if deemed warranted to lengthen the time the batteries can provide power to critical systems.

Below is an example of a recent set of EVAs where the “space weather” forecast was favorable, such that upon PCU failure no additional safing action is required.

There are no constraints (aside from EVA safety) when to unshunt the solar arrays. Commanded unshunting of the solar arrays may occur during insolation or eclipse, with the array pointing at any combination of SARJ and BGA positioning, at any point in the orbit.

Matthew

CONTROL NUMBER:	SUBJECT:		REQUEST ORG:	STATE:
011386	Request for VIPER Short-Term Plasma Forecast for US EVA 22 (36-1)		MOD	DISPOSITIONED
ACTIVITY: Increment 36	GMT CREATED: 2013/156:00:05	GMT ACTION REQD: 2013/189:00:00	RESPONSE ORGs: IMC, ISSMER	

MOD REQUEST

contact: Barrett, Elizabeth A. (SPARTAN), 45301

SPARTAN requests VIPER provide short-term plasma environment forecast analysis to relieve array shunting constraints for US EVA 22 being planned for July 9th (GMT 190) in the event of a PCU failure and during the planned timeframe when one PCU will be powered down (Reference Flight Rule B9-908 paragraph D). SPARTAN requests that the 1A/2B array combination remain unshunted following PCU failure during the EVA. Beyond that, the arrays which SPARTAN would prefer to be cleared, in preferred order, are 1B, 2A, 4A, 4B, 3B, 3A. SPARTAN understands that not all will likely be allowed, but the full set of preferred order is provided for completeness.

It is understood that the application of the short-term plasma environment forecast process for a pre-planned EVA represents a change to the process in Hazard Report ISS-EVA-0312 and NCR-ISS-232E. The safety community (via the safety console) is requested to concur with this application of the short-term plasma environment forecast.

In the event the plasma forecast indicates that no arrays need to be shunted, SPARTAN requests that PCU FDIR be left inhibited during the entire EVA. In this situation, enabled software would shunt the arrays but then they would be manually unshunted based on the plasma forecast. Having the software enabled would create

1

additional, unnecessary actions. It is understood that not enabling the PCU FDIR represents a change to the process in Hazard Report ISS-EVA-0312 and NCR-ISS-232E. The safety community (via the safety console), ISS MER and IMC is requested to concur with not enabling the PCU FDIR for the entire EVA if the short term plasma forecast predicts that no arrays need to be shunted or wake pointed after a PCU failure. Note that the FDIR will be inhibited when one PCU is powered down for safing as part of the nominal EVA timeline (the arrays will be appropriately safed during this timeframe).

It is understood that FPMU data will be required to produce this short-range forecast. Note that this EVA will take place in a +XVV attitude.

The preliminary forecast is needed 2 weeks prior to the start of the EVA so that the Flight Control Team can plan for the expected BGA feathering requirements and impacts in support of the planned PCU deactivation during the EVA. It is understood that the 2 week forecast is not final and is subject to change. The Flight Control Team will work to the forecast provided but also carry a separate worst-case plan as well.

The final forecast is needed at least 24 hours prior to the start of the EVA so that the Flight Control Team can uplink a revised version of Warning procedure 2.646 PCU 3B(4B) EVA Hazard to the Crew and finalize BGA feathering and powerdown plans.

Actions:
VIPER: Provide short-term plasma forecast
ISS-MER, IMC: Provide concurrence

IMC RESPONSE

contact: Cranford, Cindy (Manager), 46161

IMC has reviewed and concurs with the information in this chit.

ISSMER RESPONSE

contact: Palacios, George J. (Manager), x39456

EVA

contact: Thomas, Lawrence A. (EVA), 281-483-9163

EVA Concurs

SAFETY

contact: Daniel, Christina D. (SAFETY), 281-335-2183

Safety concurs with this chit.

VI

contact: ROMILLO, JESSICA L. (VIPER), 281-226-4428

FPMU eclipse exit Ne and Te data from June 17-24 have been compared to calculations using the IRI-2011 model. The results show that the ionosphere is currently in a nominal to –2s state. In order to be conservative, this assessment is based on a nominal environment.

Based on the solar array plan provided by VIPER, and the present ISS nominal plasma environment determined by the FPMU data, no solar arrays would need to be shunted/wake pointed in the event of a PCU failure.

Note: The Space Environments team will continue to monitor the Sun-Earth environment parameters, FPMU data, and Vehicle operations (e.g. Reboost/DAM) to determine if the forecast continues to be applicable. If the current ionospheric variability changes from the value shown in this analysis or an unplanned operation that changes the vehicle velocity occurs, there may be additional constraints. The Space Environments team will notify the VIPER console as soon as possible, if that occurs.

Attachment: US_EVA_22.docx

Attachments

US_EVA_22.docx (41 KB)

MOD DISPOSITION

contact: Barrett, Elizabeth A. (SPARTAN), 45301

SPARTAN acknowledges. Based on the forecast, both PCUs will be in discharge but the PCU FDIR will not be enabled and BGAs will not be preemptively parked for the planned powerdown of PCU 2 due to the Y-jumper installation safing. However, the timeline will maintain these callouts (which can be aborted if not required) to protect for the possibility of a change in the forecast prior to execution.

This CHIT should remain in disposition until after US EVA 22. (ECD GMT 191)

US EVA 22 was completed nominally with all BGAs remaining in autotrack for the PCU down timeframe. This CHIT can be closed.

From: Hernandez-Pelle, Amri I. (GSFC-5630) [mailto:amri.i.hernandez-pelle@nasa.gov]
Sent: Wednesday, July 31, 2013 7:23 PM
To: Scudder, Matthew P; Iannello, Christopher J. {Chris} (KSC-C104); EXT-Galvez, Ronald M
Subject: RE: ISS PCU Failure Array Shunt FDIR Algorithm

Hi Matthew,

I have two more topics related to the FDIR array shunting to ask you about:

1) The B9-908 document states:

3

The one failure deep case that removes power to both a PCU and a primary PVCU is the rationale for setting all eight arrays to shunt in the PCU FDIR versus only six arrays. This ensures that even if a PVCU failure does not allow shunting of an array pair, the necessary number of arrays are still shunted. No PVCU transition is necessary if the array pair controlled by a PVCU that shares a power channel with a PCU is allowed per paragraph D (or E if HTV is berthed).

- Are all eight arrays always shunted upon a PCU failure? If yes, does that mean the ISS going to battery power is acceptable?

2) Last time you explained us (supported by the document) that arrays are unshunted only if placed >15 degrees to wake. However, are there any rules or specifications of when can the un-shunting commands occur relative to in-sunlight, in-eclipse, time within sunlight, etc…? Or is it when needed regardless of time in orbit? Any other (non-time, nor > 105°) related restrictions to un-shunt?

Once again thank you for your support,

Amri

Hernandez-Pelle, Amri I. (GSFC-5630)

From:	Scudder, Matthew P <matthew.p.scudder@boeing.com>
Sent:	Wednesday, July 17, 2013 6:21 PM
To:	Hernandez-Pelle, Amri I. (GSFC-5630); Iannello, Christopher J. {Chris} (KSC-C104); Galvez, Ronald M. (JSC-EP511)
Subject:	RE: ISS PCU Failure Array Shunt FDIR Algorithm

Is the FDIR in charge of pointing the arrays to > 105° from the velocity vector?, Or a separate control (or software) does that?
The ground (MCCH) will command the solar arrays to their new positions, once the PCU failure is confirmed.

Does the FDIR prevents other controls from unshunting the arrays while it is enabled or can it be overwritten during operation by an external control?
Once the arrays are shunted (software will retry up to 3 times, with 15 seconds between tries) the software doesn't do anything else. Once the arrays are shunted via the FDIR, if an operator were to command a SSU to unshunt the arrays, it will go thru.

I am trying to understand where is the operational priority for the array >105 pointing and unshunting and how the FDIR fits in the commands/controls priority or hierarchy.
The primary controls for the EVA Hazard are the two PCUs. Since it's a catastrophic hazard, a third control is required. Since the hazard has been determined to only exist when the solar arrays are unshunted (providing power) and pointed towards the velocity vector (in the ram direction), the third control can be to either shunt the arrays (the FDIR) or to ensure the arrays are out of the velocity vector. Keeping the arrays out of the velocity vector leads to poor power generation thru the majority of the orbit, and to maintain power balance, the powerdowns required for the entire duration of the EVA would be severe. The program does not like the idea of the severe powerdowns unless absolutely necessary (loss of science, excessive MCCH workload, risk to single string systems, etc) therefore over the years we have made it the "backup" plan. (I'm referring mostly to paragraphs A and B in the flight rule below.)

Matthew Scudder
Boeing ISS EPS Engineering, Hardware Lead
281-226-6975

The following is Flight Rule B9-908:

B9-908 PLASMA HAZARD MITIGATION DURING EVA [HC] [RC]

A. DURING NOMINAL EVA PERIODS, HAZARD CONTROLS ARE REQUIRED AS FOLLOWS: ®[022802-5153B] ®[081811-00363B]

1. TWO PCU'S ACTIVE IN DISCHARGE MODE

2. ONE OF THE FOLLOWING:

a. CCS PCU EVA HAZARD CONTROL FDIR ENABLED

b. NO MORE THAN 2 ARRAYS UNSHUNTED WHILE ORIENTED LESS THAN 105 DEGREES FROM THE VELOCITY VECTOR. ALLOWED 2 ARRAY COMBINATIONS ARE DOCUMENTED IN PARAGRAPH D (OR E IF HTV

BERTHED). ANY ARRAY ORIENTED 105 DEGREES OR GREATER FROM THE VELOCITY VECTOR MAY BE UNSHUNTED.

B. IN THE EVENT OF PCU FAILURE DURING OR PRIOR TO AN EVA, CCS PCU EVA HAZARD CONTROL, IF ENABLED, WILL SHUNT ALL ACTIVE SOLAR ARRAYS. THE EVA MAY CONTINUE WITH ONE OR ZERO ACTIVE PCU'S AFTER THE FOLLOWING CONFIGURATION HAS BEEN ESTABLISHED:

NO MORE THAN 2 ARRAYS UNSHUNTED WHILE ORIENTED LESS THAN 105 DEGREES FROM THE VELOCITY VECTOR. ALLOWED 2 ARRAY COMBINATIONS ARE DOCUMENTED IN PARAGRAPH D (OR E IF HTV BERTHED). ANY ARRAY ORIENTED 105 DEGREES OR GREATER FROM THE VELOCITY VECTOR MAY BE UNSHUNTED.

C. IF METHOD OUTLINED IN PARAGRAPH B DOES NOT ACHIEVE SATISFACTORY PREDICTED BATTERY SOC, THEN SOLAR ARRAY POSITIONING WILL BE GUIDED BY RULE {B2-38}, SOLAR ARRAY POSITIONING PRIORITIES. ®[081811-00363B]

This Rule Continued on Next Page

B9-908 plasma hazard mitigation DURING EVA [hc] [RC] (continued)

D. THE FOLLOWING ARRAY COMBINATIONS MAY REMAIN UNSHUNTED AND/ OR POINTED IN THE VELOCITY VECTOR FOLLOWING A PCU FAILURE IF HTV IS NOT BERTHED TO ISS (TO INCLUDE ATV BUT EXCLUSIVE TO COTS VEHICLES): ®[081811-00363B]

POWER CHANNELS	STATION ATTITUDE	INBOARD OF PORT SARJ	INBOARD OF STBD SARJ	OUTBOARD OF PORT SARJ	OUTBOARD OF STBD SARJ	CENTERLINE OF VEHICLE
1A, 2B (PREFERRED)	+XVV	ALLOWED	ALLOWED	ALLOWED	ALLOWED	ALLOWED
	-XVV	ALLOWED	ALLOWED	ALLOWED	ALLOWED	ALLOWED
	+YVV	ALLOWED	ALLOWED	ALLOWED	ALLOWED	ALLOWED
	-YVV	ALLOWED	ALLOWED	ALLOWED	ALLOWED	ALLOWED
1A, 2A	+XVV	ALLOWED	ALLOWED	ALLOWED	ALLOWED	ALLOWED
	-XVV	ALLOWED	ALLOWED	ALLOWED	ALLOWED	ALLOWED
	+YVV	ALLOWED	ALLOWED	ALLOWED	ALLOWED	ALLOWED
	-YVV	ALLOWED	ALLOWED	ALLOWED	ALLOWED	ALLOWED
2B, 3A	+XVV	ALLOWED	ALLOWED	ALLOWED	ALLOWED	ALLOWED
	-XVV	ALLOWED	ALLOWED	ALLOWED	ALLOWED	ALLOWED
	+YVV	ALLOWED	ALLOWED	ALLOWED	ALLOWED	ALLOWED
	-YVV	ALLOWED	ALLOWED	ALLOWED	ALLOWED	ALLOWED
S6 1B, 3B	+XVV	ALLOWED	ALLOWED	ALLOWED	ALLOWED	ALLOWED
	-XVV	ALLOWED	ALLOWED	ALLOWED	ALLOWED	ALLOWED
	+YVV	ALLOWED	ALLOWED	ALLOWED	ALLOWED	ALLOWED
	-YVV	ALLOWED	ALLOWED	ALLOWED	ALLOWED	ALLOWED
S4 1A, 3A	+XVV	ALLOWED	ALLOWED	ALLOWED	ALLOWED	ALLOWED
	-XVV	ALLOWED	ALLOWED	ALLOWED	ALLOWED	ALLOWED
	+YVV	ALLOWED	ALLOWED	ALLOWED	ALLOWED	ALLOWED
	-YVV	ALLOWED	ALLOWED	ALLOWED	ALLOWED	ALLOWED
P4 2A, 4A	+XVV	ALLOWED	ALLOWED	ALLOWED	ALLOWED	ALLOWED
	-XVV	ALLOWED	ALLOWED	ALLOWED	ALLOWED	ALLOWED
	+YVV	ALLOWED	ALLOWED	ALLOWED	ALLOWED	ALLOWED
	-YVV	ALLOWED	ALLOWED	ALLOWED	ALLOWED	ALLOWED
P6 2B, 4B	+XVV	ALLOWED	ALLOWED	ALLOWED	ALLOWED	ALLOWED
	-XVV	ALLOWED	ALLOWED	ALLOWED	ALLOWED	ALLOWED
	+YVV	ALLOWED	ALLOWED	ALLOWED	ALLOWED	ALLOWED
	-YVV	ALLOWED	ALLOWED	ALLOWED	ALLOWED	ALLOWED
OTHER COMBINATIONS	NOT ANALYZED	NOT ANALYZED	NOT ANALYZED	NOT ANALYZED	NOT ANALYZED	NOT ANALYZED

®[062112-00554]

Column labeled as "Centerline of Vehicle" is applicable for EVA crew on the modules along the centerline of the vehicle (PMA2, Node2, U.S. Lab, Node1, PMM, Z1, PMA1, FGB, SM, DC-1, MRM1, MRM2, MLM).

Columns labeled as Inboard of Port or Stbd SARJ refer to EVA crew located on the truss inboard of the respective SARJ. It also includes EVA crew on modules that are not on the centerline of the vehicle (Columbus, JEM, JEM-EF, JEM-ELM, Airlock, Cupola, Node3).

Following a loss of both PCU's, the maximum allowed negative voltage is -45.5V. If array shunting or offpointing is maintained per this table, a second PCU failure will not result in a hazardous voltage. ®[081811-00363B]

This Rule Continued on Next Page

B9-908 plasma hazard mitigation DURING EVA [hc] [RC] (continued)

E. DURING EVA'S WITH HTV ATTACHED, THE FOLLOWING PLASMA HAZARD MITIGATION REQUIREMENTS APPLY AND SUPERSEDE PARAGRAPH D: ®[081811-00363B]

POWER CHANNELS	STATION ATTITUDE	INBOARD OF PORT SARJ	INBOARD STBD SARJ	OUTBOARD OF PORT SARJ	OUTBOARD OF STBD SARJ	CENTERLINE OF VEHICLE
1A, 2B (PREFERRED)	+XVV	NOT ALLOWED	NOT ALLOWED	NOT ALLOWED	NOT ALLOWED	ALLOWED
	-XVV	ALLOWED	ALLOWED	ALLOWED	ALLOWED	ALLOWED
	+YVV	ALLOWED	ALLOWED	ALLOWED	ALLOWED	ALLOWED
	-YVV	ALLOWED	ALLOWED	ALLOWED	ALLOWED	ALLOWED
1A, 2A	+XVV	NOT ALLOWED	NOT ALLOWED	NOT ALLOWED	NOT ALLOWED	ALLOWED
	-XVV	ALLOWED	ALLOWED	ALLOWED	ALLOWED	ALLOWED
	+YVV	ALLOWED	ALLOWED	ALLOWED	ALLOWED	ALLOWED
	-YVV	ALLOWED	ALLOWED	ALLOWED	ALLOWED	ALLOWED
2B, 3A	+XVV	NOT ALLOWED	NOT ALLOWED	NOT ALLOWED	NOT ALLOWED	ALLOWED
	-XVV	ALLOWED	ALLOWED	ALLOWED	ALLOWED	ALLOWED
	+YVV	ALLOWED	ALLOWED	ALLOWED	ALLOWED	ALLOWED
	-YVV	ALLOWED	ALLOWED	ALLOWED	ALLOWED	ALLOWED
S6 1B, 3B	+XVV	NOT ALLOWED	ALLOWED	NOT ALLOWED	NOT ALLOWED	NOT ALLOWED
	-XVV	ALLOWED	ALLOWED	ALLOWED	ALLOWED	ALLOWED
	+YVV	ALLOWED	ALLOWED	ALLOWED	ALLOWED	ALLOWED
	-YVV	ALLOWED	ALLOWED	ALLOWED	ALLOWED	ALLOWED
S4 1A, 3A	+XVV	NOT ALLOWED	ALLOWED	NOT ALLOWED	NOT ALLOWED	ALLOWED
	-XVV	ALLOWED	ALLOWED	ALLOWED	ALLOWED	ALLOWED
	+YVV	ALLOWED	ALLOWED	ALLOWED	ALLOWED	ALLOWED
	-YVV	ALLOWED	ALLOWED	ALLOWED	ALLOWED	ALLOWED
P4 2A, 4A	+XVV	ALLOWED	NOT ALLOWED	NOT ALLOWED	NOT ALLOWED	ALLOWED
	-XVV	ALLOWED	ALLOWED	ALLOWED	ALLOWED	ALLOWED
	+YVV	ALLOWED	ALLOWED	ALLOWED	ALLOWED	ALLOWED
	-YVV	ALLOWED	ALLOWED	ALLOWED	ALLOWED	ALLOWED
P6 2B, 4B	+XVV	ALLOWED	NOT ALLOWED	NOT ALLOWED	NOT ALLOWED	ALLOWED
	-XVV	ALLOWED	ALLOWED	ALLOWED	ALLOWED	ALLOWED
	+YVV	ALLOWED	ALLOWED	ALLOWED	ALLOWED	ALLOWED
	-YVV	ALLOWED	ALLOWED	ALLOWED	ALLOWED	ALLOWED
OTHER COMBINATIONS	NOT ANALYZED	NOT ANALYZED	NOT ANALYZED	NOT ANALYZED	NOT ANALYZED	NOT ANALYZED

®[081811-00363B] ®[062112-00554]

This Rule Continued on Next Page

B9-908 plasma hazard mitigation DURING EVA [hc] [RC] (continued)

Column labeled as "Centerline of Vehicle" is applicable for EVA crew on the modules along the centerline of the vehicle (PMA2, Node2, U.S. Lab, Node1, PMM, Z1, PMA1, FGB, SM, DC-1, MRM1, MRM2, MLM). ®[081811-00363B]

Columns labeled as Inboard of Port or Stbd SARJ refer to EVA crew located on the truss inboard of the respective SARJ. It also includes EVA crew on modules that are not on the centerline of the vehicle (Columbus, JEM, JEM-EF, JEM-ELM, Airlock, Cupola, Node3).

For most EVA's +XVV with HTV mated, if a PCU fails, the shunt FDIR is insufficient to control the negative floating potential voltage to comply with the -45 volt limit. With HTV docked, for EVA's, the ISS may be configured to fly -XVV or ±YVV to achieve a more optimal array configuration.

Following a loss of both PCU's, the maximum allowed negative voltage is -45.5V. If array shunting or off pointing is maintained per this table, a second PCU failure will not result in a hazardous voltage.

F. PARAGRAPHS A THROUGH E DEFINE THE GENERIC PCU HAZARD PROTECTION AND FAILURE SAFING GUIDELINES FOR ANY EVA. IN REAL TIME, THE ENVIRONMENTS MER MAY BE ABLE TO USE RECENT PLASMA DATA FROM THE FPMU AND OTHER SOURCES TO MORE SPECIFICALLY CHARACTERIZE THE EXPECTED ON-ORBIT PLASMA ENVIRONMENT AT THE TIME OF A PLANNED NOMINAL OR CONTINGENCY EVA. IF THIS INFORMATION RESULTS IN DIFFERENT REQUIREMENTS THAN THOSE LISTED IN PARAGRAPHS A THROUGH E, A CHIT WILL BE WRITTEN TO TEMPORARILY SUPERSEDE THE APPROPRIATE PORTIONS OF THIS RULE. ®[062112-00554]

The plasma hazard short term forecasting process that utilizes data from the Floating Potential Measurement Unit (FPMU) to adjust constraint real-time relief has been approved by the August 9, 2011 SRP and is documented in Hazard Report ISS-EVA-0312 and the safety non-compliance report NCR-ISS-232. If, while planning for a contingency or nominal EVA during mission or stage, real-time data shows that the plasma environment does not require as stringent a configuration for hazard control as this rule provides, MER can provide updated hazard control requirements via the CHIT process. Any event which would invalidate the short term forecast would result in the implementation of the appropriate requirements per paragraphs A-E. ®[081811-00363B]

This Rule Continued on Next Page

B9-908 plasma hazard mitigation DURING EVA [hc] [RC] (continued)

G. IF A PVCU AND PCU SHARE THE SAME POWER CHANNEL, IT MUST BE ASSUMED THAT CCS PCU EVA HAZARD CONTROL FDIR WILL NOT AUTOMATICALLY SHUNT THE TWO POWER CHANNELS CONTROLLED BY THAT PVCU. IF THE RESULTING CONFIGURATION IS 'NOT ALLOWED' OR 'NOT ANALYZED' PER PARAGRAPH D (OR E OF HTV IS BERTHED), A PVCU TRANSITION WILL BE PERFORMED PRIOR TO THE EVA. ®[081811-00363B]

The one failure deep case that removes power to both a PCU and a primary PVCU is the rationale for setting all eight arrays to shunt in the PCU FDIR versus only six arrays. This ensures that even if a PVCU failure does not allow shunting of an array pair, the necessary number of arrays are still shunted. No PVCU transition is necessary if the array pair controlled by a PVCU that shares a power channel with a PCU is allowed per paragraph D (or E if HTV is berthed).

Three hazard controls are required during EVA activities if floating potential magnitudes exceed -40V. If both PCU's are available and functional, then one additional control is required. CCS PCU EVA Hazard Control provides the third control for the nominal case. In the event of PCU failure or shutdown, the CCS PCU EVA Hazard Control detects the loss and immediately shunts all solar arrays, maintaining plasma protection until further action is taken. NCR-ISS-232 documents acceptance of voltages up to -45.5V in cases where a PCU failure results in a voltage higher than requirements. This NCR allows greater flexibility and allows particular sets of two solar arrays to remain unshunted and/or tracking, if analysis shows that the worst case voltage is within the expanded -45.5V limit.

Per the CCS PCU EVA Hazard Control as documented in the CCS SRS Paragraph 3.2.3.2.9, in the event of a PCU failure, having all solar arrays shunted provides the required controls until the ground takes additional action. Specific analysis has been performed to document two-array pairs that can be unshunted without risk of a -45.5V limit violation. Once all arrays are shunted, the operator has the option of unshunting two active solar arrays from the table in paragraph E, and placing any additional arrays 15 degrees or more to wake. 15 degrees has been chosen to account for the maximum expected attitude deviation. As long as no more than two unshunted arrays from the table are facing ram at any one time, no -45.5V violation exists and the hazard is properly controlled. ®[081811-00363B]

This Rule Continued on Next Page

B9-908 plasma hazard mitigation DURING EVA [hc] [RC] (continued)

Hazard Report ISS-EVA-312 identifies a catastrophic shock hazard to EVA crewmembers due to vehicle arcing through the EMU suit. Electrical currents generated by vehicle arcing may pass through an EMU suit and crewmember when the vehicle floating potential is more negative than -40V. ®[081811-00363B]

Fully retracted solar arrays do not require any plasma hazard control actions.

Reference Hazard Report ISS-EVA-312, Electric Shock to EVA Crew Resulting from EMU Arcing to Plasma, ISS Environments Memorandum EID684-12386 Worst-Case Plasma Charging Analysis for 15A and Beyond, NCR ISS-232 Lack of Two-Fault Tolerance to EVA Crew Shock in the Low Earth Orbit Plasma Environment, and EID684-13598, Worst-Case Plasma Charging Analysis for 17A. ®[062112-00554]

For additional reference in pointing the U.S. Solar Arrays, refer to procedure EPS 5.103 for the U.S. Solar Array pointing convention. ®[081811-00363B]

FLIGHT/STAGE EFFECTIVITY: ALL FLIGHTS

From: Hernandez-Pelle, Amri I. (GSFC-5630) [mailto:amri.i.hernandez-pelle@nasa.gov]
Sent: Wednesday, July 17, 2013 4:21 PM
To: Scudder, Matthew P; Iannello, Christopher J. {Chris} (KSC-C104); EXT-Galvez, Ronald M
Subject: RE: ISS PCU Failure Array Shunt FDIR Algorithm

Hi,
Thanks for the response Matthew. I need some clarifications too:

Is the FDIR in charge of pointing the arrays to > 105° from the velocity vector?, Or a separate control (or software) does that?
Does the FDIR prevents other controls from unshunting the arrays while it is enabled or can it be overwritten during operation by an external control? I am trying to understand where is the operational priority for the array >105 pointing and unshunting and how the FDIR fits in the commands/controls priority or hierarchy.

Thanks
Amri

From: Scudder, Matthew P [mailto:matthew.p.scudder@boeing.com]
Sent: Wednesday, July 17, 2013 2:42 PM
To: Iannello, Christopher J. {Chris} (KSC-C104); Galvez, Ronald M. (JSC-EP511); Hernandez-Pelle, Amri I. (GSFC-5630)
Subject: RE: ISS PCU Failure Array Shunt FDIR Algorithm

In order to maintain ISS power balance, we'll want to unshunt arrays when allowed. So given your scenario, once the arrays are shunted and the PCU verified failed (shunting wasn't due to a false trigger) the arrays will be pointed > 105° from the velocity vector, then we'd unshunt the arrays.

Matthew

7

From: Iannello, Christopher J. {Chris} (KSC-C104) [mailto:christopher.j.iannello@nasa.gov]
Sent: Wednesday, July 17, 2013 11:49 AM
To: EXT-Galvez, Ronald M; Hernandez-Pelle, Amri I. (GSFC-5630)
Cc: Scudder, Matthew P
Subject: RE: ISS PCU Failure Array Shunt FDIR Algorithm

Guys,

Thanks for this.

Just one clarification I am unclear on.

Is there a circumstance that: after a PCU failure and we've shunted XX arrays, crew are on EVA, that we'd unshunt any arrays?

Sounds like no below but want to make sure.

Chris Iannello

Chris Iannello, Ph.D.
NASA Technical Fellow for Electrical Power
NASA Engineering and Safety Center
Kennedy Space Center, Florida, 32899
Cell: 407-252-8448

http://www.nasa.gov/offices/nesc/team/Chris_Iannello_bio.html

From: Galvez, Ronald M. (JSC-EP511)
Sent: Friday, July 12, 2013 5:59 PM
To: Iannello, Christopher J. {Chris} (KSC-C104); Hernandez-Pelle, Amri I. (GSFC-5630)
Cc: SCUDDER, MATTHEW P. (JSC-OB6)[THE BOEING COMPANY]
Subject: FW: ISS PCU Failure Array Shunt FDIR Algorithm

Chris,

Below answers courtesy of Matt Scudder, the Boeing EPS Hardware focal.

Ron

From: <SCUDDER>, Matthew Scudder <matthew.p.scudder@boeing.com>
Date: Friday, July 12, 2013 4:53 PM
To: Ronald Galvez <Ronald.m.galvez@nasa.gov>, Casey Adams <casey.j.adams@boeing.com>, "SHAH, DHARMESH D. (JSC-OB)[THE BOEING COMPANY]" <dharmesh.d.shah@boeing.com>, "Kaminski, Raymond (JSC-OA)[BOEING]" <raymond.j.kaminski@boeing.com>
Cc: Rustin Robetorye <rustin.c.robetorye@boeing.com>
Subject: RE: ISS PCU Failure Array Shunt FDIR Algorithm

Ron, Sorry didn't see email until now. I'm assuming you'll pass this on to Chris. Thanks!

1. question is what happens to the SSU when the PCU fails – do one or more array shunt?

8

Upon detection of a PCU "failure", the CCS will issue commands to shunt up to 8 SAWs via their SSUs. "Up to 8" is pre-defined by MCC-H via a "weather forecast". In other words, if the "space weather" is relatively benign, and 3 active arrays result do not result in a hazardous condition with no PCUs, MCCH can set the FDIR to shunt 5 solar arrays.

2. When do we enable PCU (I believe this may be environments related)

PCUs are only enabled to discharge during EVAs, both Russian and US.

3. Recovery plan appears to be an operations call, but, not sure

Two main recovery paths are possible. 1) (Nominal response) Maintain XX (See "space weather" above) Solar Arrays a minimum of 105° out of the velocity vector. When a SAW is > 105° from the velocity vector, it is deemed not a contributor to the EVA Hazard, and thus may be unshunted. This requires placing both the SARJ and BGAs into directed position to ensure the >105° requirement (and no LOAC). 2) Terminate EVA. Once the crewmembers are inside the Airlock, and the door shut, the Solar Array Wings may be unshunted.

4. Could crew be on EVA? Not sure when you have the PCU active without a crew.

The only time PCUs are placed into discharge now is during EVAs

0. Specifically, how is it enabled and when?

In preparation for an EVA, several hours before the crew is scheduled to go out the door, the PCUs are commanded from Standby Mode to Discharge Mode. After verifying the two PCUs are operating nominally, commands are issued to the C&C MDM to enable the EVA Hazard Control Function (aka PCU Failure Array Shunt FDIR Algorithm). At the conclusion of the EVA, MCCH issues commands to disable the EVA Hazard Control Function before the PCUs are returned to Standby Mode.

Matthew

From: EXT-Galvez, Ronald M
Sent: Friday, July 12, 2013 3:46 PM
To: Adams, Casey J; Shah, Dharmesh D; Scudder, Matthew P; Kaminski, Raymond J
Cc: Robetorye, Rustin C
Subject: Re: ISS PCU Failure Array Shunt FDIR Algorithm

Have you guys had a chance to look at this? Kinda hard when you are on travel. Can you look at this early next week?

Thanks

Ron

From: <Galvez>, Ronald Galvez <Ronald.m.galvez@nasa.gov>
Date: Wednesday, July 3, 2013 12:26 PM
To: Casey Adams <casey.j.adams@boeing.com>, "SHAH, DHARMESH D. (JSC-OB)[THE BOEING COMPANY]" <dharmesh.d.shah@boeing.com>, Matthew Scudder <matthew.p.scudder@boeing.com>, "Kaminski, Raymond (JSC-OA)[BOEING]" <raymond.j.kaminski@boeing.com>
Cc: Rustin Robetorye <rustin.c.robetorye@boeing.com>
Subject: FW: ISS PCU Failure Array Shunt FDIR Algorithm

Casey/Dharmesh/Matt/Ray

Hate to dump but, the FDIR is something that may be in your neck of the woods. Can you point me in the right direction?

1. question is what happens to the SSU when the PCU fails – do one or more array shunt?
2. When do we enable PCU (I believe this may be environments related)
3. Recovery plan appears to be an operations call, but, not sure
4. Could crew be on EVA? Not sure when you have the PCU active without a crew.

Thanks

Ron

From: <Iannello>, "Christopher J. {Chris} (KSC-C104)" <christopher.j.iannello@nasa.gov>
Date: Wednesday, July 3, 2013 12:04 PM
To: Ronald Galvez <Ronald.m.galvez@nasa.gov>
Subject: ISS PCU Failure Array Shunt FDIR Algorithm

Ron,
Are you knowledgeable on how the FDIR works? We are relooking at the necessity of PCUs at JSC's (koontz's) request.

Specifically, how is it enabled and when?

If a PCU fails when FDIR is enabled, do all array's get shunted or just some?

What is recovery plan to unshunt an array? Could crew be on EVA when that happens?

Thanks Ron...Chris

Chris Iannello

Chris Iannello, Ph.D.
NASA Technical Fellow for Electrical Power
NASA Engineering and Safety Center
Kennedy Space Center, Florida, 32899
Cell: 407-252-8448

http://www.nasa.gov/offices/nesc/team/Chris_Iannello_bio.html

Appendix G. Maximum Magnetic Induction Potential Along ISS Truss

Inductive potential differences exist between two points on the ISS metallic structure due to motion of the vehicle across the Earth's magnetic field. The magnitude of the potential difference $\varepsilon_{induced}$ between two points separated by a distance **L** is given by the vector equation

$$\varepsilon_{induced} = (\mathbf{v} \times \mathbf{B}) \bullet L \qquad (1)$$

where **v** is the ISS velocity and **B** the Earth's magnetic field strength at the location of ISS. Values of $\varepsilon_{induced}$ are small near the equator where the dominant component of the Earth's magnetic field vector lies along the direction of the ISS truss (in the typical +/-XVV flight attitude) and the dot-product between **v x B** and the vector components of **L** along the Truss is small. The extremes in potential difference between the ends of the ISS truss due to magnetic induction will occur at high latitudes where geomagnetic field lines are steeply inclined relative to the Earth's surface (and the ISS truss in typical flight attitudes), maximizing the **v x B** components along the length of the truss. In this case, the vector equation can be reduced to the scalar form

$$\varepsilon_{induced} = vB_rL_T \qquad (2)$$

where the ISS velocity v is assumed to be parallel to the Earth's surface, B_r is the radial component of the Earth's magnetic field, and L_T is the length of the ISS Truss.

The ISS coordinates of the Truss tips are (D. Schmidl, personal communication, 2013):

Starboard Truss Tip	X = +0.73 meters
	Y = +47.15 meters
	Z = +0.73 meters
Port Truss Tip	X = +0.02 meters
	Y = -47.13 meters
	Z = +0.73 meters

The distance between the Truss tips is L_T = (+47.15 meters + 47.13 meters) = 94.28 meters along the y-axis. The small contribution from the different locations of starboard and port tips in the x-direction has been neglected for this analysis.

Variation in ISS velocity as a function of altitude can be estimated from the equation for velocity of a circular orbit:

$$v = \sqrt{\mu/(z + R_E)} \qquad (3)$$

where $\mu = 3.986 \times 10^{14}$ m^3/s^2 and $z+R_E$ is the geocentric radial distance of the circular orbit at altitude z above the mean Earth radius R_E =6371 km. For example, ISS orbital velocity at an altitude of 400 km is 7673 m/s assuming the orbit is circular.

Magnetic field intensity also varies as a function of altitude with the field intensity decreasing with increasing altitude. Numerical B_r magnetic field component values are conveniently obtained from NASA's Community Coordinated Modeling Center's implementation of the International Geomagnetic Reference Field (IGRF) model (http://ccmc.gsfc.nasa.gov/modelweb/models/igrf_vitmo.php).

The values used here are obtained from the IGRF model for the current year (2014) at latitudes of +51.6 degree in the northern hemisphere and -51.6 degree in the southern hemisphere. Because the magnetic field intensity varies with longitude, the model was run as a function of longitude between 0 degree longitude and 360 degree longitude in 1-degree increments to find the maximum value of the radial magnetic field component in order to estimate the worst case induction potential along the ISS orbit.

Maximum IGRF B_r magnetic field components in the northern and southern hemisphere and orbital velocity values from equation (3) as a function of altitude are listed in Table G-1 along with the corresponding magnetic induction potential between the ISS Truss tips computed from equation (2). The distance 94.28 meters is used in all calculations.

Table G-1. Maximum Induction Potential Between ISS Truss Tips

Altitude (km)	ISS Velocity (m/s)	Northern Hemisphere		Southern Hemisphere	
		Br (nT)	$\varepsilon_{induced}$	Br (nT)	$\varepsilon_{induced}$
330	7713	48046.1	34.9	55271.7	40.2
340	7707	47800.4	34.7	55002.5	40.0
350	7701	47556.3	34.5	54735.1	39.7
360	7695	47314.0	34.3	54469.4	39.5
370	7690	47073.3	34.1	54205.4	39.3
380	7684	46834.3	33.9	53943.2	39.1
390	7678	46596.9	33.7	53682.6	38.9
400	7673	46361.2	33.5	53423.8	38.6
410	7667	46127.0	33.3	53166.6	38.4
420	7661	45894.5	33.1	52911.1	38.2

Extreme inductive potential differences of approximately 40V between the tips of the ISS Truss may occur when the ISS orbital altitude is low. For example, ISS orbital altitudes were allowed to drop to approximately 335 km during 2001 and again in 2007. Mean ISS orbital altitudes in 2014 have all exceeded 400 km with typical mean altitudes between 413 km and 418 km. A good estimate of the extreme inductive potential difference between the Truss tips for current ISS altitudes reported to the nearest volt is therefore 38V.

Appendix H. International Space Station Electrical Power Systems Training Manual ISS EPS TM 21109 (Section 2.3.4)

01.04.05(0)T0005
Version 1.0
(supersedes TD9707)

International Space Station Electrical Power Systems Training Manual

ISS EPS TM 21109

Mission Operations Directorate
Space Flight Training Division

August 26, 2004

National Aeronautics and
Space Administration

Lyndon B. Johnson Space Center
Houston, Texas

Contract NAS9-20000

2.3.3.4 Monitoring

There is no telemetry specific to the UOP.

2.3.3.5 Replacement/Location

The UOPs are located in the standoffs of the Node, Lab, and Airlock and can be changed out on orbit as needed.

2.3.4 System/User Protection

System protection encompasses the architecture's ability to detect that a fault condition has occurred, confine the fault to prevent damaging connecting components, and execute an appropriate recovery process to restore functionality, if possible. This process is usually referred to as FDIR. For example, upon detection of a fault, components can be isolated, thereby preventing propagation of faults. In response to overcurrent conditions, the architecture is designed such that each downstream circuit protection device is set to a lower current rating and responds more quickly than the protection device directly upstream. This ensures that electrical faults or "shorts" in the system do not propagate toward the power source. The architecture's system-protection also shuts down power production when array output voltage drops below a specified lower-limit threshold. This prevents the PV cells from operating in low-voltage, high-current applications, causing cell overheating. In summary, all the various implementations of system-protection work together to isolate faults or shorts at the lowest level. This approach minimizes impacts to the users of the EPS and also protects the EPS from complete failure from low-level faults.

User protection encompasses the architecture's ability to protect the crew from electrical shocks. This is can be accomplished via grounding, specific hardware fault isolators (such as a Ground Fault Isolator (GFI) circuit), or through procedure or operational constraints.

In addition to the fault detection and isolation capabilities of the secondary power system, several other specific functions provide further protection for both the electrical components and the crew: Load shed software, grounding, the Rack Power Switch (RPS), and the PCU.

2.3.4.1 Components

Load shedding is a software process by which the C&C MDM automatically shuts down equipment to prevent channel overloading; this can also be initiated manually via the PCS. The grounding function is accomplished with the SPG architecture that maintains all components on the USOS are at a common potential. RPSs are used to remove power from an entire rack so that the crew will be protected during maintenance or installation activities. Finally, a PCU is used to minimize the difference in potential between the ISS and the surrounding space environment.

Load Shed Software

Load shed can be commanded or initiated automatically by an overcurrent condition on a power channel (i.e., high BCDU output or a low BCDU bus voltage). Except for system malfunctions, resource management should normally account for power demand on the power channel and prevent the need for load shedding.

When the Tier II EPS MDM (PMCU MDM) detects a load shed condition on a power channel, an indication is sent to the C&C MDM. The load shed function acts to reduce loads on that power channel by commanding RPCs open in approximately 500 W blocks. This function is based upon predetermined load shed tables that can be uploaded from the ground to the C&C MDM. For example, if 1200 W needs to be shed to remove the load shed condition on power channel 2B, the C&C MDM will load shed 3 blocks (assuming 500 W per block and thus potentially 1500 W total). However, because not all components in the load shed table may be operating, 1500 W may not actually be shed. If the load shed condition persists, the process will be repeated, and load shed will be repeated, again removing loads in approximately 500 W blocks until the load shed condition no longer exists.

Single Point Ground

The primary purpose of the SPG design is to protect crew and equipment from power surges and unbalanced loads that can present an electrical shock hazard. Unbalanced loads can be avoided by tying neutral electrical lines to a conductive single point ground. In doing so, USOS loads will have the same reference point, thus eliminating differences in potential (voltage levels) and balancing the load. During a current fault, the USOS EPS utilizes the entire conductive metal structure of the USOS as an electrical return to which neutral electrical lines are grounded. The ISS structure will not be used as a return at any time unless a fault is present.

Grounding straps (see Figure 2-44) connect the neutral side of an electrical power generator and any power converters, such as a DDCU, to the metal boxes that contain them. The grounding straps are physically placed as close as possible to the power source to maximize shock protection. The chassis and/or structure of all equipment associated with a power source must also be grounded or bonded to prevent shock hazards. Bonding is the physical contact between two objects that results in electrical conductivity. Bonding or grounding the metal boxes to the USOS structure completes a grounding path back to that ORUs power source and provides two distinct advantages. The ORU, its power source, and structure are now at the same reference potential eliminating any differences in potential and possible shock hazards. Second, the grounded box provides a current path that aids in identifying electrical shorts. When a short occurs in a load and comes into contact with a grounded box, a path of negligible resistance is provided back to the load's power source causing a sharp increase in current flow. This will cause a trip within the power circuit, removing power from the component and eliminating a hidden shock hazard.

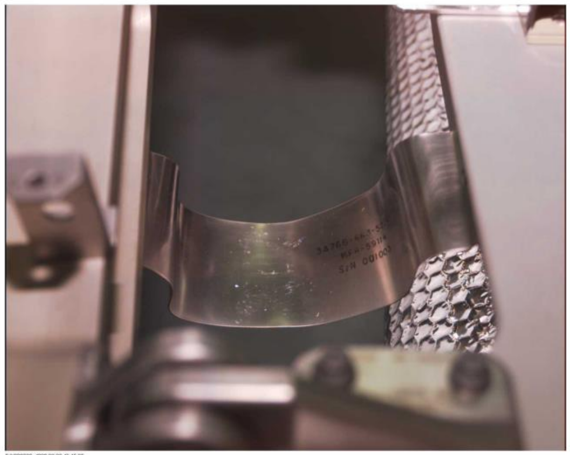

Figure 2-44. Grounding strap

Rack Power Switch

The RPS is an emergency power shutdown switch for a Lab rack. It can also be used to protect the crew during mate/demate operations while maintaining or replacing a rack or its ORUs. When the switch is changed to the OFF position, all power feeds to the rack are commanded off ***and*** the Tier I C&C software blocks all power "ON" commands to the rack. This includes crew, ground and software commands. In Figure 2-45, three different versions of the RPSs are shown. The first type is for a rack with no smoke detector inside the rack, the second is for a rack containing a smoke detector, and the third is for a payload rack. The smoke indication led is illuminated in the event the smoke detector inside the rack detects smoke.

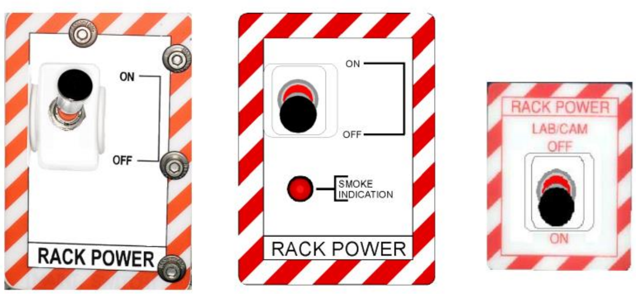

Figure 2-45. Rack power switch

If an RPS has failed, the MCC ground control workaround is to disable the RPS monitoring function at the local MDM level. This tells the software to ignore the RPS position sensor information as though the switch did not exist. The crew cannot disable the RPS MDM Monitoring function from onboard. The workaround for the crew in the rare case of a failure that would inadvertently prevent power to flow to the rack is to cut one of two wires on the RPS circuit at the location of the RPS.

Plasma Contactor Unit

Although the SPG architecture maintains all components of the USOS EPS are at a common potential, this potential may not correspond to the surrounding space environment. The potential difference between the ISS structure and the plasma environment in orbit could be as much as ~140 V dc during insolation. This difference in potential can result in micro-arcing between the space environment and the ISS structure, potentially damaging the arrays or thermal coating that covers the ISS. To minimize this potential difference, PCUs located on the Z1 truss generate plasma from xenon gas and emit a stream of electrons into space. This electron emission results in a “grounding-strap” that effectively grounds the ISS to the space environment, minimizing the potential difference as well as related hazards to the ISS and crew.

The emitted gas is nonpropulsive and does not affect EVA. During operations, the Hollow Cathode Assembly (HCA), which heats the xenon gas, can reach temperatures up to 600^{o} C. To protect EVA crewmembers, the PCU HCA is shielded by a screen to protect against inadvertent contact.

2.3.4.2 Interfaces

The RPS interfaces with the local MDM (LA-1, LA-2, OR LA-3) responsible for control of the rack components.

The PCUs are powered by RPCM Z13B_B and RPCM Z14B_B and controlled by the N1-1/2 MDMs. There is no thermal interface to the PCU since they are located on the Z1 truss.

2.3.4.3 Control

The only system protection functions that are controlled via MDMs are the load shed function, the RPS, and the PCU. The load shed function is controlled by the C&C MDM upon receiving a request from a lower tier MDM. The RPS position is monitored by the C&C software and all commands to close the RPC to the rack will either be blocked or allowed depending upon the state of the RPS.

The PCUs nominally function in a completely autonomous fashion. However, before initial operation, both PCUs must run a one-time only conditioning routine. This routine includes heating of the xenon tank, as well as heating and cooling of the HCA, baking out any contaminants that might have been absorbed during delivery to the ISS. While in the conditioning mode, the PCU consumes less than 115 W. In a worst case scenario, heating of the xenon tank may take up to 200 hours to complete, depending on the pressure and thermal conditions. A more reasonable time estimate is 10 hours. The conditioning routine will be done on both PCUs at the same time. After the conditioning routine is completed, the PCUs can be activated. Nominally, this activation includes starting the PCU, conditioning the cathode, stabilizing the xenon tank temperature, making adjustments allowing gas feed lines to reach the correct operating temperatures, and finally igniting the HCA, all autonomously. The PCU will then proceed to the nominal ON state in which xenon gas is discharged. The PCU can also be placed in a manual mode in which all steps and functions in the startup process are manually controlled, including the valves, heaters, etc. Xenon is consumable and is expected to support 1.5 to 2 years of continuous operation. Presently, the PCU is planned to continuously emit xenon gas, even in eclipse where the PCU is not necessary. The rationale is that if the xenon flow were to be controlled, it would have to be turned on and off over 8000 times, which might shorten the life of the ORU. It was also determined that the life of the xenon reserve would be shortened. The PCU modes and associated power consumption rates are described in Table 2-31.

Table 2-31. PCU modes and power consumption after the conditioning routine

PCU mode	PCU mode description
Shutdown State	Both valves are closed, heater control is disabled, cathode heater is off and the anode voltage supply is also off. The PCU will not exceed 20 W during this routine
Standby Routine	The tank temperature is sampled for 10 minutes. If the temperature is stable, the tank heaters are enabled and valve 1 is opened. Once the tank temperature is in range (73.8° to 126.2° F). The tube heaters are also enabled and monitored in the same temperature range. The PCU will not exceed 115 W during this routine
Ignition Routine	The tank heaters are disabled after they reach their upper limit and after a 3-½ minute time delay, valve 2 is opened and the cathode heater is activated. The tube pressure is monitored until the tube pressure exceeds 33.4 psia. At this point, ignition pulses enable the HCA anode output. Once the anode current is greater than 0.5°A, the ignition pulses cease and the anode current is monitored again. If there is a constant current output at the anode, the PCU disables the cathode heaters, leaves the ignition routine and enters the discharge state. If the anode does not show constant current after 30 minutes, the cathode heater is disabled and valve 2 is closed. The Ignition Failed indicator is set and the PCU returns to standby. The PCU will not exceed 290 W during this routine
Discharge Mode	The PCU will remain in this mode as long as the anode current is greater than 0.5 A. If the current falls below 0.5 A, the PCU will return to the ignition routine. Presently, the PCU is planned to continuously emit xenon gas, even in eclipse where the PCU is not necessary. The rationale is that if controlled, the xenon flow would have to be turned on and off over 8000 times in 2 years, which might shorten the life of the ORU as well as the xenon reserve

2.3.4.4 Monitoring

The RPS position is ultimately monitored by the C&C software in order to prevent inadvertent powering of a disabled rack.

The following data is provided on the PCU:

- Plasma current
- Anode voltage
- Cathode heater voltage
- Tank and tube temperature
- Tank and tube pressure

The PCU has FDIR that will react to failures in the following manner:

a. For loss of discharge or low discharge, the low discharge indicator is set to the active state and the PCU modes to the ignition routine.

b. If the PCU does not reach the discharge state 30 minutes after entering the Ignition routine, the ignition-failed indicator is set and the PCU modes to the Standby state.

c. For low temperature or low tube pressure, the appropriate indicator is set to the active state and the PCU modes to the standby state.

d. Other indicators that are set during a fault are high tank pressure, low anode voltage, and heater stuck on.

2.3.4.5 Replacement/Location

Of the system protection devices, the PCU is the only replaceable component on-orbit. Upon depletion of the xenon gas tank assembly, the ORU is returned to the ground for replenishment, and then reflown. Figure 2-46 shows the location of the PCUs on the Z1 truss.

Note: If an RPS fails, the entire rack will need to be replaced.

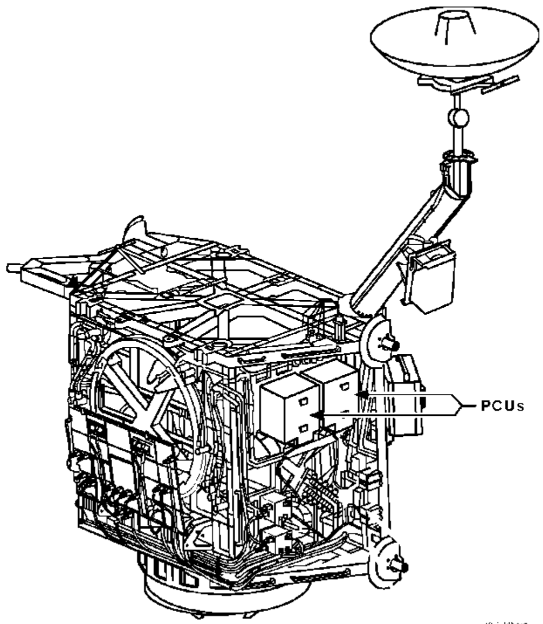

Figure 2-46. Plasma contactor units on the Z1 truss

Appendix I. International Space Station (ISS) Plasma Contactor Unit (PCU) Utilization Plan Assessment Update: Key Points Summary

International Space Station (ISS)
Plasma Contactor Unit (PCU)
Utilization Plan Assessment Update
TI-13-00869

Key points summary

Assessment Request

Assess the following possible additions to the PCU utilization plan:	NESC response:
Nominally leaving the PCUs off during EVA if pre-EVA hazard severity measurements and short-term ionospheric environment forecasts support that decision.	NESC Team recommends operating two PCUs during all EVAs as most reliable and low cost to provide secure control of ISS potentials. This counts as two controls of three for two-fault failure control.
Disabling the EVA shunt fault detection, isolation and recovery (FDIR) logic and the supporting operational hazard controls if two PCUs are in discharge during the EVA.	NESC Team recommends to not use FDIR at any time during any EVA as it has fault condition paths that can be more hazardous than the protection it may provide.
Possible long-term marginalization of the ISS EVA-312 shock hazard report so that no active hazard controls are required.	NESC Team recommends (again) using two PCUs during EVAs rather than using no active hazard controls. The space plasma environment can change under certain situations making somewhat hazardous conditions occur more quickly than a response can be provided to reduce those hazardous conditions.

Main Conclusion of NESC Team

- NESC team disagrees with replacing PCU active hazard control which safely and reliably controls EVA negative arcing hazard with a "forecasting" process that has only been evaluated on a cursory level, is incapable of predicting the full range of observed charging behavior on ISS, and uses tools that do not meet NASA standards for making critical decisions.
  - NESC team asserts PCUs should be used regardless of pre EVA "predictions" or planned EVA location

Primary Area of Disagreement #1

Subject	ISS	NESC Position
"Forecast" Adequacy	• "Short-term" forecast methodology exists to conduct plasma assessment 14 days in advance of EVA • "Short-term" forecast in-place and has been used successfully to support Program operational decisions. • Low Solar cycle supports using this analytical prediction to determine if hazard exists and determine if controls are needed **Reference: ISS-NCR-232G and 2013-10-01-SSPCB-Plasma-NCR-ISS-232_final.pdf presented to SSPCB 10/1/2013**	• Potentials more negative than -45V have been measured on ISS. The ionosphere forecast and PIM3.0 models are not capable of predicting these large potentials • "Forecasting" process (1) has only been evaluated on a cursory level, (2) is incapable of predicting the full range of observed charging behavior on ISS and (3) uses tools that do not meet NASA standards for making critical decisions

Primary Area of Disagreement #2

Subject	ISS	NESC Position
PCU Utilization	• Use is optional if space weather forecast calculates within limit floating potential prediction • Due to positive potential hazard PCUs will not be used for EVAs outboard of the SARJs **Reference: ISS-NCR-232G and 2013-10-01-SSPCB-Plasma-NCR-ISS-232_final.pdf presented to SSPCB 10/1/2013**	• Use PCU for all EVAs regardless of pre-EVA severity predictions or EVA location • PCUs can safely and reliably control EVA negative arcing hazard for the life of ISS • Positive potential hazard concern with running PCUs is unwarranted as demonstrated by calculations in the report *(see next page; higher fidelity model and verified by FPMU measurements)* • *PCU capability to control negative hazard much more certain than the analytical approach's ability to predict the hazard*

Primary Area of Disagreement #3

Subject	ISS	NESC Position
Positive Charging Hazard	• "Placing the PCU in discharge produces positive potential hazard in +10 to +12 V range outboard of SARJ (i.e., catastrophic hazard)" • "Positive potential hazard results from placing PCUs in discharge to prevent negative potential hazard. However, negative potentials within allowable range with PCUs not in discharge. Negative levels driven by solar array orientation" **Reference: ISS-NCR-232G and 2013-10-01-SSPCB-Plasma-NCR-ISS-232_final.pdf presented to SSPCB 10/1/2013**	• NESC team calculations (provided in the report) suggest overly conservative treatment by ISS team that overstates the severity of the current available from this "positive hazard". • EMU "positive shock hazard" is the result of making unrealistic assumptions about plasma collection that model the EMU as a bare metal sphere floating in space connected with a wire to the ISS chassis ground, then claim that the actual configuration of the "EMU cannot be used as a hazard control" for this contrived "hazard".

Secondary issues

Subject	ISS	NESC

Array Shunt FDIR utilization	• Do not use if space weather forecast calculates within limit floating potential
	• Use (along with PCUs) when the calculated floating potential is out of limit.
	    • Shunt FDIR invoked upon sensing single PCU failure
	    • All 8 solar arrays are shunted
	    • FR B9-908 governs recovery of an array pair after shunt event
	Reference: ISS-NCR-232G and 2013-10-01-SSPCB-Plasma-NCR-ISS-232_final.pdf presented to SSPCB 10/1/2013
		• Do not use at all as potentially creates larger risk
		• The effects on the floating potential of unshunting an array not pointed into ram have not been characterized.
		• Unshunting an array pair pointed in the ram directions during insolation can cause high negative peaks (short duration)
		• Evaluate using additional isolation features of the EMU along with the low probability of completing the circuit as the third control
		• Some question on how many arrays are shunted with FDIR but no bearing on conclusions either way

Secondary issues

Subject	ISS	NESC
EMU	• "The EMU is not designed or certified to insulate against electric shock per HR EMU-018." **Reference: ISS-NCR-232G**	• Evaluate what it would take to use the EMU's insulative aspects as a hazard control. • Consider isolation features added to the MMWS.

Secondary issues

Subject	ISS	NESC
Rapid Charging Events (RCEs)	• Low likelihood of a shock hazard due to the short duration nature of RCEs (<5 seconds)	• Noted several instances of RCE data being left off of data plots presented to ISS management – should present all the data with explanations • The hazards presented by these events are not well understood • No technical argument presented to assessment team that supports ignoring RCEs • PIM3.0 model does not contain the physics to predict these events

Secondary issues

Subject	ISS	NESC
Space Environment Persistence	• Solar cycles indicate benign environment through Solar Cycle 25 (~2030) • FPMU data since 2007 corroborates benign environment • "FPMU measurements since 2007 have indicated no ISS charging in excess of -45V" (**NCR-ISS-232G p.6**) • Not directly used in prediction calculation so what is the NESC concern • Predicted benign environment and lack of charging in excess of -45V used extensively as rationale in persuading ISS community to adopt forecast approach in NCR and SSPCB briefings.	• The space environment is not predictable over short or long term (ex: future solar activity) so cannot assume continued benign environment • The FPMU database only captures ~6% of the total ISS eclipse exit charging events since regular operations started in 2007. • FPMU measurements since 2007 document examples of charging more negative than -45 V. • Significant space weather events still occur during "benign" environment periods, they just occur less often.

Secondary issues

Subject	ISS	NESC
Ionosphere State	• Does not vary significantly over a period of a few weeks • Corroborated by FPMU data • Monitored daily until EVA	• Affected by a number of factors such as geomagnetic activity and auroral charging • Can change rapidly • Impact of storm time density depletions and plasma heating on forecast has not been evaluated. • Daily monitoring until EVA has been recommended by the NESC team but is an unoffical (not in release documentation) process that is not described in ISS NCR and Hazard reports which only list a "up to" 14 day forecast and hazard assessment.

Secondary issues

Subject	ISS	NESC
ISS Charging Modeling (PIM3.0)	• Uses FPMU measurements to determine what IRI model input to use. • Valid prediction model with some limited, understood shortcomings • A suitable tool for this decision making flow	• Model has too many limitations to be predictive of a hazard condition • Model is incapable of predicting the large transient charging events in excess of -45 V observed on ISS (RCEs) • The hazards presented by these events are not well understood. • Does not meet NASA standards for critical models • Climatology Inputs are not adequate to predict step function changes • Using the IRI model as environment input to PIM3.0 is inadequate for short term changes

Secondary issues

Subject	ISS	NESC
Auroral Charging	• Agree, looking into inclusion	• Not considered in PIM3.0 model and can be unlikely yet potentially significant charging source • IRI model does not provide auroral charging environments • FPMU documents auroral charging on a number of occasions but only frame charging, no data on surface charging.

Secondary issues

Subject	ISS	NESC
Negative Potential Limit	• -45.5 V approved in Jan 2009 by SRP Reference: ISS-NCR-232G	• -40 V should be maintained until further experimentation • The full range of measured ISS charging events were not presented to the SRP. The PIM3.0 model accuracy was overstated – implied error was 0%. • The -40V limit associated with vehicle charging • No voltage limit found for the EMU

Appendix J. EMU Team Email

From: "Boyle, Robert M. (JSC-EC511)" <robert.m.boyle@nasa.gov>
Date: June 13, 2014 at 5:08:18 PM CDT
To: "Hansen, Christopher P. (JSC-EC111)" <christopher.p.hansen@nasa.gov>, "Blanco, Raul A. (JSC-EC511)" <raul.a.blanco@nasa.gov>
Cc: "West, T. Scott (JSC-C105)" <timothy.s.west@nasa.gov>
Subject: RE: EMU/plasma shock hazard

I agree with conclusions in the executive summary and the recommendations in section 8. I reviewed sections 7.9 – 7.13 in detail, and had the following minor comments. They can be ignored if desired, it will not change the report conclusions.

In Table 7.9-1 the Body Seal Closure/MMWS Connection coating is noted as anodize. The parts are Stainless Steel. There is a caveat noting the coating data is suspect and not used in the calculations.

In Table 7.9-1 I don't understand why the DCM and OBS are lumped in one row. Totally different hardware.

The baseplate and MWS probably protect the SS bosses (MMWS Connection) from contacting the tether, but the statement that the baseplate is isolated seems to ignore the exposed SS.

It was a very educational read. Thanks. Good job.
Rob

From: Hansen, Christopher P. (JSC-EC111)
Sent: Tuesday, June 03, 2014 4:06 PM
To: Boyle, Robert M. (JSC-EC511); Blanco, Raul A. (JSC-EC511)
Subject: FW: EMU/plasma shock hazard

Here's the NESC report on the PCU hazard. Scott West (NESC Chief Engineer for JSC) asked that we take a look at the EMU sections and let him know if we agree with them.

Chris

From: West, T. Scott (JSC-C105)
Sent: Tuesday, June 03, 2014 10:19 AM
To: Hansen, Christopher P. (JSC-EC111)
Subject: RE: EMU/plasma shock hazard

Thanks Chris. I've enclosed the whole draft report, but sections 7.9 – 7.13 are the main sections to look at for the EMU in relation to the shock hazard. The appendices are also there with the EMU information that was presented to the assessment team that they used to do their analysis. And yes this was being looked at relative to running/not running PCUs and also enabling or not enabling the shunt FDIR. The first part of the report should help provide some context.

A reply from team member Ira Katz to the below Rob Boyle comment.

The baseplate and MWS probably protect the SS bosses (MMWS Connection) from contacting the tether, but the statement that the baseplate is isolated seems to ignore the exposed SS.

From: Katz, Ira (353B) [mailto:ira.katz@jpl.nasa.gov]
Sent: Tuesday, June 17, 2014 11:47 AM
To: Hernandez-Pelle, Amri I. (GSFC-5630); Schneider, Todd A. (MSFC-EM50); Moran, Erin (LARC-C101)[TEAMS2]
Subject: RE: REPORT FINAL COMMENTS

Amri-
I looked through the 2 suit presentations "Baseplate_-_BRT_Continuity_Test_Summary(1)" and "NESC_ISS_Shock_EVA_Actions" and the best I can interpret Rob Boyles comments are that there is some exposed stainless steel that actually can contact some of the metal, either anodized aluminum or stainless steel, inside the suit. However, they have a very small area, so they wouldn't have a big effect on either the probability or current collection calculations. I think this metal was included in the Boeing PRA. Rob Boyles's conclusion "*"The baseplate and MWS probably protect the SS bosses (MMWS Connection) from contacting the tether,..."* is basically our conclusion. I'd have to review the physical hardware with him in person if you need a better answer. I'm afraid this is the best I can do with emails and PowerPoint presentations.
Thanks - ira

Appendix K. Current Flow to EMU in Electrical Contact with +15V ISS Surface

Current Flow to EMU (Extravehicular Mobility Unit) in Electrical Contact with +15 V ISS (International Space Station) Surface

M.J. Mandell
V.A. Davis
B.M. Garner

Leidos, Inc.
10260 Campus Point Drive
San Diego, CA 92121

June 29, 1015

Submitted to:
Analytical Mechanics Associates, Inc.
Teams2_contracts@ama-inc.com

Final Report *for:*
1601-TEAMS-SAI01, Technical services in accordance with
SOW No: 1604-T2-LEI-SOW-10.160.1-R00 ISS PCU II Test

NASA LaRC TEAMS 2 Contract NNL12AA09C
WBS Number: 10.160.001/FY15
ISS Plasma Contractor Unit (PCU) II Test

Leidos CRN: 311814

This document is hereby submitted to Analytical Mechanics Associates, Inc. as the Final Report for 1601-TEAMS-SAI01, technical services in accordance with SOW No: 1604-T2-LEI-SOW-10.160.1-R00 ISS PCU II Test, with period of performance January 2, 1015 through July 31, 2015. The major product of this effort is the viewgraph package included herein as the Appendix. These viewgraphs were used in a presentation to Ms. Amri Hernandez-Pellerano, Dr. Christopher Iannello, and Scott West, of NASA/Johnson and Dr. Ira Katz of NASA/JPL on May 18, 2015. The version included in this report includes clarifying revisions made subsequent to that presentation. It does *not* include the modifications made by NASA specifically for a presentation to Dr. Steven Koontz on June 1, 2015. (NASA had added viewgraphs before the title slide and relocated the section "Conditions for Astronaut Hazard"). The viewgraphs in the Appendix contain the details of the calculations and the results, as well as tutorials on the relevant aspects of current collection and on the conditions for the hazard to occur. The text of this report is a short narrative summary of the motivation, methodology, and results of the work.

1 Objective

The hazard investigated is current flow through an astronaut during EVA (Extra-Vehicular Activity) should a metallic component of the EMU (Extravehicular Mobility Unit) inadvertently contact a positive, metallic ISS (International Space Station) surface, either directly or indirectly. Conditions for this to occur are outlined in the "Conditions for Astronaut Hazard" section of the Appendix viewgraphs, starting on page A-4. The maximum potential of an ISS surface is +15 V, resulting from the **v×B** potential gradient when the center of the ISS is grounded by the Plasma Contactor Unit (PCU). The current through the astronaut is limited by the ability of other exposed EMU metallic components to collect electrons from the ambient plasma, which is necessary to complete a circuit. (Resistance within the EMU is considered negligible.[1]) The worst-case plasma condition is taken to be plasma density 1×10^{12} m^{-3} and plasma electron temperature 0.1 eV.[2]

A complete hazard assessment must include (1) the probability of completing a circuit from the plasma through the EMU and astronaut to a positive ISS surface; (2) the maximum current in this circuit, limited by the ability of the exposed EMU metallic component to collect plasma electron current; and (3) the risk that this current poses to the astronaut. The scope of this work is limited to the second of these components: calculating the maximum plasma current collected by possibly exposed EMU components.

2 Basics of Plasma Current Collection and Previous Estimate

The basic unit of plasma current density is the "one-sided plasma thermal current" given by $J_0=ne(eT_e/2\pi m_e)^{1/2}$, for plasma density n, plasma temperature T_e , electron charge e, and electron mass m_e. For the environment considered[2] ($n = 1\times10^{12}$ m^{-3} and T_e = 0.1 eV), $J_0=8.46\times10^{-3}$ Am^{-2}. J_0 is the current density that would be collected by a large, flat plate.

For realistic three-dimensional geometry the current density to a positively biased electrode exceeds J_0 due to convergence of attracted electrons, while being limited by effects including electron angular momentum, space charge, and nearby negatively charged insulation. It is convenient to express the current to an electrode as (I/J_0A) (where I is the collected current and A is the electrode area), referred to as "Normalized Current" or "Enhancement Factor."

It is well-known that a sphere with a long-ranged potential (Orbit-Motion Limited regime) has an enhancement factor of $(1+V/T_e)$. Apparently motivated by this simple result, previous investigators[3] found that a small sample of data taken by a 4-inch diameter Langmuir Probe on the ISS FPMU (Floating Potential Measurement Unit) could be fit by an enhancement factor of $0.6(1+ V/T_e)^{0.7}$, which is 20.11 for V = 15 V and $T_e = 0.1$ eV. Despite the lack of any dependence on plasma density or electrode geometry, this enhancement factor was used to estimate current to exposed EMU electrodes in the proposed worst case plasma condition.

A more detailed discussion of plasma current collection and the "Langmuir Probe Fit" estimate can be found in the "Current Collection Tutorial" and "Application to FPMU Langmuir Probe" sections of the Appendix, starting on page A-15.

3 *Nascap-2k* Methodology

Leidos used the *Nascap-2k* computer code to calculate currents to the EMU electrodes under the proposed worst-case plasma conditions. *Nascap-2k* calculates the potential in the vicinity of a complex object immersed in plasma using a space charge formula that accounts for acceleration and convergence of attracted particles. Current distribution on the object is then found by tracking particles inward from a sheath boundary. References to previous current collection calculations using *Nascap-2k* are provided at the end of the Appendix, page A-63.

4 EMU Geometric Model

A geometric model of the EMU suitable for *Nascap-2k* calculations was constructed using information provided by T. Scott West.[4] A preliminary model was constructed based on the initially provided information, and then revised based on corrected, clarified, revised, and additional information provided later. The electrodes and neighboring fabric were zoned sufficiently finely for accurate *Nascap-2k* calculations, while the bulk of the EMU fabric was coarsely zoned. Details of the EMU Geometric Model are provided in the Appendix, starting on page A-31.

4.1 Exposed versus Unexposed Electrodes

Most of the electrodes modeled are normally covered with fabric, but are sometimes partially exposed during normal operations. These include the Fabric Attachment Rings (FARs), Sizing Rings, Waist and Arm bearings.

A few of the electrodes modeled are always exposed. These include the D-Rings (for attachment of the Body Restraint Tether (BRT)), the Neck Ring, and the EVA Baseplate.

4.2 Anodized Aluminum versus Stainless Steel

Most of the electrodes considered have stainless steel surfaces that may be exposed to plasma. However, a few electrodes (notably the Neck Ring) are anodized aluminum. The anodization layer is insulating, and acts as a capacitor to block the flow of direct current. However, a transient current will flow, lasting a few milliseconds, depending on the thickness of the anodization layer (Appendix, page A-46).

4.3 Tether Scenario

The Body Restraint Tether (BRT) may contact an EMU electrode while another EMU electrode contacts a positive ISS surface. Since the BRT is insulated at both ends, it participates in the EMU circuit as an extended current collector. Here we are only considering the case in which the tether is *not* in contact with ISS. The tether is made of stainless steel, 3/32 inch (2.4 mm) in diameter, and may have exposed length of tens of meters.

5 Current Collection Results

Nascap-2k was used to calculate currents to the EMU electrodes under the proposed worst-case plasma condition of plasma density 1×10^{12} m^{-3} and plasma electron temperature 0.1 eV. The fabric surfaces were taken to be at a negative potential of -0.2 V, which is appropriate to a ram-facing surface. (Under other conditions, the potential estimate would be more negative, for less current.)

The results are shown in Table 1. (See Appendix, starting on page A-47, for additional details.) Of the EMU components, the largest current is collected by the EVA baseplate at 1.6 mA. Most of the FAR-Sizing Ring combinations collect about 1 mA, but these are expected to be mostly (if not entirely) covered. The Neck Ring (which is known to be anodized) collects 0.7 mA. The two D-Rings together collect less than 0.4 mA. Current to the "Breast Plate" (representing the DCM) is also small. Most of the "Enhancement Factors" are in the range of 3 to 6, well below the factor of 20.11 used in Reference 3. If all EMU electrodes were exposed and conducting, the total current would be 11.4 mA. If those electrodes that are normally covered are only 90% covered, the total is reduced to 3.7 mA. Of this 3.7 mA, at least 2.4 mA is transient (milliseconds).

The Body Restraint Tether (BRT) collects in Orbit-Motion Limited (OML) fashion due to its small diameter of 2.4 mm. The cylindrical OML factor is well approximated by $\left(1+\frac{4}{\pi}\frac{V}{T_e}\right)^{1/2}$, which is 13.86 for the parameters of interest. Thus it collects nearly 1 mA of current for each meter of exposed tether, raising the possibility of 10 mA to 20 mA of current flowing in the circuit.

6 Conclusions

We used *Nascap-2k* to make realistic estimates of plasma current collected by exposed electrodes on the EMU under worst case plasma conditions. The largest individual current is 1.6 mA collected by the EVA BasePlate. Other electrodes each collect 1 mA or less if totally exposed. Enhancement factors are mostly in the range of 3 to 6, well below the previous estimate of 20.11.[3]

The Body Restraint Tether (BRT), which collects in Orbit-Motion-Limited fashion, collects nearly 1 mA per meter of exposed length. Thus, if the BRT is the plasma contacting component of the circuit through the astronaut, there is a possibility of 10 mA to 20 mA of current.

In evaluating the risk associated with these currents, it should be taken into account that currents to anodized components (e.g., the Neck Ring) are transient, with a decay period of a few milliseconds, depending on the thickness of the anodization.

This analysis does not address ram enhancement, presheath enhancement, magnetic limiting, and transients due to dynamic plasma response. Collectively, our experience is that these effects are not likely to increase the current collected by as much as a factor of two.

References

1 2014-11-10-Plasma-EMU-Area-Body-Resistance-Input-Data.pdf, page 14, Nov 10, 2014.
2 1604-T2-LEI-SOW-10.160.1-R00.docx, references "Kramer 2010".
3 EMU External Metallic Areas, Human Body Resistance Values, & Electron Current Calculations to Support NCR Update, Boeing Space Environments, Nov 10, 2014, page 25-30.
4 EMU Current Collection Areas rev 4.pptx, T. Scott West, May 4, 2015.

Table 1. Current collection results for EMU electrodes.

EMU feature	Area	Current	Material	Current for 10% of area collecting	Enhancement		
	(m^2)	mA	(**)	mA	Calculated (I/(AJ_e))	$0.6(1 + V/T)^{0.7}$	Ratio
					(Space-charge limited)	(Langmuir Probe Fit)	
Body Seal Closure	0.0328	0.87	S	0.087	3.13	20.11	0.16
Waist Bearing	0.0255	0.89	S	0.089	4.12	20.11	0.21
Leg Sizing Rings–each of two	0.0139	1.115	S	0.1115	9.48	20.11	0.47
Boot Sizing Rings–each of two	0.0197	0.95	S	0.095	5.67	20.11	0.28
Arm Bearings–each of two	0.00455	0.135	S	0.0135	2.45	20.11	0.12
Upper Arm Sizing Rings–each of two	0.0066	0.325	S	0.0325	5.77	20.11	0.29
Wrist Bearings–each of two	0.0131	0.735	S,A	0.0735	4.75	20.11	0.24
Breast Plate	0.0058	0.19		0.19 *	3.87	20.11	0.19
Neck Ring	0.0166	0.72	A	0.72 *	3.88	20.11	0.19
Boot FARs–each of two	0.01905	0.01	A	0.001	0.06	20.11	0.31
D-Rings–each of two	0.0029	0.185	S	0.185 *	7.54	20.11	0.38
EVA Base Plate	0.0552	1.62	A	1.62 *	3.47	20.11	0.17
Leg FARs–each of two	0.02535	0.08	A	0.008	0.37	20.11	0.02
Total of Electrodes	0.3661	11.36		3.746	3.72	20.11	0.19
Tether collection: 0.2694 mA/ft					Cylindrical OML		
Tether, 85 feet exposed (25.908m)	0.194	22.9	S		13.86	20.11	0.69
Tether, 55 feet exposed (16.764m)	0.125	14.8	S		13.86	20.11	0.69

*- Always Fully Exposed
** - From EMU Current Collection Areas rev 4.pptx dated 04May2015 from T. Scott West.
S – Stainless Steel
A – Anodized Aluminum

4

Appendix

The following is the viewgraph package used in the presentation by Leidos to Amri Hernandez-Pelle, Chris Iannello, Scott West, of NASA/Johnson and Ira Katz of NASA/JPL on May 18, 2015, with the addition of clarifying revisions made subsequently.

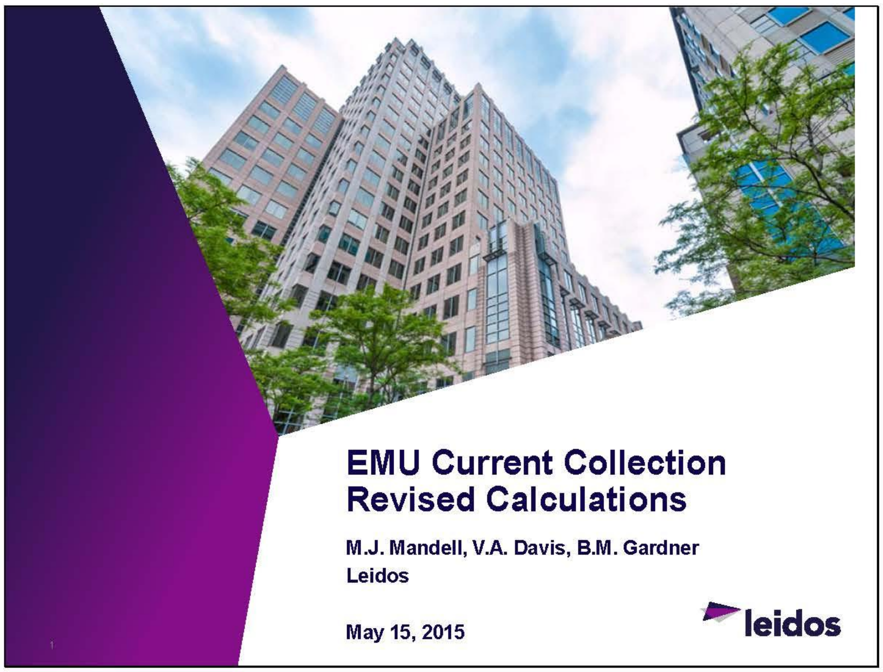

A preliminary version of these calculations was presented to NASA personnel on 17 April 2015. In addition to revised geometry based on updated information provided by NASA, this version includes a discussion of the hazard scenarios and a more detailed tutorial on the relevant aspects of plasma current collection, both of which were requested by NASA.

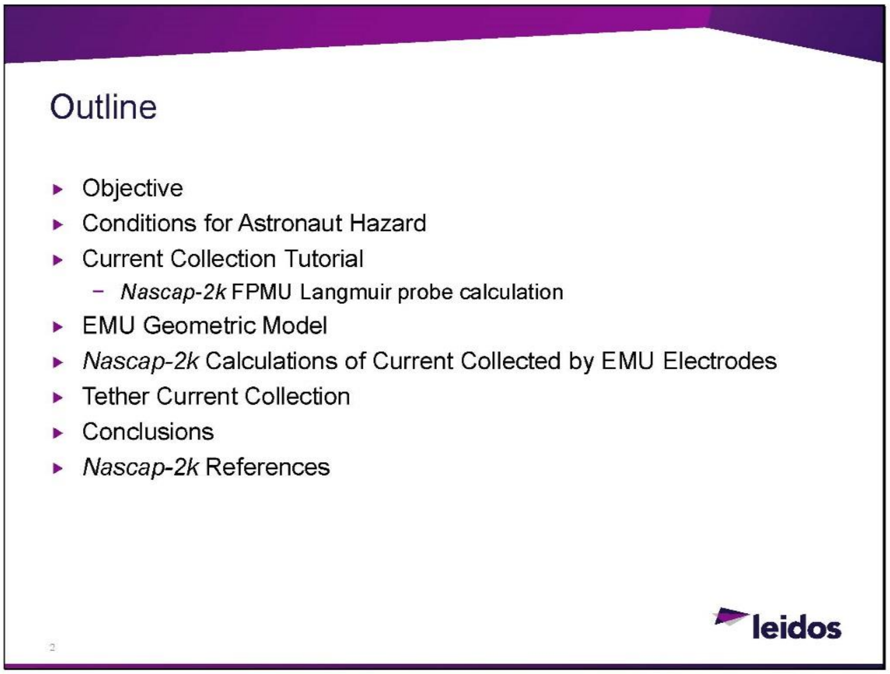
Outline
Objective
Conditions for Astronaut Hazard
Current Collection Tutorial
– *Nascap-2k* FPMU Langmuir probe calculation
EMU Geometric Model
Nascap-2k Calculations of Current Collected by EMU Electrodes
Tether Current Collection
Conclusions
Nascap-2k References
leidos

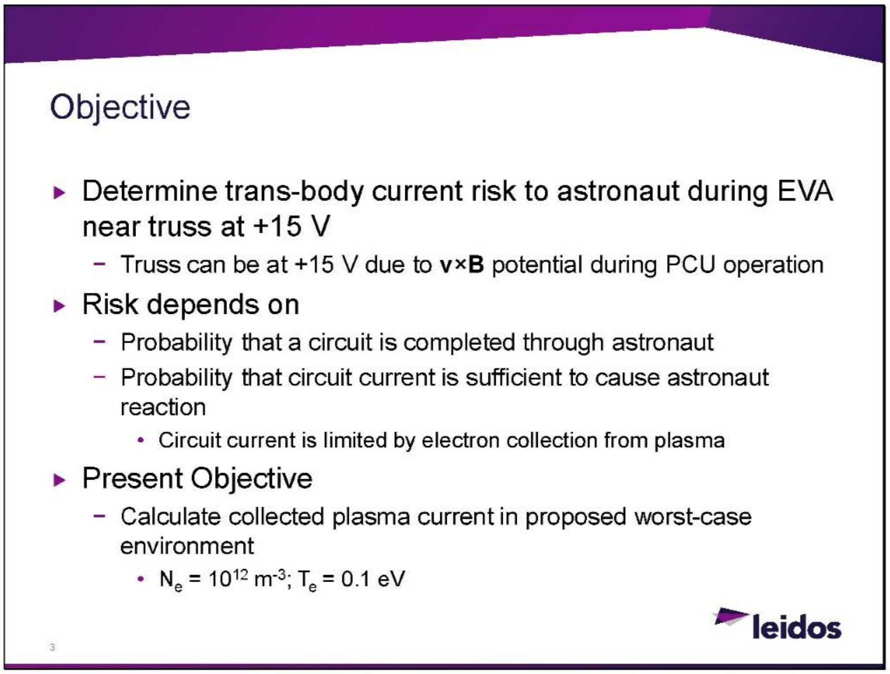

PCU operation is needed during EVA to ground ISS to the ambient plasma and avoid the occurrence of large (~40 V or higher) negative potentials on the ISS truss, which would represent a significant astronaut hazard. However, grounding ISS near its center creates the possibility of positive potentials (possibly up to 15 V) at the end of the truss due to ISS motion through Earth's magnetic field. It is possible (albeit unlikely) that a circuit can be completed by exposed metal on the EMU contacting the ISS truss while exposed metal elsewhere on the EMU collects current from the ambient plasma. The focus of this work is to perform realistic calculations of how much current can flow through this circuit (and thereby through an astronaut) in a proposed worst-case environment.


Conditions for Astronaut Hazard
leidos

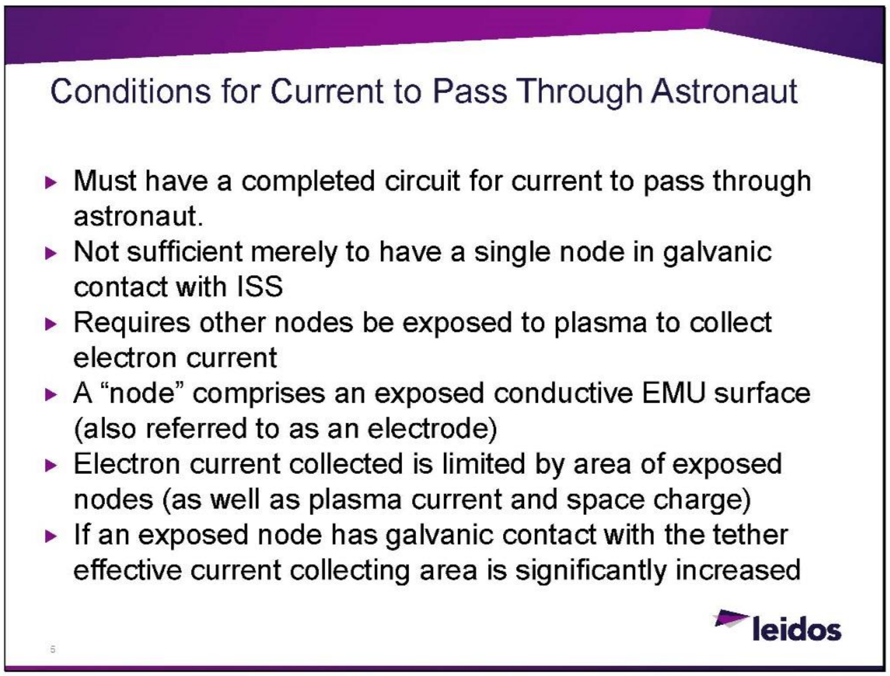

For current to pass through astronaut, there must be a completed circuit. It is not sufficient to merely have a single node in galvanic contact with ISS. Here a node refers to a conductive EMU surface. In addition to a node making galvanic contact with the 15 V ISS, other nodes must be exposed in order to collect electrons from the plasma and complete the circuit.

The current collected is limited by the area of nodes exposed to the plasma as well as the plasma current and space-charge. If an exposed node has galvanic contact with the tether, the effective current collecting area is significantly increased.

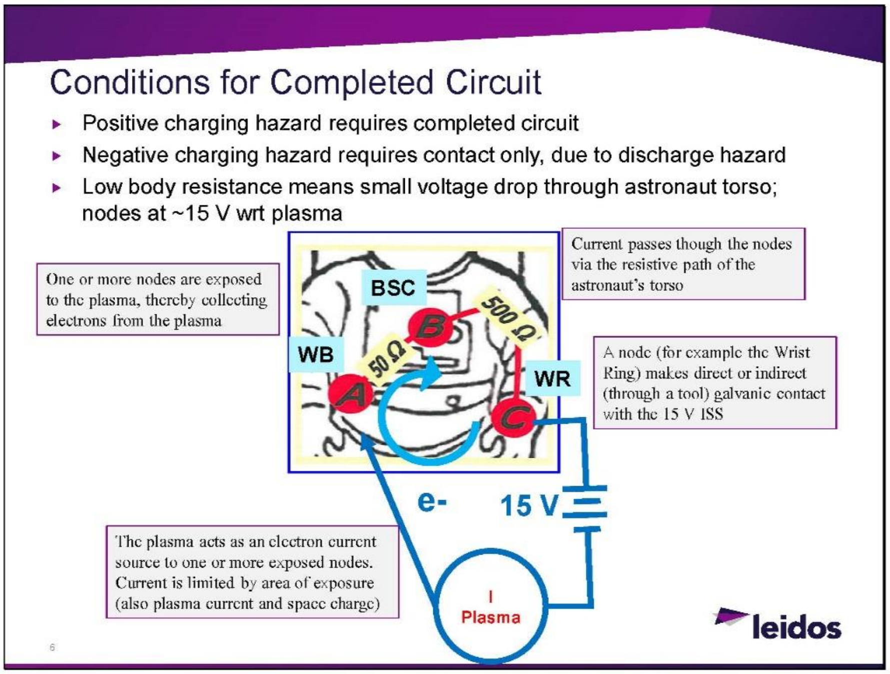

Graphic shows the EMU with the Waist Bearing (WB or node A), the Body Seal Closure (BSC or node B), and the Wrist Ring (WR or node C), and the typical resistances between the nodes. These are the nodes considered most likely to be involved in a completed circuit.

The importance of the resistance values is that they are low enough such that the voltage drop from one node to another is very small, thereby maintaining the 15 V differential between the astronaut and the ambient plasma and resulting electron collection.

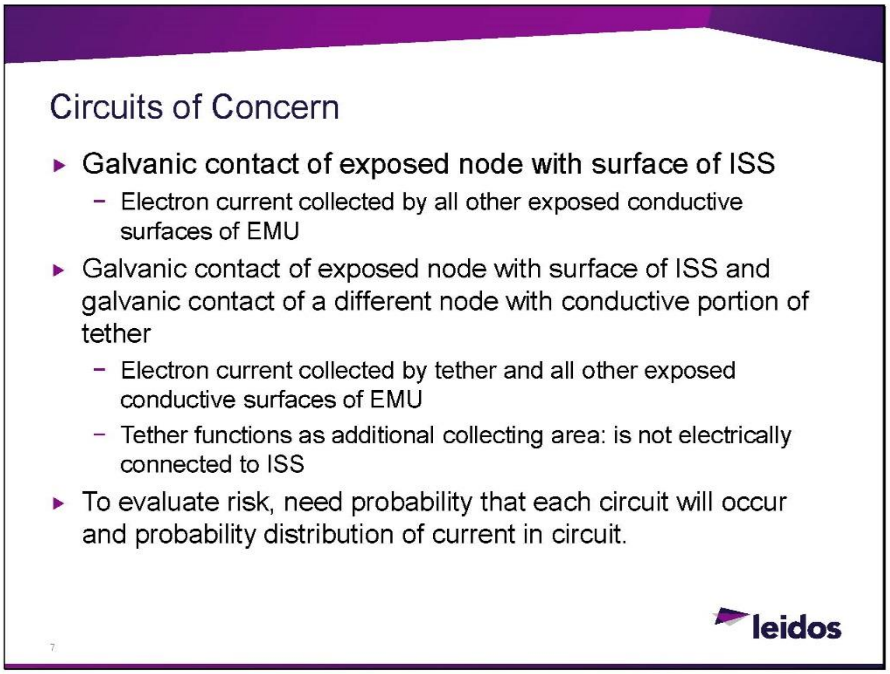

The circuits are essentially identical, with the exception that in the second case the tether provides the main contact with the plasma.

The node in galvanic contact with the 15 V ISS puts the astronaut at 15 V positive with respect to the surrounding plasma.

With resistance of the body or other materials within the EMU, other exposed nodes are also at ~15 V positive.

These positively charged exposed nodes attract electrons from the plasma, thereby completing the circuit.

If one of the exposed nodes makes galvanic contact with the tether (which is not in galvanic contact with ISS), the tether is at 15 V positive and thereby collects electrons from the plasma like any other exposed node.

To evaluate risk, we need to know the probability of each of the events involved in completing the circuit as well as a probability distribution of the amount of current in the circuit.

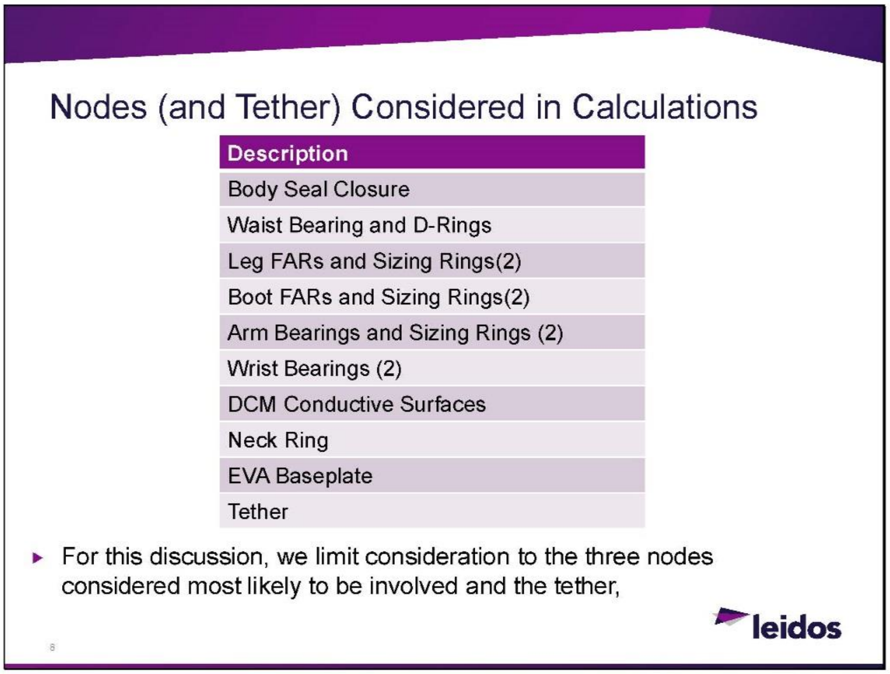

Calculations were performed for all the nodes (and tether) listed above. However, for this discussion, we limit consideration to the three nodes (and tether) noted on slide 6, as they are considered to be most likely to be involved.

Nodes (Electrodes) Considered in this Discussion

Ref: NCR-ISS-232G, page 39

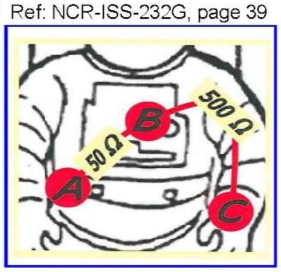

Node A: Waist Bearing (WB) including D-rings for safety tether attachment

Node B: Body Seal Closure (BSC) to which the Mini Workstation (MMWS), tools and the Body Restraint Tether (BRT) are attached.

Node C: Wrist Ring

MMWS and BRT are insulated

- NCR-ISS-232G provides resistance values as shown in the figure.
  - Values are from the waist bearing to the BSC (50Ω), and from the BSC to the wrist ring (500Ω).
  - Resistance values from NASA-STD-3000.
- Above from *2014-11-10-Plasma-EMU-Area-Body-Resistance-Input-Data.pdf*

leidos

9

Here we describe the three nodes considered in this discussion. The graphic and text on this slide were taken from the file noted at the bottom of the slide.

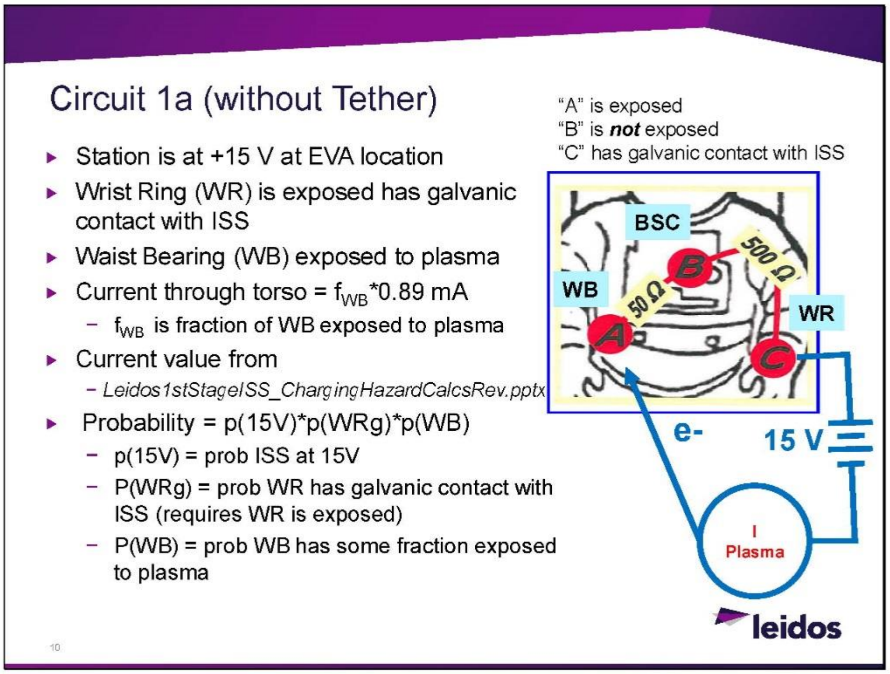

We will examine two circuit configurations, each one with and without the tether being involved. In this case, the Wrist Ring (C) is making contact with ISS and the Waist Bearing (A) is exposed to the plasma. The Body Seal Closure (B) is not exposed.

The current in the circuit is limited by the exposed area of the Waist Bearing, the plasma current, and space-charge. Here the maximum current would be f_{WB}*0.89 mA, where f_{WB} is the fraction of the Waist Bearing exposed to the plasma, and 0.89 mA is the calculated current to the entire Waist Bearing, as will be shown later.

To calculate the probability of that this scenario will occur, we need consider the probability of ISS being at 15 V at the EVA site, the probability of the WR in galvanic contact with ISS, and the probability of the BS being exposed to the plasma. To all this we need to add the probability that sufficient current will flow through the circuit to be of concern.

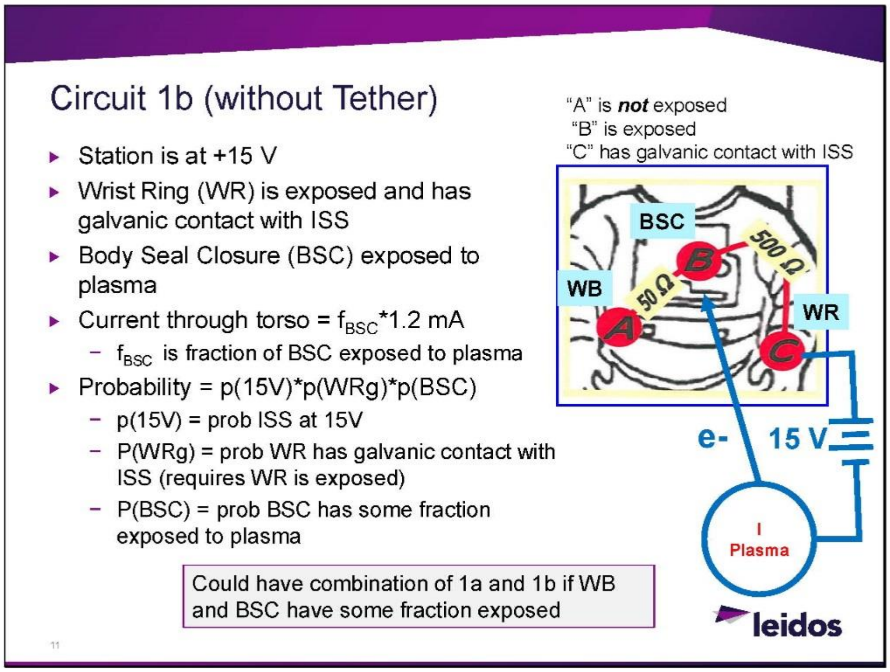

This circuit is like the previous one with the exception that the Body Seal Closure (B) is now exposed to the plasma and the Waist Bearing (A) is not. Of course, you could have a case where some fraction of A and B are exposed.

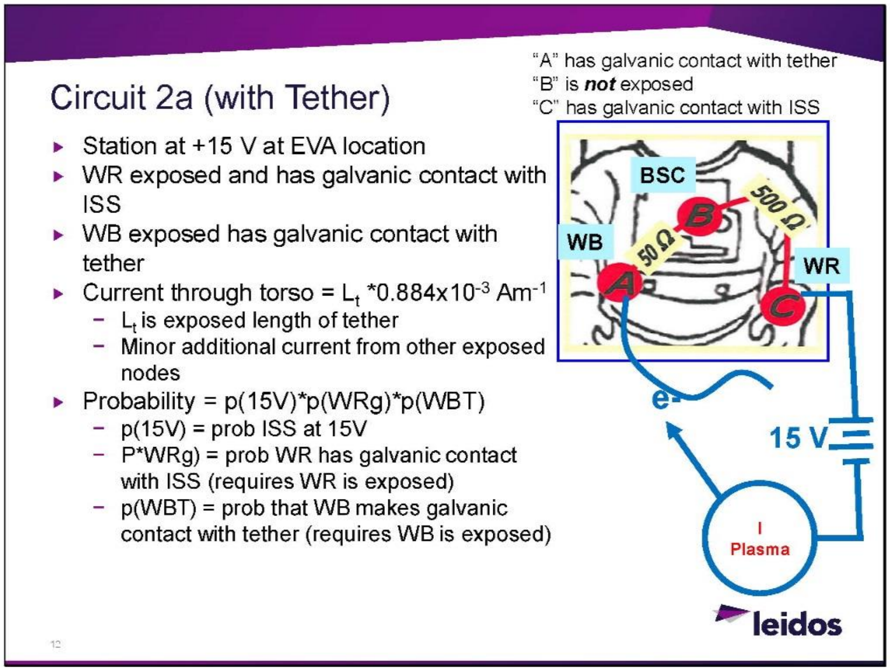

This circuit is like the first one with the addition that the tether is in galvanic contact with the Waist Bearing (A), thereby collecting electron current from the plasma. This increases the maximum possible current through the astronaut's torso to ~ L_t *0.884x10^{-3} Am^{-1} where L_t is the exposed length of the tether, and the calculation of current per unit length of exposed tether will be shown later.

The probability of occurrence now includes the probability of galvanic contact between the Waist Bearing (A) and the tether.

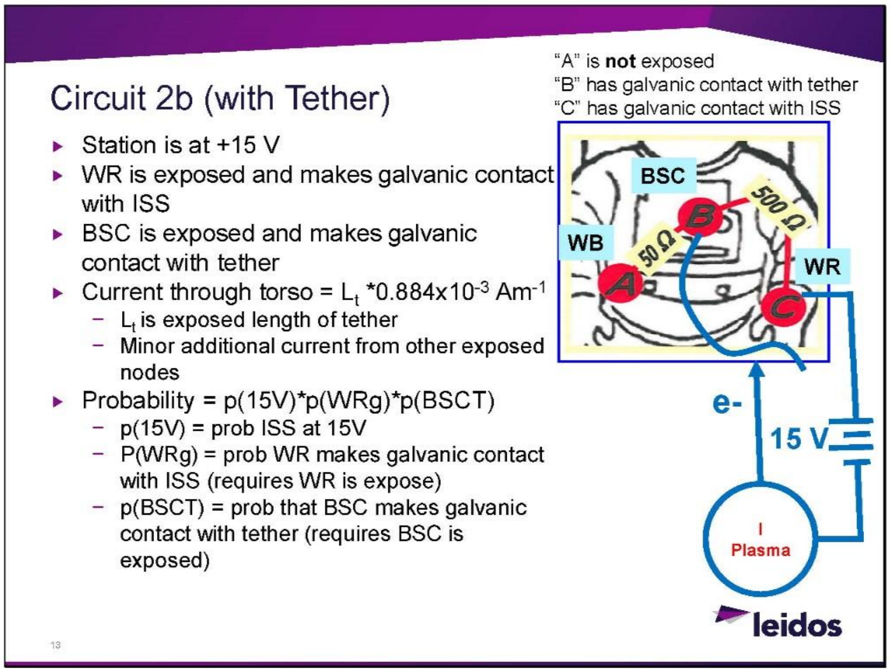

This circuit is like the previous one with the exception that the tether is in galvanic contact with the Body Seal Closure (B).

In addition to collection by the tether, additional current would be collected by any other nodes exposed to the plasma. However, the current collected by the tether would dominate.

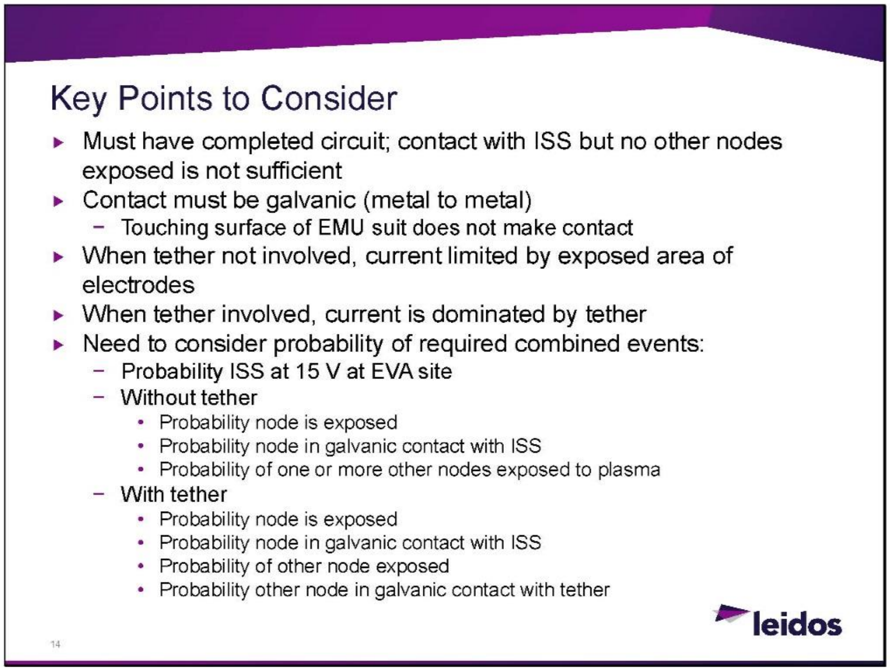

To reiterate the key points here:

In order to have current pass through the astronaut, there must be a completed circuit; contact with ISS but no other nodes exposed is not sufficient.

The contact in question must be galvanic (metal to metal). Merely touching the surface of the EMU suit does not make galvanic contact.

When the tether is not involved, current is limited by exposed area of electrodes. When the tether is involved, current is dominated by the tether.

To evaluate risk, you need to consider probability of required combined events, as well as the probability that the collected current is high enough to be of concern.

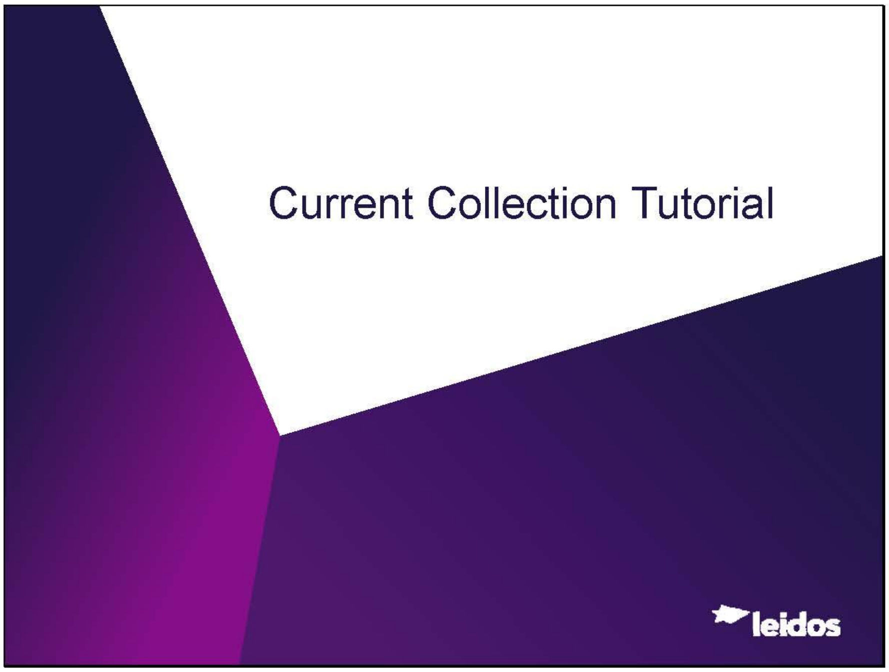

This section provides an introduction to the physical principles that govern how simple charged probes collect electron current from the ionospheric plasma. It includes calculations of electron collection by the spherical Langmuir probe (SLP) on the ISS Floating Potential Measurement Unit (FPMU), which has been invoked previously as a basis for estimation of EMU current collection.

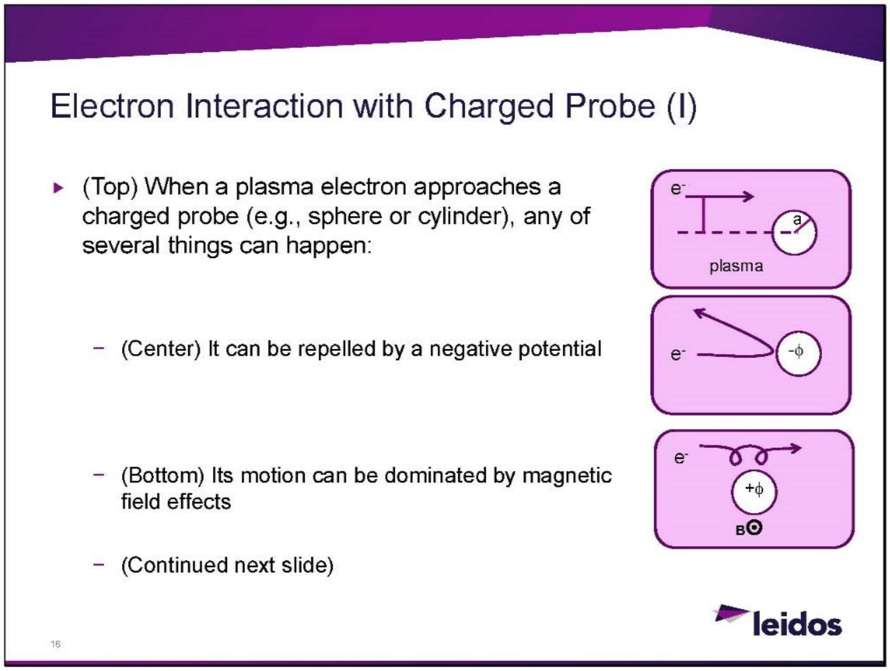

Several things can happen when a plasma electron approaches a charged probe, as shown in the top figure. In these examples the probe can be either a sphere, or an infinite cylinder with axis normal to the figure. In the latter case we will calculate the current per unit length.

The other two figures on this slide illustrate cases that are not of interest for the current purpose. The center figure shows an electron being repelled by a negative potential probe. The lower figure shows that the presence of a magnetic field can make the electron's motion rather complicated. Theories for electron collection in the presence of a magnetic field are beyond the scope of this tutorial, beyond saying that the magnetic field generally reduces the current that can be collected.

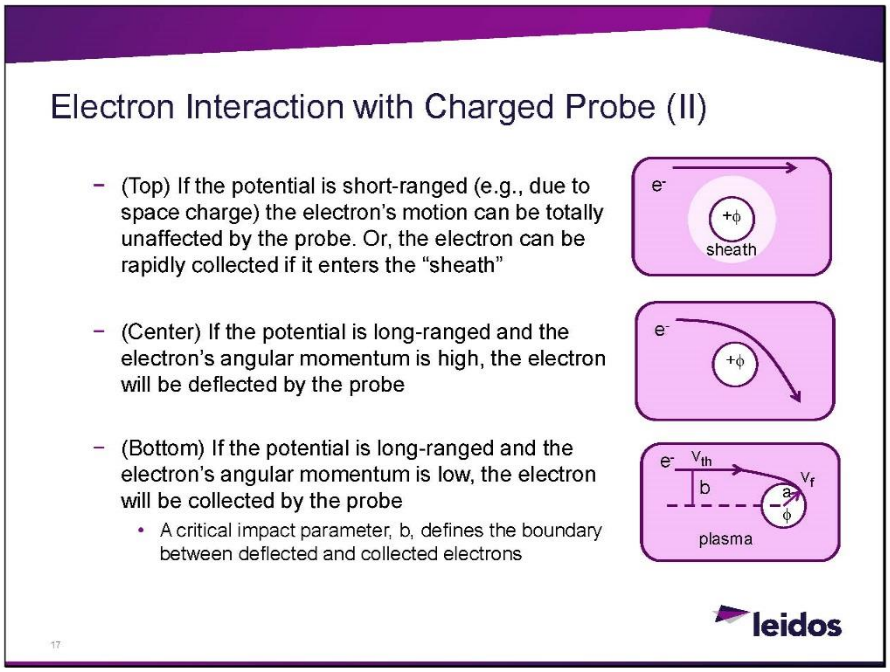

This slide shows the three scenarios that we need to understand. The top figure shows that a positive probe in plasma divides its near vicinity into two distinct regions. Positive potential excludes plasma ions from the region near the probe, leaving this region electron rich. The electron charge "screens" the probe potential, causing it to fall off rapidly to a low value that no longer excludes ions. The electron-rich region of "disturbed plasma" is called the "sheath." In practice there is a reasonably well-defined boundary between the disturbed plasma (with high electric field) and undisturbed plasma (with near zero electric field). This boundary is called the "sheath surface."

If an electron trajectory passes outside the sheath surface, then it passes through a region of near-zero electric field and sees no effect from the probe. However, if the trajectory intersects the sheath surface it suddenly sees a very strong electric field and is collected by the probe. Thus, the current collected by the probe is given by the amount of current in the undisturbed plasma that passes through the sheath surface.

For a long-range potential (to be defined later) collection of an electron is determined by that electron's angular momentum about the probe. Far from the probe the electron travels in a straight line and its angular momentum (mvr) is given by its linear momentum times its distance from a parallel line through the probe's center. That distance is called its "impact parameter." If the electron's angular momentum is large, then the electron is merely deflected by the probe's potential and not collected. For any given electron energy there is a critical impact parameter such that electrons with that angular momentum or less will be collected by the probe. The critical impact parameter is easily calculated by equating the initial angular momentum to the angular momentum of the electron when its trajectory is tangent to (barely touches) the probe surface.

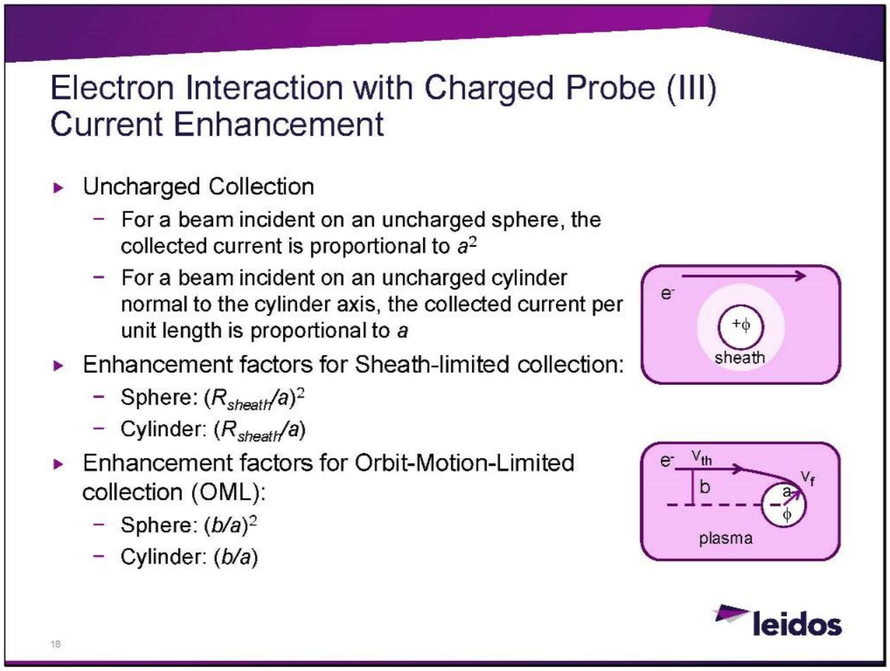

Knowing the critical impact parameter allows us to calculate the enhancement of electron collection due to positive potential on the probe.

First consider a monoenergetic beam incident on an uncharged probe. The current collected is proportional to the cross-sectional area of the probe, which is πa^2 in the case of a sphere, and 2aL for a cylinder.

If the probe is charged and has a sheath, then the probe radius is replaced by the sheath radius, and the enhancement is as shown.

If the probe collection is angular-momentum limited (usually called Orbit-Motion-Limited or OML) then the probe radius is replaced by the critical impact parameter, giving an equally simple expression for the enhancement factor.

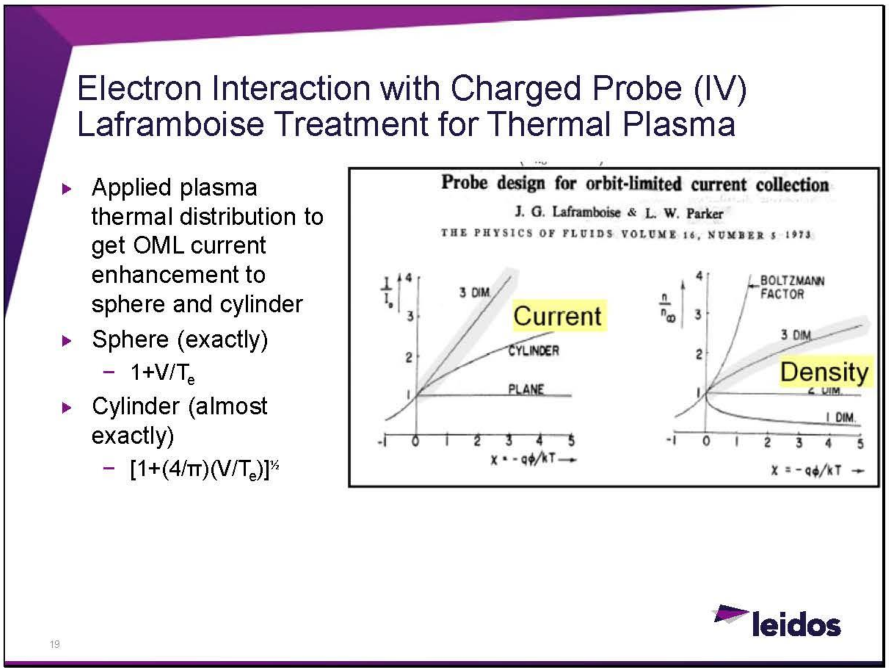

Jim Laframboise applied these principles to calculate OML current collection by a charged probe in a thermal plasma (rather than a monoenergetic beam).

For the spherical case, the very simple result is obtained that the current increases linearly with the ratio of the probe potential (in volts) to the electron temperature (in eV).

The cylindrical case is more complicated because it involves integrating the product of a square root times an exponential. However, the exact result (involving erfs) is very closely fit by the simple square root formula shown. Thus, the OML current to a cylinder increases less rapidly with applied potential than the OML current to a sphere.

Note that this enhancement depends only on the potential's being long-ranged, and has no dependence on the density of the plasma from which we are collecting.

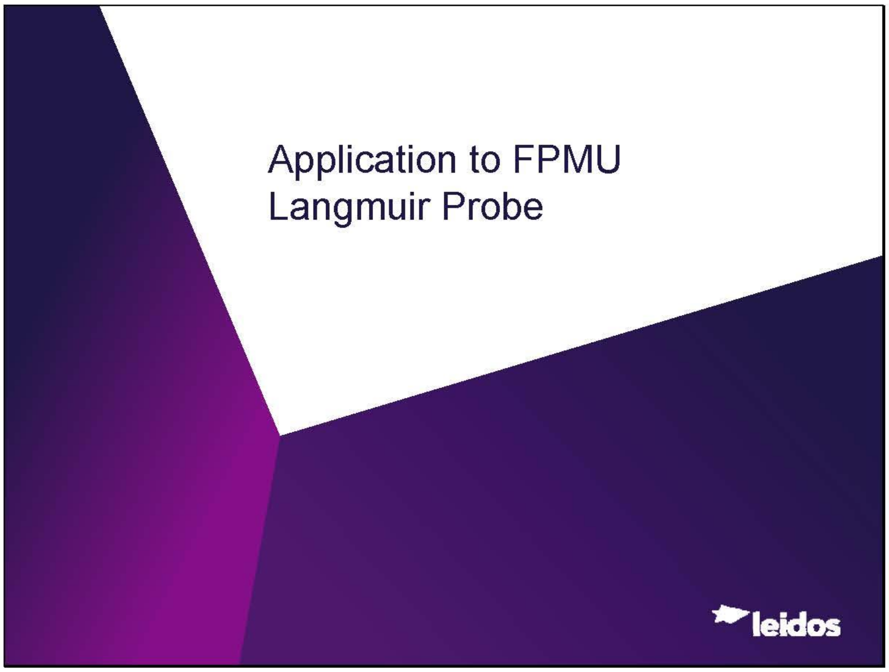

Next, we apply the current collection concepts we have been discussing to electron collection by the Spherical Langmuir Probe (SLP) on the ISS Floating Potential Measurement Unit (FPMU).

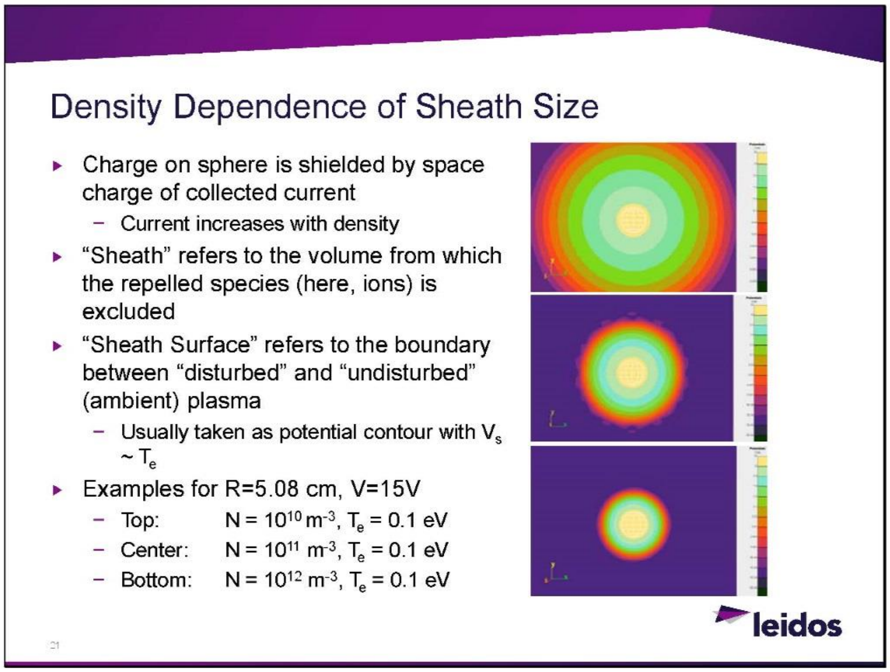

We noted earlier that OML collection did not depend on plasma density, but only on the potential's being long ranged.

That is *not* the case for sheath-limited collection, as long as the sheath potential fails the condition of being long-ranged.

This slide shows the sheath potential around the SLP for three different plasma densities. As the plasma density increases the sheath becomes markedly smaller.

We will examine these cases in detail on the following slides.

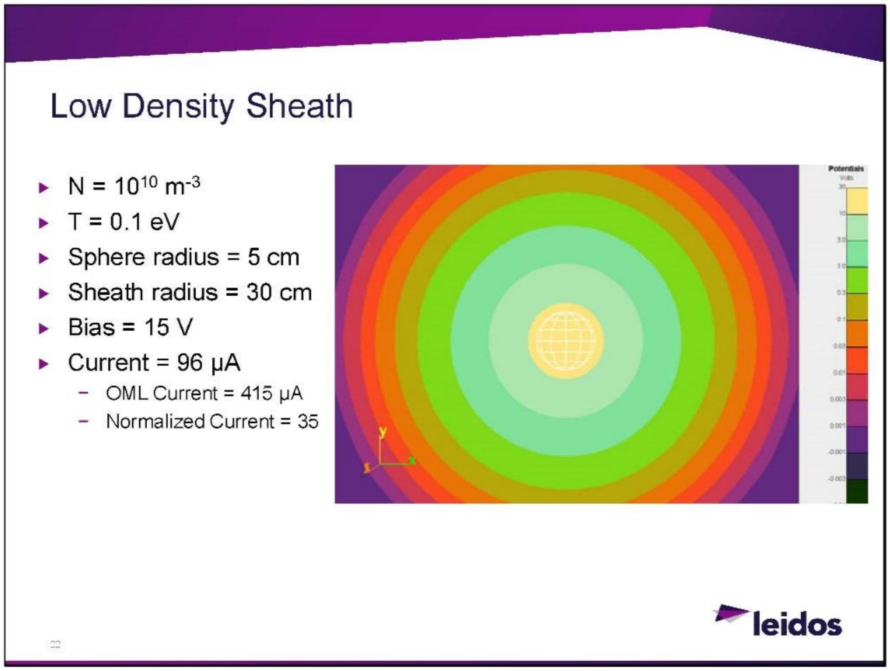

This slide shows the sheath about the SLP in relatively low density plasma.

The potential contour corresponding to the electron temperature occurs at the boundary of the dark green and orange contour regions, at a radius of about 30 cm, or six times the sphere radius. Consequently, the collected current (i.e., the current through the sheath) is 96 microamperes, or 35 times the current to the uncharged probe. Due to the electron temperature being very small compared with the applied potential, the OML current is much larger at 415 microamperes. So, the OML treatment is inappropriate to this probe, even at relatively low plasma density.

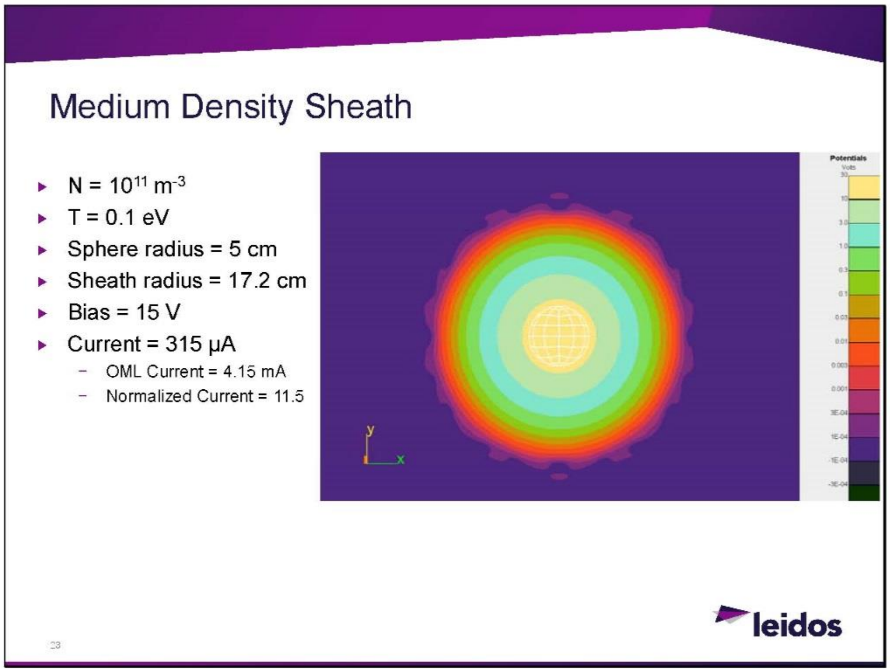

The medium density sheath contains a higher space charge density of collected electrons.

If the sheath remained the same size as for the low density case, the space charge within the sheath would increase by a factor of ten.

Consequently the sheath radius is reduced to 17 cm (compared with 30 cm in the low density case).

The sheath-limited current of 315 microamperes (11.5 times the current to an uncharged sphere) is much less than the OML current of 4.15 milliamperes (151 times the current to an uncharged sphere).

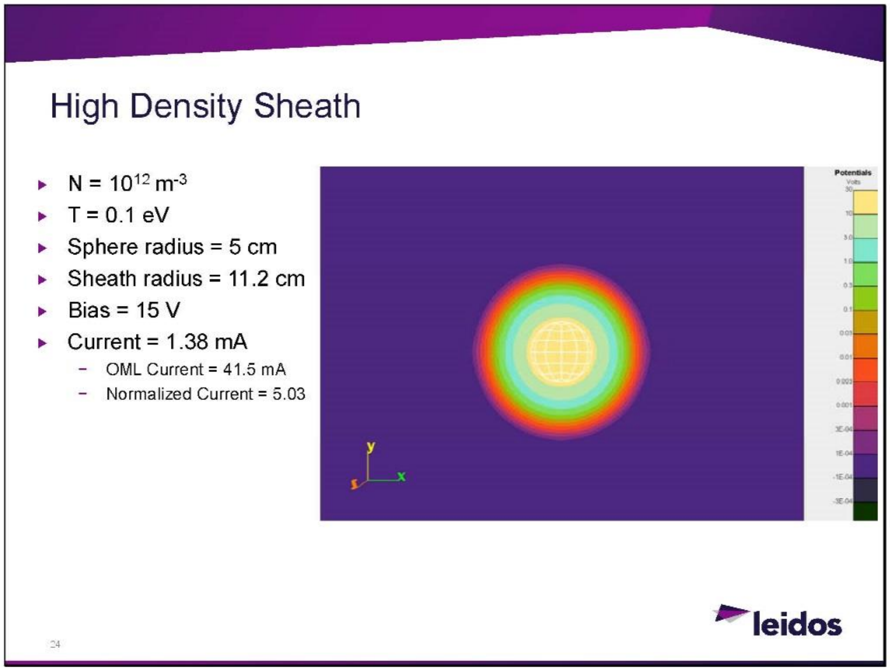

Raising the plasma density yet another order of magnitude forces the sheath to shrink even further – to 11 cm from the previous values of 30 and 17 cm.

While we are now collecting the highest current (1.38 mA vs. previous values of 0.1 and 0.3 mA), it is a mere five times what an uncharged sphere would collect, far below the OML prediction of 151.

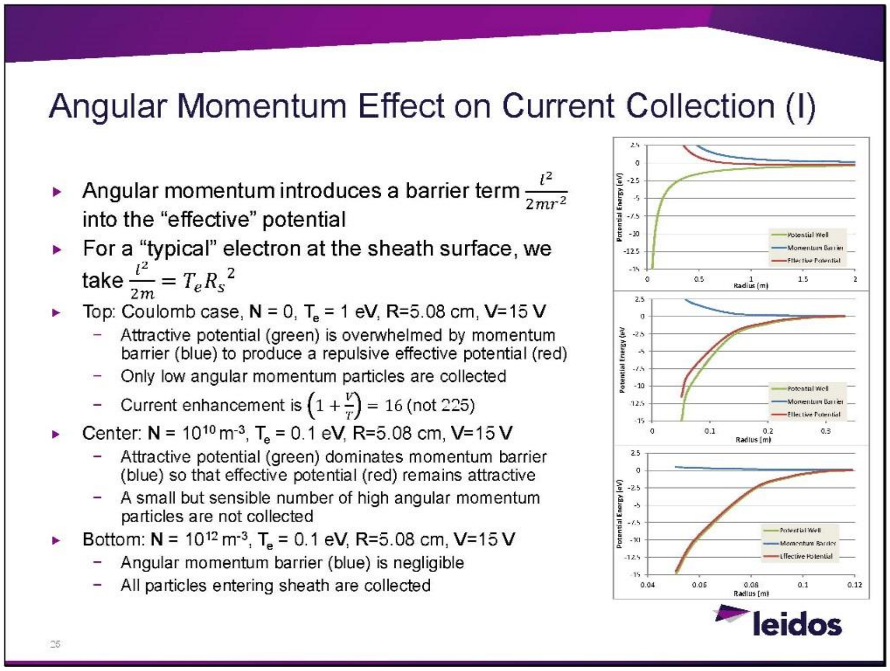

The next few slides provide a more formal treatment as to when collected current is angular momentum limited and when it is not.

The following three slides address the three cases shown here in more detail.

If you took Classical Mechanics in college, you spent a lot of time studying motion in a central force field.

You learned that the motion was always planar, and could be cast into a one-dimensional (radial) problem by introducing an "effective potential" that included a barrier term proportional to the square of the particle's angular momentum. Note that the barrier term goes as $1/r^2$, which is why we define a long-range potential as one that falls off more slowly than $1/r^2$.

To apply this to the current problem, we define the angular momentum of a "typical" electron by its having thermal energy at the sheath surface. We look at the case of a coulomb potential (corresponding to zero density plasma), and the low and high density plasma cases treated previously. The coulomb case is taken as having 1 eV electron temperature in order to not overstate the case. Potential solutions for the other two cases were taken from the previously displayed potential plots.

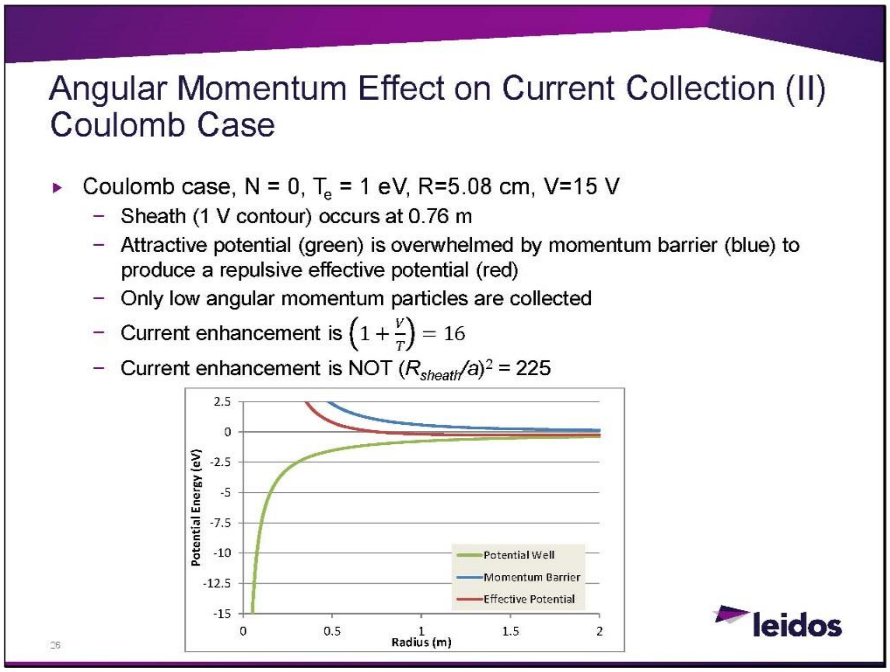

This slide discusses the coulomb (zero density) case. The attractive coulomb potential is shown as the green curve.

Since the potential goes as 1/r, it is easy to calculate that the sheath surface (taken as the -1 V contour) occurs at fifteen times the sphere radius, a radius of 76 cm.

The angular momentum barrier (blue curve) is an inverse square repulsive potential.

When we add these together to get the effective potential (red curve) we see a small minimum at large distance, but a strongly repulsive effective potential inside the sheath.

This tells us that the "typical" plasma electron is not collected; only a few atypical (low angular momentum) electrons are collected by the probe.

Specifically, even though the normalized plasma electron current entering the sheath is 225 (in normalized units), the current collected by the probe is given by the OML value of 16.

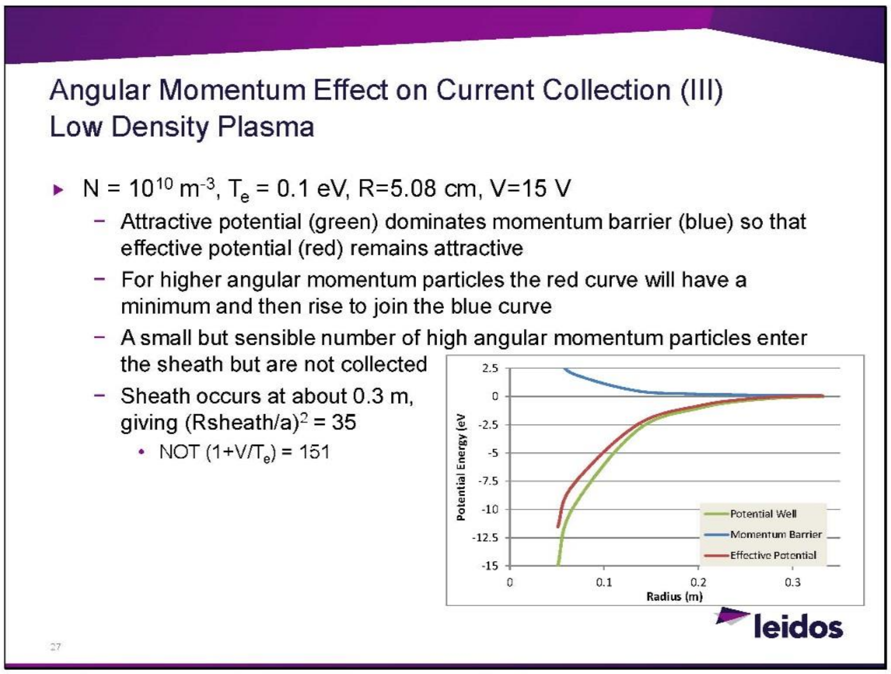

For the low plasma density case the attractive potential is given by the green curve.

The sheath edge (-0.1 V contour) occurs at 30 cm, a far smaller radius than in the higher temperature coulomb case.

(While 10^{10} m^{-3} is a low density for the ionosphere, it is *not* low density when considering the sheath around a 4-inch sphere.)

The angular momentum barrier for a "typical" electron (blue curve) is rather modest, so the effective potential (red curve) remains attractive.

This means that the "typical" plasma electron entering the sheath is collected, but a few atypical (high angular momentum) electrons will enter the sheath and merely be deflected.

The sheath enhancement for this case is 35, far smaller than the angular momentum limited current of 151.

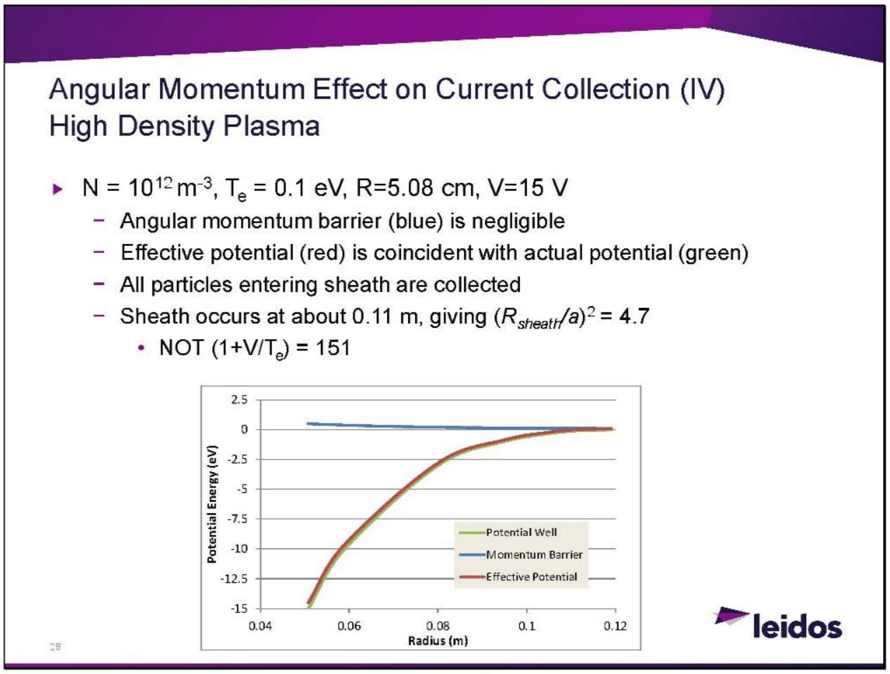

In the high plasma density case the sheath is still smaller.

Only low angular momentum particles reach the sheath, so the angular momentum barrier (blue curve) is negligible, and the effective potential (red curve) is indistinguishable from the attractive potential (green curve).

The sheath limits the collected current to 4.7 (in normalized units), while angular momentum considerations along would have allowed current of 151.

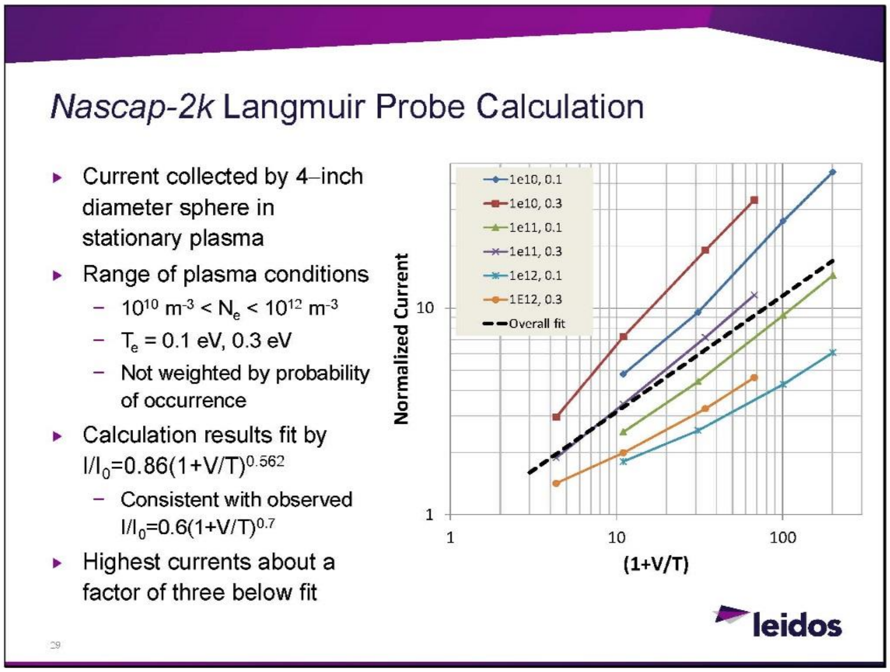

Nascap-2k was used to calculate the currents to the Spherical Langmuir Probe on the FPMU.

The probe is a 4-inch diameter sphere.

For simplicity, the currents were calculated for stationary plasma (no ram-wake effects).

The plasma parameters were chosen to bound the densities and temperatures of interest. No attempt was made to account for the frequency of occurrence of the various conditions.

The applied voltages were 1, 3, 10, and 20 volts.

The calculated currents were normalized by the electron thermal current, and plotted against (1+V/T).

The fit to all the data agrees well with the suggested fit to the actual data.

In all cases the calculated data falls far below the spherical OML factor of (1+V/T), which would be a diagonal line on the plot.

Note that the low currents (corresponding to low density) lie above the fit, while the high currents (corresponding to high density) lie below the fit.

In each case the difference is about a factor of three at the highest voltage calculated (20 V), and less at lower voltages.

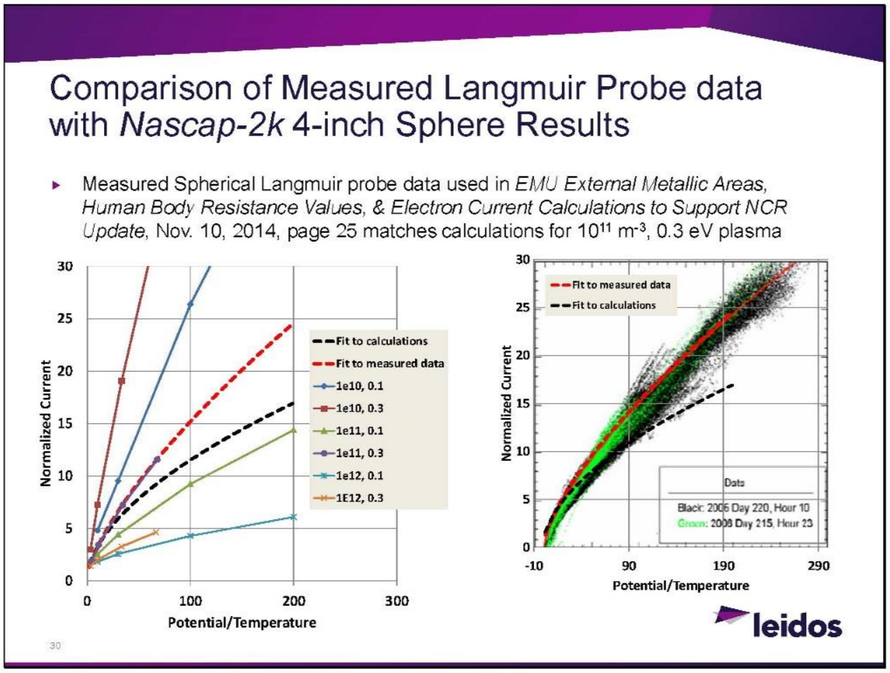

Nascap-2k calculations for a sphere in a 10^{11} m^{-3}, 0.3 eV plasma gives results similar to the data originally used to estimate the positive potential hazard.

However, the *Nascap-2k* prediction is that the normalized current at high positive potential depends only weakly on temperature, and strongly on density, whereas the data fit assumes no density dependence. I.e., that the density dependence is completely accounted for by the current normalization, and the sheath thickness is therefore independent of density.

We do not know the range of temperature (or density) that is included in the data.

However, comparison of the plot with the *Nascap-2k* results suggests a fairly narrow range of densities in the neighborhood of 10^{11} m^{-3}.

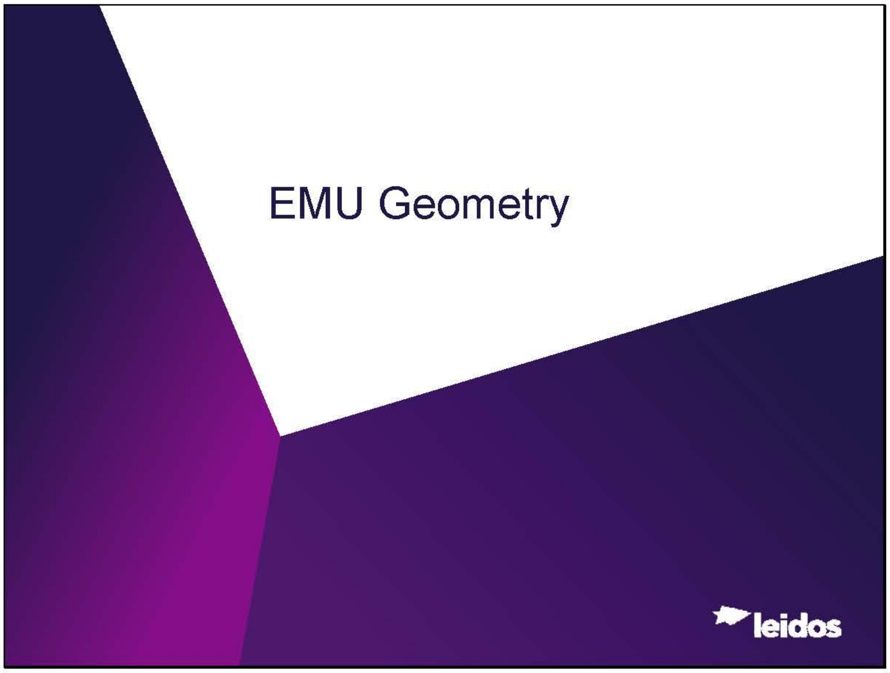

Now we turn to the detailed geometry of possible exposed electrodes on the EMU.

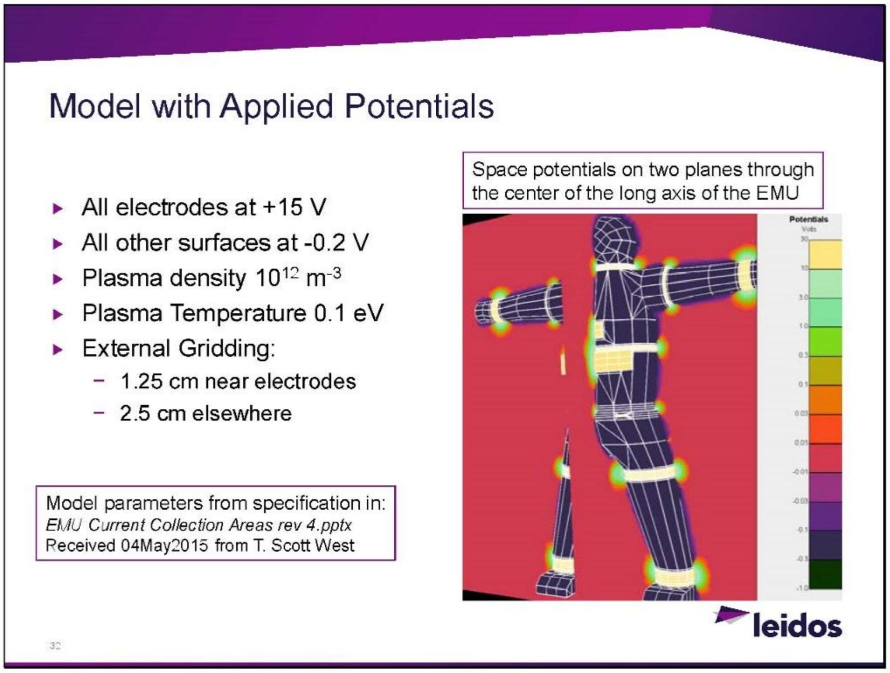

Model based on geometric information provided by Scott West. Details of these electrode geometries (including the breast plate added later) are shown on later slides.

Parameters represent the environment that has been identified as the worst case, highest current.

The electrodes are at +15 V.

The insulating fabric is set to -0.2 V, which is appropriate to a ram-facing surface; non-ram-facing surfaces will be more negative.

The plasma temperature and density are set to the values suggested for worst case.

The grid spacing near the electrodes was set to 1.25 cm, which corresponds to a few plasma Debye lengths. We considered this to be adequate because

1) *Nascap-2k* does a good job resolving a few debye lengths per zone;
2) The length scale near the electrodes with V >> Te is much larger than a debye length; and
3) Overly coarse resolution will err by overestimating the current.

Note that the potentials are plotted on a logarithmic scale; the sheath edge occurs at the edge of the green contour region.

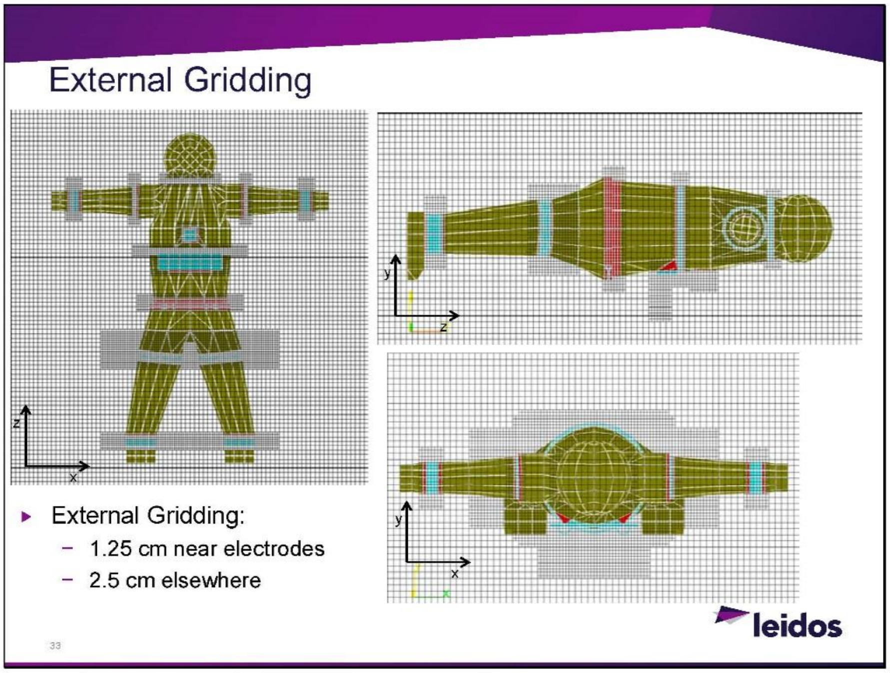

This slide illustrates the external gridding. Note that the fine (1.25 cm) gridding covers ample space near the electrodes.

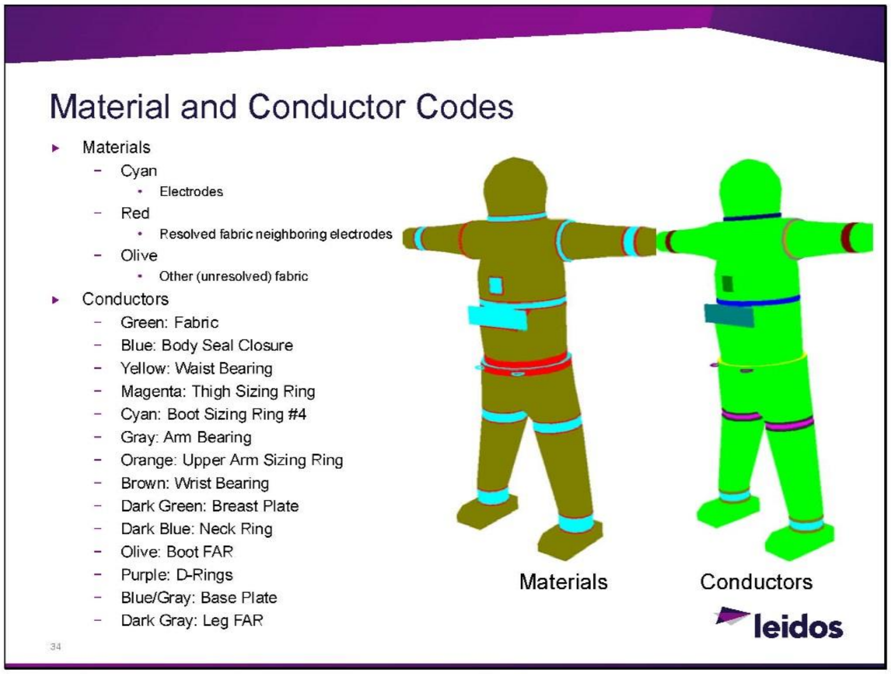

In *Nascap-2k* we use two attributes for each surface, which we call "Material Name" and "Conductor Number."

The figure on the left shows the material assignments.

The light blue indicates the metallic electrodes.

The fabric next to the electrodes (shown in red) is gridded similarly to the electrodes because the potentials are blurred over cell boundaries, and we don't want the blurring to carry high potentials to fabric far from the electrodes.

The olive areas are coarsely gridded, unresolved fabric that is uniformly at the fabric potential.

The figure on the right shows the conductor assignments. Each electrode (or pair of electrodes) is given a unique conductor number that we use to identify its current in the particle tracker output.

Area Breakdown of EMU Geometric Model

Description	Model Area (cm^2)
Unresolved Fabric	25,724
Resolved Fabric	2027
Body Seal Closure	328
Waist Bearing	255
Leg Sizing Pings (2)	278
Boot Sizing Rings (2)	396
Arm Bearings (2)	130
Upper Arm Sizing Rings (2)	133
Wrist Bearings (2)	366
Breast Plate	58
Neck Ring	219
Boot FARs (2)	381
D-Rings (2)	58
Base Plate	552
Leg FARs (2)	507
Tether (per meter of length)	75

leidos

35

These are the areas of the various electrodes in the *Nascap-2k* model.

In the preliminary version of these calculations there were several discrepancies between the areas in the model (based on the electrode dimensions) and the areas we were given.

In the present calculations all dimensional have been updated and all area discrepancies resolved.

We will examine each of these electrodes in the subsequent slides.

Boot FAR with Sizing Ring

- Total Height: 6.9 cm
- Size Ring Height: 3.9 cm
- FAR Diameter: 17.2 cm
- Size Ring Diameter: 16.75 cm
- FAR Area: 190 cm^2 (each)
  - Includes bridges between FAR diameter and size ring diameter
- Size Ring Area: 198 cm^2 (each)

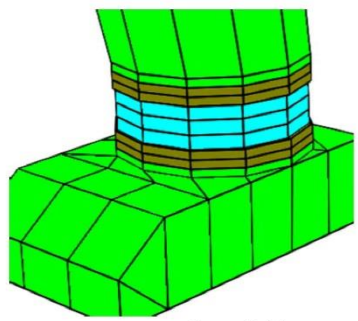

Green: Fabric
Olive: Boot FAR
Cyan: Boot Size Ring

leidos

36

The ankle was modelled with the two halves of the FAR separated by the largest sizing ring.

With this geometry we expect the current to be focused on the sizing ring, with lower current density on the FAR.

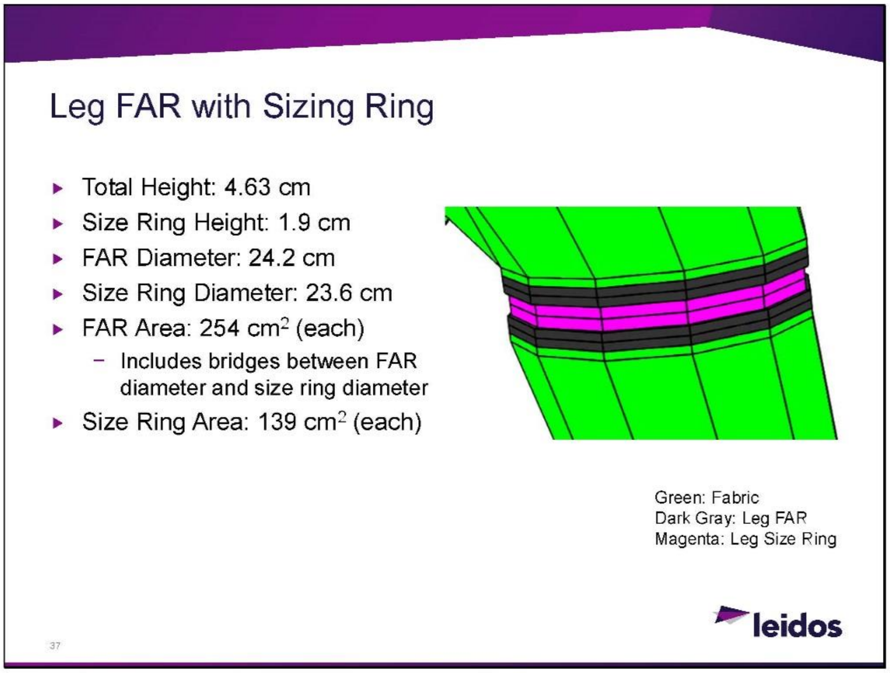

The leg disconnect was modelled with the two halves of the FAR separated by the largest sizing ring.

As with the ankle disconnect, we expect the current to be focused on the sizing ring, with lower current density on the FAR.

However, in this case the size ring area is much less than the FAR area, so the current density on the size ring may be quite high.

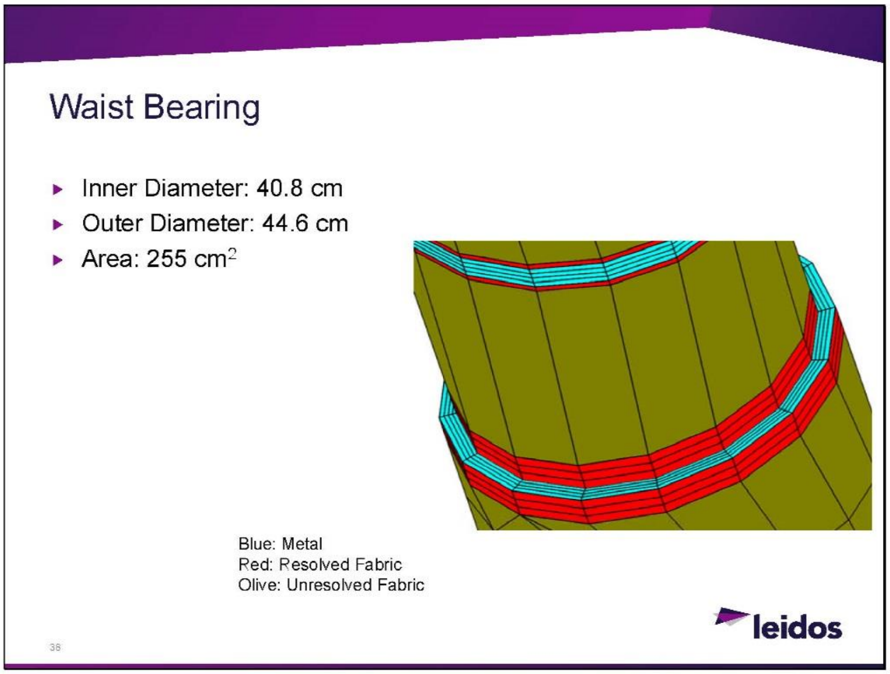

The Waist Bearing is a horizontal ledge.

The D-rings are associated with the waist bearing, and are shown in a later slide.

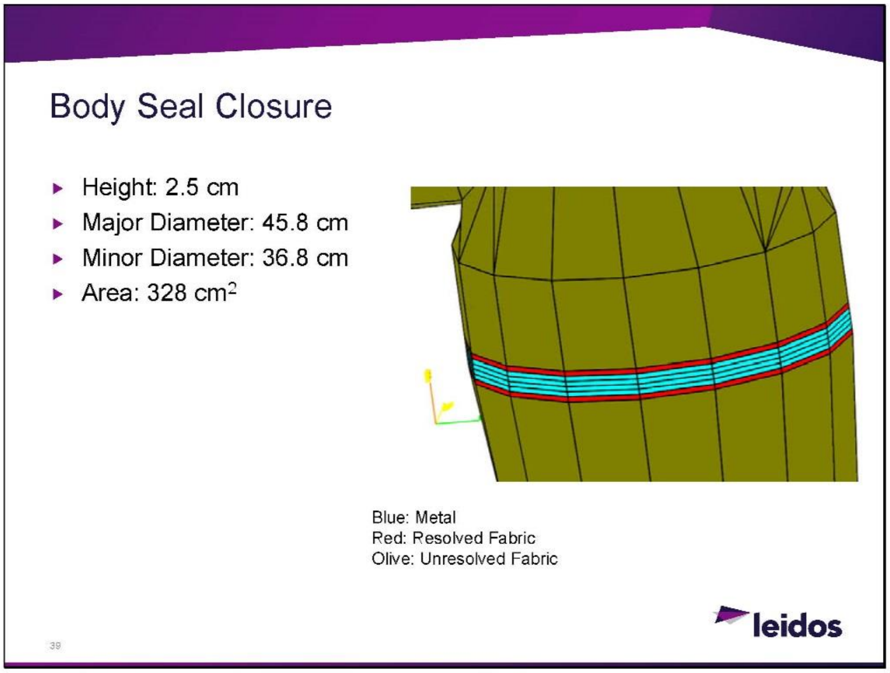

The Body Seal Closure is an elliptical ring.

Near the BSC is a three inch square breast plate (intended to represent several small possibly exposed metal surfaces of the DCM), and the EVA Baseplate, both shown in subsequent slides.

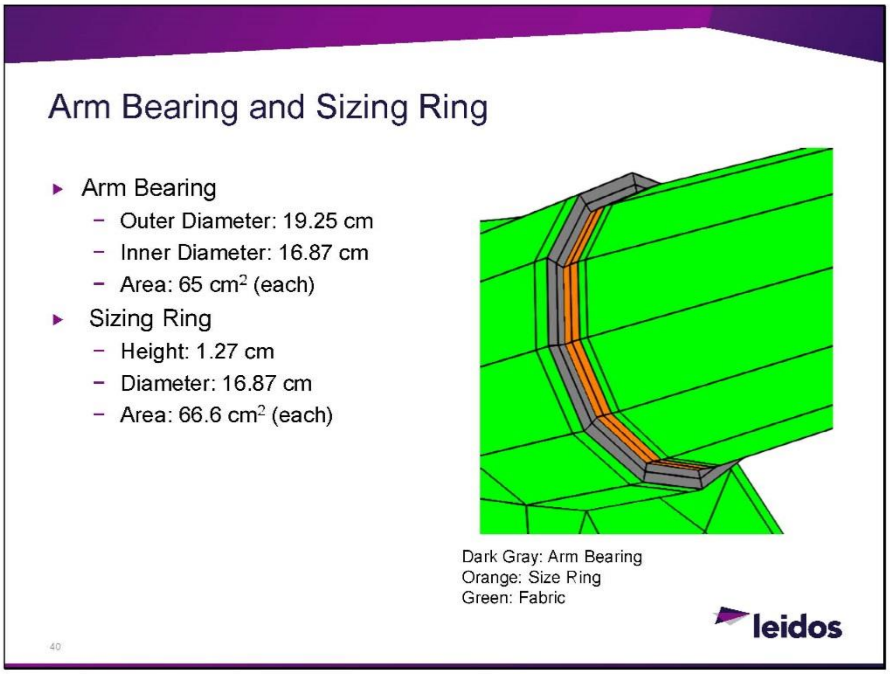

The Arm Bearing (gray) was modeled along with one half-inch sizing ring (orange).

Only the portion of the arm bearing exterior to the sizing ring is exposed to plasma.

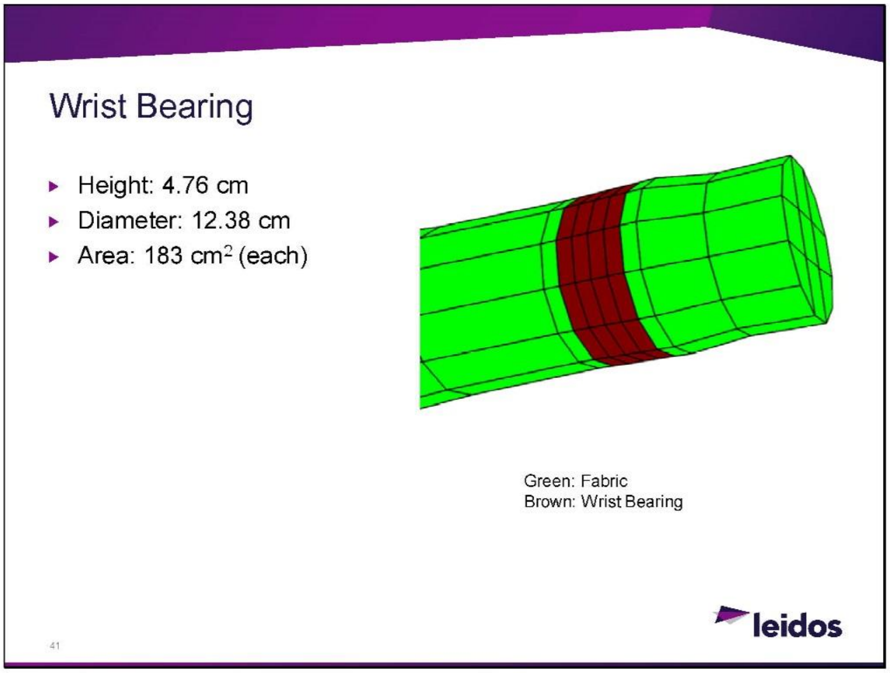

The wrist bearing is modelled as shown.

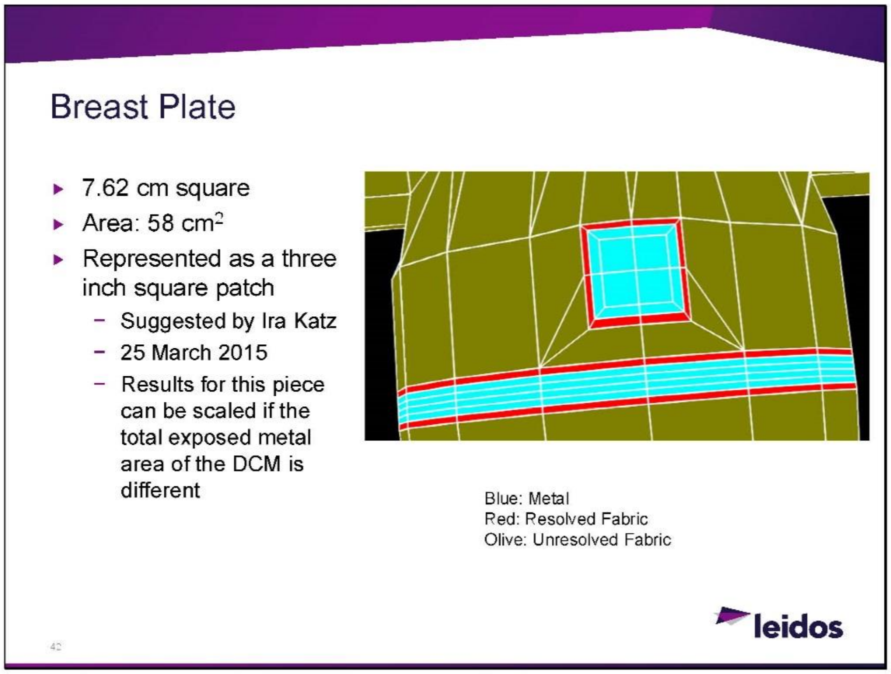

The Breast Plate was a late addition to the model, and is intended to represent several small possibly exposed metal surfaces of the DCM.

It was modeled as a three inch square in accordance with a suggestion by Ira Katz, 25 March 2015.

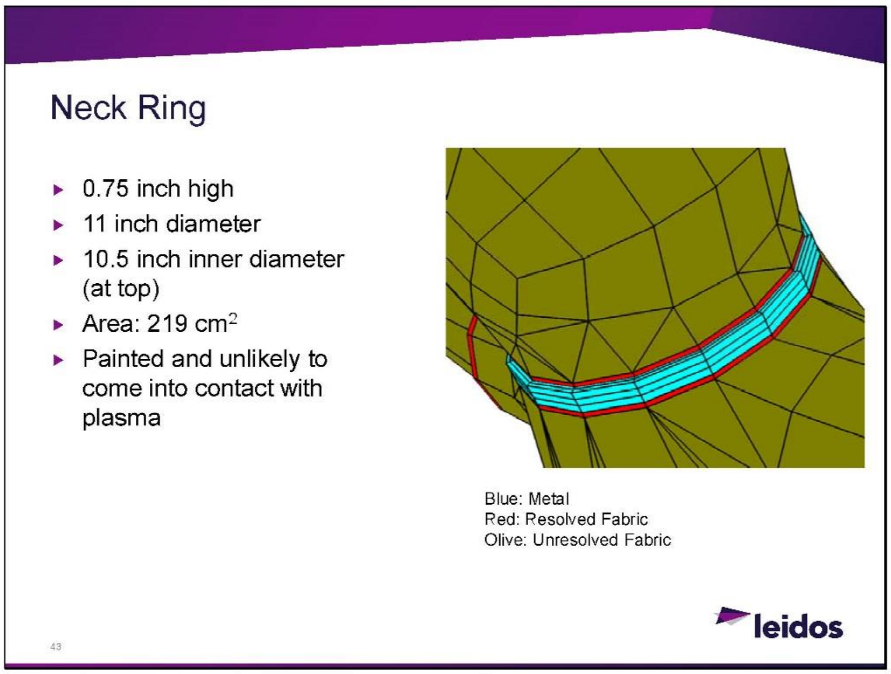

The neck ring was requested following initial submission of the slides.

It was omitted initially because "Neck Ring is painted and would be very unlikely to come into contact with Plasma or ISS structure."

D-Rings

- 2.5 inch wide
- 0.25 inch thick
- Area: 29 cm^2 (each)
- Extend through fabric cutout and are always exposed

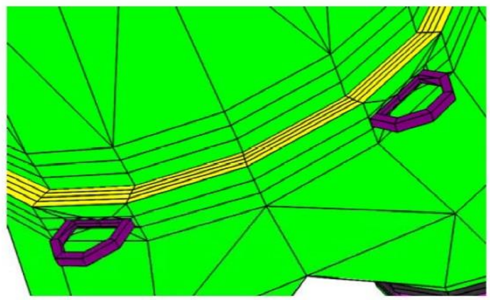

Green: Fabric
Yellow: Waist Bearing
Purple: D-Rings

leidos

44

The D-Rings are used to attach the safety restraint tether.

The tether is insulated from its hook, which is not modelled.

However, "the hook is not always attached to the D-ring – sometimes secondary fabric tethers are looped through the D-ring and then attached to the tether hook." (Per T. Scott West.)

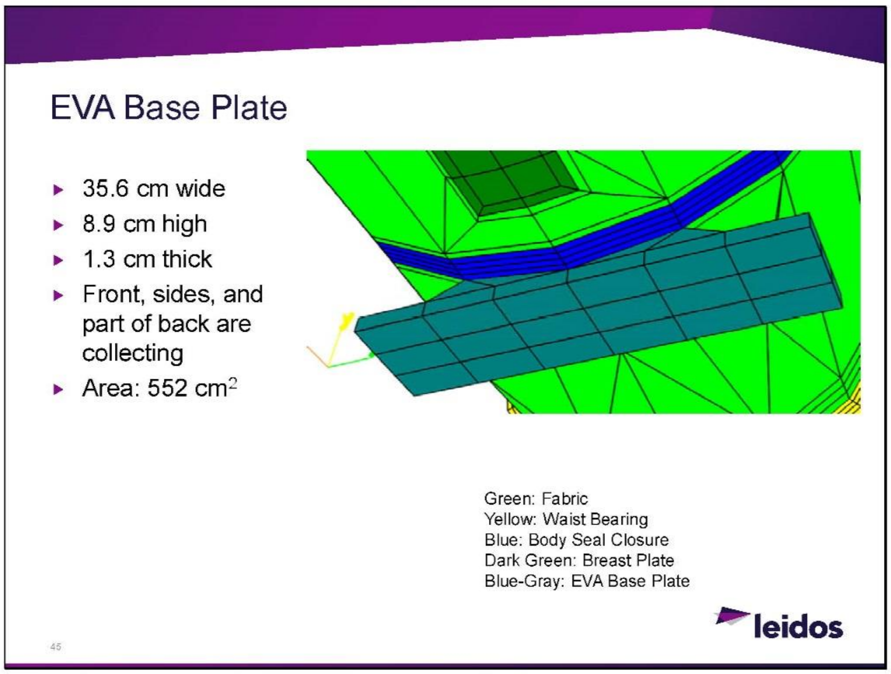

The EVA Base Plate is modeled as a rectangular plate exposed on the front and sides and partially exposed on the back.

This version of the model probably overestimates the exposed area of the base plate.

The arms (not shown) attached to the base plate are electrically isolated from the base plate.

The baseplate itself is conductive through its attachment to the BSC.

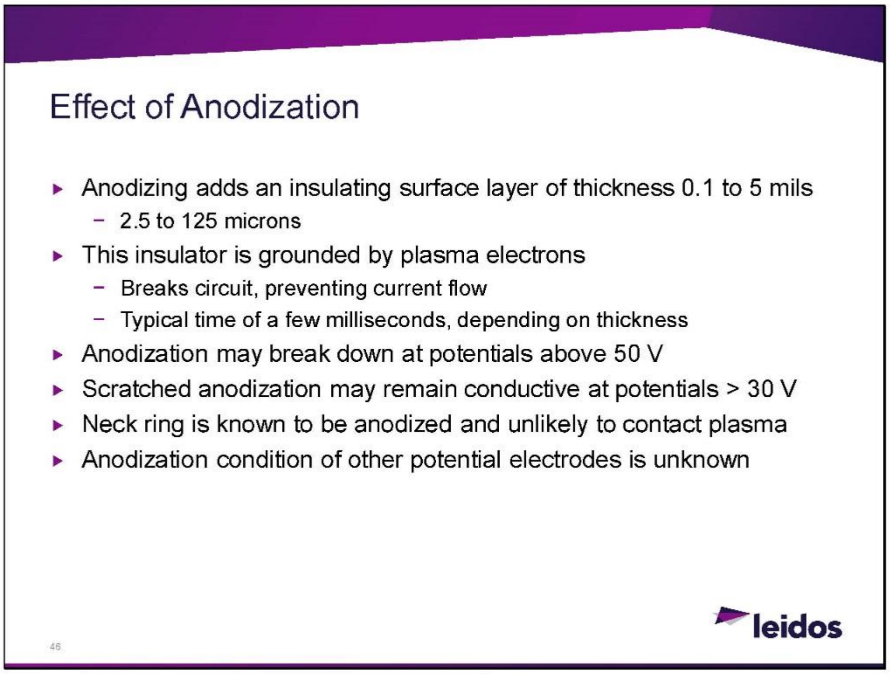
Effect of Anodization
Anodizing adds an insulating surface layer of thickness 0.1 to 5 mils
– 2.5 to 125 microns
This insulator is grounded by plasma electrons
– Breaks circuit, preventing current flow
– Typical time of a few milliseconds, depending on thickness
Anodization may break down at potentials above 50 V
Scratched anodization may remain conductive at potentials > 30 V
Neck ring is known to be anodized and unlikely to contact plasma
Anodization condition of other potential electrodes is unknown
leidos
46

Having demonstrated the code's behavior with respect to the spherical Langmuir probe data and described the geometrical model, we move on to the actual current collection calculations.

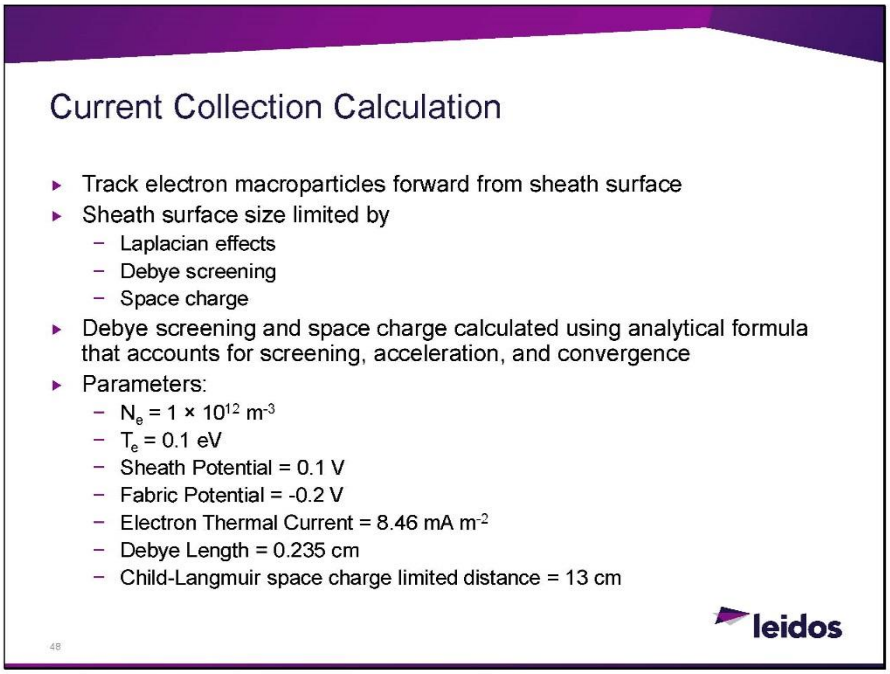

The currents to all the electrodes are calculated by tracking electron macroparticles inward from the sheath surface.

The sheath surface is taken as the potential contour at the electron temperature.

Potentials are calculated using the well-tested "Nascap/LEO Formula" for space charge, which reproduces Debye screening in low potential regions and accounts for acceleration and convergence of attracted particles in high potential regions.

While the 1.25 cm resolution near the electrodes gives about five debye lengths per zone, the more relevant Child-Langmuir space charge limited distance of about 13 cm (for applied potential of 15 V) is well-resolved.

Current Collection Results

EMU feature	Area	Current	Material	Current for 10% of area collecting	Enhancement		
	(m²)	mA	(**)	mA	Calculated (I/(AJ_e))	$0.6(1 + V/T)^{0.7}$	Ratio
					(Space-charge limited)	(Langmuir Probe Fit)	
Body Seal Closure	0.0328	0.87	S	0.087	3.13	20.11	0.16
Waist Bearing	0.0255	0.89	S	0.089	4.12	20.11	0.21
Leg Sizing Rings–each of two	0.0139	1.115	S	0.1115	9.48	20.11	0.47
Boot Sizing Rings–each of two	0.0197	0.95	S	0.095	5.67	20.11	0.28
Arm Bearings–each of two	0.00455	0.135	S	0.0135	2.45	20.11	0.12
Upper Arm Sizing Rings–each of two	0.0066	0.325	S	0.0325	5.77	20.11	0.29
Wrist Bearings–each of two	0.0131	0.735	S,A	0.0735	4.75	20.11	0.24
Breast Plate	0.0058	0.19		0.19 *	3.87	20.11	0.19
Neck Ring	0.0166	0.72	A	0.72 *	3.88	20.11	0.19
Boot FARs–each of two	0.01905	0.01	A	0.001	0.06	20.11	0.31
D-Rings–each of two	0.0029	0.185	S	0.185 *	7.54	20.11	0.38
EVA Base Plate	0.0552	1.62	A	1.62 *	3.47	20.11	0.17
Leg FARs–each of two	0.02535	0.08	A	0.008	0.37	20.11	0.02
Total of Electrodes	0.3661	11.36		3.746	3.72	20.11	0.19
Tether collection: 0.2694 mA/ft (0.8839 mA/m)					Cylindrical OML		
Tether, 85 feet exposed (25.908m)	0.194	22.9 (S)			13.86	20.11	0.69
Tether, 55 feet exposed (16.764m)	0.125	14.8 (S)			13.86	20.11	0.69

* Fully exposed

** From *EMU Current Collection Areas rev 4.pptx, Dated 04May2015 from T. Scott West*

S – Stainless Steel A – Anodized Aluminum

leidos

49

This slide shows the current collected by each electrode when totally exposed at 15 V. The sum of the currents to all totally exposed electrodes is about 11.4 mA.

The highest current is collected by the EVA Baseplate, at 1.6 mA.

Several other electrodes collect on the order of 1 mA each when totally exposed. Only small currents are collected by the D-Rings and breast plate.

The "enhancement factor" (i.e., the ratio of the calculated current per unit area to the planar plasma current per unit area) is in the range of 3 to 6, except for the Boot and Leg size rings (which have current focused on them by their respective FARs), and the D-Rings (which are small). Summing all the electrode areas and currents gives an enhancement factor of 3.72, which is a factor of five below the 20.11 enhancement factor predicted by the "Langmuir Probe Fit."

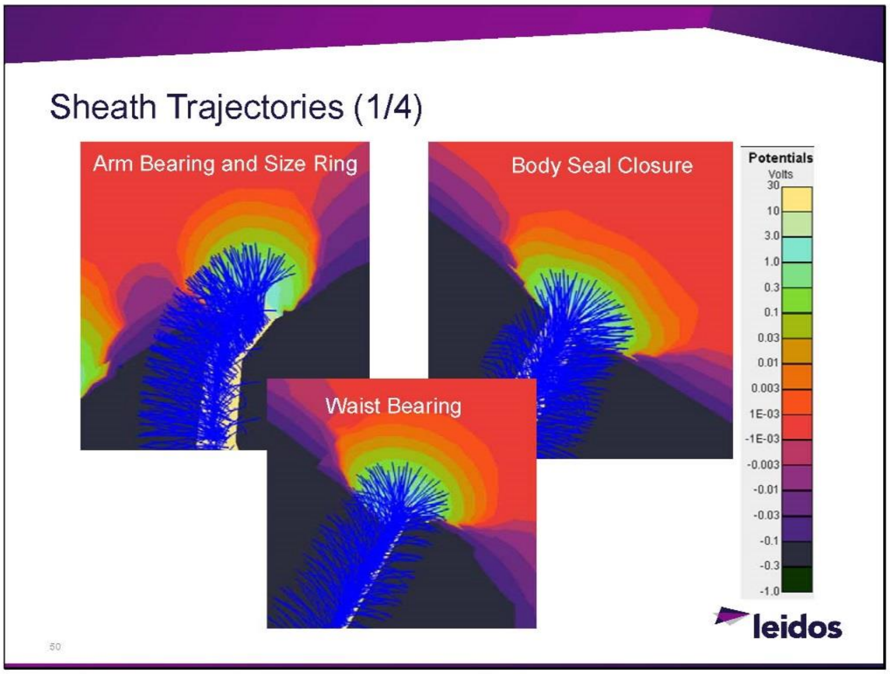

These figures show the calculated potential contours and the electron trajectories from the sheath surface to the electrode.

In these cases nearly all the tracked macroparticles reached the electrode.

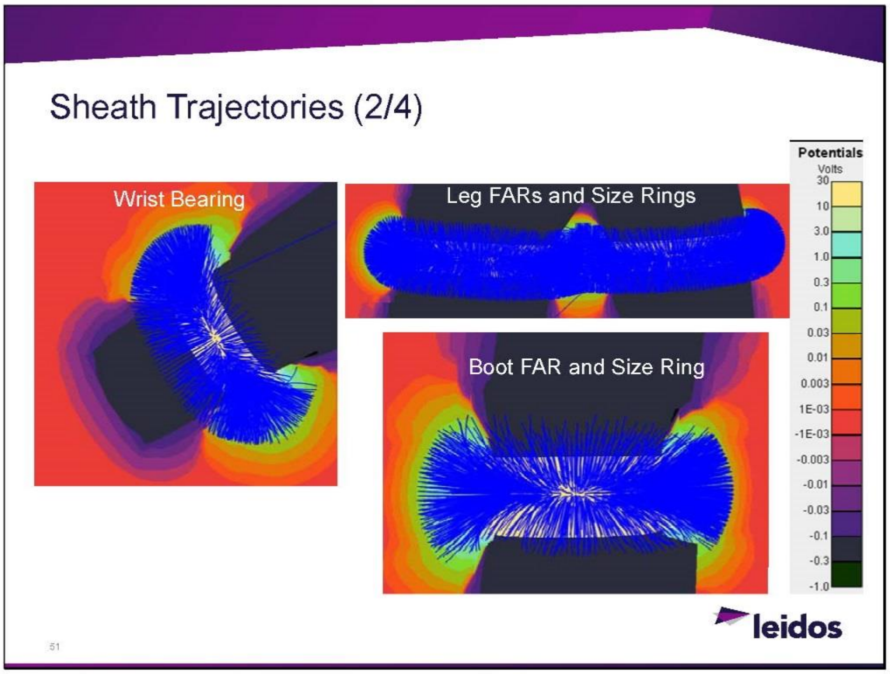

Trajectories to three more electrodes. For the wrist and the boot, focusing of current near the center of the electrode can be seen.

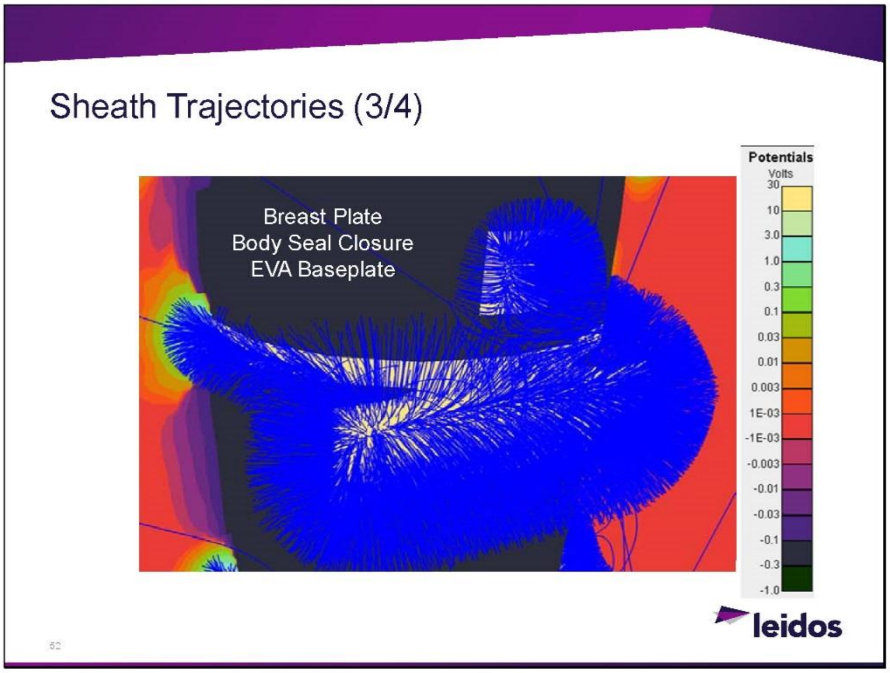

The sheath near the Breast Plate is more nearly planar than the sheaths near electrodes that have smaller dimension, and thus the enhancement factor is somewhat lower.

Note that the sheath curvature deflects electrons away from the upper edge of the breast plate and focuses current in the central region.

The current to the EVA Baseplate is enhanced by large areas of sheath wrapping around the ends and edges.

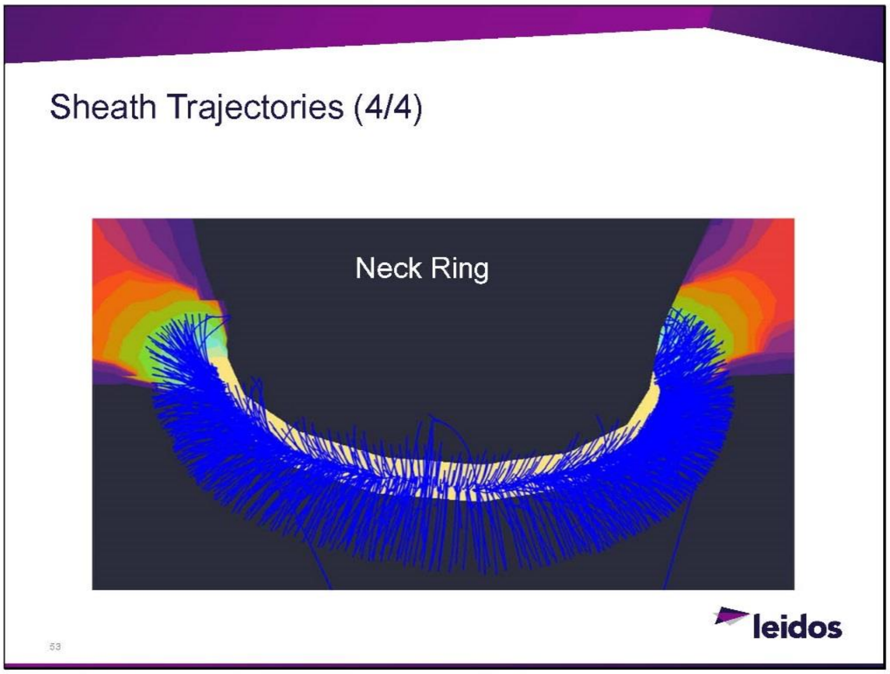

The sheath near the Neck Ring is pinched off by the potential of the negative fabric, particularly near the arm.

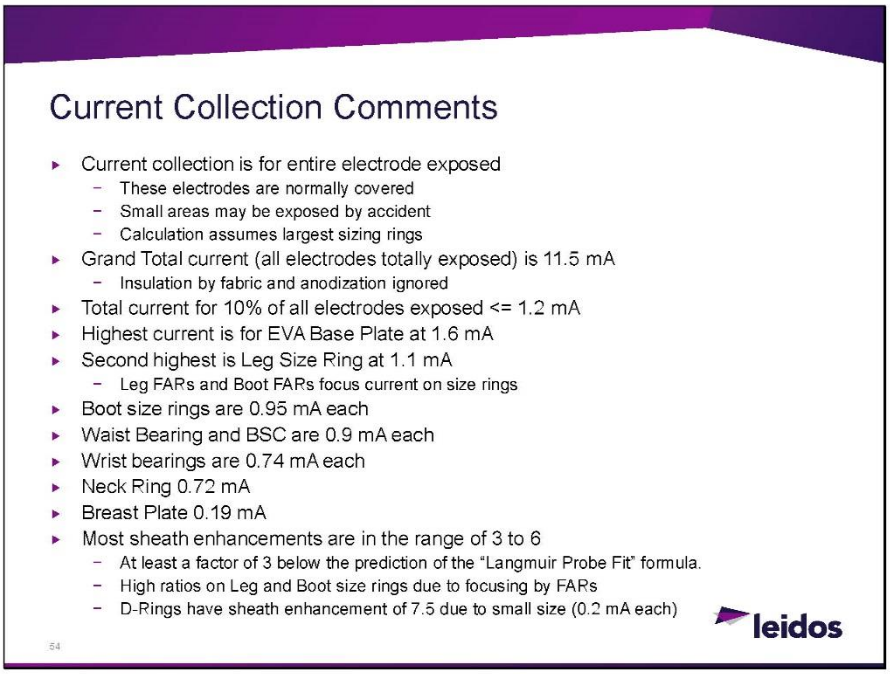

The currents we have calculated are gross overestimates, as they assume that all electrodes are totally exposed.

In practice, at most small fractions of these electrodes are exposed, with a corresponding reduction in current.

Most of the electrodes collect about three-quarters of a milliampere each if totally exposed, with the Breast Plate coming in at a mere 0.23 milliamperes.

The calculated sheath enhancements fall in the range of 4 to 6, with all currents at least a factor of three below the prediction of the "Langmuir Probe Fit" formula. The reduction is due to compression of the "sheath" both by the space charge of the collected current and by the presence of negatively-charged fabric surrounding the electrodes.

In the previous calculations we have ignored the possibility that one of the electrodes may be contacted by the restraining tether, in which case current collection by the tether dominates the hazard. So, we will treat that next.

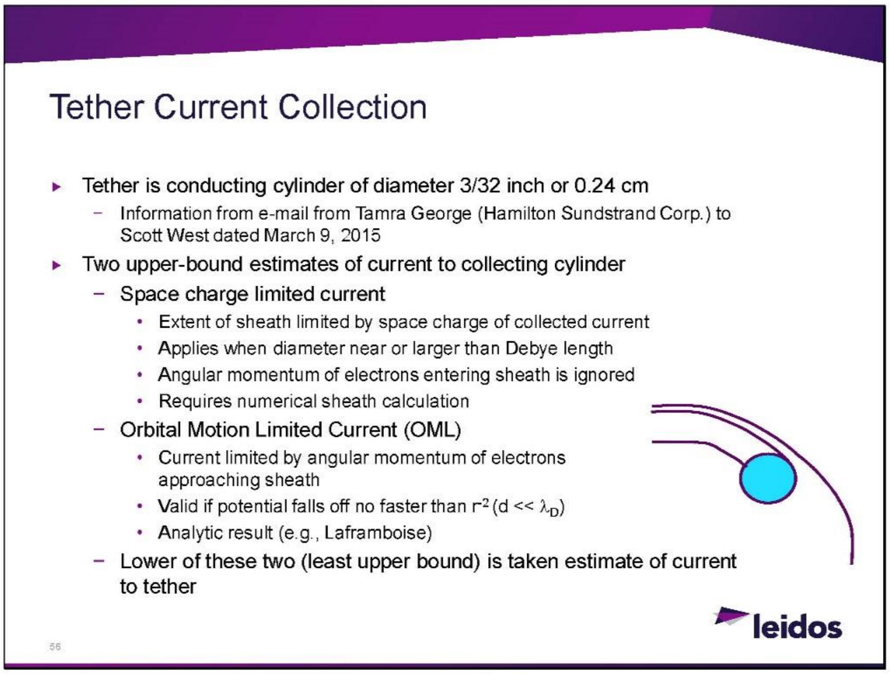

The tether is modeled as a conducting cylinder with diameter 2.4 mm.

In calculating the current to a small, symmetric object such as the tether, one must recognize that there are two common ways to obtain upper bounds to the current.

The "Sheath" method calculates the potential around the object and then launches macroparticles normally from a sheath contour. In so doing the calculation neglects the sheath normal velocity, i.e., the particle angular momentum, which may cause some of the actual electrons to be deflected by the object rather than hitting it.

The Orbit Motion Limited method, in contrast, considers ONLY the angular momentum of the particles. For the case of a monoenergetic beam, the cartoon (which could be for either a sphere or a cylinder) shows a bounding trajectory between the trajectories that strike the object and those that are merely deflected. Equating the initial angular momentum of this trajectory to its angular momentum when tangent to the object gives the boundary "impact parameter" (i.e., the distance of the particle from a parallel line through the object center), and the maximum collected current is inferred from the ratio of the boundary impact parameter to the object size.

As both of these methods provide upper bounds, the lower of the two is taken as the estimate of collected current.

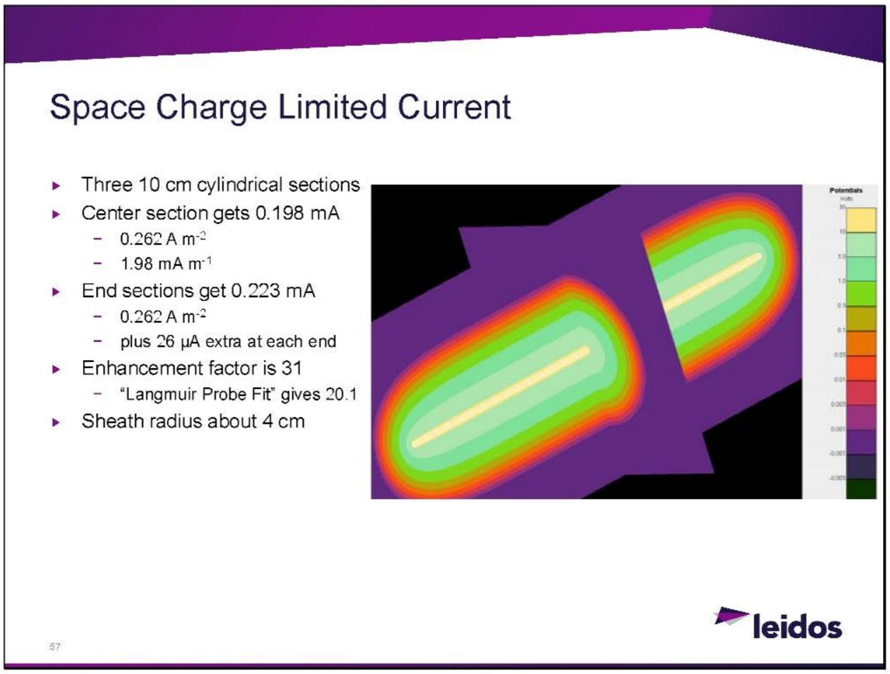

The Space Charge Limited Current is calculated using *Nascap-2k*. The tether is modeled in three 10 cm sections, so that the end current can be separated out.

The Sheath extends over 4 cm radially from the tether. The result is nearly 2 mA per meter of tether, plus 26 microamperes extra at each end.

Note that in this case the calculated enhancement factor of 31 is larger than that given by the Langmuir Probe Fit of 20.1.

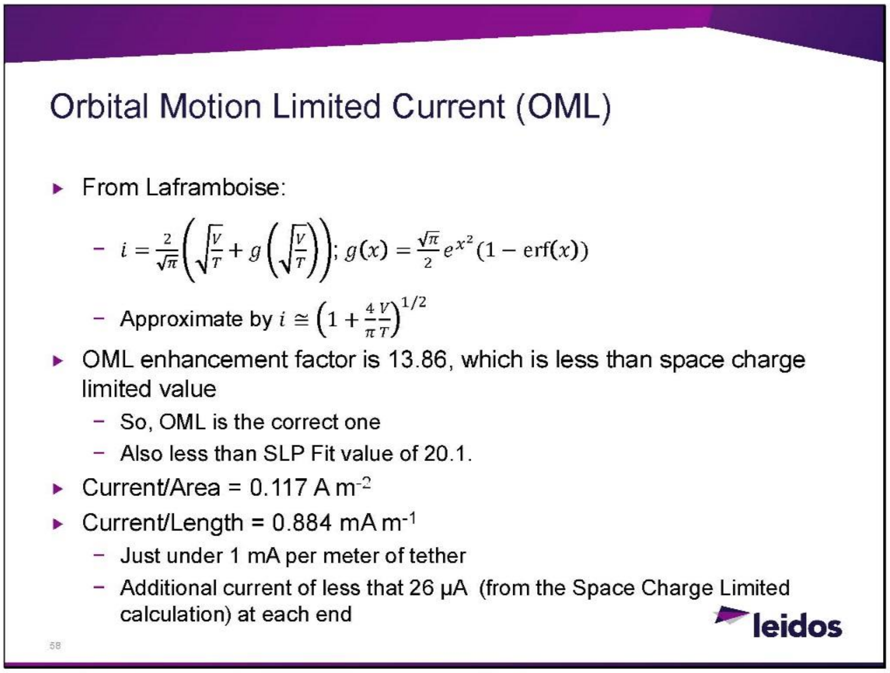

The exact solution of the OML current to a cylinder is given by Laframboise.

It is easier to use an approximate formula that gives, to very close tolerance, the same result.

(Note the factor of 4/π, which results from integrating a square root times an exponential; this occurs only for the cylindrical case.)

This gives an enhancement factor of 13.86, which is less than the 31 we got from the sheath-limited calculation, and also less than the 20.1 from the Spherical Langmuir Probe Fit.

The bottom line is collected current of just under 1 mA per meter of tether, plus additional current of less than 26 µA (from the Space Charge Limited calculation) at each end.


Conclusions
leidos

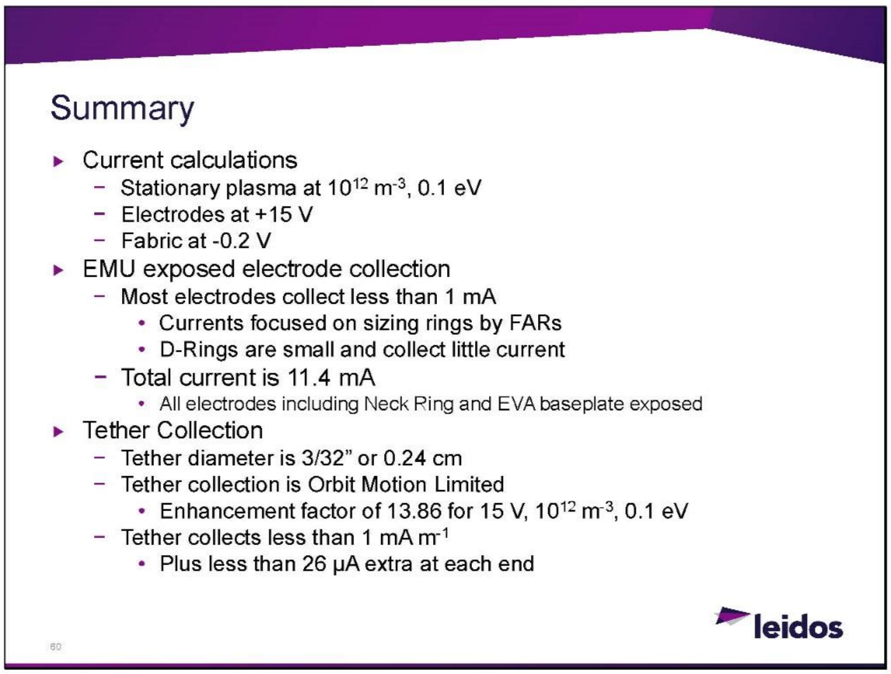

We have calculated the current to possible exposed EMU electrodes under proposed worst case conditions.

When totally exposed, several electrodes collect on the order of one milliampere, with the EVA baseplate collecting 1.6 mA.

The calculated currents are at least a factor of three below what would be estimated using the "Langmuir Probe Fit" estimate.

With the exception of the EVA baseplate, neck ring and D-rings, these electrodes are intended to be covered, and it is unlikely or impossible that more than a small area would be exposed.

The neck ring is known to be anodized and painted. The D-rings are small and collect little current. We have calculated 1.6 mA to the EVA baseplate, which is probably a high estimate.

The final issue is collection by the Body Restraint Tether. The tether collects electrons from the plasma in orbit-limited fashion, and can collect nearly 1 mA per meter of length. (This is somewhat less than predicted by the "Langmuir Probe Fit.") Thus, in the unlikely event that the tether contacts one electrode while another electrode contacts a positive ISS surface while in dense plasma, current of a few milliamperes (depending on the length of the tether) is possible.

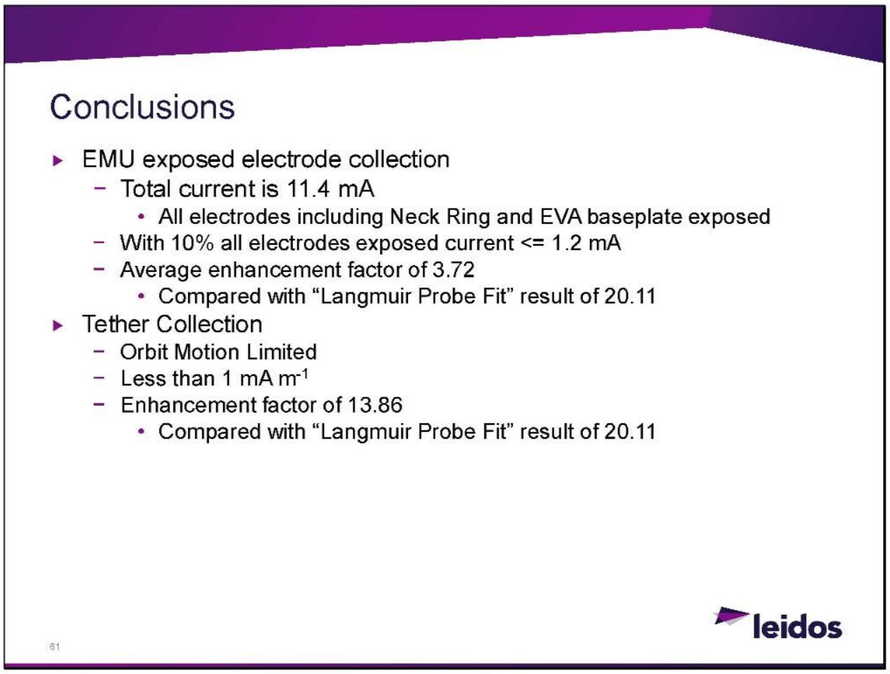

All currents are below the Langmuir Probe fit enhancement factor of 20.11

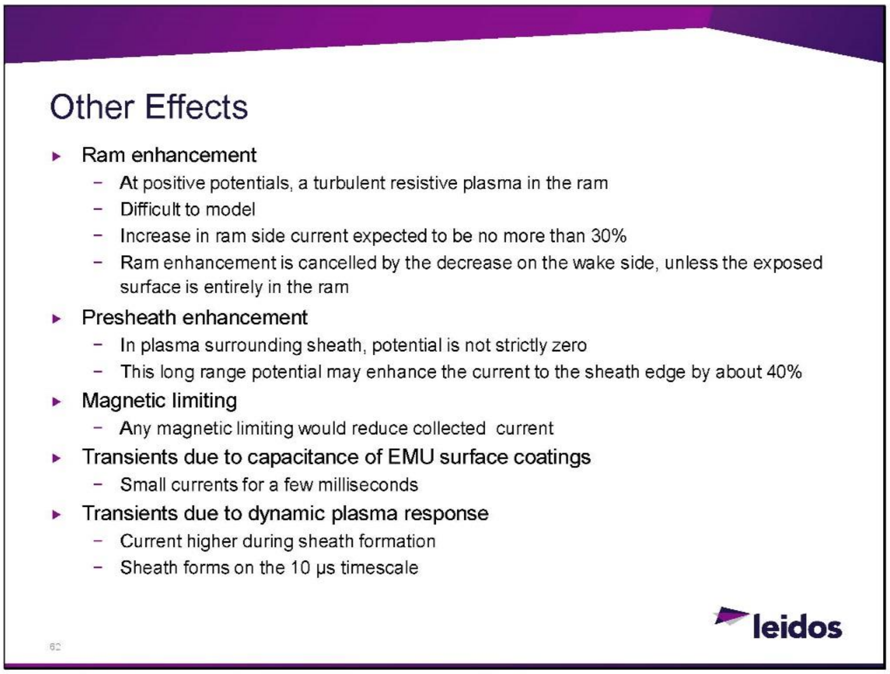

There are a few effects that have not been considered in these current collection calculations. Collectively, these would have much less than a factor of two effect on the current.

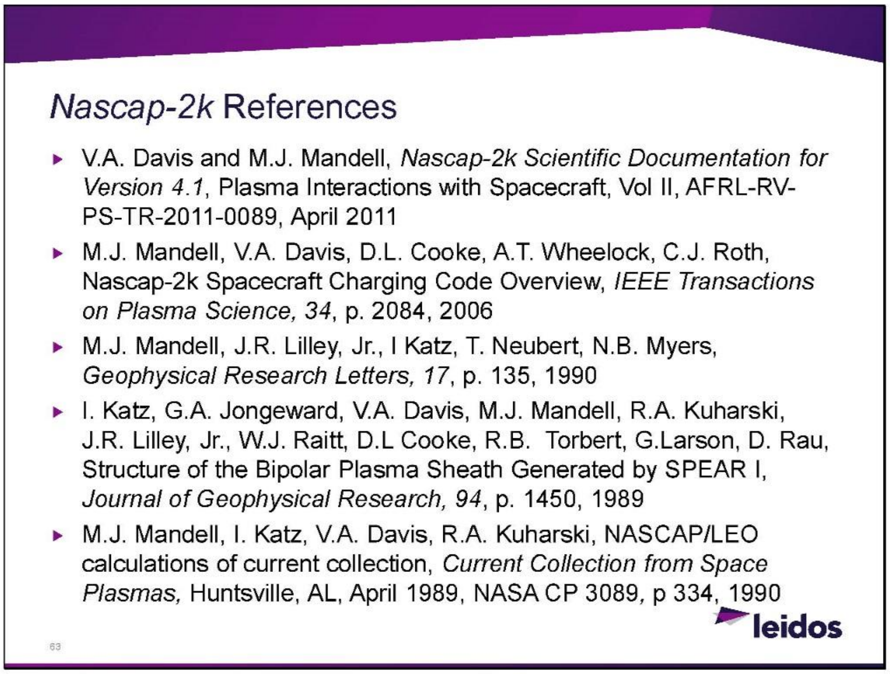
Nascap-2k References
V.A. Davis and M.J. Mandell, Nascap-2k Scientific Documentation for Version 4.1, Plasma Interactions with Spacecraft, Vol II, AFRL-RV-PS-TR-2011-0089, April 2011
M.J. Mandell, V.A. Davis, D.L. Cooke, A.T. Wheelock, C.J. Roth, Nascap-2k Spacecraft Charging Code Overview, IEEE Transactions on Plasma Science, 34, p. 2084, 2006
M.J. Mandell, J.R. Lilley, Jr., I Katz, T. Neubert, N.B. Myers, Geophysical Research Letters, 17, p. 135, 1990
I. Katz, G.A. Jongeward, V.A. Davis, M.J. Mandell, R.A. Kuharski, J.R. Lilley, Jr., W.J. Raitt, D.L Cooke, R.B. Torbert, G.Larson, D. Rau, Structure of the Bipolar Plasma Sheath Generated by SPEAR I, Journal of Geophysical Research, 94, p. 1450, 1989
M.J. Mandell, I. Katz, V.A. Davis, R.A. Kuharski, NASCAP/LEO calculations of current collection, Current Collection from Space Plasmas, Huntsville, AL, April 1989, NASA CP 3089, p 334, 1990
leidos
63

REPORT DOCUMENTATION PAGE

Form Approved
OMB No. 0704-0188

1. REPORT DATE *(DD-MM-YYYY)*
01- 08 - 2014

2. REPORT TYPE
Technical Memorandum

3. DATES COVERED *(From - To)*
May 2013 - July 2014

4. TITLE AND SUBTITLE
International Space Station (ISS) Plasma Contactor Unit (PCU) Utilization Plan Assessment Update

5a. CONTRACT NUMBER

5b. GRANT NUMBER

5c. PROGRAM ELEMENT NUMBER

6. AUTHOR(S)
Hernandez-Pellerano, Amri; Iannello, Christopher J.; Garrett, Henry B.; Ging, Andrew T.; Katz, Ira; Keith, R. Lloyd; Minow, Joseph I.; Willis, Emily M.; Schneider, Todd A.; Whittlesey, Albert C.; Wollack, Edward J.; Wright, Keneth H.

5d. PROJECT NUMBER

5e. TASK NUMBER

5f. WORK UNIT NUMBER
869021.05.07.09.37

7. PERFORMING ORGANIZATION NAME(S) AND ADDRESS(ES)
NASA Langley Research Center
Hampton, VA 23681-2199

8. PERFORMING ORGANIZATION REPORT NUMBER
L-20454 NESC-RP-13-00869

9. SPONSORING/MONITORING AGENCY NAME(S) AND ADDRESS(ES)
National Aeronautics and Space Administration
Washington, DC 20546-0001

10. SPONSOR/MONITOR'S ACRONYM(S)
NASA

11. SPONSOR/MONITOR'S REPORT NUMBER(S)
NASA/TM-2014-218512

12. DISTRIBUTION/AVAILABILITY STATEMENT
Unclassified - Unlimited
Subject Category 16 - Space Transportation and Safety
Availability: NASA CASI (443) 757-5802

13. SUPPLEMENTARY NOTES

14. ABSTRACT
The NASA Engineering and Safety Center (NESC) received a request to support the Assessment of the International Space Station (ISS) Plasma Contactor Unit (PCU) Utilization Update. The NESC conducted an earlier assessment of the use of the PCU in 2009. This document contains the outcome of the assessment update.

15. SUBJECT TERMS
International Space Station; Extravehicular activity; NASA Engineering and Safety Center; Plasma Contactor Unit; Extravehicular Mobility Unit

16. SECURITY CLASSIFICATION OF: a. REPORT	b. ABSTRACT	c. THIS PAGE	17. LIMITATION OF ABSTRACT	18. NUMBER OF PAGES
U	U	U	UU	299

19a. NAME OF RESPONSIBLE PERSON
STI Help Desk (email: help@sti.nasa.gov)

19b. TELEPHONE NUMBER ***(Include area code)***
(443) 757-5802

Standard Form 298 (Rev. 8-98)
Prescribed by ANSI Std. Z39.18